# Effect of Microbubble on the Performance of the Partial Nitrification and Anammox process

XIA ZHU

Degree of Doctor of Philosophy

Under the supervision of

Professor William Zimmerman

&

Dr. Stephen Wilkinson

Department of Chemical and Biological Engineering


University of Sheffield

November 2012

## Summary

Nitrogen pollution is an increasingly important global concern because it has multiple impacts on terrestrial, aquatic and atmospheric environments. Nitrogen is usually present in wastewater as ammonium. Ammonium can be removed from wastewater by a variety of physicochemical and biological processes, but biological processes are preferred because they are usually more efficient and environmentally friendly. Conventional biological nitrogen removal is carried out by autotrophic nitrification and heterotrophic denitrification via nitrate, which use biodegradable organic matter as electron donor. However there are some kinds of wastewater with low concentrations of biodegradable organic matter such as landfill leachate and anaerobic digester supernatant. In these cases an external organic carbon source is necessary in order to obtain a complete denitrification, which implies higher economic cost.

Partial nitrification- Anammox process as a promising and novel biological technology of removing nitrogen from high-strength ammonium wastewater with a low C/N ratio has attracted increasing attention due to its higher efficiency and cost-effectiveness compared with the conventional nitrification–denitrification nitrogen removal process. However, many challenges were faced during the development of stable and high-efficiency partial nitrification-Anammox performance, such as NOB activity, the effort to save energy, strict conditions and influent with favourable composition for Anammox. In order to improve the efficiency of Partial nitrification- Anammox process as much as possible whereas using the least energy, the microbubble generation system was firstly applied into the partial nitrification-Anammox process. The steady microbubble cloud produced by fluidic oscillator was verified size ranging from 60 μm to 600 μm which provides higher mass transfer rates and gas hold-up in gas-liquid phase bioreactor due to the fact that the microbubble was characterized by higher surface area to volume ratio and slower rising velocity. The simulation of the inner motion of the airlift loop reactor with COMSOL offered a visual difference between microbubble aeration and fine bubble aeration.

In the partial nitrification process dissolved oxygen is a key factor for the growth of ammonia oxidizing bacteria (AOB). Two contrasting experiments in sequencing batch airlift loop reactors (SBAB) with and without fluidic oscillator were conducted over 200

days to investigate the effect of microbubble aeration system on the long term partial nitrification process. The results showed the microbubble aeration system can significantly enhance the activity of AOB to speed up the biological treatment with fewer oxygen requirements and effectively prevent the production of nitrate. The performance of the partial nitrification in an airlift loop bioreactor with fluidic oscillator was greatly improved in terms of treatment capacity and stability compared to the one without fluidic oscillator. Thereafter different operational parameters such as temperature and pH were examined to optimize the operational strategies for the partial nitrification process. The microbial communities that catalyse partial nitrification were analysed by molecular biotechnology. The morphology of bacteria at different growth stages was observed by SEM and TEM. Real-time PCR was used to quantify populations of ammonia-oxidizing bacteria and nitrite oxidizing bacteria.

For the Anammox process, a strict anaerobic condition is required to operate successfully. As we all know, the stack gas is usually consists of depleted oxygen but mostly nitrogen (typically more than two-thirds) derived from the combustion, carbon dioxide ($CO_2$), and water vapour, among which $CO_2$ is considered as a greenhouse gas contributing to global warming. Bubbling the synthetic power station stack gas into the Anammox reactor by means of the microbubble generation system not only obtain this circumstance but also provide the heat required by good activity of anammox bacteria. In addition to maintaining desirable conditions, the dissolved $CO_2$ can provide a carbon source for the growth of anammox bacteria and adjust the value of pH in the reactor which is able to save substantial operational cost caused by pH control. Two contrasting experiments in round sequencing batch gas lift loop bioreactors (SBGB) with and without fluidic oscillator were carried out nearly 100 days. The performance of Anammox process in the SBGB with fluidic oscillator was noticeably improved comparing to the one without fluidic oscillator. The size distribution of granular Anammox sludge was analysed by ImageJ to investigate the effect of microbubble on the granulation. The batch assays were conducted to measure the maximum specific Anammox activity in different gas lift loop bioreactors. The morphology of Anammox bacteria at different growth stages was observed by SEM and TEM. Real-time PCR was used to quantify populations of Anammox bacteria in different stage and different bioreactors.

The kinetic model for laboratory-scale partial nitrification and Anammox (anaerobic ammonium oxidation) process with sequencing batch gas lift loop bioreactors (SBGB)

with and without fluidic oscillator were investigated. According to Monod model and Stover–Kincannon model the kinetic parameters of the model including maximum specific rates and half-maximum rate concentrations for partial nitrification and Anammox were estimated respectively from the results obtained from a laboratory-scale SBGB fed with synthetic wastewater.

## Acknowledgements

First of all, I would like to express my sincere gratitude to my supervisor Professor William Zimmerman for introducing me to the challenges of wastewater treatment with microbubble application, for all his support and for the great enthusiasm he has always shown for my work. I cannot imagine having any other supervisor than Will. Thanks for his encourage I could always find inspirations in my study. Furthermore, his careful reading of this thesis has improved its quality considerably.

I also want to thank my second supervisor Dr. Stephen Wilkinson who gave me great support in my experimental work and the research in the first two years of my PhD. I am so impressed by his carefulness and sense of responsibility.

I greatly appreciated Thomas Holmes for proofreading the thesis and providing me with huge amounts of detailed comments and suggesting important improvements with regard to the content of the thesis. In addition to this, Thomas has helped me solve various practical problems in my experiments and English Learning. At the same time, I would like to thank all the technicians at the Department of Chemical and Biological Engineering, who gave me a lot of assistance, especially Andy and Adrian. Without their help I could not finish my experiment successfully.

I have had the great honour of being part of a large, interdisciplinary research Group—Microfluidics Group, working within the field of wastewater treatment, during the last 4 years. A large amount of important research has been carried out and a lot of valuable results were obtained. Nowadays Microfluidics group is internationally recognized for its work. I would like to take this opportunity to thank all my friends and colleagues. It is my sincere wish that our group would approach more great achievements and have a promising future.

I would also like to thank Dr Hemaka Bandulasena (Lecturer in Chemical Engineering at Loughborough University) Dr Dmitriy Kuvshinov and Dr Jaime Lozano-Parada who have inspired me and provided me with valuable comments over the years. I am much indebted to them for help me order a lot of experiment devices (over and over again). Working with them has been a great experience.

I want to show my great appreciation to Dr Dayi Zhang from Department Civil & Structure Engineering who gave me significant technical support in the aspect of microbiology. Two MSc students Sisi Ge and Meng Lian also did good job as

experiment assistants under my supervision. Thanks to them I was allowed to have more time to do further research on my project.

I am also grateful to every member of our group who have contributed to my work. I would especially like to thank Kezhen Ying, Yuzhen Shi and James O Hanotu for providing the creative and friendly atmosphere which makes work a pleasure. They not only gave me great help in my experiment but also close personal friends.

Finally, I thank my parents and the other members of my immediate family for the love, support and trust that they have always shown towards me.

The work has been supported financially by China Scholarship Council and Department for Innovation, Universities and Skills and the University of Sheffield. Their support is gratefully acknowledged.

# Contents

# List of Figures

# List of Tables

# List of Symbols

ALB: Airlift Loop Bioreactor

Anammox: Anaerobic Ammonia Oxidation

Amox-SBGB: Anammox-Sequencing Batch Gas Lift Loop Bioreactor

AOB: Ammonium Oxidizing Bacteria

ATP: Adenosine Triphosphate

ASM: Activated Sludge Models

BOD: Biochemical Oxygen Demand [$mgO_2L^{-1}$]

COD: Dissolved Oxygen Saturation Concentration [$mgL^{-1}$]

$C_L$: DO Concentration [$mgL^{-1}$]

CANON: Completely Autotrophic Nitrogen Removal

COD: Chemical Oxygen Demand [$mgO_2L^{-1}$]

CRR: Coefficient of Range Ratio

CRFD: Coefficient of Regression Function Derivative

CSTR: Continuous Stirred Tank Reactor

CVR: Coefficient of Variation Ratio

DO: Dissolved Oxygen

FA: Free Ammonia [$mgL^{-1}$]

FNA: Free Nitrous Acid [$mgL^{-1}$]

FO: Fluidic Oscillator

HRT: Hydraulic Retention Time [day]

IC: Inorganic Carbon

$k_G$: Gas Phase Mass Transfer Coefficient

LFL: Long Feedback Loop

NAR: Nitrite Accumulation Ratio

NLR: Nitrogen Loading Rate [$kgNm^{-3}d^{-1}$]

NRR: Nitrogen Removal Rate [$kgNm^{-3}d^{-1}$]

NOB: Nitrite Oxidizing Bacteria

MBR: Membrane Bioreactor

OPR: Oxidation Reduction Potential [mV]

OUR: Oxygen Uptake Rate [$mgO_2L^{-1}h^{-1}$]

OLAND: Oxygen Limited Autotrophic Nitrification Denitrification

PN: Partial Nitrification

PN-SBAB: Partial Nitrification Sequencing Batch Airlift Loop Bioreactor

PCR: Polymerase Chain Reaction

qPCR: Quantitative Polymerase Chain Reaction

SAA: Specific Anammox Activity

SBR: Sequencing Batch Reactor

SBAB: Sequencing Batch Airlift Bioreactor

SBGB: Sequencing Batch Gas Bioreactor

SHARON: Single Reactor System for High-activity Ammonia Removal over Nitrite

SRT: Sludge Retention Time [day]

SFL: Short Feedback Loop

SEM: Scanning Electron Microscope

SVI: Sludge Volume Index [$mlg^{-1}$]

T: Temperature [ ℃]

TN: Total Nitrogen [$mg^{-1}L^{-1}$]

TEM: Transmission Electron Microscope

TSS: Total Suspended Solid [$mgL^{-1}$]

UASB: Upflow Anaerobic Sludge Blanket

VSS: Volatile Suspended Solid [$mgL^{-1}$]

WWTP: Waste Water Treatment Plant

$K_S$: Half Saturation Constant (mg $L^{-1}$)

$M$: Percent of AOB in total biomass (%)

$K_{S,NH4}$ : Half-maximum Rate Concentration for $NH_{+4}$ for autotrophs ($mgL^{-1}$)

$K_{S,O}$: Half-maximum Rate Aoncentration for DO for Autotrophs ($mgL^{-1}$)

$K_B$: Saturation Value Constant ($gL^{-1}$ $day^{-1}$).

$S$: Concentration of Substrate (mg $L^{-1}$)

$S_0$: Influent Substrate Concentration (mg $L^{-1}$)

$S_e$: Effluent Substrate Concentration (mg $L^{-1}$)

$S_{NH4}$: Ammonium Concentration (mg $L^{-1}$)

$S_O$: DO Concentration ($mgL^{-1}$)

$q_{ammonia}$: Specific Nitrification rate of Ammonium ($h^{-1}$)

$U_{max}$,: Maximum Utilization Rate Constant ($gL^{-1}$ $day^{-1}$)

$X_A$: Active AOB Biomass Concentration (mg SS $L^{-1}$)

$X$: Total Biomass Concentration in SBR (as mg $SSL^{-1}$)

$Y_{A:}$ Yield Coefficient for AOB (mg SS/mg$NH_4^+$-N)

$\mu_{AOB}$: Specific Growth Rate of AOB ($h^{-1}$)

$\mu_A$: Maximum Specific Growth Rate of AOB ($h^{-1}$)

$\mu$: Specific Growth rate due to Synthesis ($h^{-1}$)

$\mu_{max}$: Maximum Specific Growth Rate ($h^{-1}$)

# Chapter 1. Introduction

## 1.1 Background

Nitrogen is one of the primary nutrients critical for the survival of all living organisms. It is an indispensable component of many biomolecules, including proteins, DNA, and chlorophyll. In addition to $N_2$ and $NH_3$, nitrogen exists in many different forms, including both inorganic (e.g., ammonia, nitrite) and organic (e.g., amino and nucleic acids) forms. Therefore, nitrogen undergoes many different transformations in the ecosystem, converting from one form to another as organisms use it for growth and, in some cases, energy. The major transformations of nitrogen are nitrogen fixation, nitrification, denitrification, Anammox, and ammonification (Fig.1) (Bernhard 2010). Natural reactions of atmospheric forms of nitrogen with rainwater result in the formation of nitrate and ammonium ions. The two most important compounds that result from the reaction of these gases and rainwater are nitrate ($NO_3^-$, an anion) and ammonium ($NH_4^+$). In the atmosphere major sources of nitrate include reactions caused by lightning, photochemical oxidation in the stratosphere, chemical oxidation of ammonia, soil production of NO by microbial processes, and fossil fuel combustion. Ammonia in the air comes from fertiliser manufacturing, anaerobic decay of organic matter, bacterial decomposition of excreta, and the burning of coal (Gaillard, 1995). Many of the major sources of nitrate and ammonium come from the use and production of fertilisers and the burning of fuels. They are very common nitrogenous compound stemming from artificial processes. As the development of human society, human activities such as making fertilisers and burning fossil fuels have greatly increased the levels of these compounds, particularly in water bodies. The nitrogenous contaminant has increasing impact on the Human living environment. (Haller et al., 2012)

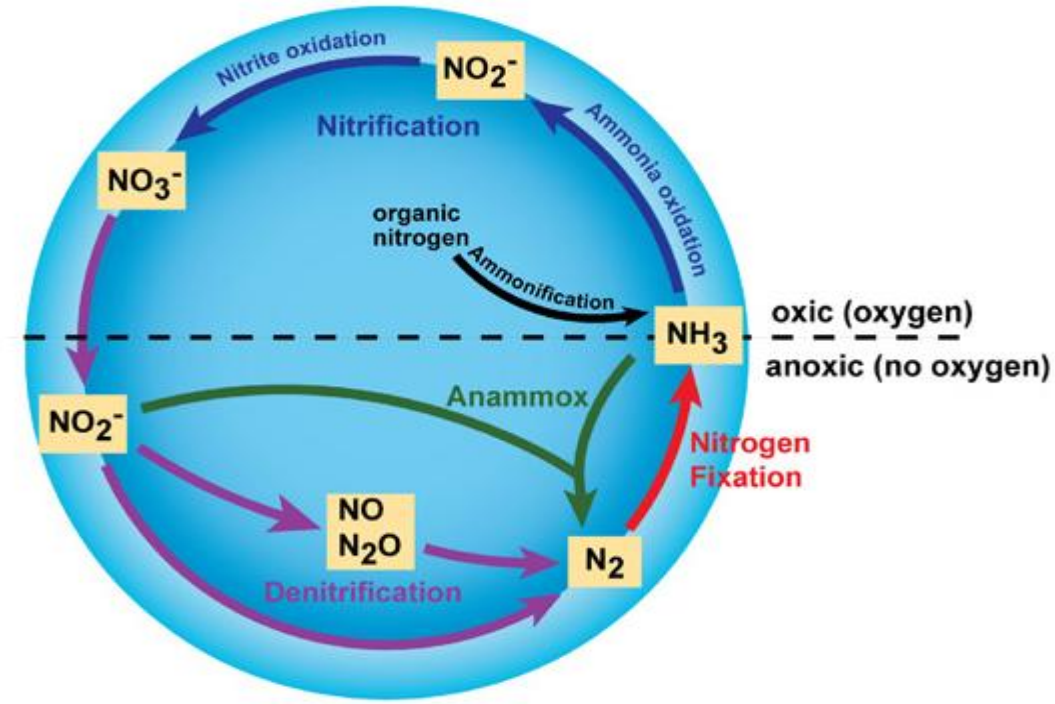


**Figure 1.1** Major transformations in the nitrogen cycle (Bernhard 2010)

Nitrogen contaminant compounds lead to eutrophication of environmental waters (i.e. severe reductions in water quality, aquatic life etc.) if the waste stream is discharged without sufficient treatment. In order to mitigate these effects, UK water companies are subject to tight regulation in the form of discharge consents. The maximum amount of ammonia nitrogen allowed in sewage effluent is 6 milligrams per litre and the fact that this limit is sometimes violated shows that it represents a serious operating constraint. In order to minimise risks of contamination and reduce the nitrogen contaminant compounds to the values lower than those required by the receiving aquatic system, a variety of technologies have been developed to remove all kinds of nitrogenous compounds from wastewater, including physicochemical and biological processes.

Up to now the most widely used biological nitrogen removal process is the conventional complete nitrification-denitrification process, which consists of an initial nitrification step that converts ammonia to nitrite and then a further step to produce nitrate under aerated conditions. Subsequently, denitrification reduces nitrate into nitrite, then into nitrous oxide, nitric oxide, and finally into gaseous $N_2$ under anoxic conditions. Due to the very high demand of organic carbon sources involved in this process, it substantially increases the cost of operation. In this project, however, we are concerned for the

treatment of wastewater characterized by high ammonium and low carbon source (i.e. low C/N ratio). Consequently this conventional process is not suitable to treat the wastewater with the low biodegradable organic matter content or even no organic carbon source.

Taking into account these constraints, a novel alternative biological nitrogen removal treatment, partial nitrification-Anammox process, has recently gained much attention due to its potentially higher efficiency and cost-effectiveness. This process is carried out totally based on the autotrophic microorganism to remove the nitrogen via nitrite instead of nitrate (Figure1.1). The partial nitrification process uses ammonia oxidising bacteria (AOB) oxidising half of the ammonia to nitrite preventing the production of nitrate. This is followed by the Anammox process which converts the 50% remaining ammonia and 50% produced nitrite into $N_2$ but utilising ammonium as electron donor instead of using organic compounds such as methanol and ethanol. In comparison with complete nitrification-denitrification, this new process saves 100% of the organic carbon demand, and it requires only 62.5% of aeration energy (Feng et al., 2007). Moreover it gives lower biomass production and therefore sludge disposal costs, which are a significant fraction of the total cost, are saved.

This project will focus on the use of microbubbles to enhance the efficiency of both the partial nitrification stage and the Anammox stage. Dissolved oxygen is the critical process variable for the growth of ammonia oxidising bacteria. A good aeration system can increase oxygen transfer efficiency to speed up the biological treatment. The main reason for poor oxygen transfer efficiency is the large size of bubbles produced by standard aeration systems. The department of Chemical & Process Engineering at the University of Sheffield has developed a novel aeration system building on microbubble technology. This new aeration system can produce bubbles which are at least 10 times smaller than bubbles produced by conventional means. The smaller the bubble size is the better the oxygen transfer into water should be. This system is demonstrated to be over eight times more efficient at oxygen transfer when producing the small bubbles than when producing large bubbles (Hu, 2006). Apart from optimizing aeration for partial nitrification process, the microbubble generation system potentially contributes to create desirable environment for Anammox process, which requires a strict anaerobic condition and narrow pH range for successful operation. In order to obtain such conditions, mixture $CO_2/N_2$ abounding in power station stack gas can be flushed into

the Anammox bioreactor by using a microbubble generation system. As result, continuously flushing mixed gas could not only maintain the anaerobiosis of Anammox bacteria, but also provide more carbon source for the growth of Anammox bacteria and $H^+$ for pH adjustment.

## 1.2 Project Overview

The aim of my PhD project is to experimentally test the difference of treatment performances between using microbubble and using normal bubble on the partial nitrification and Anammox process. Airlift loop bioreactors are applied throughout this project.

This project is divided up into three main areas of work as described below:

**A. Effect of microbubble on mass transfer efficiency for airlift loop bioreactor**

There are many factors influencing the effect of nitrogen removal, such as temperature, pH value, C:N ratio, dissolved oxygen, free ammonia and so on. Among these factors, the dissolved oxygen is the key factor and the most difficult to control. The oxygen transfer efficiency of a reactor has a direct impact on its effectiveness for wastewater treatment. Therefore aeration systems for the partial nitrification process appear to be particularly important. On the contrary, as the consequent process, Anammox required very strictly anaerobic environment. Removal of the dissolved oxygen is crucial to realise and run a stable Anammox process.

This work investigated the working performance of a biphasic airlift loop bioreactor equipped with a microfluidic oscillator producing microbubbles. Experiments were carried out to compare the performances of deoxygenation and oxygenation processes in the airlift loop bioreactor with microbubble generation system to those performances in the airlift loop bioreactor with conventional aeration system. Since the ideal aeration environment and the strictly anaerobic conditions required by the partial nitrification and Anammox processes respectively, which are potentially able to enhance these two biological processes, therefore the mass transfer study of ALB offers an essential basis for the subsequent work.

**B. Partial nitrification with microbubble aeration system.**

Partial nitrification is an oxygen consumption process which means the microbubble generator could be applied supply oxygen for the growth of AOB. The improvement of performance of partial nitrification achieved by using microbubbles rather than conventional aeration was investigated. Meanwhile, different operational conditions were applied to study optimisation of a partial nitrification biological system. The involved microorganisms were observed by SEM and QPCR to further confirm the enhancing of the partial nitrification process by using microbubble aeration system with fluidic oscillator.

### C. Anammox process with mixture of 10%$CO_2/N_2$ flushed using microbubble

Strict anaerobic conditions are required for the growth of Anammox bacteria. It was reported that researchers used $N_2$ or Argon to strip out the oxygen from the system to create the desired conditions for Anammox bacteria. Apart from the absence of dissolved oxygen, pH is another very important operational parameter to successfully run the Anammox process. Since Anammox biological process is alkali production process, increasing the pH, control of pH is indispensable throughout the entire process.

It is well known that the stack gas is usually depleted in oxygen but also consist of mostly nitrogen (typically more than two-thirds) derived from the combustion, carbon dioxide (CO2), and water vapour, in which $CO_2$ is considered as a greenhouse gas contributing to global warming. It further contains a small percentage of a number of pollutants, such as particulate matter, carbon monoxide, nitrogen oxides, and sulphur. Therefore, if the oxygen levels are sufficiently low, it should be possible to inject simulated stack gas (mixture of $CO_2/N_2$) into the Anammox reactor to maintain the desired anaerobic conditions and provide carbonate as a carbon source for the growth of related bacteria as well as preventing harmful gases (i.e. $CO_2$) being discharged into the atmosphere. This operational strategy might be a win-win solution for environment protection. In this work the author studied the performance of the Anammox reactor for nitrogen removal by using $CO_2/N_2$ with microbubble technology. The involved microorganisms were also investigated with microbiological determination technology to confirm the improvement of performance of the Anammox process achieved through introducing the microbubble generation system and the mixture of $CO_2/N_2$.

**D Kinetics Model of the partial nitrification-Anammox process with microbubble generation system**

The final object of this project is to establish a kinetics model for the partial nitrification and Anammox process in sequencing batch gas lift loop bioreactor with microbubble generation system for the treatment of wastewater with low C/N ratio. This kinetics model is able to help people to simulate the wastewater treatment process under different conditions and optimize the operating condition to treat different wastewater with minimal energy input and best result. Meanwhile the kinetic model can also be applied to predict wastewater treatment plant effluent quality. Therefore it is critical for the design and construction of wastewater treatment plant. Once the different models were built, the kinetic parameters of the models in this study will be compared with the ones in previous study. The in-depth understanding of influences of microbubble on the performance of partial nitrification and Anammox process were further discussed. Model evaluations were carried out by comparing experimental data with predicted values calculated from suitable models.

# Chapter 2. Literature Review

## 2.1 Nitrogen Pollution

Being produced industrially for over a century, nitrogen containing compounds among the most threatening pollutants for the quality of fresh water and coastal areas and attract more and more public attention. Whether they are developed or developing countries, they are committed to research and investment in nitrogen removal from wastewater in order alleviate the worsening global drinking water crisis.

Nitrate and ammonia are main problems as contaminants in drinking water (primarily from groundwater and wells) due to their harmful biological effects. For instance livestock manure is high in ammonia concentrations, and dissolved ammonia in water is not only highly toxic to fish, but can also be converted to dangerous nitrates. High concentrations of nitrate can cause methemoglobinemia and have been cited as a risk factor in developing gastric and intestinal cancer (Sustainable-Website, 2012). Due to these health risks, a great deal of emphasis has been placed on finding effective treatment processes to reduce nitrogen compound concentrations to safe levels.

### 2.1.1 Nitrogen Pollution Status and Sources

The world's supply of clean, fresh water is gradually decreased. Water demand exceeds supply in many parts of the world and as the world population continues to increase, so does the water demand. In the developing world, almost all wastewater still goes untreated into local rivers and streams (Rodriguez, 2010). It is reported that 10 million people in Europe are potentially exposed to drinking water with nitrate concentrations above recommended levels. In UK the cumulative cost of water pollution in England and Wales has been estimated at up to £1.3 billion per annum. A major new study has found that nitrogen pollution (including water body, air pollution and soil pollution) is costing each person in Europe around £130 - £650 (€150 – €740) a year. One study, carried out by 200 experts from 21 countries and 89 organizations, estimates that the annual cost of damage caused by nitrogen pollution across Europe is £60 - £280 billion (€70 - €320 billion), more than double the extra income gained from using nitrogen fertilizers in European agriculture.

There are many sources of nitrogen (both natural process and anthropogenic) that could potentially cause the pollution of the water body with different forms of nitrogen, the anthropogenic sources are really the major ones that most often lead to the amount of nitrogen contaminants to rise to a dangerous level.

In The UK one potentially large source of nitrogen pollution of groundwater is the application of nitrogen-rich fertilizers to turfgrass. This occurs on golf courses and in residential areas. Apart from the fertilizers source, other sources of nitrogen contributing to water pollutant will be discussed as follows:

*Urban and Industrial Sources

Municipal and industrial sources are considered “point sources” of nutrient pollution because they discharge nutrients directly to surface waters or groundwater via a pipe or other discrete conveyance. They are typically the most controllable sources of nutrients and are often regulated in developed countries.

**Table 2.1** Percentage of sewage treated in different regions worldwide (Selman et al., 2009)

| Percent of Sewage Treated by Region | |
|---|---|
| Region | Percent of Sewage Treated |
| North America | 90 |
| Europe | 66 |
| Asia | 35 |
| Latin America&Caribbean | 14 |
| Africa | <1 |

*Chemical fertilizers

Unlike point sources the agricultural pollution is know n as an area pollution source. Between 1960 and 1990, global use of synthetic nitrogen fertilizer increased more than sevenfold, while phosphorus use more than tripled.

*Manure

Another potential source of nitrogen compounds leaching to the groundwater is the storage of manure. Farmers commonly store manure in large holes in the ground. While this is convenient and relatively inexpensive for the farmer in the short term, it results in

excessive leaching of nitrates. It has also been found that an empty manure storage facility can be more hazardous to groundwater than a full one. The sides of an empty lagoon are directly exposed to the sun and air. This results in the drying and cracking of the soil material. Precipitation containing large amounts of dissolved oxygen will then convert the ammonium in the contaminated soil and leftover manure to nitrates which can easily be leached out (Lagoon Reclamation, 1993) (Haller et al., 2012) Over the last century the rapidly changing nature of raising livestock has also contributed to a sharp increase in nutrient levels. Animal production is intensifying, and as a result, more production is occurring further away from feedstock supplies, making it harder to spread the manure.

*Aquaculture

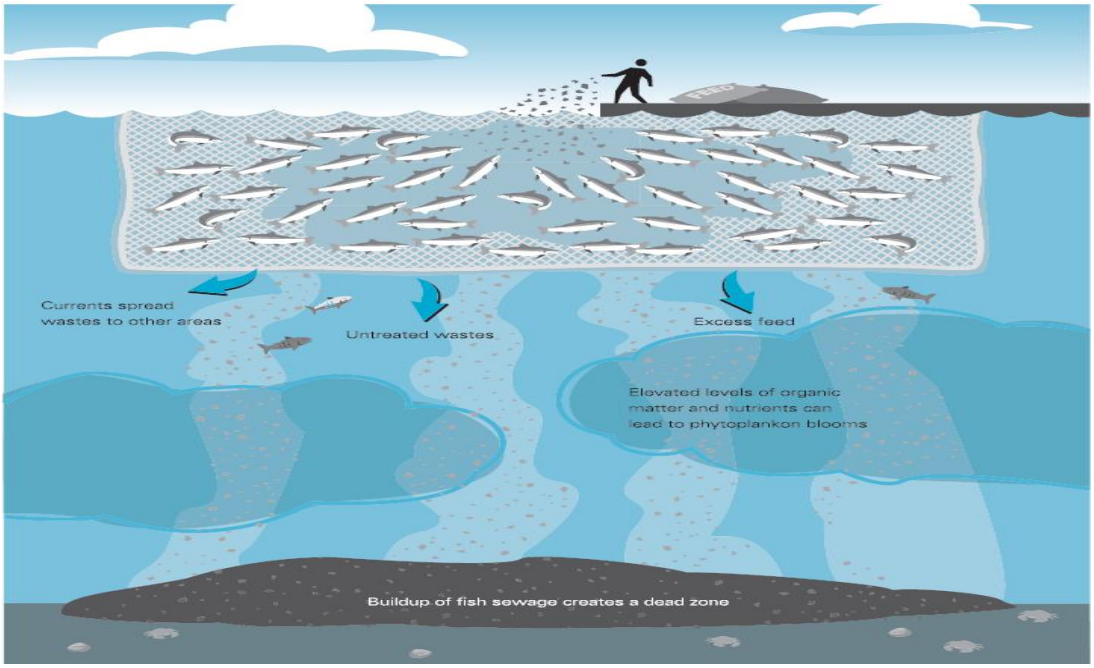


**Figure 2.1** Diagram illustrating the mechanisms by which aquaculture can contribute to eutrophication and hypoxia

Fish farming generates concentrated nitrogen and phosphorus from excrement, uneaten food, and other organic waste. If nutrient wastes are discharged directly into the surrounding waters without proper management, aquaculture operations can have severe impacts on aquatic ecosystems. For every ton of fish, aquaculture operations produce between 42 and 66 kilograms of nitrogen waste and between 7.2 and 10.5 kilograms of phosphorus waste (World Resources Institute 2012).

### 2.1.2 Hazards of Nitrogen Pollution

Nutrient over-enrichment in aquatic ecosystem, resulting from the contributions of Nitrogen from untreated sewage effluent and agricultural run-off carrying fertilizers etc., could lead to many adverse environmental and ecological effects. The most important negative impact on environment is eutrophication caused by the addition of artificial or natural substances, such as nitrates and phosphates. Eutrophication can cause excessive production of algal biomass and aquatic plants followed by undesirable consequences：

1. Dissolved oxygen depletion
2. Increased biomass of benthic and epiphytic algae
3. Increased incidences of fish kills
4. Increased biomass of phytoplankton
5. Loss of desirable fish species
6. Reductions in harvestable fish and shellfish
7. Decreases in perceived aesthetic value of the water body
8. Toxic or inedible phytoplankton species
9. Increases in blooms of gelatinous zooplankton
10. Changes in macrophyte species composition and biomass
11. Decreases in water transparency (increased turbidity)
12. Colour, smell, and water treatment problems

Ammonia is the nutrient source of nitrifying bacteria； therefore nitrification consumes a lot of dissolved oxygen in the water. At 20 ° C the saturation concentration of dissolved oxygen (DO) in water is about $9mgL^{-1}$. Generally speaking the dissolved oxygen concentrations required by fish is above 5mg / l, which calls for saturation of dissolved oxygen in water is greater than 56%. Ammonia consumption of dissolved oxygen can lead to serious impacts on aquatic ecosystems.

Due to the hazards of nitrogen pollution, more and more attention has been paid to the nitrogen pollution control. In the research of development and application of nitrogen removal technology, the emergence of a large number of effective treatment processes constitute a nitrogen removal system, which can be divided into two categories of

physical-chemical nitrogen removal technology and biological nitrogen removal technology. Physical-chemical nitrogen removal comprises air stripping, selective ion exchange, breakpoint chlorination and magnesium ammonium phosphate precipitation method. At present, however, the biological nitrogen removal is the most widely used technology in wastewater treatment around the world， which usually refers to nitrification and denitrification.

## 2.2 Conventional Biological Nitrogen Removal from Wastewater

Nitrogen is present in wastewater in several forms, the important ones being inorganic nitrogen (both soluble and particulate), ammonium/ammonia and possibly some nitrate.

The biological conversion of ammonium to nitrate nitrogen is called Nitrification. Ammonium can undergo the process of nitrification, which is an oxidation reaction. Through this mechanism, the nitrogen in the ammonium ion is released back into the atmosphere (Berner, 1987). Nitrate that leaves the atmosphere can be converted back into elemental nitrogen, through the process called denitrification. This often takes place in the soil through the activity of bacteria that reduce the nitrate to $N_2$. After the conversion from elemental into nitrogenous ions in solution in rainwater, the nitrogen in these compounds can be transformed back to the atmosphere by the pathways previously described, thus completing the cycle.

Conventional biological nitrogen removal from wastewater based on these two natural process is carried out in two steps which involve well-known natural autotrophic nitrification with ammonium ($NH_4^+$) as the electron donor and oxygen as the electron acceptor followed by heterotrophic denitrification with organic matter or carbon source as the electron donor and nitrite ($NO_2^-$) or nitrate ($NO_3^-$)as the electron acceptor. (Than Khin et al, 2004; Pongsak et.al., 2009) The cost of this process resides mainly in aeration (bringing oxygen into the reactor) and the addition of an external carbon source (e.g. methanol) for the denitrification (Feng et al., 2007).

Complete nitrification implies a chemolithoautotrophic [Metabolism that uses chemicals as the energy source (chemo) (compared with phototrophic metabolism, which utilizes light as the energy source), inorganic compounds (litho) as electron donors, and carbon dioxide as a carbon source (auto)] oxidation of ammonium to nitrate under aerobic conditions. There is no bacterium which can directly oxidize ammonium into nitrate in one step. Thus this

process is conducted in two sequential oxidative stages: ammonia to nitrite by means of ammonia oxidizing bacteria (AOB) known as *Nitrosomonas* and then nitrite to nitrate by means of nitrite oxidizing bacteria (NOB) called *Nitrobacter*, in which ammonia and nitrite perform as an energy source and molecular oxygen performs as an electron acceptor, while carbon dioxide is used as a carbon source (Ahn, 2006). The relevant reactions are as follows:

$$NH_3 + 1.5\ O_2 + \text{Nitrosomonas} \rightarrow NO_2^- + H_2O + H^+ \qquad (2\text{-}1)$$

$$NO_2^- + 0.5\ O_2 + \text{Nitrobacter} \rightarrow NO_3^- \qquad (2\text{-}2)$$

The nitrification process produces acid. This acid formation lowers the pH in the aeration tank and can cause a reduction of the activity of nitrifying bacteria. The optimum pH for *Nitrosomonas* and *Nitrobacter* is between 7.5 and 8.5; most treatment plants are able to effectively nitrify with a pH of 6.5 to 7.0. Nitrification stops at a pH below 6.0. The nitrification reaction (that is, the conversion of ammonia to nitrate) consumes 7.1 $mgL^{-1}$ of alkalinity as $CaCO_3$ for each $mgL^{-1}$ of ammonia nitrogen oxidized. An alkalinity of no less than 50-100 $mgL^{-1}$ is required to insure adequate buffering (Nitrification & Denitrification).

Ammonia oxidizing bacteria form two monophyletic groups the β- and γ-proteobacteria (Purkhold et al., 2000). The most studied ammonia oxidizing bacteria belong to the *genera Nitrosomonas and Nitrosococcus.* The second step (oxidation of nitrite into nitrate) is mainly done by bacteria of the genus *Nitrobacter*. Both steps produce energy to be coupled to ATP synthesis. Nitrifying organisms are chemoautotrophs, and use carbon dioxide as their carbon source for growth.

The biological reduction of nitrate ($NO_3^-$) to nitrogen gas ($N_2$) by facultative heterotrophic bacteria is called Denitrification. “Heterotrophic” bacteria need organic carbon source as food to live. “Facultative” bacteria can get their oxygen by taking dissolved oxygen out of the water or by taking it off of nitrate molecules. Denitrification is carried out by a heterotrophic bioconversion process under oxygen-reduced or anoxic conditions. The oxidized nitrogen compounds like nitrite and nitrate are reduced to gaseous nitrogen by heterotrophic microbes that use nitrite or nitrate instead of oxygen as electron acceptors and organic matter as a carbon and energy source.

Denitrification is performed under anoxic conditions; that is, when the dissolved oxygen concentration is less than 0.5 $mgL^{-1}$, ideally less than 0.2 $mgL^{-1}$. When bacteria break apart

nitrate ($NO_3^-$) to gain the oxygen ($O_2$), the nitrate is reduced to nitrous oxide ($N_2O$), and, in turn, nitrogen gas ($N_2$). Since nitrogen gas has low water solubility, it escapes into the atmosphere as gas bubbles. Free nitrogen is the major component of air, thus its release does not cause any environmental concern (Nitrification & Denitrification) .

Denitrifying bacteria are generally found among the Gram–negative $\alpha$ and $\beta$ classes of the Proteobacteria, such as *Pseudomonas, Alcaligenes, Paracoccus,* and *Thiobacillus*. Some Gram-positive bacteria (such as *Bacillus*) and a few *halophilic Archaea* (such as *Halobacterium*) are capable of denitrification (Ahn, 2006). This process results in a reduction in effluent ammonia toxicity but releases higher concentrations of nitrate, a groundwater pollutant. The addition of an external organic carbon source is necessary when biodegradable organic matter is not present in the wastewater to be treated or when its concentration is not enough in order to complete denitrification. (Rodr ́guez, 2010) The organic carbon source is needed to act as a hydrogen donor and to supply carbon for biological synthesis. Some typical electron donors are small chain alcohols (methanol, ethanol), acetate and glucose. Usually, methanol is the cheapest available carbon source, thus it is the most used compound in industry around the world. The need of organic matter per unit of mass of nitrogen is about 3.7 g COD $(gN)^{-1}$ when methanol is employed. In addition its ease of application and not leaving a residual BOD in the process effluent make methanol the most popular external carbon source. In fact, the cost of methanol makes the widespread application of denitrification process unsatisfactory in wastewater treatment. Thus a lot of alternatives were developed. The anoxic denitrification involves the following reactions:

$$5CH_3OH+6NO_3^-\rightarrow 3N_2+5CO_2+7H_2O+6OH^- \qquad (2\text{-}3)$$

According to the stoichiometry it can be observed that denitrification produces alkalinity therefore it is able to compensate, to some extent, for the consumption of alkalinity caused by the nitrification.

Different reactor types can be used to carry out the conventional nitrification and denitrification such as SBR (Figure 2.2), CSTR, MBR.

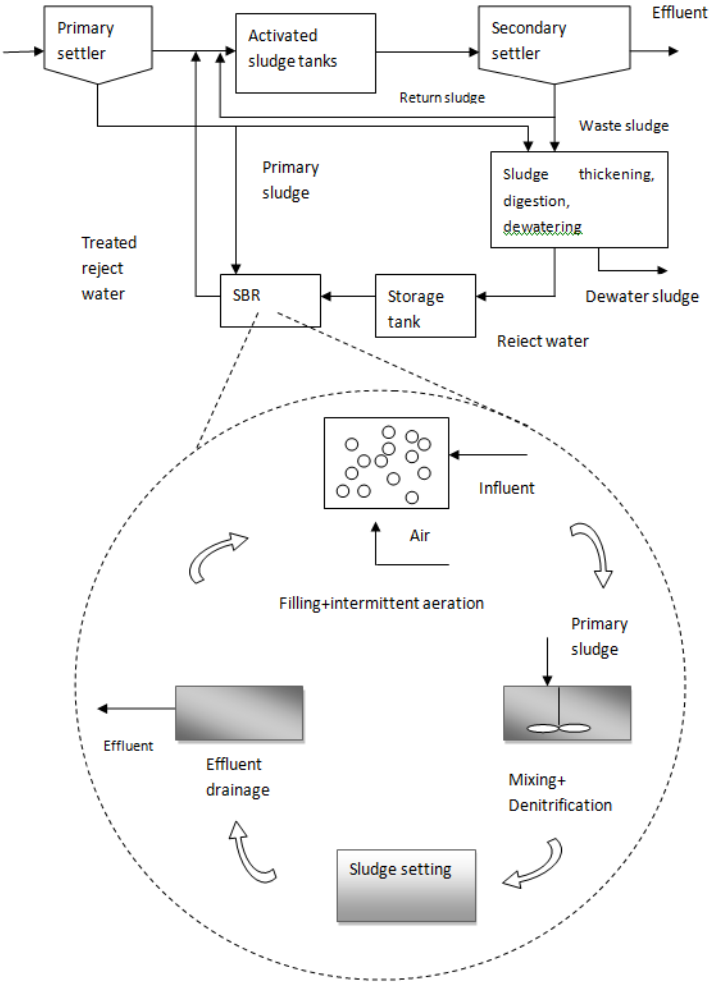


**Figure 2.2** An SBR process for Nitrification/Denitrification (Wett et al 1998)

Because the organic carbon presenting in the real wastewater is always quite insufficient for the denitrification process, complete nitrogen removal needs an external carbon source. All these external carbon sources are expensive and substantially increase the cost of operation (Noophan et al., 2009). Due to the requirement of a large amount of aeration and carbon source increasing the cost of operation for conventional biological nitrogen removal process, a novel process called Partial Nitrification and Anammox is becoming a focus of wastewater treatment, which is able to successfully eliminate nitrogen compounds accompanied by a saving of 62.5% oxygen consumption and 100% organic carbon.

## 2.3 Partial Nitrification Process

Recently, a new biological nitrogen removal process, partial nitrification and Anammox, has drawn increasing attention as an alternative to the conventional nitrification-

denitrification process. Nitrite is used as an intermediary compound between the partial nitrification and Anammox process units. The Anammox process converts $NH_4^+$ and $NO_2^-$ to $N_2$ gas with $NH_4^+$ as the electron donor and $NO_2^-$ as the electron acceptor under anaerobic conditions using autotrophic bacteria. For this reason, partial nitrification is required as a pretreatment for Anammox instead of complete nitrification (Fig 2.3).

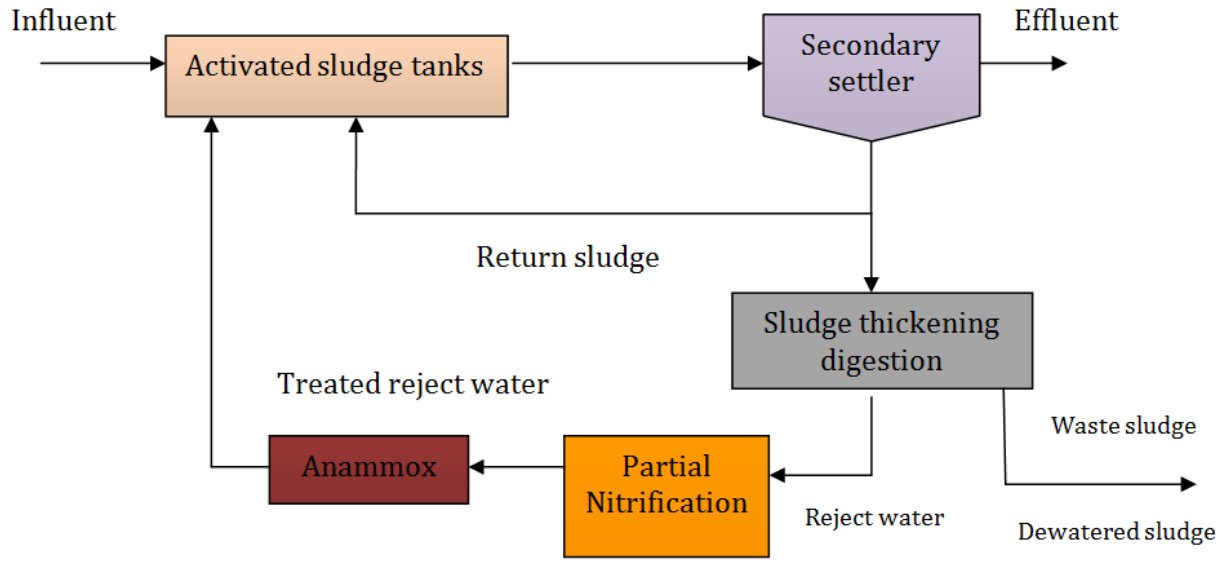


**Figure 2.3** SBR process for partial nitration coupled with an Anammox-reactor

### 2.3.1 Basic Principle of Partial Nitrification

The complete nitrification involves two steps which are oxidation of ammonia to nitrite and further oxidation to nitrate (as equation below). Partial nitrification implies nitrification is prevented at stage of nitrite (Eq 2-1), not to nitrate(Eq 2-2) so as to the partial nitrification can be used as a pretreatment of Anammox to provide the desired effluent to feed the Anammox process, which is characterized by ammonium to nitrite molar ratio of 1:1.32.

$$NH_4^+ + 1.5O_2 \rightarrow NO_2^- + H_2O + 2H^+ \text{ (nitrification, by AOB)} \quad (2\text{-}1)$$

$$NO_2^- + 0.5O_2 \rightarrow NO_3^- \text{ (nitrification, by NOB)} \quad (2\text{-}2)$$

*Nitrosomonas* bacteria are chemolithotrophic microorganism that obtains their energy for growth from aerobic or anaerobic ammonia oxidation, illustrated in Figure2.5. The first step in the metabolic path way is accomplished by the enzyme ammonia monooxygenase (AMO) followed by the second step which is accomplished by

hydroxyl-amine oxidoreductase (HAO). Both enzymes are co-dependent because they generate the substrate and electrons, respectively, for each other. AMO catalyzes the oxygenation of ammonia to hydroxylamine (Eq 2-4). Two electrons required in this biological process are derived from forming the oxidation of hydroxylamine to nitrite by HAO (Eq2-5). One of the oxygen atoms in nitrite derives from oxygen, the other coming from water. Two of the four electrons generated by HAO are transferred via the tetra-heme cytochrome c554 either to AMO or diverted into an electron transport chain, where many of the carriers involved and the intermediates have not been completely characterized. The overall reaction converts ADP to ATP an energy rich compound, see Figure 2.4.

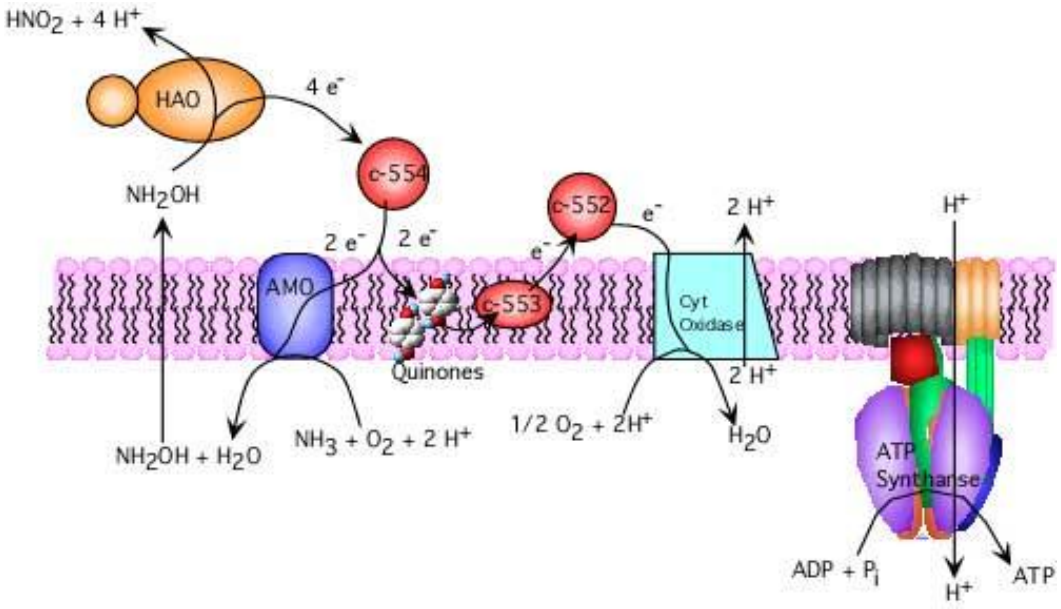


**Figure 2.4** Outline of Metabolic Pathways of *Nitrosomonas* (Timothy, 2000)

$$NH_3 + O_2 + 2H^+ + \text{-}2e^- \rightarrow NH_2OH + H_2O \qquad (2\text{-}4)$$

$$NH_3 + N_2O_4 + 2H^+ + 2e^- \rightarrow NH_2OH + 2NO + H_2O \qquad (2\text{-}5)$$

The hydroxylamine resulting from ammonia oxidation is further oxidized to nitrite (Eq2-6) by hydroxylamine oxidoreductase (HAO) (Hooper et al.,1993; Schmidt 2001).

$$NH_2OH + H_2O \rightarrow HNO_2 + 4H^+ + 4e^- \quad (2\text{-}6)$$

### 2.3.2 The Feature of Enrichment Cultures of Partial Nitrification

In terms of morphology, partial nitrification sludge is similar to the conventional activated sludge of which the color is yellowish-brown or reddish. The sludge by appearance is classified into floccus sludge, membranous sludge and granular sludge, which have different physiological characteristics. For this research floc sludge was cultivated. Floc sludge has a larger surface area which is capable of enhancing the contact area between the sludge and substrate, however settling performance of the floc sludge is relatively poor; the SVI is usually greater than 80ml·g-1. Generally cumulative concentration of sludge in the bioreactor would not exceed 5gVSS ·$L^{-1}$.

In the partial nitrification, ammonia is not only involved in the energy-generating reaction as an energy source, but is also involved in cell synthesis reactions as a nitrogen source. If the empirical formula of AOB was $C_5H_7NO_2$ the total AOB metabolic reaction is obtained by coupling the energy-generating reactions and biosynthesis of the cell. The stoichiometric coefficients of reaction can reflect the cell yield, oxygen consumption, pH changes during the biological process.

Catabolism of ammonium oxidation can be described by Equation 2-7:

$$NH_4^+ + 1.5\,O_2 + 2\,HCO_3^- \rightarrow NO_2^- + 3\,H_2O + 2\,CO_2 \qquad (2\text{-}7)$$

If the cellular growth is taken into account, the stoichiometry would be:

$$NH_4^+ + 1.382\,O_2 + 1.982\,HCO_3^- \rightarrow 0.018\,C_5H_7O_2N + 0.982\,NO_2^- + 2.927\,H_2O + 1.891\,CO_2 \qquad (2\text{-}8)$$

And for the oxidation of nitrite:

$$NO_2^- + 0.5\,O_2 \rightarrow NO_3^- \qquad (2\text{-}2)$$

If bacterial growth is included in Equation2-9:

$$NO_2^- + 0.003\,NH_4^+ + 0.488\,O_2 + 0.010\,H_2CO_3 + 0.003\,HCO_3^- \rightarrow 0.003\,C_5H_7O_2N + NO_3^- + 0.008\,H_2O \qquad (2\text{-}9)$$

$$NH_4^+ + 1.5O_2 \rightarrow NO_2^- + H_2O + 2H^+ \qquad (2\text{-}10)$$

$$NH_4^+ + 1.5CO_2 \rightarrow 10NO_2^- + 3C_5H_7NO_2 + 4H_2O + 23H^+ \qquad (2\text{-}11)$$

Yields for the most common AOB and NOB, Nitrosomonas and Nitrobacter, are 0.12 mg Cells (mg $NH_4^+$-N)$^{-1}$ and 0.02 mg cells(mg $NO_2^-$-N)$^{-1}$,respectively. (Rodr ́guez, 2010)

According to the above equation, the partial nitrification is a high oxygen-consumption reaction, where the oxygen consumption is 3.43g$O_2$ $g^{-1}NH_4^+$-N. At 30 ℃, saturated concentration of DO in the water is 7.56$O_2$g $L^{-1}$. Continuous oxygen supply leads to low mass transfer efficiency. Therefore DO is very crucial parameter to realize successful partial nitrification.

On the basis of Eq 2-18, the yield rate of AOB is 0.29gVSS $g^{-1}NH_4^+$-N, lower than the actual bacterial production rate; only 10% of the heterotrophic bacteria productivity. The reasons are: ① Less substrate for cell growth: Only 14% of the released electrons in the general ammonia oxidation process are used for cell growth, much lower than the 60-70% of the heterotrophic bacteria (Ritmmann and McCarty, 2001). ② High energy consumption for synthesis: Assimilation of $CO_2$ by AOB to cytoplasm needs to consume massive reducing power and ATP (Gallert and Winter, 2005). In addition, both reactions produce the $H^+$ leading to rapid decline in pH. Partial nitrification stops when the pH drops below 6.3.

The different environmental preferences of AOB and NOB bacteria strains can be exploited to maximize production of the nitrite intermediate. The discovery of the Anammox process provides the feasibility for nitrite as the electron acceptor to be reduced to gaseous nitrogen under anaerobic conditions with ammonia as the electron donor. Thus $NH_4^+ \rightarrow NO_2^- \rightarrow NO_3^- \rightarrow N_2$ nitrification-denitrification could be achieved by bypassing the nitrate stage. Nitrite accumulation is a prerequisite for the stable new nitrogen removal process from wastewater, referring to the requirement for a product of ratio of $NO_2^-/(NO_3^- + NO_2^-)$ value greater than 0.5.

The accumulation of Ammonia Oxidizing Bacteria (AOB) and the limitation-inhibition-washout of NOB is the critical point for partial nitrification (Hellinga et al., 1998, Guo et al, 2009, Yuan et al., 2007). NOB can be washed out selectively by controlling the appropriate operating variable, including dissolved oxygen (DO) concentration, temperature, sludge retention time (SRT), substrate concentration, aeration pattern, and inhibitors (Zhu, 2008). Because AOB have higher affinity for oxygen than NOB (Shahabadi *et al*.,2009; Anceno et al.,2009 ), the activity of NOB can be inhibited by controlling DO at low concentrations (commonly lower than 1 $mgL^{-1}$) (Chung et al.2005, Aslan and Dahab.2008). On the contrary, low DO concentrations may lead to a low nitrification rate, sludge bulking (In treatment of sewage one process used the activated sludge process in which air is passed through a mixture of sewage and old

sludge to allow the micro-organisms to break down the organic components of the sewage. Sludge is continually drawn off as new sewage enters the tank and this sludge must then be settled so that the supernatant can be separated to pass on to further stages of treatment. Sludge bulking occurs when the sludge fails to separate out in the sedimentation tanks) or increasing nitrite production (Guo et al., 2009). Elimination of NOB from the system can also be achieved at high temperatures (Bougard et al., 2006; Kim et al., 2008), high free ammonia (FA) concentrations (Vadivelu et al.,2007, Anthonisen et al.,1976, Aslan and Dahab, 2008), high free nitrous acid (FNA) concentrations (Vadivelu et al., 2007; Park and Bae, 2009; Kim and Seo, 2006) and high pH (Villaverde et al., 1997). However, most research indicated the partial nitrification and denitrification via nitrite is suitable for treating the wastewater with high ammonia concentration and high temperature, such as anaerobic sludge digestion liquor and landfill leachate (Gali and Dosta, 2007; Ganigue′ et al., 2007; Yang et al., 2007). However, the stable partial nitrification is difficult to achieve when treating wastewater with low nitrogen concentration. So far, there are a few reports concerning partial nitrification to nitrite obtained to treat municipal or domestic wastewater by using aerobic duration control (Yang et al., 2007; Blackburne et al., 2008).

Generally it is not common to find effluents with the required composition ($NH_4^+$ :$NO_2^-$ ≈1:1.3) to feed the Anammox process. To reach this objective, half of the ammonium fed has to be converted into nitrite by AOB and therefore, the further oxidation of nitrite to nitrate carried out by NOB has to be avoided. Several alternatives have been tested to obtain an influent with these features successfully. Both SBR and Chemostat could be effectively used to produce a 50%/50% ammonium-nitrite effluent suitable for a subsequent Anammox process. Kinetic and stoichiometric parameters of the partial nitrification process are similar for both reactors. Biomass retention in the SBR will result in a smaller reactor volume for the given influent ammonium concentrations to be converted. The SHARON process showed, however, a better stability. (Galı and Dosta, 2007)

Apart from Anammox, the partial nitrification can be also combined with conventional denitrification. The benefit for this combined process is less consumption of COD, as only nitrite not nitrate has to be reduced to gaseous nitrogen.

### 2.3.3Partial Nitrification Operational Parameters

In order to obtain the stable and cost-effective partial nitrification processes, nitrite oxidation must be restrained so as to accumulate ammonium oxidizing bacteria and washout nitrite-oxidizing bacteria or surpress the activity of NOB. To date, various factors such as pH, temperature, dissolved oxygen (DO), free ammonia, free nitrous acid, etc. have been investigated as operational parameters to achieve successful partial nitrification (Cho et al., 2011*).*Among these factors, the dissolved oxygen is the key factor and the most difficult to control. The operational costs of the biological nitrogen removal process are to a great extent related to the oxygen.

#### 2.3.1.1 Free Ammonia Concentration (FA) & Free Nitrous Acid (FNA)

Several studies have shown that non-ionized forms of ammonium and nitrite, free ammonia (FA) and free nitrous acid (FNA) can inhibit activities of ammonium oxidizing bacteria (AOB) and nitrite oxidizing bacteria (NOB). However, NOB organisms are more sensitive than AOB organisms to elevate concentrations of these compounds and reactors operating at high ammonium concentrations may lead to an inhibition of NOB activity. According to the research by Anthonisen et al.(1976), a free ammonia concentration in the range 0.1-1.0mg$L^{-1}$ will restrain the activity of nitrite oxidizing bacteria. When the free ammonia concentration rises up to 0～150mg$L^{-1}$, the activity of AOB is inhibited. If the concentration level of the FA is higher than the inhibition concentration threshold of NOB and lower than the inhibition threshold of AOB, then accumulation of nitrite would take place. However, researchers have presented different opinions on the inhibition level of free nitrious acid (Anthonisen et al., 1976; Vadivelu et al. 2006, 2007). The anabolism of AOB and NOB were inhibited completely at 1.3 mg $L^{-1}$ and 0.1 mg $L^{-1}$of FNA concentrations respectively compared with 0.2 mg $L^{-1}$of FNA concentration inhibiting both AOB and NOB by Anthonisen et al.,(1976). Optimum FNA concentration can be concluded as 0.1-0.2 mg$L^{-1}$. The strategy, using inhibition by FA and FNA on NOB activity to prevent nitrate production, was successfully applied by Lai et al., (2004) in a batch reactor. Yamamoto et al. (2008) also relied on FA and FNA inhibition to out-compete NOB from an attached biomass reactor treating swine wastewater digested liquor.

### 2.3.1.2 pH Value

The partial nitrification process is sensitive to the value of pH. At pH value below 6.8 the reaction rate significantly declines. The optimum pH values for the growth of AOB and NOB are 7.0-8.5 and 6.0-7.5 respectively. The relationship between pH value and the growth of nitrite oxidizing bacteria as well as the growth of ammonium oxidizing bacteria were studied indicating that higher AOB growth rate will be achieved at a relatively high pH level, which can promote the accumulation of the nitrite. The author holds the view in terms of previous experiments that keeping the pH value in the range of 7.5-8.5 is favorable for nitrite accumulation.

### 2.3.1.3 Dissolved Oxygen

Nitrobacteria are aerobic autotrophic bacteria, so the availability of dissolved oxygen (DO) in the medium is essential for the growth of AOB and NOB. Physiological differences between ammonia oxidizing bacteria (AOB) and nitrite oxidizing bacteria (NOB) lead to different affinities of these two bacterial groups to DO. In general AOB microorganisms have a higher affinity for oxygen than NOB, therefore, nitrite accumulation will occur under low dissolved oxygen (DO) conditions (Garrido et al., 1997; Ruiz et al., 2003). The research indicates that the saturation constant of NOB to oxygen is 1.2-1.5 $mgL^{-1}$, while the saturation constant of AOB to oxygen is 0.2-0.4 $mgL^{-1}$. These ranges suggest that the DO should be kept low enough to be below the saturation value for NOB but high enough to be above the saturation of AOB. According to Ruiz's research, when DO concentration level is in the range of 0.7-1.4 $mgL^{-1}$, there is significant accumulation of nitrite as ammonia is oxidized but no accumulation of nitrate in the second step as required.

### 2.3.1.4 Temperature

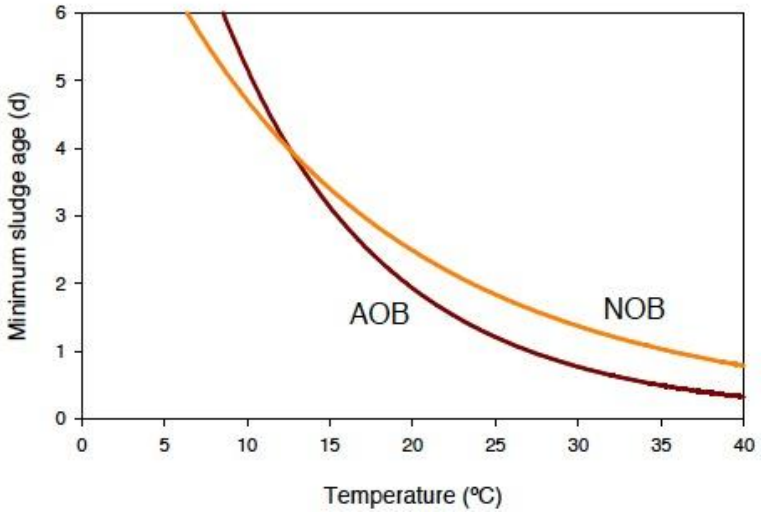


**Figure 2.5** Minimum residence time for AOB and NOB as a function of temperature (Hellinga et al., 1998)

Temperature has different effects on AOB and NOB activity. The optimum temperature ranges for the growth of AOB and NOB are 28℃-38℃ and 20℃-30℃ respectively (J. Dosta et al., 2008). Within the temperature range generally found in WWTP (10℃-20℃), NOB grow faster than AOB, in addition under such conditions ammonium tends to be completely oxidized to nitrate (Ganigue et al., 2008). However at temperature above 20℃ the situation is the opposite: ammonium oxidizers grow faster than nitrite oxidizers which means nitrite is accumulated (Yamamoto et al, 2008). To illustrate this issue, Fig2.5 shows the minimum sludge retention time needed for the development of both communities, as a function of temperature. At higher temperatures the growth of the NOB becomes slower than that of the AOB, but if the temperature is increased above around 40℃ the reaction rate will decline.

Temperature also governs the solubility of oxygen in water. A temperature increase leads to a reduction in the solubility of gases, which in turn may increase aeration costs. (Yamamoto et al., 2008)

### 2.3.1.5 Sludge Age

The differences between the growth rates of the two types of bacteria can also be exploited by manipulation of the sludge age. The sludge age (or SRT - sludge retention time) is the average residence time of the sludge (i.e. the microbial cells) in the reactor.

In general this is greater than the HRT (hydraulic retention time) since partial nitrification is an autotrophic biological process in which the growth rate of autotrophic bacteria is lower than that of heterotrophic bacteria. Taking advantage of higher growth rate of AOB microorganisms at specific conditions (by controlling DO, pH, temperature, FA and FNA) mentioned above the SRT can be optimized to eliminate ('wash-out') the NOB from the system in order to successfully achieve partial nitrification.

#### 2.3.1.6 Toxics

Nitrification can also be affected by inorganic toxins such as heavy metals (Dahl et al., 1997). For instance Skinner and Walker (1961) reported complete inhibition of ammonia oxidation at 0.25 $mgL^{-1}$ of nickel, 0.25 $mgL^{-1}$ of copper. In addition, organic compounds might also inhibit nitrifying activity (Blum and Speece, 1991; Ganigue et al., 2009).

### 2.3.4 Physiology of Microorganisms Involved in Partial Nitrification

In order to design and operate a wastewater treatment system (activated sludge system) efficiently, it is necessary to understand the biochemistry of the microorganisms involved and basic research is the keystone to optimize established processes and to invent new and innovative systems. (Schmidt et al., 2003)

**Table 2.2**. Differentiation of the genera of the ammonia-oxidizing bacteria (Koops et al., 2005)

| Characteristic | ***Nitrosomonas*** | ***Nitrosospira*** | ***Nitrosovibrio*** | ***Nitrosolobus*** | ***Nitrosococcus*** |
|---|---|---|---|---|---|
| Cell shape | Spherical to ro d shaped | Tightly coiled spirals | Slender, curved rods | Lobular | Spherical to ellipsoidal |
| Intracytoplasmic Membranes | Peripherally located flattened vesicles | Occasional tubular invaginations | Occasional tubular invaginations | Cell compartmental ized by cytoplasmic membranes | Centrally located stack of membranes |
| Flagella | Polar flagella | Pertirichous | Polar to subpolar flagella | Peritrichous flagella | Tuft of flagella |

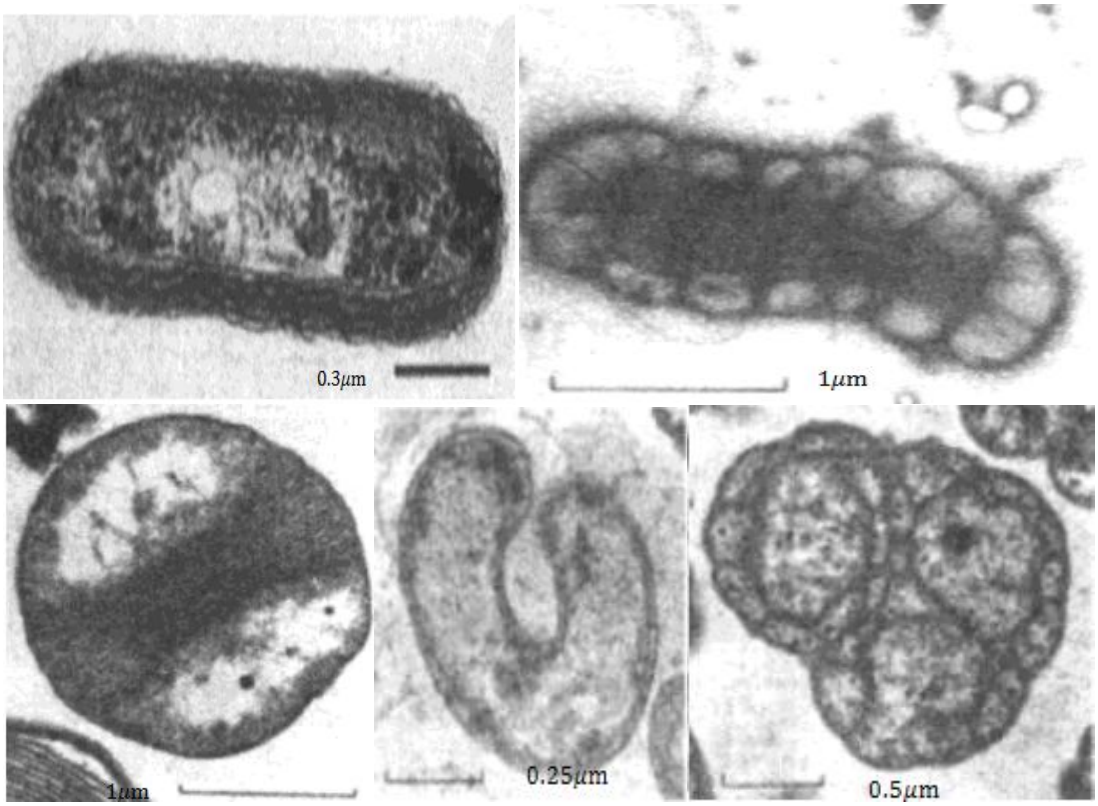


**Figure 2.6** *Nitrosomonas, Nitrosospira, Nitrosococcus, Nitrosovibrio& Nitrosolobus*(TEM)

Nitrifying organisms are primarily chemoautotrophs, and use carbon dioxide as their carbon source for growth, although recently organic compounds have been described that can provide them with carbon and energy sources (Schmidt et al., 2003). Many species of nitrifying bacteria have complex internal membrane systems that are the location for key enzymes in nitrification: ammonia monooxygenase which oxidizes ammonia to hydroxylamine, and nitrite oxidoreductase, which oxidizes nitrite to nitrate. As mentioned above, nitrification is a two-step process. In the first step $NH_4^+$ is oxidized to $NO_2^-$ by ammonia oxidizing bacteria. The second stage of the nitrification reaction is the oxidation of $NO_2^-$ to $NO_3^-$ by nitrite oxidizing bacteria. (Rittmann and Perry 2001). Due to the identical basic metabolism in all representatives of the AOB group, only morphological characteristics (shape and ultrastructure of the cells) can be used as discriminating properties which had led to the definition of five distinct genera, namely *Nitrosomonas, Nitrosococcus, Nitrosospira, Nitrosovibrio and Nitrosolobus*. Ammonia oxidizing bacteria can be found among the *β*- and γ-*proteobacteria* (Purkhold et al., 2000). The *β*-ammonia oxidizers comprise the well-known genera *Nitrosolobus,*

*Nitrosomonas and Nitrosospira*, *Nitrosococcus* belongs to the γ-proteobacterial genus. However, it should be noted that other members of this group – notably *Nitrospira* (Helical to vibroid-shaped cells; nonmotile; no internal membranes), *Nitrospina* (Long, slender rods, nonmotile, no obvious membrane system), *Nitrococcus* (Large Cocci, motile [one or two subterminal flagellum] membrane system randomly arranged in tubes), and *Nitrobacter (*Short rods, reproduce by budding, occasionally motile (single subterminal flagella) or non-motile, membrane system arranged as a polar cap) are known to sustain themselves from the second-stage nitrite oxidation reaction. *Nitrobacter* is the most well-known genus of the nitrite oxidizers. Both steps – ammonia oxidation and nitrite oxidation produce energy to be coupled to ATP synthesis.

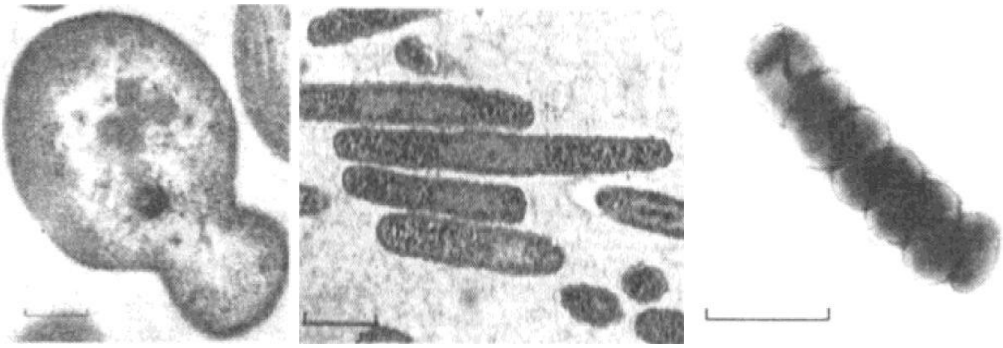

**Figure 2.7** *Nitrobacter, Nitrospina, Nitrospira* by TEM

In most environments both mircoorganisms (AOB and NOB) are found together, yielding nitrate as the final product. It is possible however to design systems in which nitrite are selectively formed. This is known as the Sharon Process (Hellinga et al., 1998). Together with ammonification, nitrification forms a mineralization process which involves the complete decomposition of organic material, with the release of the available nitrogen compounds. This replenishes the nitrogen cycle.

Nitrifying bacteria are widespread in soil and water, and are found in the highest numbers where considerable amounts of ammonia are present (areas with extensive protein decomposition and sewage treatment plants) (Purkhold et al., 2000). Nitrifying bacteria thrive in lakes and streams with high inputs of sewage and wastewater because of the high ammonia content.

## 2.4 Anammox

### 2.4.1 History of Anammox

Until the end of the 20th century the general consensus was that ammonium is an inert molecule under anoxic conditions: activation by oxygen was assumed to be required for its metabolism as known for nitrifying bacteria (Jetten et al., 2009). However more and more research has reported high nitrogen losses that are unaccounted for. Under anoxic conditions, a considerable part of the nitrogen load was eliminated from wastewater at the leachate treatment plant of the landfill in Mechernich (Hippen et al., 1997; Fux et al., 2002). Massive nitrogen loss, up to 70%, was also detected in a nitrifying rotating biological contactor in Koelliken treating ammonium-rich leachate from a hazardous waste landfill (Siegrist et al., 1998). Heterotrophic denitrification was excluded due to COD removal in previous processes (Fux et al., 2002).

The Austrian theoretical chemist Engelbert Broda, from the point of view of chemical reaction mechanisms and their thermodynamic calculations, was the first to predict the existence of microorganisms capable of oxidating ammonium with nitrite or nitrate as the electron acceptor in 1977 (Brochier and Philippe , 2002). Equation:

$$NH_4^+ + NO_2^- \rightarrow N_2 + 2H_2O \qquad (2\text{-}14)$$

$$-\Delta G^0 = 335kJ/(molNH_4^+)$$

Ten years later, Mulder discovered anaerobic ammonium oxidation in biological denitrification fluidized bed reactor (Mulder et al., 1995) which initiated an active search for the microorganisms involved. Afterwards van de Graaf proved that the anaerobic ammonium oxidation is a biological reaction by a variety of methods (van de Graaf et al., 1995). After long-term efforts Strous successfully separate anaerobic ammonium oxidizing bacteria by means of density gradient centrifugation technology (Strous et al., 1999).

### 2.4.2 Anammox Reaction Mechanism

#### 2.4.2.1Chemical Reaction Model

The Anammox process is also chemolithotrophic, which generally implies microorganisms characterized by low growth rates (0.069 $day^{-1}$, Van de Graaf et al.,

1996) and yields due to the low Gibbs free energy involved in the reaction. In this case, the Gibbs free energy and the activation energy calculated by Strous (2000) are 357 KJ (mol $NH_4^+$)$^{-1}$ and 70 kJ (mol $NH_4^+$)$^{-1}$, respectively. Carbon dioxide is the main carbon source for the growth of ANAMMOX bacteria (van de Graaf et al., 1996). The Anammox process (an abbreviation for anaerobic ammonium oxidation) is a stage in the nitrogen cycle. (Rodriguez, 2010)

Van de Graaf et al. (1997) conducted researches to study the reaction mechanisms of the Anammox organisms. These researchers employed different combinations of nitrogen compounds to test the formation and consumption of possible intermediate products. They discovered that the intermediates for Anammox were hydrazine and hydroxylamine (Rodr ́gue., 2010). Schalket et al. (1998) confirmed that hydrazine was an intermediate of the Anammox process. They hypothesized the metabolic pathway for anaerobic ammonium oxidation which is shown in Figure 2.8. Ammonium is oxidized by $NH_2OH$ (hydroxylamine) to produce $N_2H_4$ (hydrazine) (step 1). The hydrazine could be converted to dinitrogen gas and generate four reducing equivalents (4 electrons) ($\Delta G0'$ = -271 kJ mol-l) which then are transferred to the nitrite reducing system to form hydroxylamine (steps 2, 3 and 4) (Khin et al., 2004; van de Graaf et al., 1997). The oxidation of nitrite into nitrate generates reducing equivalents needed for the $CO_2$ fixation (the reduction of inorganic carbon (carbon dioxide) to organic compounds ), in other words for biomass growth (step 5).

Schalk et al. (1998) found that when excess hydrazine was added to an Anammox culture, the final products were ammonium and $N_2$ in a ratio of 4:1, while with the addition of hydrazine and nitrite as an electron acceptor the ultimate product was $N_2$. These authors also found that hydrazine was toxic in long-term periods and that it was not possible to grow Anammox bacteria directly from hydrazine and nitrite.

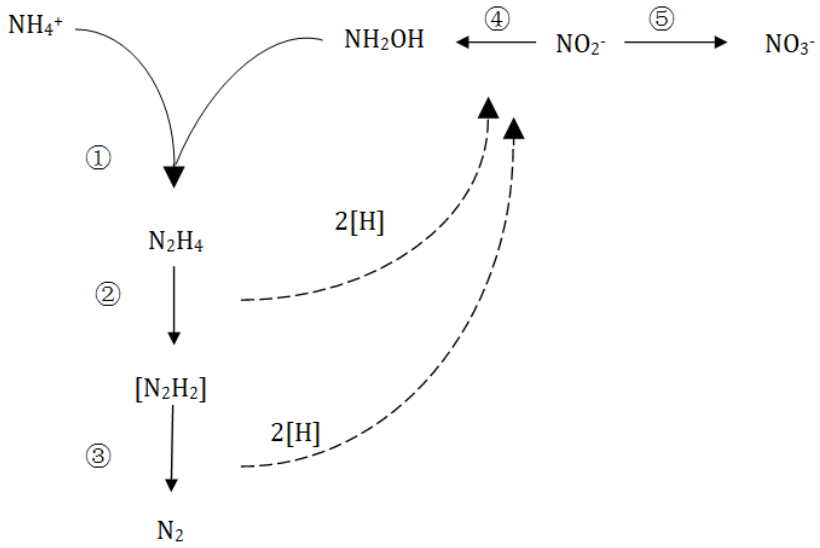


**Figure 2.8** Possible metabolic pathways for anaerobic ammonium oxidation, consumption and production of $H_2O$ and $H^+$ are not showed (van de Graaf et al., 1997)

*Chemical Reactions involved in the ANAMMOX

$$NH_2OH + NH_3 \rightarrow N_2H_4 + H_2O \quad (2\text{-}12)$$

$$N_2H_4 \rightarrow N_2 + 4[H]$$

$$HNO_2 + 4[H] \rightarrow NH_2OH + H_2O \quad (2\text{-}13)$$

$$NH_3 + HNO_2 \rightarrow N_2 + H_2O$$

$$HNO_2 + H_2O + NAD^+ \rightarrow HNO_3 + NADH_2 \quad (2\text{-}14)$$

### 2.4.1.2 Cells Reaction Model of Anammox

The Anammox bacteria form a separate and distinct group in the microbial world shown in Fig2.9. Their catabolic reactions take place on a cell internal membrane, whereas for all other acteria such an internal energy generating membrane is absent. Normally the energy is generated on the outer membrane. Anammox microbes have a unique intermediate in their catabolism, hydrazine. Whereas normal denitrifying bacteria have $N_2O$ as intermediate, this compound is absent in the Anammox physiology. This means that this strong greenhouse gas will not be produced by Anammox bacteria. The Anammox growth yield is similar to that of nitrifying bacteria. In Anammox process nitrate is produced. This is due to oxidation of nitrite to nitrate, which compensates the reduction of $CO_2$ to cellular organic matter. Therefore, in a fully autotrophic process

this anoxic nitrate generation is a measure for the biomass growth of Anammox and a very good indication of Anammox of activity (Henze et al., 2008).

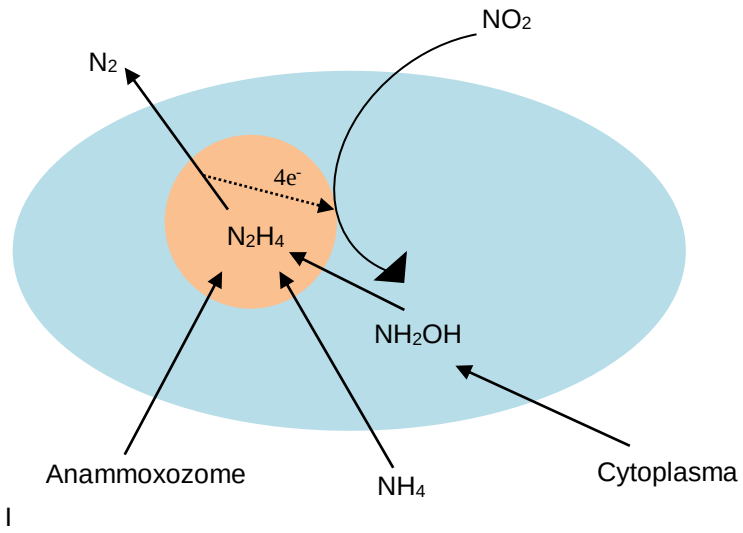


**Figure 2.9** Mechanisms of anaerobic ammonium oxidation in *Candidatus Brocadia anammoxidans*

### 2.4.1.3 Biochemical Reaction Model of Anammox

Jetten et al. (2001) postulated a biochemical reaction model (Fig2.10) in accordance with the Anammox chemical reaction model (Fig 2.8) and catalytic properties of HAO. According to this model Nitrite-reducing Enzyme (NR) located on the cytoplasmic side of the cell membrane catalyzed nitrite reduction to hydroxylamine ($NH_2OH$). Transmembrane hydrazine hydrolase (HH) which is the assumed product catalyzed hydroxylamine and ammonia to generate hydrazine via a condensation reaction; hydrazine-oxidising enzyme( HZO) located on the anammoxosome side of the cell membrane, catalyzes hydrazine into $N_2$ and in addition releases electrons which are delivered to nitrite reductase through electron transport chain.

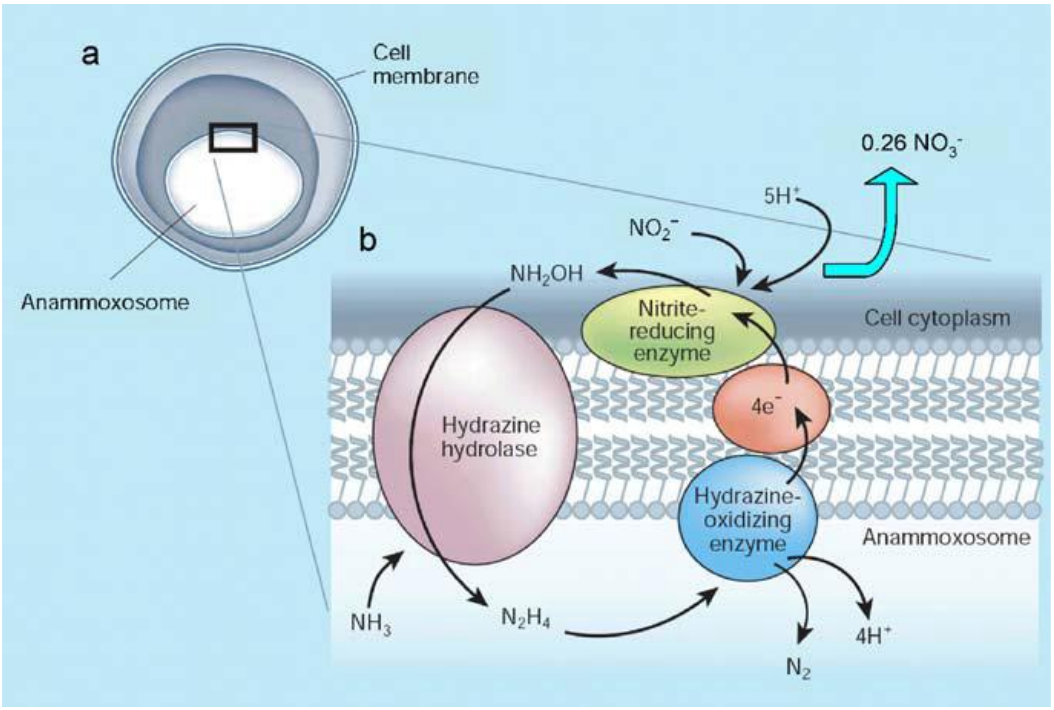


**Figure 2.10** Biochemical pathway of Anammox reaction (Ahn, 2006)

'a' simply depicts the Anammox microbe, anammoxosome. 'b' describes the anammoxosome membrane, which consists of the ladderane lipid bilayer identified by Sinninghe Damste et al.,(2002) and the Anammox reaction pathway. Intermediate in the cycle are hydrazine ($N_2H_4$) and hydroxylamine ($NH_2OH$), which are highly toxic. The dense, impermeable membrane may serve to contain them (Ahn, 2006)

### 2.4.3 Anammox Process Principle

In this biological process, nitrite and ammonium are converted directly to dinitrogen gas making use of autotrophic Anammox bacteria under strictly anaerobic conditions, but about 10% of the Nitrogen feed (nitrite and ammonium) was converted to $NO_3^-$. This process contributes up to 50% of the dinitrogen gas produced in the oceans. From several basic studies, the stoichiometry of the Anammox reaction based on mass balance over Anammox enrichment cultures was represented by Eq. 2-15. Anammox bacteria derive their energy for growth from the 1:.32 chemolithotrophic conversion of ammonium and nitrite into $N_2$. Bicarbonate serves as the sole carbon source for the synthesis of cell biomass ($CH_2O_{0.5}N_{0.15}$), making the organisms autotrophs. Cell carbon fixation involves the acetyl-CoA pathway (Strous et al., 2006). Based on the formation of biomass and nitrate and on stoichiometric calculations it was hypnotized that the

reducing equivalents for the reduction of $CO_2$ are derived from the oxidation of nitrite to nitrate (Strous et al., 1998).

The overall nitrogen balance gave a ratio of ammonium to nitrite conversion of 1:1.31 ±0.06 and 1:0.22 ±0.02 for the ratio of nitrite conversion to nitrate production (Van de Graaf et al., 1996). However, the $NO_2$-N/$NH_4$-N removal in the various Anammox reactors is in the range of 0.5–4 depending on substrate, operating conditions and reactor configuration (Ahn, 2006)

$$NH_4^+ + 1.32NO_2^- + 0.066HCO_3^- + 0.13H^+ \rightarrow 1.02N_2 + 0.26NO_3 + 0.066CH_2O_{0.5}N_{0.15} + 2.03H_2O \quad (2\text{-}15)$$

According to the reaction above, Anammox is equivalent to the classical denitrification which converts ammonia into $N_2$ but utilizes ammonium as electron donor instead of using organic compounds such as methanol. The nitrite form is the oxidised compound that should be available for the process in an ammonium/nitrite ratio of 50% since nitrate cannot be used as an electron acceptor (Galı´, 2007). Hydrazine and hydroxylamine are intermediate products in the process (Shivaraman, 2003). The Anammox process is suited to wastewater with low C:N ratios. At C:N ratios above 1, the Anammox bacteria are no longer capable of outcompeting the heterotrophic denitrifying bacteria (Güven et al., 2005, Molinuevo et al., 2009).

To obtain a stable process for Anammox, an appropriate influent ratio of $NH_4^+$-N and $NO_2^-$-N at 50% is indispensable. It is important to transform high concentration ammonia streams into the correct Anammox influent flow, which means having $NH_4^+$-N, $NO_2^-$-N and avoiding $NO_3^-$-N formation. (Galı, 2006). The partial nitrification process discussed above presents a possible path to achieve the required Anammox influent in which half ammonium is oxidized to nitrite and prevented from further oxidation to nitrate by working at temperatures over 20 ℃ with a biomass retention time (SRT) below 2 days (Hellinga et al., 1999; Van Dongen et al., 2001), controlling the pH around 7~ 8 or working with high ammonium concentrations.

The key to obtain the appropriate influent ratio of $NH_4^+$-N and $NO_2^-$-N is the bicarbonate/ammonium ratio. From equation 2-1 the molar stoichiometric relationship for complete ammonium oxidation to nitrite must be 2 mol $HCO_3^-$/mol $NH_4^+$. Thus, to achieve a 50% ammonium oxidation, ammonium and bicarbonate should be present in a molar ratio of 1:1. If the waste stream for the partial nitrification process is not able to

provide this relationship, the pH would have to be controlled in the process. (Galı´ 2006).

In 2002 the combined system of partial nitrification and Anammox was put into operation in Dokhaven Wastewater Treatment Plant (WWTP) in the Netherlands. Fundamental information, e.g. how constrained the stoichiometry is and the duration of the startup period for these processes are required for the implementation at larger scales. (Noophan et al., 2009). Implications of Anammox for large scale municipal and industrial wastewater treatment plants are summarized in Table 2.3 (Mogens *et al*., 2008)

Compared with the traditional nitrification/denitrification process, the partial nitrification and Anammox process has the following advantages.

(1) Less demand for oxygen up to 62.5% (Feng et al., 2007) and potentially high energy savings up to 60-90%

(2) No extra carbon source is needed. Since the Anammox bacteria are autotrophic, the carbon source necessary for the heterotrophic bacteria in the traditional denitrification process is no longer needed.

(3) Less sludge production.

(4) After a suitable startup period, the system is not expensive to maintain and is simple to operate (Noophan et al., 2009). On the other hand, due to slow growth rates of Anammox bacteria (the doubling time was reported to be approximately 11 days), long start-up times for Anammox is a primary limitation (Jin and Zheng, 2009). Moreover, the Anammox reactor must be efficient in biomass retention.

(5) Reduction of $CO_2$ emission (up to 90%) because during the process bicarbonate is consumed instead of carbon dioxide formed (as in conventional denitrification). Thus this process has much lower contribution to greenhouse effect.

(6) Strong greenhouse gas $N_2O$ is not an intermediate in the Anammox reaction

The conventional denitrification process and some of the Anammox process will be compared in terms of Energy production ($CH_4$), $CO_2$ emission, power consumption and sludge production. The reduced need for energy and an electron donor means that use of an Anammox process strongly contributes to increasing the sustainability of wastewater treatment operation. Implication of Anammox for large scale municipal Abd

Ubdystruak wastewater treatment plants are summarized in table below (Mogens *et al*., 2008).

**Table.2.3** Implication of Anammox: comparison of nitrogen removal in municipal wastewater treatment plants with conventional denitrification and Anammox process in the Netherlands (Mogens *et al*., 2008)

| Item | Unit | Conventional | Pre-treatment, Anaerobic treatment Anammox | Difference |
|---|---|---|---|---|
| Energy production ($CH_4$) | MW | 0 | 40 | 40 |
| CO2 emission | kton/year | 400 | 6 | 394 |
| Power consumption | MW | 80 | 41 | 39 |
| Sludge production | ktonVSS/year | 370 | 270 | 100 |

**Table.2.4** Implication of Anammox: comparison of nitrogen removal in industry wastewater treatment plants with conventional denitrification and Anammox process in the Netherlands (Mogens et al., 2008)

| Item | Unit | Conventional | Pre-treatment, Anaerobic treatment Anammox | Difference |
|---|---|---|---|---|
| Energy production | MW | 0 | 2 | 2 |
| ($CH_4$) | kton/year | 30 | 6 | 24 |
| CO2 emission | MW | 2.3 | 0.3 | 2 |
| Power consumption | ktonVSS/year | 30 | 4 | 26 |

### 2.4.4 Key Operational Parameters in Anammox Process

#### 2.4.4.1 Effect of Temperature

The influence of temperature on the rate of the Anammox process was studied earlier by several authors and its increase up to the levels of 40 led to increase of Anammox rate in most studies (Malovanyy et al., 2009). The further increase of temperature up to 45 ℃ had a negative effect on process activity (Dosta et al., 2008). In addition, a temperature of 45 ◦C was found to cause an irreversible decrease of the Anammox activity due to biomass lysis (Dosta et al., 2008). The maximum activity of non-adapted Anammox biomass was observed between 30 and 40 ℃. However, Dalsgaard and

Thamdrup (2002) and Rysgaard et al. (2004) who worked on establishing temperature dependence for Anammox bacteria in marine sediments, reported the highest activity at the temperature of 35 ℃ and loss of activity at the temperatures higher than 40 ℃.

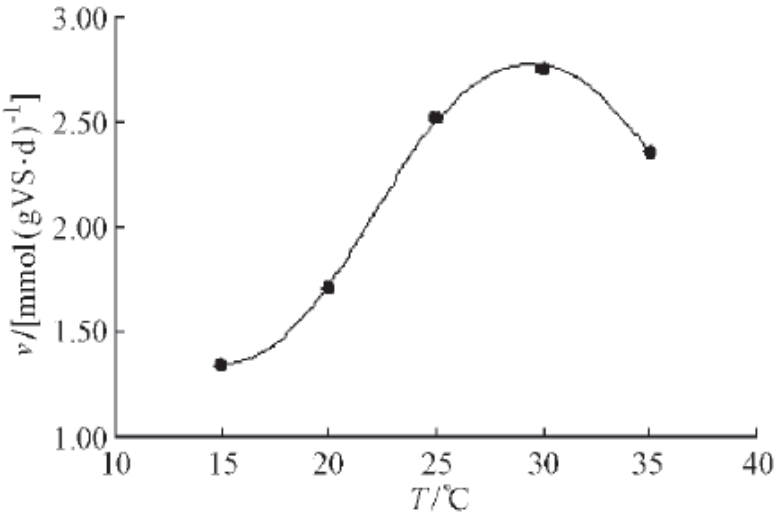


**Figure 2.11** Effect of temperature on Anammox activity (Zheng, 2001)

### 2.4.4.2 Effect of pH

In the Anammox process, pH is a very important environmental condition. The values of pH affect the Anammox activity by their impact on the Anammox bacteria and the substrate forms.

Strous (2000) studied the relationship between Anammox activity and pH, finding a physiological interval of pH of 6.7-8.3. The optimum pH value for operation was around 8 reported by Strous 1997. Nevertheless Egli et al. (2001) observed Anammox activity even at a pH range of 8.5-9.0.

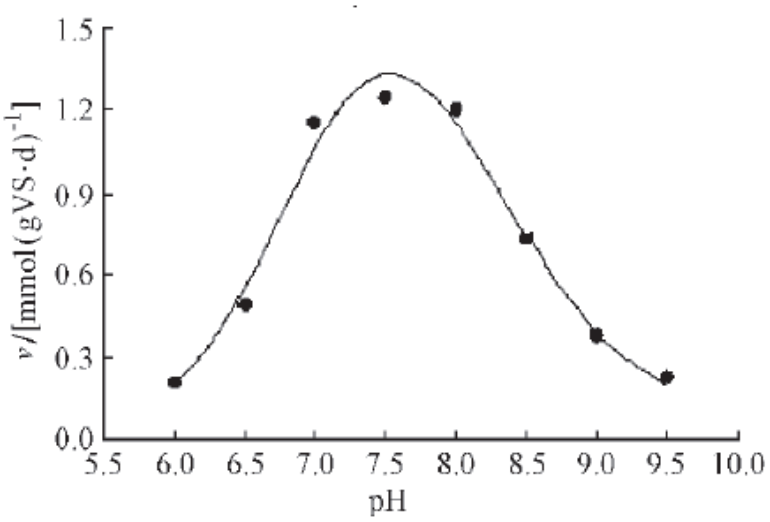


**Figure 2.12** Effect of pH on Anammox activity (Zheng, 2001)

Ammonia and nitrite are the substrate of Anammox bacteria, however, the active ingredient is $NH_3$ and $HNO_2$.The value of pH has tremendous impact on the percentage distribution of $NH_3$ and $HNO_2$ in the liquid phase.

Effect of pH on $NH_3$

Ionic equilibrium of $NH^+_4$ and $NH_3$ in liquid phase

$$NH_4^+ \leftrightarrows NH_3 + H^+ \quad (2\text{-}16)$$

Reaction equilibrium

$$K_a = \frac{[NH_3][H^+]}{[NH_4^+]} \qquad (2\text{-}17)$$

$$\text{or} \qquad \frac{K_a}{[H^+]} = \frac{[NH_3]}{[NH_4^+]} \qquad (2\text{-}18)$$

Where $K_a$ is ionization constant; $[NH_4^+]$ is concentration of $NH_4^+$; $[H^+]$ is concentration of $H^+$

According to Mass balance the percentage of $NH_3$ is

$$NH_3\,\% = \frac{[NH_3]}{[NH_4^+]+[NH_3]}100\% \qquad \text{III}(2\text{-}19)$$

Or

$$\frac{NH_3}{\%} = \frac{100}{1+[NH_4^+]/[NH_3]} \qquad (2\text{-}20)$$

Put Eq 2-18 into Eq 2-20 get

$$\frac{NH_3}{\%} = \frac{100}{1+\frac{K_a}{[H^+]}} \qquad (2\text{-}21)$$

Or

$$\frac{NH_3}{\%} = \frac{100}{1+\frac{10^{-pH}}{K_a}} \qquad (2\text{-}22)$$

At 25 ℃ $K_a$ *is* $5.6\times10^{-10}$ When pH are 7.0, 8.0, 9.0, respectively, the percentage of $NH_3$ are 0.56%, 5.3% and 35.9%.

Effect of pH on $HNO_2$

Ionic equilibrium of $HNO_2$ and $NO_2$ in liquid phase

$$HNO_2 \leftrightarrows NO_2^- + H^+ \qquad (2\text{-}23)$$

Reaction equilibrium

$$K_a = \frac{[NO_2^-][H^+]}{[HNO_2]} \qquad (2\text{-}24)$$

Or

$$\frac{K_a}{[H^+]} = \frac{[NO_2^-]}{[HNO_2]} \qquad (2\text{-}25)$$

Where $K_a$ is the ionization constant; $[NO_2^-]$ is concentration of $NO_2^-$

According to Mass balance the percentage of $HNO_2$is

$$\frac{HNO_2}{\%} = \frac{[HNO_2]}{[HNO_2]+[NO_2^-]}\times100 \qquad (2\text{-}26)$$

Or

$$\frac{HNO_2}{\%} = \frac{100}{1+\frac{[NO_2^-]}{[HNO_2]}}\times100 \qquad (2\text{-}27)$$

Put Eq 2-25 into Eq2-27 get

$$\frac{HNO_2}{\%} = \frac{100}{1+\frac{K_a}{[H^+]}} \qquad (2\text{-}28)$$

or

$$\frac{HNO_2}{\%} = \frac{100}{1+\frac{K_a}{10^{-pH}}} \qquad (2\text{-}29)$$

At 12.5℃ $K_a$ *is* $4.6\times10^{-4}$ When pH are 6.0, 7.0 and 8.0 respectively, the percentage of $HNO_2$ are 0.217%, 0.022% and 0.002%.

### 2.4.4.3 Effect of Dissolved oxygen (DO)

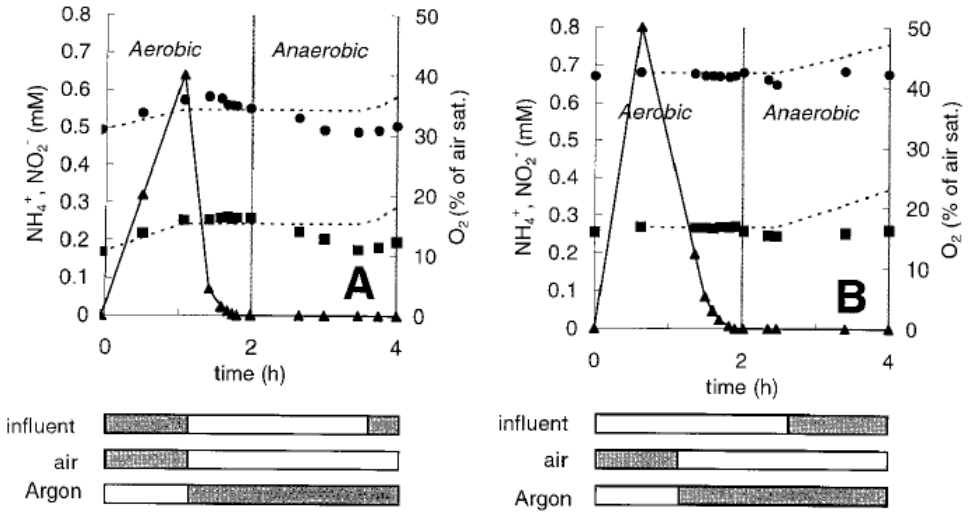


**Figure2.13** Anammox process under alternating aerobic and anaerobic conditions. (Strous et al., 1997)

Strous (1998) used the sequencing batch reactor (SBR) to test the effect of dissolved oxygen on anaerobic ammonium oxidation. Under alternating aerobic and anaerobic conditions no ammonium was oxidized during the aerobic periods; the Anammox activity in the anaerobic periods remained constant throughout the experiments, indicating that the oxygen inhibition was reversible (Fig 2.13). During 20 days, no aerobic ammonium oxidation was observed (Strous et al., 1997).

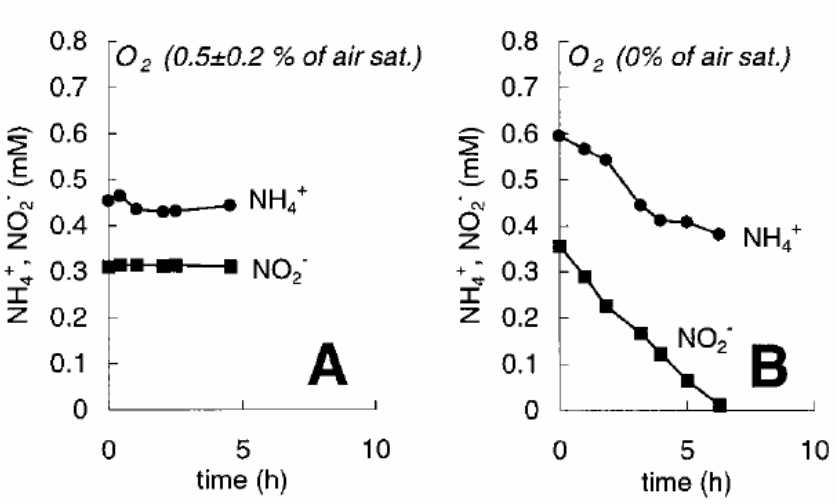

**Figure. 2.14** Anammox activity at air saturations (sat.) of 0.5% ± 0.2% (A) and0% (B). Only when no oxygen was present (B) was Anammox activity observed (Strous et al., 1997).

Strous et al. further investigated the sensitivity of Anammox organisms to concentration of oxygen under microaerobic conditions. They found that no Anammox activity was detected in the presence of 2, 1, and 0.5% of air saturations. Ammonium and nitrite were consumed again after reactor was flushed with argon until it was completely anaerobic (0% $O_2$). Nevertheless, Sliekers et al. (2002 and 2003) operated Anammox in SBR and a gas-lift reactor under oxygen-limited conditions and interestingly they found the maximum Anammox activity declined. However, a stable coexistence of Anammox and aerobic ammonium oxidizers permitted a completely autotrophic removal of nitrogen from both systems. These studies indicated that the existence of Anammox in the presence of oxygen is possible because it is consumed by the nitrifying organisms and organic matter.

### 2.4.4.4 Effect of Substrate and Product Concentrations

Strous (2000) exposed Anammox biomass to high ammonium and nitrate concentrations (up to 1 $gNL^{-1}$) in a SBR for one week and did not observe negative effects on the activity. Ammonia and the product of nitrate have little effect on the anammox bacteria. Anammox activity would not be inhibited as long as the concentrations of ammonia and nitrate are lower than $1000mgL^{-1}$. Nevertheless, the inhibition of the substrate of nitrite on the Anammox activity was significant. Strous et al. (1999) found that nitrite concentrations in the range of 0 ~ $750mgL^{-1}$ activity of anammox biomass decreased with increasing nitrite concentration. Rodr ́guez (2010) found that the biomass (Candidatus Brocadia anammoxidans) completely lost its activity at concentrations of nitrite of 98 mg $NO_2$-$NL^{-1}$. Furthermore, if the biomass was subjected to nitrite concentrations higher than 5 mM (70 mg $NO_2^-$-$NL^{-1}$) for a period of 12 h, the process was totally inhibited.

Egli et al. (2001) showed that Candidatus Kuenenia Stuttgartiensis has a relatively important tolerance to nitrite concentrations up to 180 mg $NO_2^-$-$NL^{-1}$. On the contrary, Fux et al. (2002) reported an inhibition of the Anammox process in a pilot plant fed with the effluent of a Sharon reactor that treated a sludge digester effluent. In this case,

the organisms (Candidatus Kuenenia Stuttgartiensis) were strongly inhibited by a nitrite concentration of 60 mg $NO_2^-$-$NL^{-1}$ (Rodr ́guez, 2010).

### 2.4.4.5 Effect of Organic Matter

The presence of organic matter (OM) is considered to affect anammox process adversely, (van de Graaf et al., 1996), while practically wastewaters containing ammonia are not free from OM. The effects of organic matter on anammox bacteria have been investigated in previous studies. Güven et al. (2005) found that alcohols inhibited anammox bacteria, while organic acids stimulated the anammox process. They also revealed that even 0.5mM of methanol leading to the complete and irreversible inactivation of anammox activity; however glucose had almost no effect on the anammox process, in addition propionate promoted the reaction. Zheng et al. (2006) reported that the effect of organic materials on anammox performance is related to the type and concentration of organic compounds and the state of existence of the anammox bacteria. In their experiment, yeast extract was added to the reactor and its inhibitory effects on performance were reported. Chamchoiet (2008) and Molinuevo (2009) reported both COD concentrations and COD to N ratios affect the performance of anammox bacteria. At COD to N ratio of 0.5, COD inhibitory organic load threshold concentration (defined when ammonia removal dropped to 80%) could be 142 and 242 $mgL^{-1}$, depending on pre-anammox process, partial nitrification (Molinuevo et al., 2009). Some researchers found heterotrophic denitrifiers will exist in presence of organic materials in anammox process. Since anammox bacteria are anaerobic autotrophs and grow at a slower rate than heterotrophic denitrifiers when organic matter coexists with ammonium and nitrite, they cannot compete with heterotrophic denitrifiers for space in the anammox reactor. Thus the anammox bacteria would be eliminated and the anammox performance would be suppressed (van de Graff et al., 1995; Tang et al., 2010; Li et al., 2011).

Surprisingly, Sabumon (2007) found that in the presence of OM, ammonia was oxidized anoxically to nitrate by an unknown mechanism unlike anammox process (Sabumon, 2007). This study also proved anoxic ammonia removal was feasible in the presence of OM and nitrite was the most effective inorganic electron acceptor. This indicated that

anammox might still play a role in anoxic ammonia removal in existence of OM (Ni et al., 2012).

#### 2.4.4.6 Effect of sludge retention time (SRT)

The application of the Anammox process is limited by its long start-up periods due to very low growth rates and biomass yields of the involved biomass (Jetten et al., 1997). Minimizing the washout of biomass in the effluent by improving its retention becomes critical when biomass with such a long duplication time (0.003 $h^{-1}$, Strous et al., 1998) is used. Systems where the improvement of biomass retention is achieved reduce the duration of the start-up period and provide better conditions to implant the Anammox process at an industrial scale (Fernández, 2010). Thus the SRT for anammox process is applied for as long as possible.

### 2.4.5 Physiology of Anammox Bacteria

The anammox bacteria are classified to the bacterial *phylum Planctomycetes*, of which *Planctomyces* and *Pirellula* are the best known genera. The diversity and activity of anammox bacteria has been studied in various environments, yet knowledge about their abundance and population dynamics is rare. The first anammox bacterium was named "*Brocadia anammoxidans*". Strous et al. (1999) successfully physically purified Anammox cells from a laboratory enrichment culture at where he first describe the Anammox bacteria "*Brocadia anammoxidans*". To date five anammox genera have been described, with 16S rRNA gene sequence identities (Jetten et al., 2009). They are "*Candidatus Kuenenia", "Candidatus Brocadia", "Candidatus Anammoxoglobus"* and *"Candidatus Jettenia" (all fresh water species ) and "Candidatus Scalindua"* ( marine species) (Quan et al., 2008; Schmid et al., 2000; Strous et al., 2006; Strous et al., 1999; Kuenen and Jetten, 2001; Kartal et al., 2008; Kartal et al., 2007;Kuypers et al., 2003; Schmid et al., 2003; van de Vossenberg et al., 2008). All fresh water anammox genera have been enriched from activated sludge whereas marine species have often been found in natural habitats, particularly in marine sediments and oxygen minimum zones (OMZ) (Dalsgaard et al., 2005; Penton et al., 2006; Schmid et al., 2007; Woebken et al., 2008; Jetten et al.,2009).

**Table 2.5** ANAMMOX bacteria discovered up-to-date

| Genus | Species | Source |
|---|---|---|
| *Brocadia* | *Candidatus Brocadia anammoxidans* (Strous et al., 1999a) | Wastewater |
| | *Candidatus Brocadia fulgida* (Kartal et al., 2004) | Wastewater |
| | *Candidatus Brocadia brasiliensis* (Araujo et al. 2011) | Wastewater |
| | *Candidatus Brocadia caroliniensis'* (Vanotti et al. 2011) | Wastewater |
| | *Candidatus Brocadia sinica* ( Hu et al. 2010) | Wastewater |
| *Kuenenia* | *Candidatus Kuenenia stuttgartiensis* (Schmid et al. 2000) | Wastewater |
| *Scalindua* | *Candidatus Scalindua brodae* (Schmid et al., 2003) | Wastewater |
| | *Candidatus Scalindua wagneri* (Schmid et al., 2003) | Wastewater |
| | *Candidatus Scalindua sorokinii* (Schmid et al., 2003) | Seawater |
| *Jettenia* | *Candidatus Jettenia asiatica* (Quan et al., 2008) | Not reported |
| *Anammoxoglobus* | *Candidatus Anammoxoglobus propionicus* (Kartal et al., 2007) | Synthetic water |

Despite the fact that there is a relatively large phylogenetic distance between those anammox genera, all anammox organisms belong to the same monophyletic cluster (order) named the Brocadiales which is deeply inside the phylum Planctomycetes (Strous *et al.*, 1999). The monophyletic branch consists of five distinct genera with about 10% sequence divergence to each other. The sequence divergence of the Planctomycetes from other Bacteria (indicated as outgroup) is high. The Fig 2.15illustrates the relationships of the different families of anaerobic ammonium oxidation (anammox) bacteria among the Planctomycetes (Kuenen, 2008).

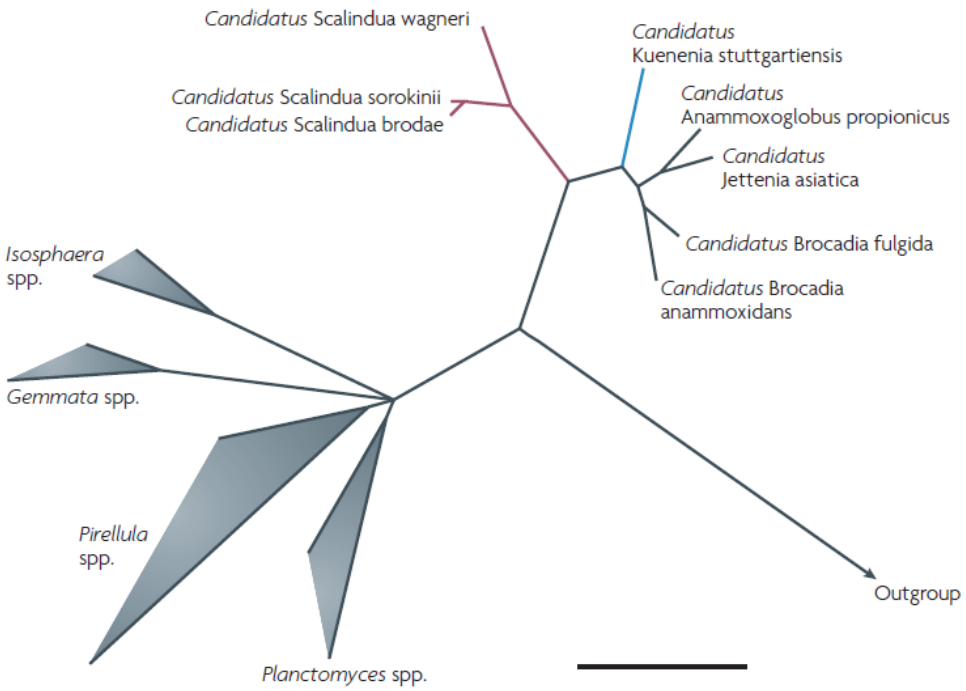


**Figure 2.15** 16s ribosomal RNA-gene-based phylogenetic tree of Anammox bacteria

Anammox cells display complex cell architecture (Fig 2.16) with a central compartment, reminiscent to that of other members of the Planctomycetes, to which anammox bacteria are phylogenetically related (Jetten et al., 2009). The anammox bacteria are characterized by several striking properties: they all possess one anammoxosome, one of the cellular compartments, which comprises 30-60% of the cell volume and where energy conservation takes place, a membrane bound compartment inside the cytoplasm which is the locus of anammox catabolism. Furthermore, the membranes of these bacteria mainly consist of ladderane lipids so far unique in bacteria (Damste et al., 2002; van Niftrik et al., 2004).

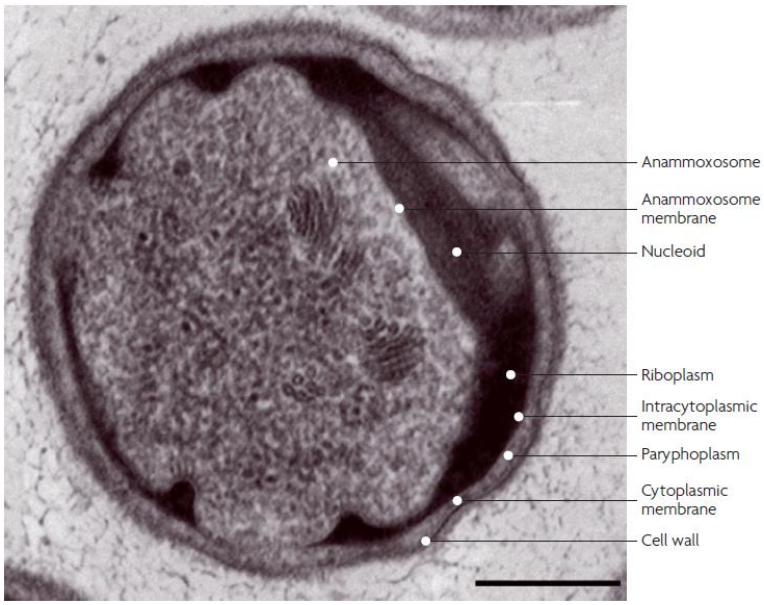


**Figure 2.16** Microstructure of Candidatus Kuenenia stuttgartiensis with subcellular compartments including the anammoxosome. The sample was high pressure frozen, freeze substituted and Epon embedded. The riboplasm is the equivalent of the ribosome-containing cytoplasm in most other bacteria. The scale bar represents 200 nm. (Kuenen, 2008)

Anammox granular sludge has a characteristic reddish color (Fig 2.17) and impressive sedimentation performance. The yield and specific growth rate reported for Anammox are low. The bacterium has a doubling time of around 11 days and the biomass yield is 0.13g dry weight ($gd^{-1}$ $NH_3$-N) (Strous, M.,1998). It has a higher affinity for the substrates ammonia and nitrite than either nitrifying bacteria or denitrifying bacteria under appropriate conditions (Strous, M.,1999). It can be reversibly inhibited by oxygen and irreversibly by nitrite (at concentrations in excess of 70 mg $N1^{-1}$for several days) and phosphate (>60 mg P $L^{-1}$ for several days) (Strous et al., 1997; Van de Graaf, 1996; Strous et al., 1999; Kuenen, 1997).

The cell is autotrophic, and the reduction of inorganic carbon to the oxidation state of cellular carbon is via the oxidation of nitrite to nitrate. Nitrite is also the nitrogen source:

$$5CO_2+14NO_2^-+H_2O+H^+\rightarrow C_5H_7O_2N+13NO_3^- \quad (2\text{-}15)$$

**Figure 2.17** Granular biomass from a One-Step-Anammox reactor Courtesy of Paques & Typical Anammox sludge granule (Mogens et al., 2008)

### 2.4.6 Status of Application of Anammox

**Figure 2.18** Full scale Anammox reactor at Dokhaven STP, The Netherlands Courtesy by Paques

The world's first Anammox demonstration plant with a volume of $80m^3$ was built in Rotterdam, The Netherlands, in 2002 to treat high-ammonium sludge water from Dokhaven-Sluisjesdijk wastewater treatment plant (Fig 2.18). This reactor was scaled-up directly from laboratory scale to full-scale without building a pilot plant. By third quarter 2006, this reactor was in full operation and was converting 8-10kg of nitrogen per $m^3$every day, twice its design capacity.

The first industrial anammox reactor took very a long time to startup, which was more than three years; henceforth the time to start the new reactors was dramatically reduced. Although this significant improvement has several different reasons the most important was the fact that unlike in the case of the first reactors which were inoculated with the biomass containing no Anammox bacteria, enriched Anammox biomass was available to inoculate new plants as seed sludge. As a result of the seed of anammox biomass, the most recent Anammox systems were started up in few months

The discovery of the Anammox process opens up a new era to treat effluents characterized by low C/N ratio and high ammonia concentrations. In the early days the

main two areas of application of Anammox process are treatment of anaerobic digestion liquors (including dewatering liquors from sewage sludge digestion, dewatering liquors from (Thermal) Hydrolysis Plants, organic waste digestate liquors, anaerobic effluents from industry) and treatment of landfill leachate. However most of the existing full scale plants (Table 2.6) were built to treat rejected water from anaerobic digestion in municipal wastewater treatment plants. The advantage of this effluent is its high temperature, which allows operation of the Anammox reactor at good rates: no need for extra energy to meet the temperature demand.

As more increasingly in-depth studies are conducted on anammox, the application of anammox is spreading to the broader wastewater treatment field. Some of them have realized the full-scale however some are still limited to the laboratory study:

1. Organic solid waste treatment (landfills, composting, digestion)
2. Food industry (Abeling and Seyfried, 1992)
3. Manure processing industry ( Hwang et al., 2006)
4. Fertilizer industry
5. (Petro) Chemical industry
6. Metal and Mining industry
7. Fish canning industry (Dapena-Mora et al, 2006)
8. Chemical industries
9. Power plants
10. Tannery wastewaters (Paques, 2007).
11. Slaughterhouse wastewaters (Siegrist et al, 2006)

Effluent of sludge digesters or fertilisers industry containing concentrations of ammonia nitrogen ($NH_4^+$-N) of 1.0 $gL^{-1}$ (Mahne et al., 1996), manure treatment of 2.3 $gL^{-1}$ (Wiesmann, 1994) and fish canning industry of 0.9 $gL^{-1}$ (Soto et al., 1991), are some examples of waste streams with high nitrogen concentration. This shared characteristic makes Anammox a possible process of treatment for such wastewaters. (Dapena-Mora, 2004)

The Anammox process was initially implemented only in wastewater treatment plants in the Netherlands, but has quickly been adopted globally, as it can be applied to any stream with high concentrations of ammonia or organic nitrogen. Up to now more than 30 full-scale variant plants are in operation in the Netherlands, Austria, China, Japan and USA etc.

In UK, wastewater and sewage travels into a drain, then into a sewer pipe that joins others in the sewer network. Eventually it reaches wastewater treatment plants (WWTP) works across the region. Most WWTPs in UK, such as those operated by Yorkshire Water and Severn Trent Limited treat the wastewater and sewage with activated sludge namely conventional complete nitrification and denitrification. Currently there is no Anammox plant in UK, however when installed Anammox® at Minworth will be the first UK installation and the largest sludge liquor application in the world. The process has a low whole life cost (WLC) when compared to alternative deammonification processes, as it has a smaller footprint and uses less air and chemicals. (Shorrock et al., 2012)

**Table 2.6** Full scale Anammox plants around the world (Abma et al., 2007; Wett, 2007; Joss et al., 2009; SYVAB, 2009; Gut, 2005)

| **Company** | **Country** | **Wastewater from:** | **ANAMMOX reactor vol** | **Ammonia load kg/day** | **Year** |
|---|---|---|---|---|---|
| Kuaijishan Shaoxing Winery | China | Distillery | 560 | 900 | 2011 |
| Waterboard Hollandse Delta, | The Netherlands | Municipal (reject water) | 72 | 750 | 2002 |
| Strass | Austria | reject water) | 500 | 350 | 2004 |
| Himmerfjarden WWTP | Sweden | reject water) | 700 | 240 | 2005 |
| Glanerland | Switzerland | Reject water | 400 | 250 | 2007 |
| Zurich | Switzerland | Reject water | 14000 | 625 | |
| Jiangsu Hangguang Bio-engineering | China | Sweetener | 1600 | 2180 | 2011 |
| St. Gallen | Switzerland | Reject water | 300 | 108 | 2009 |
| Waterschap Groot | The Netherlands | Reject water | 425 | 600 | 2010 |

| | | | | | |
|---|---|---|---|---|---|
| Salland* | | sludge treatment | | | |
| Meihua II | China | Monosodium glutamate | 4100 | 9000 | 2010 |
| Meihua I | China | Monosodium glutamate | 6600 | 11000 | 2009 |
| Angel Yeast | China | Yeast | 500 | 1000 | 2009 |
| ARA Niederglatt | Switzerland | Reject water sludge treatment | 180 | 60 | 2008 |
| Semiconductor plant Mie prefecture | Japan | Semiconductor | 50 | 220 | 2006 |
| Waterstromen Steenderen | The Netherlands | Potato | 600 | 1200 | 2006 |
| Industry Water Lichtenvoorde | The Netherlands | Tannery | 100 | 325 | 2004 |
| Xinjiang Meihua Amino Acid | China | Monosodium glutamate | 5400 | 10710 | 2011 |
| Confidential client | Poland | Distillery (Wheat stillage) | 900 | 1460 | 2011 |
| Shandong Xiangrui | China | Corn starch and MSG | 4300 | 6090 | 2011 |

### 2.4.7 Restrictions of Anammox Process

Compared with conventional biological nitrogen removal processes, Anammox as a biological wastewater treatment technology possess is lower running costs, higher efficiency, lower sludge production etc. and is especially suitable for wastewater with low ratio of C/N . From the moment of discovery of Anammox it was realized that the Anammox process had great promising perspectives. In fact, as it was discussed along the previous section, more and more full-size plants have been or are being built around the world (Table 2.6). However there are still some important drawbacks which limit the full scale application of the Anammox process at full-scale. To solve these problems, scholars have put forward a variety of potential solutions.

**A. High biomass retention**

Two of the biggest problems for the industrial implementation of the Anammox process are its low duplication time (11days) and its low cell yield of biomass leading to a very long start up time period. Furthermore, big amounts of inoculum are not always easily available. Therefore, it is indispensable to improve the retention of biomass as much as possible and minimize its wash out. To achieve this, various efforts have been tried such as option appropriate inoculation, the use of SBR reactors or the use of membranes.

The biomass retention ability of reactor will directly affect the nitrogen loading rate and the activity of Anammox process. Generally, these features of the reactor are in proportion to the biomass retention. In addition, the performance of the Anammox process to adapt to the environmental changes such as substrate concentration are, to a certain extent, influenced by the morphological characteristics of the biomass (biofilms, granular sludge, the general floc body).

The bacteria are the source of the function of a bioreactor. As the Anammox bacteria are such slow growing species, the choice of inoculation sludge is particularly important. Much different conventional sludge (Denitrifying sludge, nitrifying activated sludge, anaerobic granular sludge, rivers, lakes and marine Sediments, etc.) can be inoculated to successfully start up the anammox process. Tsushima et al. (2007) selected denitrifying sludge as seed sludge to start-up the anammox process and obtained a higher nitrogen removal efficiency.

Improving reactor configuration and operation was adopted to enhance sludge retention capacity. In 1998, Strous et al. noted that the sequencing batch reactor was a good alternative for the enrichment of Anammox biomass, reducing the sludge wash-out. Other benefits observed in this system were: the stability of the treatment, since a good distribution of substrates in the reaction mass is achieved, and the easiness of reactor operation. Strous et al. (1998) managed to treat a NLR about 1 g N $(L\ d)^{-1}$. Several authors (Van Dongen et al., 2001; Fux et al., 2002; Third et al., 2005) subsequently chose to use SBR reactors to enrich Anammox biomass with good results. Recently a biofilm reactor has increasingly been applied to the anammox process. Tsushima et a1. (2007) used non-woven biofilm reactor, with excellent inoculated sludge, effectively suspended the microorganisms within the system and achieved the total nitrogen removal rate up to 26 kg $\cdot m^{-3} \cdot d^{-1}$.

Vazquez-Padin (2009) aggregated biomass by means of increasing of ionic strength of the medium (i.e. higher saline concentration) to reduce biomass wash out. This strategy minimizes the electrostatic repulsion between cells and allows stronger interactions.

**B. Potential inhibition factors**

To achieve the successful implementation of the Anammox process, the possible inhibition and its extent in relation with the concentration of the substance must be considered. The presence of any of these inhibitors could compromise the stability of the Anammox reactor. If this destabilization causes the irreversible loss of activity of the biomass or any biomass wash-out, a new inoculation and start-up will be necessary followed by loss of time and money associated.

As it was mentioned before, Anammox activity is seriously affected by the organic matter in wastewater. When treating waste water with high organic matter（OM） content (COD: 600～25700mg$L^{-1}$) denitrification reaction is higher than the anammox reaction, moreover the anammox bacteria is very hard to adapt to the organic wastewater containing toxicity substances for instance phenol, cyanide and thiocyanate (Toh, et al., 2002; Toh and Ashbolt, 2002).

Beyond that, as noted above, Anammox suffers inhibition by substrate (nitrite and ammonium). Therefore, substrate ratios far from the stoichiometry (1~1.3) can result in the loss of the activity. This fact will be more likely to take place during the start-up of the partial nitrification stage when ammonium to nitrite ratio is still not very well controlled. When the combination of partial nitrification and Anammox is implemented as a one stage process, the problem can also occur during its start up. Taking into account the difficulties for the start-up of Anammox reactors and the chance of needing a very long time to achieve the design NLR removal, episodes of inhibition by substrates are strongly undesirable. Therefore, it would be very interesting to have the inhibitory effects and the concentration thresholds for each of the substrates well established.

To solve these problems, apart from the avoidance of these inhibitors, we also can take advantage of the physiological characteristics of the anammox bacteria, to the greatest extent possible to meet its requirements on environmental and nutrient conditions. The strain improvement and bacteria amplification is an important task for the biological

waste treatment. Compared with the modern biotechnologies of mutagenesis, fine Cell fusion and DNA restructuring etc. which directionally change bacterial metabolic pathways and obtain more efficient genetically engineered bacteria, optimizing environmental and nutritional conditions for growth of functional bacteria and metabolism in terms of their physiological requirements is more simple.

## 2.5 Novel biological Nitrogen removal

Conventional wastewater treatment for nitrogen removal requires a lot of energy to maintain aerobic conditions for nitrification to take place. Fifty percent of the energy that is currently consumed in wastewater treatment is used for aerobic processes, followed by sludge treatment and the use of pumps which consume 30% and 15% respectively. With such high energy requirement, there is a pressing need to look into alternative technologies to reduce energy consumption.

As the advantages of partial nitrification and the Anammox process draw more public attention, a series of novel and cost-effective biological nitrogen removal processes based on these principles are currently under development. These include the following processes: SHARON-ANAMMOX, CANON, OLAND which are further described below.

### 2.5.1 Sharon – Anammox process

The Sharon/Anammox process achieves nitrogen removal by combining two separate treatment steps: a partial nitrification process (Sharon) followed by an anaerobic ammonium oxidation process (Anammox). In the following Fig2.19, the treatment sequence of the combined Sharon/Anammox process is schematically depicted.

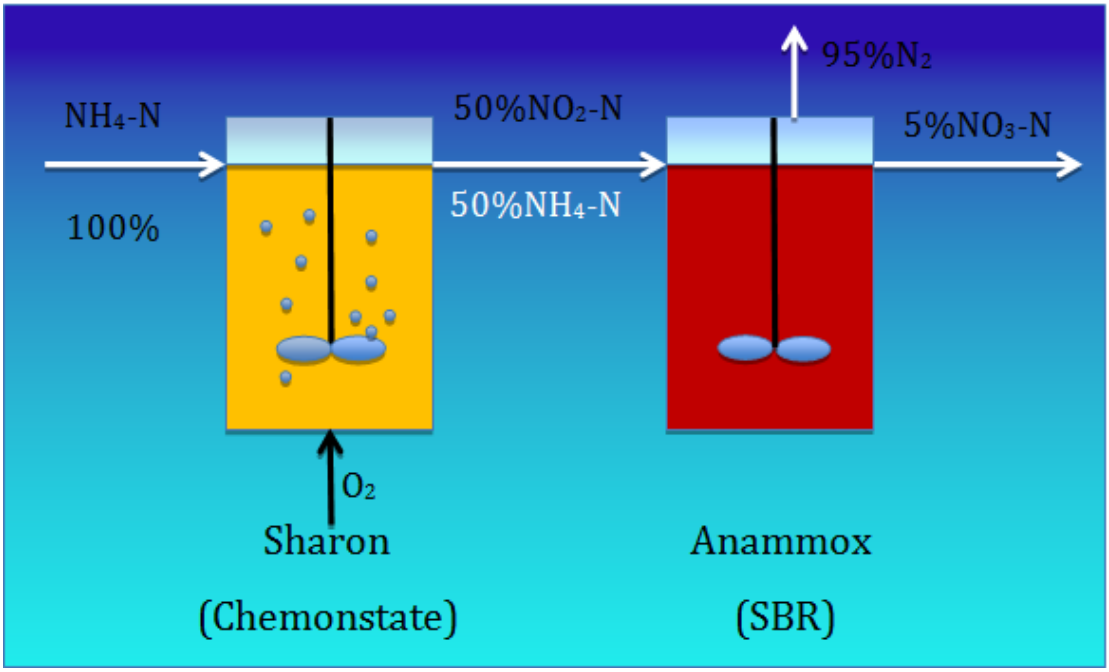


**Figure 2.19** Combined Sharon/Anammox process

Step 1 SHARON PROCESS

In the late 1990s, the SHARON (Single reactor system for High Ammonia Removal Over Nitrite) process was first successfully developed by the Technical University Delft, in The Netherlands (Hellinga et al., 1998) using nitrite as an intermediate in biological nitrogen removal achieved under stable conditions (van Kempen et al., 2001). The SHARON process is ideally suitable for the removal of nitrogen from wastewater with a high ammonium concentration (> 0.5 g $NL^{-1}$).

Compared with the traditional biological nitrogen removal technology, the SHARON process shows certain advantages: (1) Short-cut partial nitrification takes place in a single reactor in a shorter time than that required for full nitrification. (2) Relatively little initial investment is required since there is no need for an installation for sludge retention (Hellinga et al., 1998). (3) A 25% reduction of oxygen demand and a 40% reduction of carbon source demand during denitrification, because the oxidation is stopped at the nitrite stage.

The core of the process is to make use of different growth rates of ammonium oxidizer and nitrite oxidizer at high temperatures (30℃～40℃) to achieve partial nitrification. This occurs in a simple continuous stirred tank reactor with a hydraulic retention time

higher than the growth rate of nitrite oxidizers but lower than ammonia oxidizers (around 1 day). Because this process has no biomass retention, the nitrite oxidizing bacteria are not able to remain in the SHARON reactor and they are washed out. Furthermore, due to the high temperature, no biomass retention and the fixed hydraulic retention, the volumetric ammonium reactor loading depends on the ammonium concentration of influent. Therefore the process costs also depend on the ammonium concentration of the waste stream rising costs with decreasing ammonium concentration (Schmidt et al., 2003).

In order to achieve the stable partial nitrification, the operating variables (temperature, pH, HRT, substrate concentration, DO) are controlled in a chemostat-like operation. This process is operated at a relatively high temperature of around 35 ℃ with a pH above 7 (Brouwer et al., 1996; Hellinga et al., 1997) and HRT about 1 day. As discussed earlier, the growth rate of NOB is lower than that of AOB at higher temperatures. By controlling temperature, pH and sludge age, the ammonium oxidizers play the dominant role in the reactor resulting in the fact that nitrite oxidizer can be readily removed from the system.

The process has been successfully applied to Dokhaven WWTP located at Rotterdam in The Netherlands. Wastewater treatment has been apparently improved. But the largest defect of the technology lies in need for higher temperatures and pH. Therefore, it is only applied to cope with high ammonia wastewater at high temperature (otherwise the wastewater needs to be heated).

The SHARON-ANAMMOX suspension system technology developed by Strous has been applied to treat high concentrations of ammonia wastewater. A Sharon reactor has been installed on the WWTP in 1998 and was successfully operated from 1998 until mid-2002. In 2002, an Anammox reactor was built to realize the combined Sharon/Anammox concept. The Anammox reactor has been designed similarly to anaerobic granular sludge reactors. The installation was started up in June 2002. Afterwards the combined system was put into operation in Dokhaven WWTP in The Netherlands. The table 2.7 shows indicative comparison between nitrogen removal by conventional denitrification and the Anammox process (Mogens *et al*., 2008).

**Table2.7** Comparison between conventional N-removal system and SHARON/ Anammox process for N-removal

| Item | Unit | Conventional treatment | SHARON/Anammox |
|---|---|---|---|
| Power | kWh/kgN | 2.8 | 1.0 |
| Methanol | kg/kgN | 3.0 | 0 |
| Sludge Production | kgVSS/kgN | 0.5-1.0 | 0.1 |
| CO2 emission | kg/kgN | >4.7 | 0.7 |
| Total costs* | € | 3.0-5.0 | 1.0-2.0 |

*Total costs include both operational costs and capital charge

### 2.5.2 CANON

CANON is an acronym for Completely Autotrophic Nitrogen removal Over Nitrite which is the combination process of partial nitrification and Anammox as well. This process performs two sequential reactions simultaneously in a single reactor or biofilm under oxygen-limited conditions to realize short-cut nitration and anaerobic ammoxidation (Khin and Annachhatre, 2004; Ahn, 2006). Two groups of autotrophic microorganism populations (Nitrosomonas-like aerobic microorganisms and Planctomycete-like anaerobic bacteria) cooperating in a single system under oxygen-limited conditions (< 0.5% air saturation) (Strous, 2000) are responsible for the CANON activity.

Under oxygen-limited conditions, the ammonium oxidizing bacteria oxidize ammonia to nitrite and consume oxygen so as to create the anoxic conditions which the Anammox process requires. CANON has been tested extensively (Hanaki et al., 1990; Strous, 2000) and the overall reactions are as follows:

$$NH_4^+ + 0.75O_2 + HCO_3^- \rightarrow 0.5NH_4^+ + 0.5NO_2^- + CO_2 + 1.5H_2O \quad (2\text{-}30)$$

$$NH_4^+ + 1.32NO_2^- + 0.066HCO_3^- + 0.13H^+ \rightarrow 1.02N_2 + 0.26NO_3^- + 0.066H_2O_{0.5}N_{0.15} + 2.03H_2O \quad (2\text{-}15)$$

The nitrite also performs as an electron donor for the formation of biomass from carbon dioxide (Strous, 2000):

$$NH_4^+ + 0.85O_2 \rightarrow 0.44N_2 + 0.11NO_3^- + 1.43H_2O + 0.14H^+ \quad (2\text{-}31)$$

The advantages of the CANON process are that, in a single reactor, biological denitrification is realized thus saving cost and room. As it is operated in an anoxic condition, a large amount of oxygen (up to 63%) is saved (Khin and Annachhatre, 2004). Organic carbon source is not necessary. The key to controlling the process is to transform only 50% of the ammonia into nitrite. If substantially more than 50% of the ammonia is oxidized then the alkalinity will be reduced and the pH value may drop to a level at which the ANAMMOX reaction will cease (Schmidt et al., 2003).

### 2.5.3 OLAND

The OLAND (Oxygen-Limited Autotrophic Nitrification and Denitrification) process was first presented by University of Ghent Belgium in 1998. It is possible, when oxygen and nitrite are both limited, that nitrite oxidizers may be effectively excluded from the N-removal process (Hao et al., 2002). In this process, unlike the CANON process, the ammonia-oxidizing bacteria are able to convert ammonium to nitrogen gas in one reactor under oxygen limitation. The Nitrosomonas species can use, due to shortage of an electron donor, hydrogen and ammonia as electron acceptors to reduce to $N_2$. A mature OLAND biofilm under high $NH_4^+$ loading rates consists primarily of two major groups of bacteria responsible for autotrophic nitrogen removal. The aerobic ammonium oxidizing bacteria convert $NH_4^+$ to $NO_2$ with oxygen as an electron acceptor and the anaerobic ammonium-oxidizing bacteria oxidize $NH_4^+$ with $NO_2^-$ as the electron acceptor (Strous et al., 1998). No extra organic carbon source is required for denitrification as in CANON. It seems that OLAND is based on the CANON process but it makes use of individual autotrophic aerobic nitrifiers instead of cooperation of ammonia oxidizing bacteria and anammox bacteria in the CANON process (Kuai and Verstraete, 1998)

The OLAND process enables bio-denitrification to operate stably in low temperatures (22～30℃). The process can save massive oxygen consumption and 100% of the electron donor (organic carbon source). It also gives less sludge output in comparison with traditional nitrification and denitrification. The key parameter to control the process is dissolved oxygen concentration. The current problem is that it is hard to control the pH value in the system with the continuous operation of the culture of mixed bacteria. This lack of stable designs is the biggest obstacle to implementation so the

technology is still under further research and development.

### 2.5.4 NOx

The NOx process is featured by the control and stimulation of the denitirification activity of Nitrosomonas-like microbes by adding nitrogen oxides into the waste stream. When $NO_X$ exists, nitrobacteria like Nitrosomonas can simultaneously support nitrification and denitrification. With sufficient aeration they produce $N_2$ as the final product. $NO_X$ stimulates and controls the denitrification activity of the ammonium oxidizing bacteria during the whole process. Only a little $NO_X$ is needed (ratio of $NH_4^+/NO_2$ between 1000/1 and 5000/1). As a result about, 50% of the reducing equivalent of protons is gained by nitrite, at an additional cost of €0.05-€0.08 per kg $NH_4$ but with a saving of 80% carbon source and 50% oxygen consumption (Schmidt et al., 2003; Ahn, 2006).

## 2.6 Microbubble Generation & Application

Microbubbles are miniature gas bubbles with diameters ranging between 1μm - 1mm, which mostly contain oxygen, air or carbon dioxide etc. and can remain suspended in the liquid phase for an extended period. Gradually, the gas within the microbubbles dissolves into the liquid and the bubbles disappear. These bubbles are generated by various types of technologies now available in the market.

The widely used methods for generating microbubbles based on the cavitation principle include compression of the air stream, power ultrasound (sonication), and an air stream delivered under low offset pressure. Amid these technologies compression of the air stream is the most commonly used. The microbubbles released through the nozzle system of special design subsequently grow into much larger bubbles. Although these two methods are widely applied to different areas, they are significantly reliant on high-energy consumption.

Considered from the aspect of the environment, resources and energy, the third case has absolute superiority, which uses the air stream to break off the bubbles due to the use of additional feature, including mechanical vibration, flow focusing and fluidic oscillation (Zimmerman et al., 2008).

### 2.6.1 The Challenge of Small Bubble Generation

It is very interestingly but true fact that making the aperture of the diffuser as small as possible is not sufficient to try to generate the correspondingly small bubbles. The bubble generation process starts as the gas-liquid interface protrudes from the nozzle and gradually, the bubble size increases. Zimmerman (2009) reported that the growth of bubbles can be attributed to the following: Firstly, when a bubble is created from a single aperture, the liquid attached to its perimeter tenders an anchoring effect as the wetting force attaches the growing bubble to the solid surface. The bubbles continue to grow under continuous flow until such a point when their buoyant force, which varies in direct proportion to their size is strong enough to overcome the anchoring constraint on the bubble, leading to it finally breaking off. Under this low-pressure state, the force difference is the key to bubble up detachment from source. In general, the fact is that the force balance always breaks off the bubble in low pressure offset scenario at a size an order of magnitude larger than the size of the aperture. Likewise, the formation of larger bubbles as a result of coalescence effects by reason of irregular spacing between the neighbouring bubbles and polydispersity of bubble sizes, rapidly occurred as long as bubbles were created from in the openings (Zimmerman et al., 2009).

Since the behaviour and property of microbubbles are chiefly dependent on their size and size distribution, the demand for preparing microbubbles with desired size and narrow size distribution is increasing. To this end, the Department of Chemical and Biological Engineering at the University of Sheffield has patented a novel fluidic oscillator to create microbubbles more efficiently. Fluidic oscillation technology is currently a most eye-catching method for preparing microbubbles, which is only just depending on offset pressure instead of high-power density but also effectively overcoming the major difficulties discussed above creating microbubbles of the scale of the aperture diameter, rather than an order of magnitude higher.

Microbubble technology is currently used in various industries and is expected to offer a broad range of applications, some of which are reviewed below.

### 2.6.2 Microbubble Generation by Microfluidics Oscillator

Generation of small bubbles can be carried out through various processes. Researchers have reported that microbubbles can be generated by electrostatic spraying and ultrasound waves, and also through electro flotation and dissolved air flotation. Compared with these conventional microbubble generation systems, a low-cost, energy efficient generation of microbubbles with significant influence on the mass transfer and mixing efficiencies by using the fluidic oscillator was first put forward by The University of Sheffield (Zimmerman et al., 2008, 2009). Up to now, this novel technology has been reported to achieve clouds of fairly uniformly spaced and sized microbubbles on the scale of the pore size used to disperse the bubbles. Investigation of power consumption shows an 18% reduction of electricity over that of steady flow with the same volumetric flow rate. (Mashhadani et al., 2012) In this subsection, the generation mechanism for microbubbles by fluidic oscillation is discussed.

#### 2.6.2.1Fluidic Oscillator Design

Zimmerman et al. (2008) proposed that for the purpose of microbubble generation, the key idea is to reduce the bubble growth time by the duration of the period of an oscillator that supplies air into the bubble-formation apertures, which may be a variety of forms, e.g. nozzles and diffusers, microporous materials, etc. If done so, the growth of the bubble is stopped at the end of each oscillation half-period. It is capable of restricting further bubble growth. The bubble then goes off the aperture. Therefore, a new bubble is produced at once in the next period thanks to the oscillation gas stream. No bubble can reach the large sizes typical for steady flow.

Generally, this limitation of growth time might be provided by a gas flow produced by an oscillation generator with moving mechanical components, which is in essence a mechanically operated valve, periodically opened and closed. In contrast to conventional control valves with moving parts, Zimmerman et al. (2008) introduced a non-moving fluidic oscillator that is supplied with a steady fluid flow, which it converts into a pulsatory or even alternating flow at its outputs. The fluidic oscillator of the no-moving-part type is superior for its simplicity, reliability, robustness, low price and- last but not least – no need for electric energy supply.

The fluidic oscillator is an essential element of the microbubble aeration system. The fluidic oscillator comprises of a feedback loop, an amplifier, two amplifying ports and two discharging ports (Fig 2.20). It is inserted along the gas supply where its task is to limit the growth of the bubbles produced by percolation through restricting the available growth time to one half of the oscillation period. Its main component is the fluidic amplifier shown in the left part of Fig. 2.20. Its operation principle is to create pressure pulses periodically between two cavities through the feedback loop at certain frequencies. As Fig 2.20 shows the feedback loop is a very simple structure comprising nothing more than just a tube of suitable length to connect the two control terminals X1 and X2. Steady gas flow is injected into the supply terminal S at high pressures and its flow into either one of two output terminals Y1 and Y2 and is controlled by the control action applied to control terminals X1 and X2. The control action redirects the gas flow between the output terminals Y1 and Y2 through the pressure difference. The device as described above consists of an amplifier component because the output stream through the terminals Y1 of Y2 has a much higher flow rate and relatively greater momentum than the control flows input into the control terminals X1 and X2, nevertheless, in this case the former has to be controlled by the latter. (Zimmerman et al., 2009) In other words, the feedback loop gives the amplifier an opportunity to settle temporarily to a particular (either open or closed) state before it is forced to move back. This is achieved by the phase shifter in the loop. The magnitude of the shift also determines the oscillation frequency (Zimmerman et al., 2011).

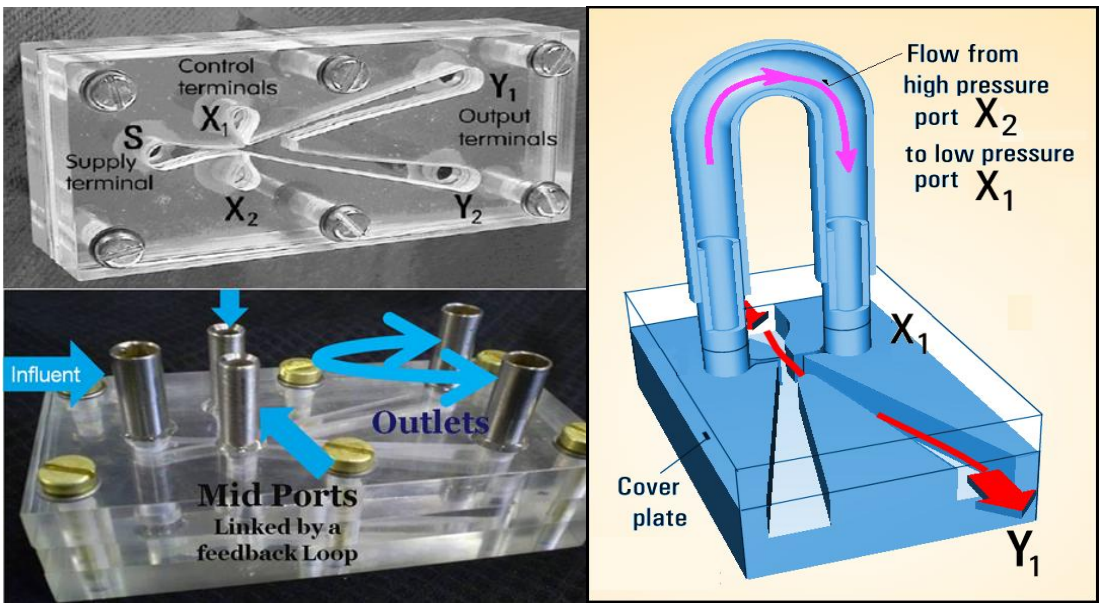

**Figure 2.20** Left: the model of the fluidic jet-deflection amplifier used in the project. It is a stack of PMMA plates with laser-cut cavities – containing no moving mechanical parts. The screws are 1/4 inch heads. Right: the fluidic oscillator is made from the amplifier by providing it with the feedback loop (shown here of adjustable length for tuning the oscillation frequency) connecting its two control terminals.

### 2.6.2.2 Energy Efficient Microbubble Generation by Fluidic Oscillation

Observations exploiting the ability of no-moving-part fluidic oscillators described that the microbubbles "shoot" out of apertures like "bullets" and further achieve clouds of fairly uniformly spaced and sized microbubbles as small as an average diameter of 28 μm from 20 μm pores in a metallic membrane instead of conventional slow pushing out from the pore along with the bubble growth as under steady flow (Zimmerman et al, 2011).

As shown in the right-hand part of Fig. 2.21 the pressurized air jet issuing from the main supply terminal gets attached to either one of the two attachment walls and is thereby flowed into one of the two output terminals. The performance can be illustrated using the "Coanda effect". The Coanda effect is the phenomena in which a jet flow attaches itself to a nearby surface and remains attached even when the surface curves away from the initial jet direction. As a consequence of the deflection the airflow trajectories inside the jet in the vicinity of cavities are curved. The curvature induces a radial pressure gradient across the jet, which leads to descending pressure at the control terminal X1. This pressure difference then draws the airflow through the feedback loop from control terminal X2 where the pressure is correspondingly higher to control terminals X1. Shortly thereafter the control airflow suffices at X1 when the air flow in the feedback loop tube gains momentum in the opposite direction. The amplification effect, therefore, switches the main air jet from Y1 and diverts it into to the other terminal Y2. Because the fluidic oscillator is a geometrically symmetric structure, this jet switching motion reappears in the opposite way resulting in a periodic switching process. By this periodic switching process the fluidic oscillator induces an oscillation in the air supply, limiting the period for bubble growth (Zimmerman et al., 2009). As the oscillator used to create the microbubbles in Fig 2.21 achieves 1–100 Hz fundamental frequencies, it is estimated that higher frequencies of the oscillation in the

fluidic oscillator chamber are responsible for the smallest bubbles generated. It was reported that frequency of oscillation to a great extent depends on the length of the feedback loop and supply flow rate (Tesaˇr et al. 2006).

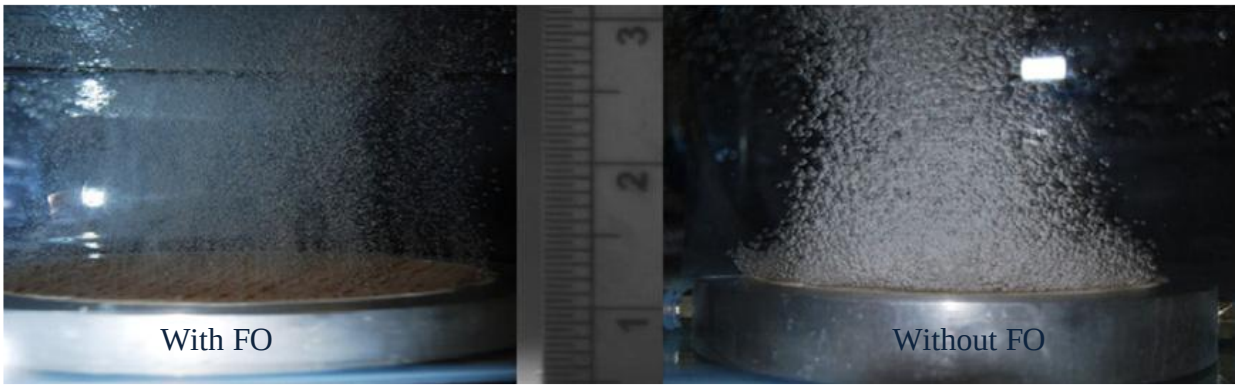


**Figure 2.21** Images of bubbles generated from the same microporous diffuser under different conditions. (Right) Bubbles generated under steady air flow. Bubbles are coalescent, non-uniform and several folds larger than the diffuser pore size. (Left) Bubbles generated under oscillatory flow. Formation of a uniformly sized non-coalescent mist of microbubbles almost same size as diffuser pores.

The frequency of oscillation is denoted by "f" and can be defined by cycles it can complete during the certain time period. It is expressed using the expression:

$$f = \frac{1}{T} \qquad (2\text{-}32)$$

Where T is period of oscillation and it can be expressed as a function of length of the feedback loop "l", the transmission time "$\tau_t$" and the time it takes for the flow to switch between the cavities "$\tau_s$". Hence, T can be expressed as $\tau$

$$T=2(\tau_t+\tau_s) \qquad (2\text{-}33)$$

The conventional bubble generation for dissolved air flotation is primarily affected by the surface tension of the liquid. By contrast, the fluidic oscillator operates on pulsation to convert steady air supply into the oscillatory flow with a regular frequency to generate microbubbles. Beyond these, the other benefit of air pulsation from the fluidic oscillator is that it is possible to avoid producing bubbles in a streak, preventing coalescence and hence limiting bubble growth. It was therefore concluded that with the

fluidic oscillator, there is a high potential for generating microbubble bubbles on the scale of the pore size.

### 2.6.3 Benefits and Application of Microbubble in Different Areas

#### 2.6.3.1 Benefits of Microbubble

Compared to larger bubbles in the millimetre range produced by conventional aeration systems, microbubbles present novel and unique features, such as a higher surface area to volume ratio, slower rising velocity in the liquid phase and higher internal pressures in which the higher ratio of higher surface area to volume is most important. Because of a common thread among these benefits of microbubbles is in their transport behaviours for instance, mass, momentum, and heat transport at the interface of microbubbles. Improvement of nearly all transport behaviours of microbubbles are attributed to the enlargement of surface area of the interface between gas and liquid phase.

It is very difficult to assess the mass transfer coefficient of a single bubble or droplet due to the hydrodynamics of the bubble rise, its environment, and the constitutive properties of the medium and material transferred. (Deshpande and Zimmerman, 2005) however, the mass transfer coefficient of bulk flow is determined by convection forces and therefore, can be globally calculated by a mass transfer coefficient phenomenological equation in which the overall flux is proportional to the interfacial area S of the dispersed phase. Consequently, transfers dynamics, mass, momentum and heat transport are improved by increasing the interface area of bubbles through decreasing the bubble size. The common chemical engineering phenomenological description of interface mass transfer flux J can be represented as (mol/s):

$$N_A = K_l a(C_{Al}^* - C_{Al}) \quad (2\text{-}34)$$

where $K_l$ is the mass transfer coefficient , $a$ is the interfacial area, and $C_{Al}$ and $C_{Al}$ are molar concentrations. $N_A$, the molar flux of component A, all things being equal, increases proportionate to an increase in $a$, and therefore, inversely proportionate to the diameter $d$ of the microbubble.

Furthermore, based on geometry, the surface area to volume ratio of a spherical bubble is inversely proportional to its radius or diameter, as represented.

$$\frac{S}{V} = \frac{4\pi r^2}{\frac{4}{3}\pi r^3} = \frac{3}{r} \qquad (2\text{-}35)$$

If it is supposed that the total volume of the bubble phase is maintained as constant $v_0$, then 2-34 transferred to

$$S = \frac{3}{r} V_0 \qquad (2\text{-}36)$$

S is the surface area that the total phase exhibits. For instance, if X l of air is distributed in 100 μm size bubbles, there are 10X$m^2$ of the interfacial area, easily comparable or greater than a reasonable sized air–liquid interface of the continuous phases in a tank open to the atmosphere. To sum up, there is no doubt that decreasing bubble size contributes to markedly higher mass transfer rates compared to the fine bubble.

The larger interface area is just one of the advantages of microbubbles. The other crucial advantage brought by microbubbles is a long residence time. The classical Stokes law serves as a guide for the residence time of a microbubble in a viscous liquid:

$$v_s = \frac{2}{9} \frac{(\rho_p - \rho_f)}{\mu} g R^2 \quad (2\text{-}37)$$

where:

1. $v_s$ is the particles' settling velocity (m/s) (vertically downwards if $\rho_p > \rho_f$, upwards if $\rho_p < \rho_f$),
2. g is the gravitational acceleration ($m/s^2$),
3. $\rho_p$ is the mass density of the particles ($kg/m^3$), and
4. $\rho_f$ is the mass density of the fluid ($kg/m^3$).

Due to the square, it is clear that the residence time of the microbubbles is strikingly longer for the same height of liquid than for larger bubbles. Thus smaller bubbles take much longer to transfer their momentum from the gas phase to the liquid phase, even though they have less momentum to transfer. These two effects would offset each other for transfer efficiency, but for the surface area to volume ratio –momentum is also transferred, by shear stress, across the surface area of the bubble. Therefore the flux of momentum is markedly increased by the decreasing the bubble size, by the same ratio of Eq. (3-26). It is easy to conclude that the longer residence time in the height of liquid permits higher holdup at lower volumetric flow rates (Zimmerman et al., 2009).

The advantages of microbubbles have been tested and proved by Zimmerman and his microfluidics group in both lab and pilot scale experiments. Shi (2006) demonstrated 8-fold smaller bubbles produced by oscillatory flow than those generated under the same volumetric flow rate steady flow through the same diffuser, measuring an 8-fold increase in dissolved oxygen transfer efficiency according to the standard ASCE test. Subsequently 3-fold promotion in aeration rates using the faster frequency oscillation was found in pilot scale experiments over steady flow through the same flexible membrane diffuser array with the same volumetric flow rate. Moreover, they also recorded a decrease in power draw on the blower to achieve this flowrate of 13%. (Zimmerman et al., 2009)

### 2.6.3.2 Application of Microbubble in Different Domain

Recently, extensive research has been devoted to the application of the microbubble in various fields such as wastewater treatment, algal biofuels production, flotation separations, biogas yield from digested sludge, Chemical reactions, therapy and remediation or bio-remediation of contaminants, etc.

*** Algal biofuels production**

Zimmerman et al., (2011) introduced a microbubble aeration system with fluidic oscillator into an airlift loop bioreactor (ALB) for growing microalgae on steel plant exhaust gas, generated from the combustion of offgases from steel processing, which has a high $CO_2$ content. The field trials' results demonstrated steady growth of biomass and obtained 100% survival rate. An uptake rate of 0.1g/L/h, an average 14% of the $CO_2$ available in the exhaust gas with a 20% composition of $CO_2$ led to a steady production of chlorophyll and total lipid constituency in the bioreactor, and an accelerating exponential growth rate of biomass, with a top doubling time of 1.8 days. Through analysing the gas composition a negative-correlation between $CO_2$ uptake and $O_2$ production was found. Smaller bubbles are also used to extract the oxygen produced by the algae, which stunts its growth and eventually kills it**.** Due to the apparent stripping of the $O_2$ to the equilibrium level by the microbubbles the bioreactor is demonstrated not to be mass-transfer limited, nor $O_2$ inhibited, which results in high growth rates and high density of biomass.

Shortly after Ying (2012) operated analogical lab scale experiments to test the how much efficiency of microalgal culture growth being promoted by an airlift loop bioreactor engaged with fluidic oscillator compared with both the ALB without microbubble generation system and a shake flask culture. The results showed that approximately a 20% - 40% increase in specific growth rate was found in ALB the with microbubble generation system than in normal ALB cultures and approximately 6 – 8 times higher chlorophyll content was achieved in ALB cultures than that in the conventional shake flask.

***Wastewater treatment**

Microbubbles, being of extremely small size, are characterized by having electrical charges which allow them to attract suspended floating particles very effectively. This particular property has been used in sludge treatment during wastewater treatment by using the microbubbles to capture and float organic matters, thus reducing the time required for the wastewater treatment.

The activated sludge process is most widely used as biologic treatment of wastewater from both industrial and municipal sources around the world. Energy is used throughout the biological wastewater treatment process; however, pumping and aeration operations are typically the largest energy users. Actually, the role of aeration in the activated sludge process is not only to simply provide oxygen for the growth of functional bacteria but also to strip the produced $CO_2$, consequently accelerating the natural life cycle of the bacterial consortium and facilitate growth by the provision of nutrients and extraction of waste products. Implementation of the microbubble aeration system with relatively high oxygen transfer is able to promise to save more energy usage as well as enhance the performance of the biological processes in addition to the permanent benefit of gas exchange.

*** Microflotation separations**

Induced Gas Flotation (IGF) is injecting gas bubble into the water where the small bubbles adhere to the suspended matter such as some colloidal, emulsified, and dissolved substances causing the suspended matter to float to the surface of the water. IGF is very widely used in treating the industrial wastewater effluents from oil refineries, petrochemical and chemical plants, natural gas processing plants and similar industrial facilities. A very similar process known as dissolved air flotation (DAF) is to

dissolve air in water under pressure and then release the air at atmospheric pressure in a flotation tank or basin. The released air forms tiny bubbles which tend to have more surface area-to-volume ratio compared to the bubbles generated by other methods, thereby resulting in better separation efficiency. In practice the latter is more employed than the former. In spite of wide implementation of these gas lift separation processes they have some major drawbacks such as being labour intensive and expensive operation (Cheremisinoff, 2011). Flotation separation is commonly used in the mineral industry to separate fine particles from solutions and the oil industry to separate oil-water emulsions. In adsorbing colloid flotation, heavy metals are removed by fine tiny bubbles.

In view of the principle and restrictions of the technology of DAF and IGF microbubble flotation was deemed to be more efficient for gas lift flotation as it saves the compression stage and saturation thus it has the potential to replace dissolved air flotation by achieving the same scale of bubble size distribution but through simply blowing air rather than pumping saturated liquid. The microbubbles produced by the fluidic oscillator, vitally without the turbulent release, will no longer require the saturated recycle flow, 90-95% of the electricity cost for the DAF process, which means leaving out the saturator can save capital costs per unit of $500k, and similar costs for pumping systems (Zimmerman et al., 2011).

Hanotu et al., (2011) studied the performance of microflotation, dispersed air flotation with microbubble clouds with bubble sizes of about 50 microns generated by using fluidic oscillation for algae separation. Owing largely to benefits of microbubbles as discussed in (2.5.3.1), particle flotation by microbubble clouds occurs more rapidly and efficiently. By comparison, the performance of microbubble flotation overwhelmed that of conventional dissolved air flotation (DAF) benchmarks which have highly turbulent flows, whereas microflotation is laminar with a several orders of magnitude lower energy density.

*** Production of biogas**

Microbubbles have also been introduced by the University of Sheffield to Anaerobic digestion in order to remove and recycle the biogases produced in the digested sludge. Biogases are readily available from landfill sites and wastewater treatment plants but are typically 60 per cent methane and 40 per cent $CO_2$. The dissolved biogases remaining in

the digested sludge for extended lengths of time can still cause environmental degradation, as well as violation of operational facilities such as corrosion of piping and process equipment. Not only that, but continuous generation of biogas in digested sludge increases cavitation phenomena and exacerbates pump loads.

Currently water scrubbing is used to remove some $CO_2$, but a lot of electricity is demanded, and microbubbles can potentially provide a much more efficient alternative. Through 170 hours of operation, the experimental data showed that the removal efficiency of carbon dioxide and hydrogen sulphide, in gas lift loop anaerobic digester with microbubble generated by fluidic oscillator were much greater than that for the conventional digester ( Mashhadani et al.,2012).

*** Ozone dosing by microbubbles**

Ozone is a powerful oxidant (far more so than dioxygen) and has many industrial and consumer applications related to oxidization. Conventional ozone generation is tied up with high-power consumption and the requirements of near vacuum operation and high voltage. In terms of these drawbacks, Zimmerman et al., (2010) invented a novel microchannel plasma reactor in a MicroNit Microfluidics microchip that was used to generate ozone at atmospheric pressure, relatively low voltage, and room temperature. Throughout a series of experiments, the upshot showed ozone could be reliably produced with a low voltage (170VCAC) at atmospheric pressure and room temperature, with a 36.6Hz AC electric field.

The application of ozone is limited by very low solubility and poor stability in water. The effectiveness of ozonation can be potentially improved by using ozone microbubbles. Thus, after successful achievement of ozone generation with a more efficient method, the dispersal of ozone catches the eyes of the research group. Conventional dosing of ozone is by insertion of a gas jet into the water stream, with subsequent in-line mixers used to disperse the gas, however, this procedure is plagued by low mass transfer rates. A substantial quantity of the ozone remains unspent and must be destroyed for safety reasons in a post-processing plant room. Greater dispersal rates of ozone are promised by microbubble dispersal. Zimmerman *et. al*, (2009) demonstrated a new fluidic oscillator technique to produce microbubbles. Since microbubbles have a low carrying capacity and ozone is highly reactive, therefore delivering ozone with such a microbubble dispersal system has the promise of such

higher dispersal rates and it should be possible to tune the production and dispersal so as to completely consume all the ozone generated (Zimmerman, 2011).

* **Medical applications**

A new emergent usage of microbubbles is in the area of clinical medicine. It is not widely known that not all bubbles in the bloodstream are detrimental. Over the last decade, contrast-enhanced ultrasound has evolved from a purely investigational tool to a routine diagnostic technique. This transformation has been facilitated by advances in the microbubble contrast agents and contrast-specific ultrasound imaging techniques. The ability to non-invasively image molecular events with targeted microbubbles is likely to be important for characterizing pathophysiology and for developing new therapeutic strategies in the treatment of cardiovascular and neoplastic diseases (Lindner, 2004).

Lately some scientists are putting great effort into developing a method of diagnosing cancer lesions by injecting microbubbles into the blood stream. During the ultrasonic scan for cancer lesions, the microbubbles contract and expand rapidly due to the pressures produced by the ultrasonic beam. Groups of the microbubbles at cancerous tumours will show up very visibly on ultrasonic scans to indicate the presence of cancerous cells.

***Other applications**

In the yeast industry, biomass production mainly depends on oxygen transfer efficiency of the aeration system. In the production processes of some biopharmaceutical products, bioreactors require microbubble aeration systems.

In addition to wastewater treatment aeration system, oxygen supplied in the form of microbubbles can also be used in other oxygen-consuming processes (e.g. aerobic fermentation aquaculture, hydroponic cultivation, and aerobic treatment of sewage). Microbubble technology has found applications in enzyme extraction, protein recovery, bacterial harvest, and oil removal or recovery (Xu et al., 2011; Onari et al., 2005; Hoage and Messer, 2005).

The property of a large surface area to volume ratio of microbubbles can enable them to penetrate deeply into a surface for effective cleaning. This cleaning effect of microbubbles is used in cleaning the inside of vegetables such as cabbage and radish sprout, as well as maintenance of freshness with vegetables in one particular vegetable processing centre in Japan. On a more personal level, the microbubbles can penetrate

deeply into human and animal skin for a cleaning without the need for any shampoo or soap. This skin treatment has been introduced within some spas in Japan as well as shops specializing in bathing pets. Needless to say, the baths are especially helpful for pets which have skin allergies to pet shampoos (Yap, 2012).

## 2.7 Conclusion

With the serious shortage of water resources and the pollution of water, conventional processes have already hardly meet the severe discharged standard of sewage. As result the novel partial nitrification and Anammox process were developed, which are able to save more energy and treat more complicated wastewater with better result. As aeration bioprocess the partial nitrification needs continuously oxygen supply which was consider to be the major contribution to the operating cost. While, the Anammox process, on the contrary, was assured to run successfully under strictly anaerobic condition. Although the Anammox process no long needs extra organic carbon source which is necessary for convention denitrification, low growth rate of Anammox biomass and strictly demanding operating condition mentioned in 2.4.7 still to large extent limit the improvement of this biological nitrogen removal process. Compared to the conventional biological nitrogen removal process, the partial nitrification and Anammox impressively reduced the duration of the wastewater treatment process, energy consumptions and emission of $CO_2$. Meanwhile, as learn more about physiology of bacteria involved in the biological process, this novel technology has been optimized in different ways to overcome or impair the restrictions.

Due to the advantages of microbubble, some traditional industries, such as biofuels production, flotation separations and biogas yield from digested sludge, more and more applied microbubbles instead of normal bubble in order to optimize the process design. It has been found that those industrial processes without exception were enhanced by microbubble in aspects of efficiency and saving of energy.

Considering the constraints in the existed partial nitrification and Anammox process the effort of researchers is to try and seek different ways to improve the efficiency and capacity with less energy and capital input. From the perspective of enhance performance of the involved microorganism, this project was forced on creating a more

appropriate environment for the growth of biomass with less energy consumption. The introduction of microbubble provides the potential way to optimize partial nitrification and anammox process because of the characteristics of microbubble. For partial nitrification, microbubble aeration system could reduce the oxygen consumption, while, for anammox, gas exchange with microbubble can more efficiently remove oxygen with less inert gas or other gases. Besides, $CO_2$ rich gases was first engaged in the anammox process acting as deoxygenating gas and pH control system. The stack gas with high temperature from power station containing a quantity of $CO_2$ was regarded as an ideal gas mixture for gas exchange because of oxygen depleting and offering the heat for the Anammox bacteria which needs warm condition to growth.

It can be thus deduced from this chapter that theoretically, the application of microbubble in the biological nitrogen removal process could be a very promising technology to bring much more economic benefit. However how the microbubble could benefit the wastewater treatment, how much improvement could be achieved and what are the problems which could be confronted with during its application still remained as major issues before its industrial application. This thesis is therefore focused on solving these questions to pave the way for the industrial scale application.

# Chapter 3. Materials and methods

In this chapter, the materials and methods employed to carry out the experimental work in this thesis are explained. Firstly, the methods employed to analyse the properties of the liquid phase are detailed. They are followed by the techniques for the physical and microbiological characterization of the biomass. Finally, the composition of the partial nitrification and Anammox medium are included. This medium was used to prepare the synthetic partial and Anammox feeding medium.

The specific analytical methods used only in a single part of the work are described in the corresponding chapter, as well as the subsequent experimental setups and strategies.

## 3.1 Chemical Analysis

### 3.1.1 Ammonium-Nitrogen ($NH_4^+$-N)

Ammonium nitrogen was determined by a colorimetric method using Nessler's reagent. Nessler's reagent (potassium tetraiodomercurate (II)) reacts rapidly with ammonia under alkaline conditions to form a yellowish brown colloidal dispersion, whose intensity of colour is directly proportional to the amount of $NH^+_4$ present. The yellow colour or reddish brown colour typical of ammonia N can be measured in a spectrophotometer (HACH DR2800) in the wavelength 420 nm. The sample containing ammonia must be analysed immediately after collection.

**Reagents**

1. Sodium potassium tartrate tetrahydrate solution
2. Distilled water
3. Nessler's reagent
4. Wastewater sample

**Procedure**

1. Water samples were filtered by filter paper and diluted proportionally
2. Add 0.5ml sodium potassium tartrate tetrahydrate solution to each diluted sample

3. Add 7.5 mL of Nessler's reagent (proportional amount to be added if the sample volume is less).
4. A blank sample using distilled ammonia free water is treated with Nessler's reagent as above. The observance is fixed at zero.
5. Then the sample is put in cuvette of spectrophotometer (HACH DR2800) and the absorbance was noted at 420 wavelengths.
6. The same experiment was repeated more than 3 times, the calibration curve was generated using the average values

A calibration curve is prepared in advance

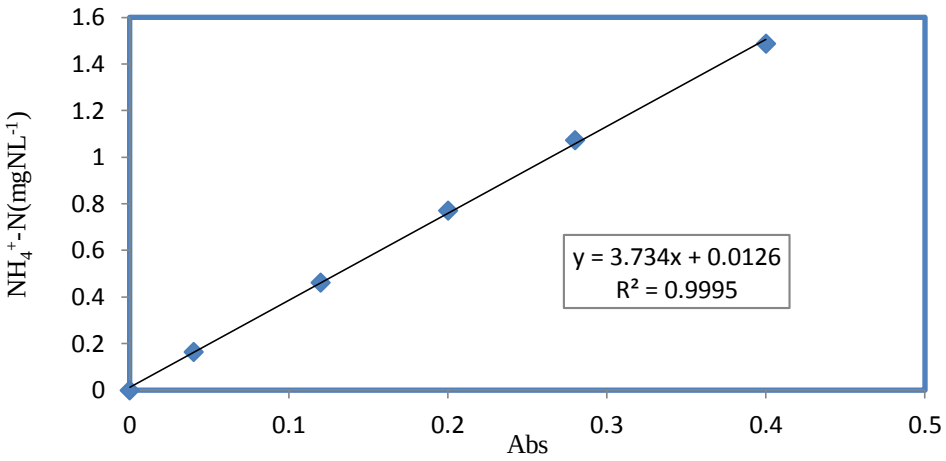


**Figure 3.1** Calibration curve for ammonium concentration determination

### 3.1.2 Nitrite-Nitrogen ($NO_2^-$-N)

Nitrite concentration was determined following the 4500-$NO_2^-$B. Colorimetric Method described in Methods for Chemical Analysis of Water and Wastes (Environmental protection agency. 1979). Nitrite ($NO^-_2$) is determined through formation of a reddish purple azo dye produced at pH 2.0 to 2.5 by coupling diazotized sulfanilamide with *N*-(1-naphthyl)-ethylenediamine dihydrochloride. (NED dihydrochloride).

**Reagents**

1 Distilled water

2 Color reagent (To 800 mL water add 100 mL 85% phosphoric acid and 10 g sulfanilamide. After sulfanilamide dissolved completely, add 1 g N-(1-naphthyl)

ethylenediamine dihydrochloride. Mix to dissolve, then dilute to 1 L with water. Solution is stable for about a month when stored in a dark bottle in refrigerator.)

3 Wastewater sample

**Procedure**

1. Wastewater samples were filtered through a 0.45-μm-pore-diam filter paper and diluted proportionally.
2. Colour development: If the sample pH is not between 5 and 9, adjust to that range with 1N HCl or $NH_4OH$ as required. To 25.0 mL sample, or to a portion diluted to 25.0 mL, add 0.5mL colour reagent and mix.
3. Photometric measurement: Between 10 min and 2 h after adding colour reagent to samples and standards, measure absorbance at 540 nm.
4. A blank sample using distilled nitrite free water is treated with the colour reagent as above. The absorbance is fixed at zero.
5. Prepare a standard curve by plotting absorbance of standards against $NO2^-$-N concentration. Compute sample concentration directly from the curve.
6. The same experiment was repeated more than 3 times, the calibration curve was generated using the average values.

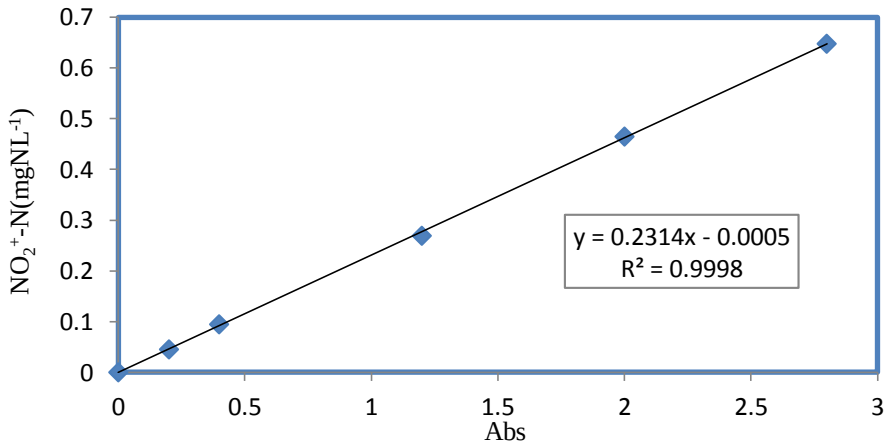


**Figure 3.2** Calibration curve for nitrite concentration determination

### 3.1.3 Nitrate- Nitrogen ($NO_3^-$—N)

Ammonium nitrogen was determined using Ion selective electrode for nitrate. A pH/mV meter (Mettler Toledo SevenMulti) or an ion meter is needed to connect to Nitrate electrode (Cole-Parmer® Ion-selective electrodes WZ-27502-31).

A calibration curve is constructed on semi-logarithmic paper when using the pH/mV meter in the millivolt mode. The measured electrode potential in mV (linear axis) is plotted against the standard concentration (log axis).

The same experiment was repeated more than 3 times, the calibration curve was generated using the average values.

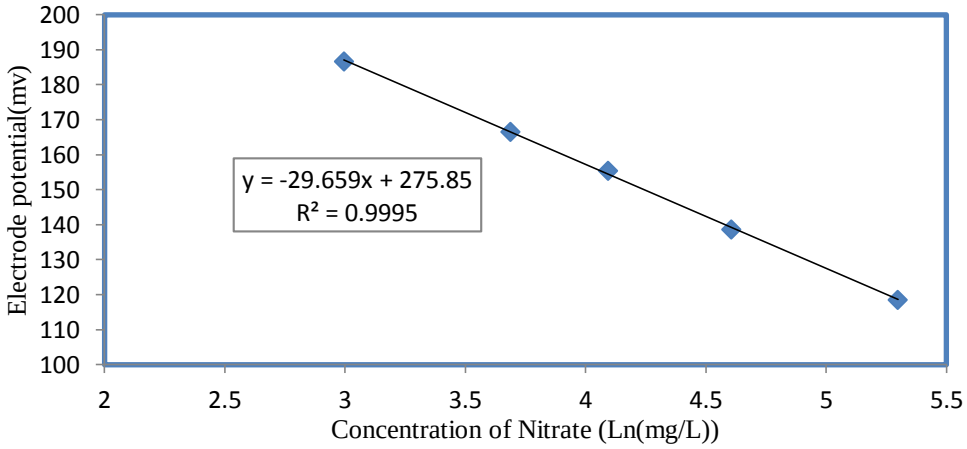


**Figure 3.3** Calibration curve for nitrate concentration determination

### 3.1.4 pH

The pH measurements were implemented with an electrode connected to a measuring instrument (pH mV-1) SevenGo Duo Pro Portable pH Meter. The sensibility of the system was ±1 mV, corresponding to 0.01 pH units. The electrode was calibrated at room temperature with three standard buffer solutions of pH 7.01, 4.01 and 10.1.

### 3.1.5 Dissolved Oxygen (DO)

The dissolved oxygen concentration ($mgL^{-1}$) is a key parameter for biological reaction and its concentration can enhance partial nitrification process or even inhibit a reaction

as in the case of Anammox. The DO is measured by SevenGo Duo Pro Portable DO probe and Meter.

### 3.1.6 Oxygen Uptake Rate (OUR) Measurements

In the aerobic partial nitrification system and assuming no outflow is taking place and only a negligible oxygen supply from the inflow, the DO mass balance in the mixed liquor can be represented by Equation 3.1

$$OUR(t) = K_L a^T \left(DO_{sat}^T - DO^{(T)}\right) - \frac{dDO}{dt} \qquad (3\text{-}1)$$

Where OUR is the calculated oxygen uptake rate ($mgO_2 \cdot L^{-1} \cdot h^{-1}$), $K_La^{(T)}$ is the mass transfer coefficient($h^{-1}$), DO is the dissolved oxygen in the SBR ($mgO_2 \cdot L^{-1}$) and $DO_{sat}$ is the saturation dissolved oxygen as a function of temperature (T) ($mgO_2 \cdot L^{-1}$)

Oxygen uptake rates (OUR $mgO_2 \cdot L^{-1} \cdot h^{-1}$) were calculated off-line and based on the general oxygen mass balance in the bioreactor. Therefore, oxygen uptake rates were calculated from the slope of the oxygen decrease over time in accordance with the method described by Puig et al. (2005).

### 3.1.7 Oxidation Reduction Potential (ORP)

Oxidation Reduction Potential (ORP) or Redox is an electrochemical parameter that shows the activities of oxidizers and reducers in respect to their concentration. Positive values of ORP show that oxidizing substances (the ones that attract electrons, electron acceptors) are dominant in the analysed environment and negative values show that reducing conditions (electron donors) prevail. In the area of wastewater treatment ORP is used in biological nutrient removal systems, sewage prechlorination and dechlorination, chromate or cyanide reduction ORP level can also be viewed as the level of bacterial activities of the water because a direct link occurs between ORP level and bacteria count in the water. ORP, dissolved oxygen (DO) and pH are key parameter indicators (KPI) providing valuable information about the biological nitrification – denitrification process. In bio-treatment processes, ORP reflects the variations in DO concentration, organic substrate, microorganism activity and process inhibition (Mart ń, 2012). It was reported that ORP has been used as a tool for controlling operation of the

SBR reactor for separate treatment of filtrate water (Haker, 1999). However, Malovanyy (2009) first introduced ORP application into partial nitrification/Anammox.

An ORP meter measures very small voltages generated with a probe placed in wastewater water. The electrode is made of platinum or gold, which reversibly loses its electrons to the oxidizer. A voltage is generated which is compared to a silver (reference) electrode in a silver salt solution, similar to a pH probe. The more oxidizer available, the greater the voltage difference between the solutions. In this work we used ORP meter and electrode (HANNA HI 991003) to measure ORP.

## 3.2 Biomass Characteristics

### 3.2.1 Total Suspended Solid (TSS)

A well-mixed sample is filtered through a weighed standard 42 µm Whatman® qualitative filter paper and the residue retained on the filter is dried to a constant weight at 103 ℃ to 105 ℃. The increase in weight of the filter represents the total suspended solids. If the suspended material clogs the filter and prolongs filtration, it may be necessary to increase the diameter of the filter or decrease the sample volume. To obtain an estimate of total suspended solids, calculate the difference between total dissolved solids and total solids. (2540 D Standard Methods 1997).

Calculation

$$\text{Total suspended solids (mg /L)} = (A\text{-}B) \times 1000 \text{ /sample volume (mL)} \quad (3\text{-}2)$$

Where: A = weight of filter + dried residue (mg) and B = weight of filter (mg)

### 3.2.2 Volatile Suspended Solids (VSS)

Ignite residue produced by measurement of TSS to constant weight in a muffle furnace at a temperature of 550 ℃. Ignite a blank glass fibre filter along with samples. Have furnace up to temperature before inserting sample. Usually, 15 to 20 min ignition is required for 200 mg residue. However, more than one sample and/or heavier residues may overtax the furnace and necessitate longer ignition times. Let dish or filter disk cool partially in air until most of the heat has been dissipated. Transfer to a desiccator for final cooling in a dry atmosphere. Weigh disk as soon as it has cooled to balance

temperature. Repeat cycle of igniting, cooling, desiccating, and weighing until a constant weight is obtained or until weight change is less than 4% or 0.5 mg, whichever is less (2540 E Standard Methods 1997).

4. Calculation

$$Volatile\ Solids\left(\frac{mg}{L}\right) = \frac{(A-B)\times 1000}{Sample\ volume,mL} \quad (3\text{-}3)$$

Where:

$A$ = weight of residue + dish before ignition, mg

$B$ = weight of residue + dish or filter after ignition, mg

### 3.2.3 Average Diameter of the Granules

Biomass samples were observed with a digital camera (Coolsnap, Roper Scientific Photometrics). Images of the granular sludge were taken and least 100 granules were photographed per sample. The programme ImageJ was later employed for the digital image analysis.

### 3.2.4 Sludge Volume Index (SVI)

The Sludge Volume Index (SVI) determination is defined in the Standard Methods for the Treatment of Water and Wastewater (2710 D Examination of Water and Wastewater. 20th Ed1, 1997). The sludge volume index (SVI) is the volume in millilitres occupied by 1 g of a suspension after 30 min settling. SVI typically is used to monitor settling characteristics of involved sludge. Determine the suspended solids concentration of a well-mixed sample of the suspension (See Section 3.2.2).

$$SVI = \frac{Settled\ sludge\ volume(\frac{ml}{L})\cdot 1000}{Suspended\ solids\left(\frac{mg}{L}\right)} \quad (3\text{-}4)$$

## 3.3 Microbiological Determinations

### 3.3.1 Scanning Electron Microscopy (SEM)

The morphology of the microorganism in different bioreactors will be examined with high resolution SEM (Philips PSEM 501B Scanning Electron Microscope). The

specimens were fixed in 3% Glutaraldehyde in 0.1 M phosphate buffer at 4℃.The specimens were then washed in 0.1M phosphate buffer. The specimens were washed three times within 30 min interval at 4℃.Secondary fixation was carried out in 2% osmium tetroxide aqueous for 1 hour at room temperature. Dehydration was through a graded series of ethanol: 75% ethanol for 15min; 95% ethanol for 15min; 100% ethanol for 15min; 100% ethanol for 15min; 100% ethanol dried over anhydrous Copper sulphate for 15mins. All the above steps were carried out at room temperature.

The specimens were then air dried from Hexamethyldisilazane. Initially they were placed in a 50/50 mixture 0f 100% ethanol for 30mins followed by 30 mins in 100% Hexamethyldisilazane. The specimens were then allowed to air dry overnight before mounting.

Upon completion of drying, the specimens were mounted on 12.5mm diameter stubs and attached with Sticky Tabs and then coated in an Edwards S150B sputter coaster with approximately 25nm of gold.

The specimens were examined in a Philips PSEM 501B Scanning Electron Microscope at an accelerating voltage of 20Kv. Electron micrographs were recorded on Ⅱford.

### 3.3.2 Transmission Electron Microscope (TEM)

*Negative staining of samples

Prior to be stained with negative stain solution, carbon coated grids were performed by glow discharged for 30-40 sec (mainly depends on time length grids have been stored) by using a Cressington 208 power unit. 5 μl of the sample at a proper concentration was loaded onto the coated side of the grids and left for 1 min to adsorb. Excess sample was blotted out using Whatman filter paper and then quickly washed in one drop of distilled water and blotted again. Once blotted, immediately washed the grid in the second drop of distilled water and again blotted it. The grids were washed in the first drop of uranyl formate and blotted it once again and finally stained the grids in the other drop of uranyl formate for 20 sec. The grids were blotted by filter paper and remaining moisture was removed by a small vacuum pump. Grids were stored in a grid box before EM session.

*TEM identification of negatively stained samples

All negatively stained samples were examined and photographed using Philips CM100

transmission electron microscope (TEM) at an accelerating voltage of 100 kV. Digital micrographs were collected by size 1k x 1k using a Gantan Multiscan 794 CCD camera and viewed using Gatan Digital Micrograph (DM, Gatan Inc).

### 3.3.3 DNA Extraction

Sludge samples from partial nitrification and anammox bioreactors were respectively collected for further DNA analysis at different operation stage. The MoBio PowerSoil DNA extraction kit (MoBio Laboratories, Inc., USA) was utilized for DNA extraction process, following the manufacturer's instructions.

### 3.3.4 PCR Amplification

The DNA samples were amplified by polymerase chain reaction (PCR) using Bio-Rad (USA) thermal cycler C1000, with specific primers listed in the following Table 3.1&3.2. Each PCR was manipulated in 50 μL reaction system, containing 3 μL DNA template, 5 μL deoxyribonucleotide triphosphate (250 μM for each nucleotide), 0.5 μL DreamTaq DNA polymerase (New England Biolabs, UK), 1 μL BSA, 5 μL each pair of primers (5 μM) and 30.5 μL molecular water. The PCR programs for each reaction are illustrated in Table 3.3 with respective steps of initial denaturation, denaturation, annealing and elongation.

The presence and size of the DNA extraction or amplification product were determined by agarose gel (1% w/v) electrophoresis in in TAE buffer (40mM Tris-HCl, 20mM acetic acid, 1mM EDTA pH 8.0) containing Ethidium Bromide (Fisher Scientific). The electrophoresis was run at 70 volts for 25 minutes and the DNA bands were visualised using Versadoc imaging system with Quantity One software (Biorad).

### 3.3.5 qPCR Quantification

qPCR was performed in this research to quantify the copy numbers of the target genes, through SyBr Green dye to fluoresce when bound to dsDNA. The fluorescence signal of the target dsDNA template and products will be measured, calibrated by the standard curve which obtained by specific cloned plasmid with known copy number of target genes (Smith and Osborn, 2009).

All the target genes, including all the potential fragments mentioned in Table 3.1&3.2, were amplified and cloned into pGEM-T (Promega). Subsequently, the clone library was transferred into *E. coli* DH5α by heat shock, selected on LB agar plate with 30 μg/ml ampicillin as antibiotic pressure. The target plasmid was therefore extracted from the right clones after 37ºC overnight in a liquid LB medium with 30 μg/ml ampicillin as selection antibiotics, with Pure Yield™ plasmid extraction kit (Promega). The quantity of plasmid was verified by agarose gel (1% w/v) electrophoresis and digested by SalI restriction enzyme (New England Biolab, UK) to be linearized. The digestion was carried out in appropriate Buffer IV (New England Biolab, UK) for 2 hours at 37 ºC and the enzyme was inactivated by 65 ºC heating for 20 minutes.

The copies of dsDNA were determined by Picogreen assay (Promega), and subsequently diluted to 108 to 103 copies per micron liter as standard DNA template for qPCR. The reaction system of qPCR contained 25 μl IQ Supermix (Biorad), 0.25 μl SYBR GREEN I Nuclid DNA stain probe stock solution, 23.75 μl molecular water and 2 μl target DNA template. 2 μl molecular water was added instead of DNA template as 'No Template Control' (NTC) and all the reactions were carried out in duplicate.

The extracted DNA from AOB, NOB and anammox bacteria was amplified and quantified in CFX96 real time PCR detection system (Biorad) with the same program as shown in Table 3.3. Particularly, after the last cycle of the final extension step (72ºC, 5 minutes), the generation of a melting curve was carried out to determine the profiles of amplified DNA. qPCR analysis was carried out by Biorad's CFX Manager software in accordance with the calibration curve were obtained. The number of target sample DNA copies was calculated through comparison with the fluorescence of the standard curve. Copy numbers from samples that have a threshold cycle (Ct) greater than the cutoff cycle cannot be estimated with confidence. The cutoff cycle is either the threshold cycle for the NTC minus 3.3 or, if the NTC does not amplify, the total number of cycles minus 2.3. This ensures that copy number is at least one order of magnitude greater than the NTC (Smith and Osborn, 2009)

**Table 3.1** Primers for DNA amplification for AOB and NOB

| Group | Primer | Target gene | Orientation | Sequence (5' to3') | Reference |
|---|---|---|---|---|---|
| **Ammonia oxidizing bacteria** | **NSMmob-988F** | *Nitrosococcus mobilis*-cluster (pNmob) | Forward | GCTTGGAATTTTACGGAGAC | Lim et al., 2007 |
| | **NSMmob-1282R** | | Reverse | CTACGAAGTGCTTTGTGAG | Lim et al., 2007 |
| | **NSMeur-828F** | *Nitrosomonas europaea*-cluster (pNeur and pNhal) | Forward | GTTGTCGGATCTAATTAAG | Lim et al., 2007 |
| | **NSMeur-1028R** | | Reverse | GTGTCTTGGCTCCCTTTC | Lim et al., 2007 |
| | **NSMcry-211F** | *Nitrosomonas cryotolerans*-cluster (pNcry and pN343) | Forward | AGACCTTRTGCTTTTGGAG | Lim et al., 2007 |
| | **NSMcry-434R** | | Reverse | TTTTCTTCTCRACTGAAAGAG | Lim et al.,2007 |
| | **NSS-209F** | *Nitrosospira* genus (pNmul) | Forward | CAAGACCTTGCGCTYTT | Lim et al., 2007 |
| | **NSS-478R** | | Reverse | TCTTCCGGTACCGTCAKT | Lim et al., 2007 |
| **Nitrite oxidizing bacteria** | **F1370** | *nxrA* | Forward | CAGACCGACGTGTGCGAAAG | Wertz et al., 2008 |
| | **F2843R** | | Reverse | TCCACAAGGAACGGAAGGTC | Wertz et al., 2008 |
| | **FGPS27F** | *Nitrobacter* | Forward | GAGTTTGATCCTGGCTCAG | van der Star, et al., 2007 |
| | **FGPS1269R** | | Reverse | TTTTTTGAGATTTGCTAG | van der Star, et al., 2007 |

**Table 3.2** Primers for DNA amplification for Anammox Bacteria and Denitrifiers

| Group | Primer | Target gene | Orientation | Sequence (5' to3') | Reference |
|---|---|---|---|---|---|
| **Anammox bacteria** | **Pla46F** | *Planctomyctales* | Forward | GGATTAGGCATGCAAGTC | Stara et al.,2007 |
| | **Amx667R** | | Reverse | ACCAGAAGTTCCACTCTC | Stara et al.,2007 |
| | **Amx336** | *Anammox A* | Forward | AGTGGCGAAAGGGTGAGTAA | Fujii, et al.,2002 |
| | **Amx337** | | Reverse | TGTCTCAGTCCCAGTGTGGC | Fujii, et al.,2002 |
| | **Amx260** | *Anammox B* | Forward | TGGCGGCGTGGTTTAGGC | Fujii, et al.,2002 |
| | **Amx362** | | Reverse | GGTTACCTTGTTACGACT | Fujii, et al.,2002 |
| | **Pla461F** | *Anammox C* | Forward | GACTTGCATGCCTAATCC | Schmid et al., 2005 |
| | **1390R** | | Reverse | GACGGGCGGTGTGTACAA | Schmid et al., 2005 |
| | **Amx368F** | *Anammox D* | Forward | TTCGCAATGCCCGAAAGG | Schmid et al., 2005 |
| | **Amx820R** | | Reverse | AAAACCCCTCTACTTAGTGCCC | Schmid et al., 2005 |
| **Denitrifiers** | **338** | Bacteria 16S | Forward | ACTCCTACGGGAGGCAGCAG | Lopez et al., 2003 |
| | **530R** | Bacteria 16S | Reverse | ATTACCGCGGCTGCTGG | Lopez et al., 2003 |
| | **nirS4QF** | *Pseudomonas fluorescens* | Forward | GTSAACGYSAAGGARACSGG | Throback et al., 2004 |
| | **nirS6QR** | | Reverse | GASTTCGGRTGSGTCTTSAYGAA | Throback et al., 2004 |
| | **nirK876F** | Cloned from real samples | Forward | ATYGGCGGVCAYGGCGA | Henry et al., 2004 |
| | **nirK1040R** | | Reverse | GCCTCGATCAGRTTRTGGTT | Henry et al., 2004 |

**Tale 3.3** PCR reaction programs

| **Primers** | **Forward** | **330F** | **Pla46F** | **Amx336F** | **Amx260F** | **Pla461F** | **Amx368F** | **nirS4QF** | **nirK876F** |
|---|---|---|---|---|---|---|---|---|---|
| | **Reverse** | **530R** | **Amx667R** | **Amx337R** | **Amx362R** | **1390R** | **Amx820R** | **nirS6QR** | **nirK1040R** |
| **Initial denaturation** | **Temperature ($^{o}$C)** | 94 | 94 | 94 | 94 | 94 | 94 | 94 | 94 |
| | **Time (min)** | 10 | 4 | 5 | 5 | 5 | 4 | 5 | 5 |
| **Denaturation** | **Temperature ($^{o}$C)** | 94 | 94 | 94 | 94 | 94 | 94 | 94 | 94 |
| | **Time (min)** | 0.5 | 0.5 | 0.5 | 0.5 | 0.5 | 0.5 | 0.5 | 0.5 |
| **Annealing** | **Temperature ($^{o}$C)** | 58 | 56 | 56 | 56 | 56 | 56 | 58 | 58 |
| | **Time (min)** | 0.5 | 0.75 | 1 | 1 | 1 | 0.75 | 0.5 | 0.5 |
| **Elongation** | **Temperature ($^{o}$C)** | 72 | 72 | 72 | 72 | 72 | 72 | 72 | 72 |
| | **Time (min)** | 1 | 0.75 | 0.75 | 0.75 | 0.75 | 0.75 | 1 | 1 |
| **Final Elongation** | **Temperature ($^{o}$C)** | 72 | 72 | 72 | 72 | 72 | 72 | 72 | 72 |
| | **Time (min)** | 5 | 5 | 5 | 5 | 5 | 5 | 5 | 5 |
| **Cycle** | | 35 | 35 | 35 | 35 | 35 | 35 | 35 | 35 |

.

| Primers | Forward | NSMmob-988F | NSMeur-828F | NSMcry-211F | NSS-209F | Pla461F | F1370 | FGPS27F |
|---|---|---|---|---|---|---|---|---|
| | Reverse | NSMmob-1282R | NSMeur-1028R | NSMcry-434R | NSS-478R | 1390R | F2843R | FGPS1269R |
| Initial denaturation | Temperature (ºC) | 94 | 94 | 94 | 94 | 94 | 94 | 94 |
| | Time (min) | 10 | 10 | 10 | 10 | 10 | 10 | 10 |
| Denaturation | Temperature (ºC) | 94 | 94 | 94 | 94 | 94 | 94 | 94 |
| | Time (min) | 0.5 | 0.5 | 0.5 | 0.5 | 0.5 | 0.5 | 0.5 |
| Annealing | Temperature (ºC) | 56 | 56 | 56 | 56 | 56 | 56 | 56 |
| | Time (min) | 0.5 | 0.5 | 0.5 | 0.5 | 0.5 | 0.5 | 0.5 |
| Elongation | Temperature (ºC) | 72 | 72 | 72 | 72 | 72 | 72 | 72 |
| | Time (min) | 1.5 | 1.5 | 1.5 | 1.5 | 1.5 | 1.5 | 1.5 |
| Final Elongation | Temperature (ºC) | 72 | 72 | 72 | 72 | 72 | 72 | 72 |
| | Time (min) | 5 | 5 | 5 | 5 | 5 | 5 | 5 |
| Cycle | | 35 | 35 | 35 | 35 | | 35 | 35 |

## 3.6 Synthetic Wastewater

Table 3.4 and 3.5 shows the composition of the partial nitrification and Anammox (Modified from van Dongen et al., 2001; Trigo et al., 2006; Noophan et al., 2009) mineral medium and traces solution respectively. This medium was used as a base to prepare the different synthetic feedings treated by some of the reactors employed in this Thesis, as it is detailed in the Materials and methods section of each chapter.

**Table 3.4** Composition of growth medium for Partial nitrification

| Composition | Concentration(mg/L) | Composition | Concentration(mg/L) |
|---|---|---|---|
| $(NH_4)_2SO_4$ | Variable | EDTA | 250mg/L， |
| $NH_4Cl$ | Variable | $FeSO_4 \cdot 7H_2O$ | 25 mg/L |
| $MgSO_4 \cdot 7H_2O$ | 7.005 mg/L | $ZnSO_4 \cdot 7H_2O$ | 11 mg/L |
| NaCl | 205.72 mg/L | $CaCl_2 \cdot 2H_20$ | 27.7mg/L |
| $KHCO_3$ | Variable | $MnCl_2 \cdot 4H_20$ | 25.3mg/L |
| $KH_2PO_4$ | 25.72 mg/L | $CuSO_4 \cdot 5H_20$ | 7.85 mg/L |
| | | $(NH_4)_6Mo_7O_{24} \cdot H_2O$ | 5.5 mg/L |
| | | $CoSO_4 \cdot 6H_2O$ | 9.5 mg/L |

**Table 3.5** Composition of growth medium for Anammox

| Composition | Concentration(mg/L) | Composition | Concentration(g/L) |
|---|---|---|---|
| $NaNO_2$ | Variable | EDTA | 0.016g/L |
| $(NH4)_2SO_4$ | Variable | $FeSO_4$. | 0.186g/L |
| $KHCO_3$ | Variable | $ZnSO_4 \cdot 7H_2O$ | 0.43g/L |
| $KH_2PO_4$ | 180mg/l | $CoCl_2 \cdot 6H_2O$ | 0.24g/L |
| $CaCl_2 \cdot 7H2O$ | 47mg/l | $MnCl_2 \cdot 4H_2O$ | 0.99g/L |
| $MgSO_4 \cdot 7H_2O$ | 52mg/l | $CuSO_4 \cdot 5H_2O$ | 0.25g/L |
| $FeSO_4$/EDTA | 9.08/6.25mg/l | $NaMoO_4 \cdot 2H_2O$/L | 0.22g/L |
| Traces solution | 10ml/l | $NiCl_2 \cdot 6H_2O$; | 0.19g/L |
| | | $NaSeO_4 \cdot 10H_2O$ | 0.21g/L |

# Chapter 4. Performance of Airlift Loop Bioreactor with Microbubble Generation by Fluidic Oscillation

This work investigated the working performance of a biphasic airlift loop reactor equipped with a fluidic oscillator producing microbubbles. Experiments were carried out to examine the effect of microbubble on the performance of deoxygenation and oxygenation processes for an airlift loop bioreactor. Since an ideal aeration environmental and the strictly anaerobic conditions required by Partial nitrification and Anammox process respectively are potentially able to enhance these two biological processes, this study offers an essential basis for the subsequent work.

## 4.1 Introduction

Recently, how to improve the gas-liquid mass transfer efficiency is growing to become the focus of investigation for enhancing the efficiency of performance of the biochemical process, for instance wastewater treatment and biopharming. Mass transfer rates in a bioreactor are largely influenced by the fluid properties, liquid circulation, superficial gas velocity, the geometric structure and type of bioreactor (Reyna-Velarde et al., 2010). In turn the overall volumetric mass transfer coefficient, $k_La$, is an essential engineering data to measure and characterise the mass transfer capacity of the gas-liquid contactor (Schugerl, 1990), as well as one of the critical parameters for designing a biphasic (gas-liquid) or triphasic (gas–liquid–solid) reactors adapted for the bioprocess especially aerobic process where the solubility of oxygen is very low.

An ideal reactor should be the one possessing of a maximum mass transfer rate with a minimum energy input (Gaddis, 1999; Rainer et al., 1990; Gogate et al., 1999). Airlift loop reactor (Zimmerman et al., 2009) is increasingly employed in biotechnology and multiphase chemical reactions due to its loads of benefits: low cost and simple structure without moving mechanisms, higher shear stress favouring to settling-ability of microbes and low energy costs compared with mechanically stirred tank (Blaz Ej et al.,2004). As an airlift loop bioreactor consisted of the upflow region and the downflow region, a liquid circulation, the major cause of the good mixing and high mass transfer efficiency, is induced by the hydrostatic unequilibrium as a result of the density difference between the riser and the downcomer (Dhaouadi et al.,2001).

The volumetric mass transfer coefficient $k_La$ is the rate of gas transferring across the gas–liquid interface per unit liquid volume and per unit driving force (Juraˇsˇc´ık et al., 2006). Hence, apart from the application of the novel airlift loop reactor, the other method of enhancing gas–liquid mass transfer for the ALB is to decrease the size of gas bubble, which means increasing gas-liquid interfacial area and prolonging the residence time of gas bubbles in the aquatic media before leaving the system. The early literature reported many ways to provide a larger interfacial surface area to volume ration for the gas bubbles, including the use of static mixers, perforated plates (Krichnavaruk et al., 2002) and baffles ( Fadavi et al., 2005). Below a novel fluidic oscillator, which had proved to be capable of producing 10 to 100 times smaller than the size of bubbles generated by conventional aeration systems (Zimmerman et al. 2008), was used to produce fine distributions of microbubbles with a range of diameter approximately 60~600 μm.

It should be noted that hydrodynamic stabilisation avoids coalescence between these small bubbles. The fluidic oscillator approach also decreases the friction losses in pipe networks and nozzles or diffusers due to boundary layer disruption; therefore big energy savings are possible.

The performance of aeration process and deoxygenating process for a square gaslift loop reactor with microbubble generation system was in depth investigated in this experiment at different airflow rates. In terms of Xiaoping Lu's finding the characteristics of the square airlift loop reactor appear better than those of round airlift loop reactor.

The performance of the gaslift loop reactor was evaluated when the oscillator was applied as microbubble generator compared to that without this device in order to determine to what extent volumetric mass transfer coefficient can be improved. Afterwards the performances of the gaslift loop reactor were simulated using sing COMSOL Multiphysics version 4.1.

## 4.2 Design of Air Lift Loop Bioreactor with Microbubble Generation by Fluidic Oscillation

The airlift loop reactor was first clearly defined and patented by Lefrancois in 1955. Initially, the device was mainly applied to large-scale microbiological processes, such

as single cell protein (SCP) production (Merchuk and Siegel, 1988). Airlift loop reactor offers the possibility of very simple and highly effective fluidisation which suggests a high potential for application in three phase processes where gas, liquid, and solids must be brought into contact. In other words airlift loop reactors are believed to possess advantages over both bubble columns and stirred tank bioreactors for many applications. Thus over the last few years airlift loop reactors have received wide interest in the research and development technical literatures for many different applications such as environmental biotechnological and Production of citric acid.

Airlift loop reactors have no mechanical agitators (stirred tank). The transformation is achieved by fluid circulation as a result of hydrostatic pressure difference in a defined cyclic pattern through channels built specifically for this purpose. Indeed, all the properties of the airlift loop reactor are linked and are a consequence of this cyclic circulation and the two- or three- phase flow characteristics.

There are multiple objectives for the optimisation of ALB design to increase energy efficiency. Given the importance of energy usage in the operation of ALBs, the sparging system is a crucially important consideration, as it is the central power consumption feature for the ALB. A design of an airlift loop bioreactor with fluidic oscillation producing microbubble was put forward by Zimmerman et al. (2009). The microbubble generation mechanism has been demonstrated to achieve high mass transfer efficiency by the decrease of the bubble size, by longer residence times that offsets slower convection, and by hydrodynamic stabilisation that avoids coalescence increasing the bubble diameter. Moreover, as a result of boundary layer disruption, the fluidic oscillator approach was able to decrease the friction losses in pipe networks and in nozzles/diffusers. As consequent there is actually an energy consumption savings by using the fluidic oscillator over the steady flow. From the point of view of these dual advantages a novel airlift loop bioreactor engaged with the microbubble generation approach is bound to be promising for various biological processes.

All airlift reactors, regardless of the configuration (external loop or baffled vessel), comprise four distinct sections with different flow characteristics. Therefore, each section may have different characteristics in terms of momentum, mass and heat transfer, as well as yield. The four sections are (Merchuk and Marc, 1987; Zimmerman et al., 2009)

1. The riser: Upwards flow is predominant in this section of the airlift reactor. The diffuser is usually installed at the bottom of the riser; the gas from the bottom is injected into the reactor. The riser is the phase transfer workhorse of the ALB. The gas–liquid mass transfer and liquid–bioculture mass transfer are the dominant features of this region. This section is the major target for performance enhancement for the introduction of microbubbles.

2. The downcomer: This section is parallel to the riser and connected to it at the bottom and at the top. The dispersion recirculates in a downward direction in the downcomer. This is probably the least dynamically important region of the ALB, because its composition and bioculture occupation depend on the particulars of the riser design. The driving force of this recirculation is the difference in mean density or hydrostatic pressure between these two sections, the lower the gas fraction in the downcomer. Thus this region has the highest multiphase density, largely occupied with liquid, and perhaps lowers dissolved oxygen (gas) concentration and lower gas phase hold up. However the microbubble introduced into the ALB will be small enough to make it possible that the bubble rise will sufficiently transfer momentum to the liquid so that the liquid phase flow will be strong enough to entrain some of the microbubbles in the downcomer.

3. The base: In the majority of airlift designs, the bottom connection zone between the riser and downcomer is very simple and usually not considered as significantly affecting overall reactor behaviour. However, the design is focusing on this part as the gas sparger and the bubble distribution are located in the base (Fig. 4.1) where fluidic oscillator and ceramic diffuser distribution system has been substituted for the traditional base. The free and forced convection flow supplied by the injection flow and contributed by the dragging of the liquid by the rising bubbles has only a finite amount of kinetic energy available. Therefore friction losses should be minimised all over the ALB as the flow is holistic throughout the ALB. In this respect, the oscillatory flow responsible for lower friction is very significant for the pipework design of the wastewater treatment.

4. The gas separator: This section is at the top of the reactor connecting the riser to the downcomer and has the obvious function of communicating between these two sections, allowing for liquid recirculation and gas disengagement.

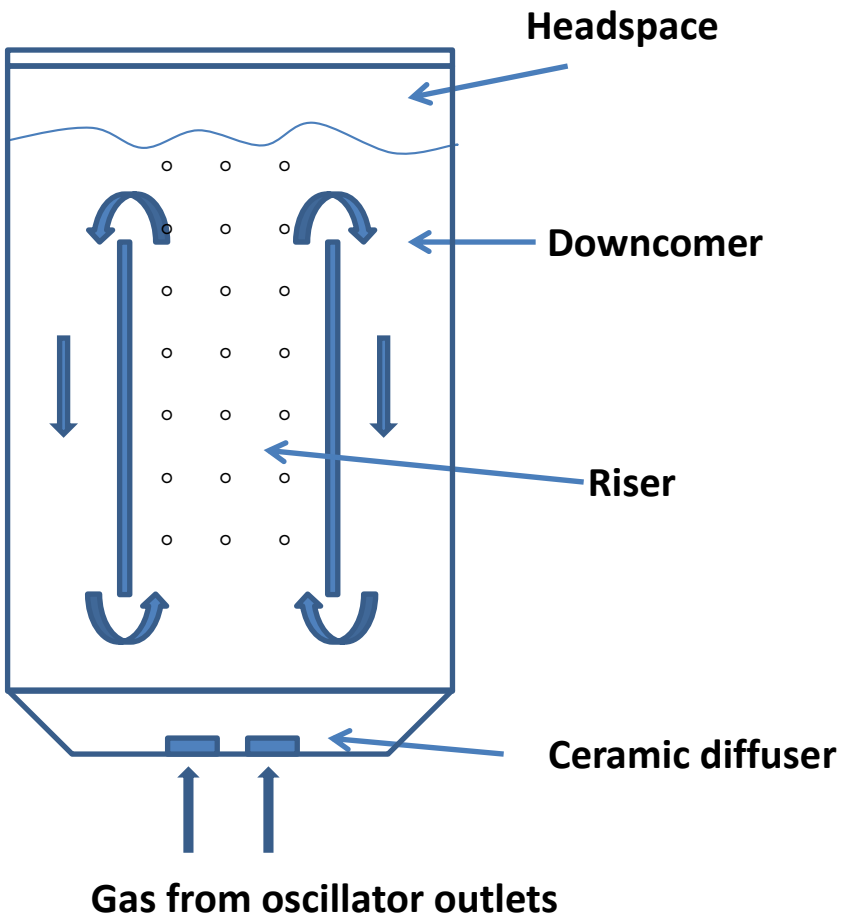


**Figure 4.1** Schematic diagram of an internal ALB with draught tube configured with ceramic diffuser fed from the two outlets of the fluidic oscillator

## 4.3 Bubble Size Distribution

According to the study of Hanotu et al. (2011) the average bubble size generated through the fluidic oscillator is approximately only twice larger than the diffuser pore size while the average bubble size achieved under steady air flow is several orders of magnitude lager than the exit aperture size and the difference is huge surprisingly up to 967 μm. As we discussed above, the fluidic oscillation proved to successfully generate microbubbles of the scale of diffuser aperture size, yet the fluidic oscillation is hardly to release equal-sized microbubbles. Difference in bubble size is simply attributed to the fluidic oscillator. In practical application, bubble size and number of bubbles making great contribution to behaviour and property of microbubbles is a vital operating and control variable (Edzwald, 2010), therefore the observation of bubble size distribution appears especially essential

There are assorted methods developed for measuring the size of bubbles generated in a liquid phase such as optical detectors, acoustical techniques and in situ measurement device ( Junker et al., 2007). By far optical means in bubble size characterisation is the most widely employed technique. Often many times visual observation is believed to be painstaking and time consuming to carry out due to the size and number of bubbles at issue. The accuracy of measurement is a function of different factors such as light and medium clarity as well as the software engaged in bubble analyses, any of which if not properly represented can bring errors to estimations of the bubble diameter particularly in high bubble flux conditions and turbid media.

Microfluidics group from University of Sheffield employed a high speed camera at 1000fps and resolution of 1024 x 1024 to analyse the microbubble generated by fluidics oscillator. Snap shots and video images were captured and the files were uploaded into a computer. A dark coloured material was placed at the opposite side of the flotation tank to aid the visualisation of the bubbles. Also, external lighting was utilised to avoid dark areas or dark bubble images and to help obtain clear images. The calibration of the field of view was carried out using a scale rule with known dimension in order to get the number of pixels that is equivalent to a certain length. Experiments were conducted with the no-moving fluidic oscillator. The image analysis was conducted using digital image analyser software "Image J". Parameters such as the bubble diameter, average size and standard deviation can then be calculated. Hence, a bubble size distribution can be determined from the results obtained.

The Fig 4.2 shows the distribution of microbubbles produced at a supply flow rate of 80L/min through the oscillator from the 20mm pore-sized ceramic diffuser at operating pressure of 0.5 bar (Table 4.1). A portion of the air supply downstream the oscillator was bled-off to match diffuser and the Fig4.3 shows the distribution of fine bubble produce under the same conditions. The result illustrated minimum and maximum sizes recorded were 163.5μm and 621.08μm respectively with an average bubble size of 311.87μm and standard deviation of 199.5 mm. For fine bubble the minimum and maximum sizes recorded were 632.1μm and 1314μm respectively with an average bubble size of 995μm.

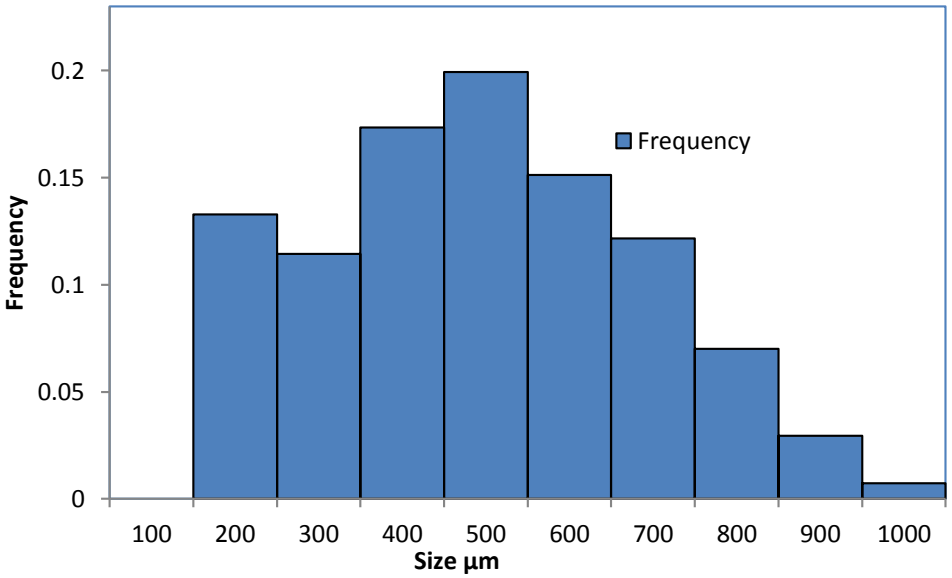


**Figure 4.2** Microbubble size distribution from a microporous ceramic diffuser at 0.5bar

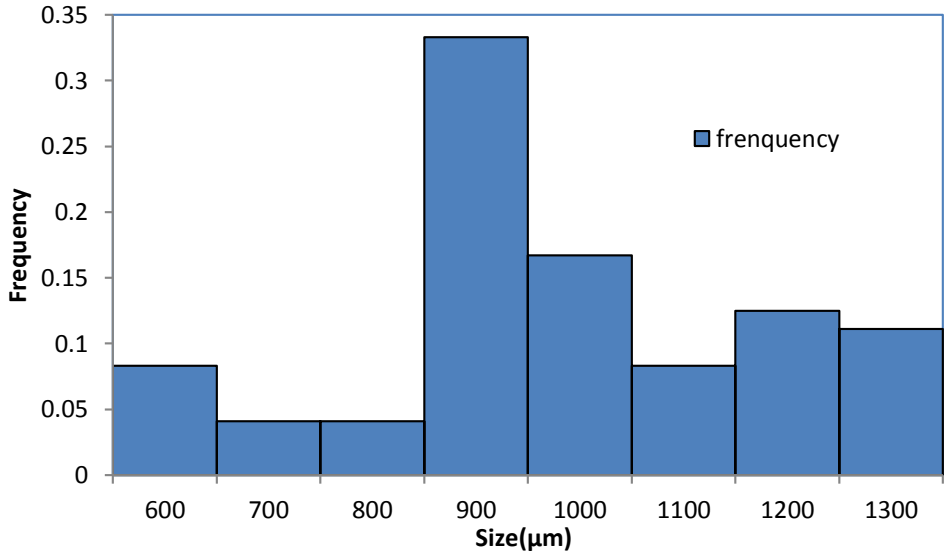


**Figure 4.3** Fine bubble size distribution from a microporous ceramic diffuser at 0.5bar

**Table 4.1** Operational parameters for Bubble size distribution from a microporous ceramic diffuser

| Experiment | Bubble Size Distribution Analysis |
|---|---|
| Diffuser | Square Ceramic Diffuser |
| Pore size | 20 microns |
| Fluidic Oscillator | Yes- Four Plate Valve I |
| Feedback Loop Length | 30cm |
| Air pressure | 0.5bar |
| Main Flow rate | 80L/min |
| Water Height Above Diffuser | 0.13m |
| Camera | Photron |
| Frames per Second | 500 |
| Shutter speed | 1/frame |

## 4.4 Thin Film Theory of Mass Transfer Coefficients. ($K_La$)

Gas-liquid mass transfer is of paramount importance in bioprocess because of the requirement for oxygen in aerobic bioreactors and the exclusion of oxygen for anaerobic bioprocess. Rates of volumetric mass transfer are directly proportional to the concentration driving force and the area available for the transfer process to take place. This can be expressed as

Transfer rate= (mass transfer coefficient)×(transferarea)×(driving force)

For each fluid on either side of a phase boundary, the driving force for mass transfer can be expressed in terms of a concentration difference. Therefore, the rate of mass transfer to a phase boundary is given by the equation

$$N_A = ka \triangle C_A \qquad (4\text{-}1)$$

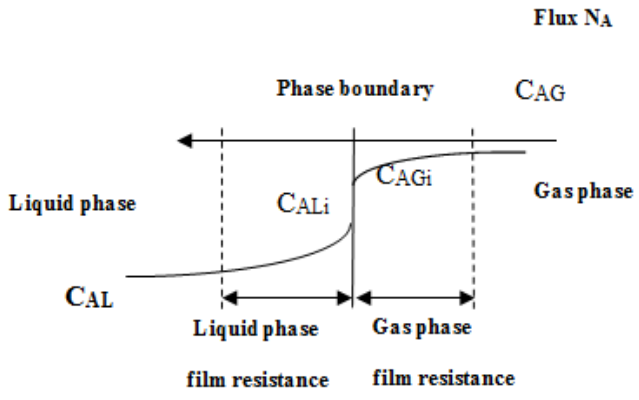


**Figure 4.4** Concentration gradients for gas-liquid mass transfer for a general component A

Fig.4.4 shows the situation an interface between gas and liquid phase containing a general component A which is transferred from the gas phase into liquid phase. The bulk concentration of A in the liquid is $C_{AL}$ in the bulk and $C_{ALi}$ at the interface.

The equation rate of mass transfer of A through the liquid boundary layer is :

$$N_{AL}=k_L a(C_{ALi}-C_{AL}) \qquad (4\text{-}2)$$

Similarly, the equation rate of mass transfer of A through the gas boundary layer is :

$$N_{AG}=k_{Ga}(C_{AG}-C_{AGi}) \qquad (4\text{-}3)$$

where $k_G$ is the gas-phase mass-transfer coefficient and $k_L$ is the liquid-phase mass-transfer coefficient. For dilute concentrations of most gases and for a wide range of concentration of some gases, the equilibrium concentration in the gas phase is a linear function of liquid concentration. Therefore we can write:

$$C_{ALi} = \frac{C_{AGi}}{m} \qquad (4\text{-}4)$$

where, m is distribution factor. This equilibrium relationship can be incorporated into 4-2 to give:

$$N_A = \left(\frac{1}{mk_G a} + \frac{1}{k_L a}\right) = \frac{C_{AG}}{m} - C_{AL} \qquad (4\text{-}5)$$

The overall liquid-phase mass transfer coefficient $K_L$ is defined as:

$$\frac{1}{K_L a} = \frac{1}{mk_G a} + \frac{1}{K_L a} \qquad (4\text{-}6)$$

The rate of mass transfer in gas-liquid systems can therefore be expressed using the equation:

$$N_A = K_L a(\frac{C_{AG}}{m} - C_{AL)} \qquad (4\text{-}7)$$

In Eq. 4-7 above, $\frac{C_{AG}}{m}$ is equal to $C^*_{AL}$, the liquid-phase concentration of A in equilibrium with $C_{AG}$. Eq. 4-7 becomes

$$N_A = K_L a(C^*_{AL} - C_{AL}) \qquad (4\text{-}8)$$

During the re-oxygenation step, the rate of change in dissolved-oxygen concentration during this period is equal to the rate of oxygen transfer from gas to liquid

$$\frac{dC_{AL}}{dt} = N_A = k_L a(C^*_{AL} - C_{AL}) \qquad (4\text{-}9)$$

Assuming $k_La$ is constant with time, we can integrate Eq. 4-9 between t1 and t2 to give the following equation for $k_La$:

$$k_L a = \frac{ln(\frac{C^*_{AL} - C_{AL1}}{C^*_{AL} - C_{AL2}})}{t_1 - t_2} \qquad (4\text{-}10)$$

$k_La$ can be estimated using two points from several values of ($C_{AL1}$,$t_1$) and ($C_{AL2}$,$t_2$).

By plotting $\ln\left(\frac{C^*_{AL} - C_{AL1}}{C^*_{AL} - C_{AL2}}\right)$ versus ($t_2$-$t_1$) , the $k_La$ could be determined from the slope of the line.

For this experiment, the thin film theory described above was used to determine the volumetric mass transfer coefficient $k_La$ in the airlift bioreactor.

## 4.5 Materials and Methods

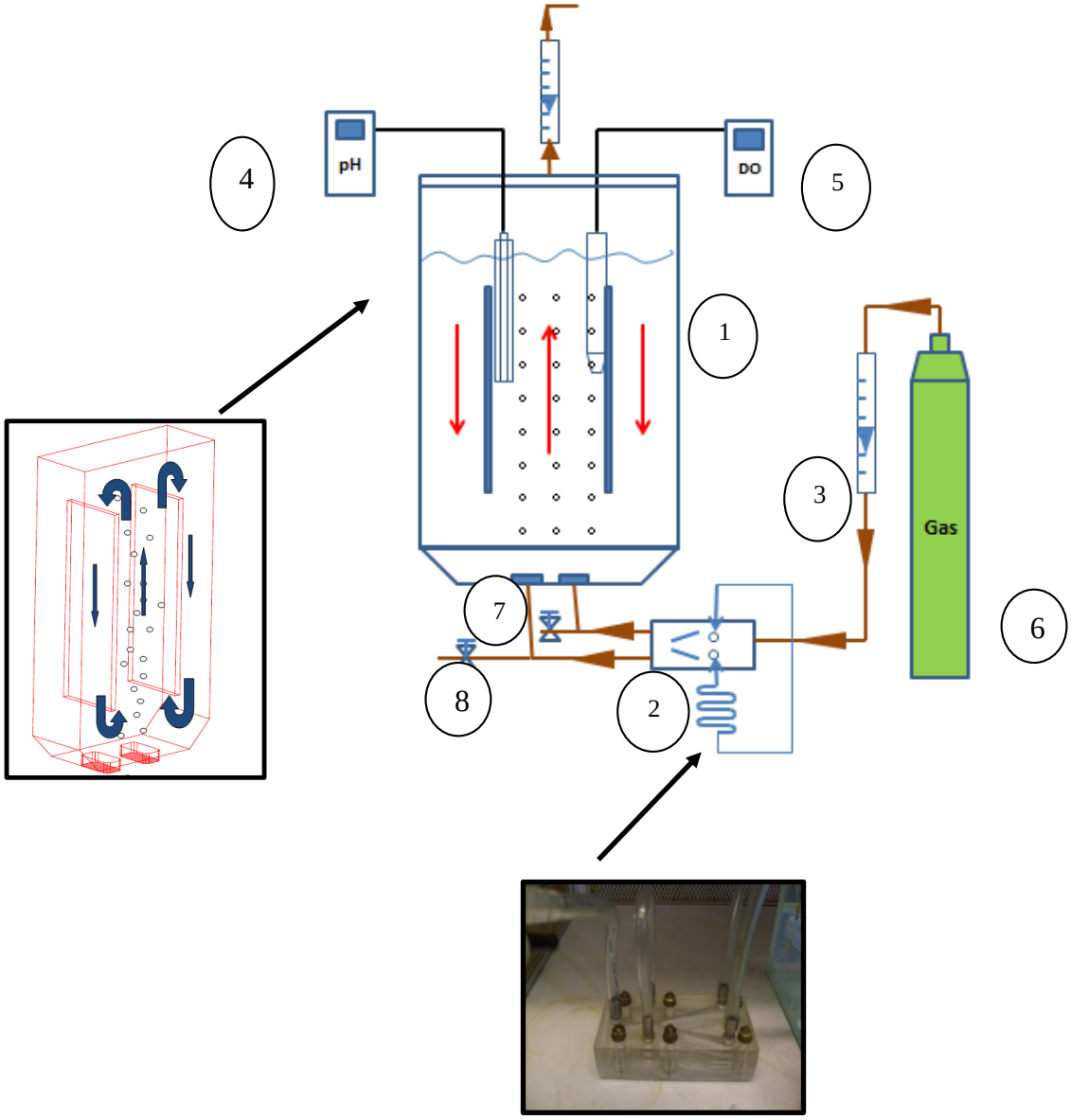


**Figure.4.5** Experiment schematic 1. Gaslift reactor, 2. Fluidic oscillator, 3. Rotameter, 4 pH meter and Probe rotameter, 5. DO meter and probe, 6 Gas (Air/$CO_2$ 10%/N2), 7.Ceramic Diffuser, 8. Bleeding off

A schematic diagram of the experimental setup for this work is shown in Fig.4.5. The square airlift loop reactor applied in this work was made of clear plexiglass to enable visual observation for the behavior of the whole system. The airlift loop reactor with 5 liters working volume was divided into the riser area and two downcomer areas by insertion of gas-liquid partition plate shown in Fig 4.5 Air supplied from a laboratory compressor was injected through two identical diffusers with twenty microns pore size. This diffusers made of ceramic plate were installed at the base of the reactor. An oxygen probe (EXTECH Model 407510) and pH probe located 10 cm above the base of the rise

region of the airlift loop reactor was used to measure the change in dissolved oxygen concentration and pH with time. Due to the characteristics of the construction of the microfluidic oscillator, gas flow rate was controlled by one master calibrated rotameter on the main airflow and one branch calibrated rotameter on the top of the reactor to control the main air flow rate and the real air flow rate into the reactor. To do so is because oscillation of gas input could not be simply measured by rotameters.

All experiments were operated under atmospheric pressure with water temperature of 26.6℃ whilst compressed air or mixed gas $CO_2$10%/$N_2$ were used as gas phase respectively for aeration and deoxygenating processes. The gas flow rate varied from 0.3 to 0.7 $Lmin^{-1}$. Deionized water was used as liquid phase. Blazej (2004) reported there is no difference between air and pure oxygen as gas phase when volumetric oxygen transfer coefficient $K_La$ was object investigated. For the deoxygenating process liquid phase is flushed with mixture of $CO_2$ 10%/$N_2$ by using fluidic oscillator while pH and DO were recorded with certain interval of time until approaching constant. The same experiments were repeated under different conditions with and without microbubble generator respectively.

The volumetric mass transfer coefficient, $K_La$ for the airlift loop reactor was determined experimentally using the film theory discussed above. Cobalt chloride (0.044g) (role as a catalyst) and sodium sulphite (1.5g) were added into the water in order to completely remove dissolved oxygen from the liquid phase in an airlift loop bioreactor. Subsequently aeration commenced and increasing of dissolved oxygen concentration with time was recorded by DO meter until the oxygen concentration was nearly saturated in the liquid. $k_La$ was calculated with reference to the airlift loop reactor from the following expression obtained by simplifying Eq4-10 (H. Dhaouadi et al.,2001)

$$K_La = \frac{1}{t}\ln\left(\frac{C^*-C_0}{C^*-C_L}\right) \quad (4\text{-}11)$$

Where C* is the dissolved oxygen (DO) saturation concentration, $C_0$ was chosen to be 1, and $C_L$ is the DO concentration at time $t=t_L$. $C_L$ was collected through experiment. When plotting the right-hand-side of the equation above against time, the slope of the line was $-k_La$. Several different air flow rates and feedback lengths were used as indicated in the results.

## 4.6 Results and Discussion

### 4.6.1 Oxygen Mass Transfer Efficiency

Dissolved oxygen is an important substrate in aerobic bioprocess. Since oxygen is sparingly soluble in water, it may be the growth-limiting substrate in these bioprocess. For bacteria and yeast cultures, the critical oxygen concentration is about 10% to 50% of the saturated DO (dissolved oxygen concentration).

The effect of bubble size on the dissolution rate of oxygen has been investigated through a series of tests using DO variation with time. Fig 4.6 shows the time required for dissolved oxygen concentration to increase from zero to 7mg/L in different airlift loop reactors with and without fluidic oscillator under different air flow rates, which indicated that the dissolved oxygen in the air lift loop reactor with fluidic oscillator achieved saturated concentration faster than that in the airlift loop reactor without fluidic oscillator. It was observed that more obvious improvement, 40% time saving, was found at low air flow rate 0.3L/min while 30% time was saved to get saturated oxygen concentration at air flow rate of 0.7L/min. The gas-liquid mass transfer is responsible for the oxygen concentration increasing during the aeration process and the different times needed was attributed to different gas-liquid mass transfer coefficient. As shown in Fig 4.6, it is clear that ALB equipped with fluidic oscillator always obtained higher oxygen mass transfer coefficient $k_La$ compared with the ALB with fine bubble aeration system. In order to confirm this result the volumetric mass transfer coefficient $k_La$ was calculated based on the method described above. Fig.4.7 shows the evolutions of the oxygen mass transfer coefficient $k_La$ with the air flow rate for different aeration systems. In both cases, oxygen volumetric mass transfer coefficients $k_La$ increased with air flow rate. Under the same operating conditions a remarkable improvement of approximate 38.9% in oxygen mass transfer efficiency was obtained by adoption of fluidic oscillator. The air transfer coefficient $k_La$ is a device-dependent parameter. The larger the contact surface area between the gas phase and liquid phase, the better the gas transfer efficiency is. Clearly this expected progress is attributed to the unique properties of microbubble, which mainly characterized by diameter of 100~600μm. Compared with fine bubbles, it has two distinct advantages: larger interface mass transfer areas and lower rising velocity causing the increasing of gas-liquid mass transfer efficiency of the reactor. Fluidic oscillator is capable of producing microbubble simply depending on its unique configuration through inducing mechanism

of oscillation and no need to consume a great deal energy. In this work the new aeration device was introduced to the biological nitrogen removal process to investigate to what extent the performance of the partial nitrification process can be promoted compared to the normal aeration system applied.

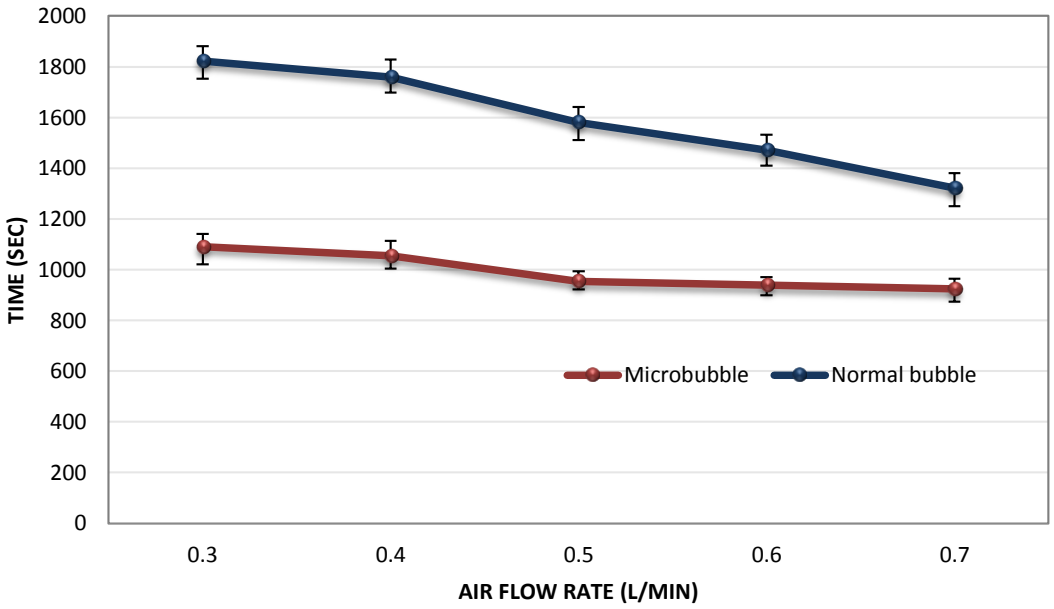


**Figure 4.6** Time needed for dissolved oxygen in the ALB from zero to saturation under different air flow rate

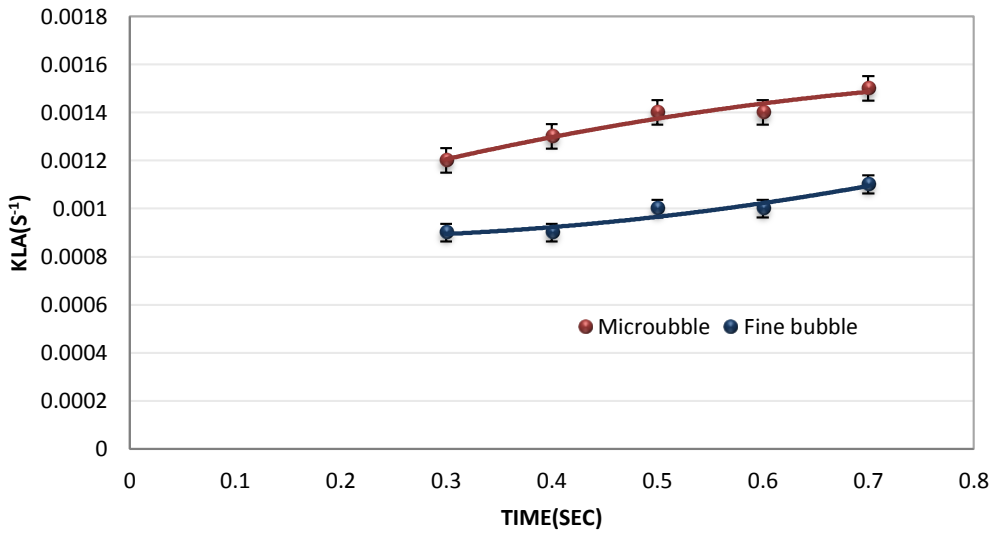


**Figure 4.7** Evolutions of the oxygen volumetric transfer coefficient with the air flow rate for different aeration systems

## 4.6.2 Deoxygenating Performance of Gaslift Loop Bioreactor Equipped with Microbubble Generation System

### 4.6.2.1 Relationship between pH and Dissolved Carbon Dioxide

It is feasible that the concentration of dissolved $CO_2$ is deducible from the pH presuming equilibrium and a well-mixed System. The dissolved $CO_2$ is in equilibrium with $HCO_3^-$ and $CO_3^-$, which can be described by the following chemical reactions. (Livansky, 1990)

$$H_2O \xleftrightarrow{K_w} H^+ + OH^- \tag{4-12}$$

$$CO_{2aq} + H_2O \xleftrightarrow{K_1} H_2CO_3 \longleftrightarrow HCO_3^- + H^+ \tag{4-13}$$

$$HCO_3^- \xleftrightarrow{K_2} CO_3^{2-} + H^+ \tag{4-14}$$

where the relevant equilibrium constants are:

$$K_w = [OH^-][H^+] = 10^{-14} \tag{4-15}$$

$$K_1 = \frac{[HCO_3^-][H^+]}{[CO_{2aq}]} = 10^{-6.381} \tag{4-16}$$

$$K_2 = \frac{[CO_3^{2-}][H^+]}{[HCO_3^-]} = 10^{-10.377} \tag{4-17}$$

The system must satisfy the electro-neutrality constraint, therefore

$$[H^+] + [Cat^+] = [OH^-] + [HCO_3^-] + 2[CO_3^{2-}] + [An^-] \tag{4-18}$$

Assuming constant concentrations of other cations and anions, it gives

$$[H^+] = [OH^-] + [HCO_3^-] + 2[CO_3^{2-}] \tag{4-19}$$

Combining (4-15)-(4-17) and (4-19), we have

$$[CO_{2aq}] = \frac{[H^+] - \frac{K_w}{[H^+]}}{\frac{K_1}{[H^+]} + \frac{2K_1K_2}{[H^+]^2}} = \frac{(10^{-pH} - \frac{10^{-14}}{10^{-pH}})(10^{-pH})^2}{10^{-6.381}10^{-pH} + 2\times10^{(-6.381-10.377)}} \quad (mol/L) \tag{4-20}$$

Eq 4-20 can be used to calculate the concentration of $CO_{2aq}$ in medium/water based on pH, but only exclusive of any buffer solution and when the pH is less than 7. When pH becomes more than 7, the concentration of $CO_{2aq}$ in the medium is almost close to 0.

### 4.6.2.2 Gas Volumetric Mass Transfer Coefficients $k_La$ in Deoxygenating Process

The application of microbubbles enhances the oxygen volumetric transfer efficiency in the aeration process (section 4.6.2.1). Similarly, the effects of bubble size on the dissolution rate of $CO_2$ and oxygen removal rate have been investigated through a series deoxygenating tests in gaslift loop bioreactor using the relationship between dissolved $CO_2$ and pH discussed earlier. Due to the poor solubility of $N_2$ in water, the consideration of mass transfer between $N_2$ and water is excluded. The $CO_2$ volumetric transfer coefficient and oxygen volumetric removal coefficient using microbubble were compared with using fine bubbles. Figure 4.8 shows the effect of dissolved carbon dioxide on the pH value of water with time. As shown in Fig 4.8, the values of pH represented a more remarkably rapid decline in the gaslift loop reactor with microbubbles generation system in comparison with fine bubbles at the same airflow rate. Likewise the values of pH of ALB with fluidic oscillator reached the solubility limit sooner. The initial pH of the liquid phase was close to 7. With $CO_2/N_2$ flushed, the pH values of ALB with fluidic oscillator dropped from 7 to 5.7 in 5 L of water after 10-30 min in contrast with the 25-50 min in ALB without fluidic oscillator. Fig.4.9 shows the response curve for stripping out the dissolved oxygen from water by injecting mixture of $CO_2$10%/$N_2$. The dissolved oxygen concentrations decreased sharply in ALB equipped with fluidic oscillator and dropped to zero within 8-25 min. By comparison, there is a prominent difference on the stripping-out time between using microbubbles and fine bubbles. Despite of the different airflow rates, it is clearly observed that the application of fine bubble led to dramatically long stripping out time more than one hour. Fig 4.9 shows the time needed for dissolved oxygen decreasing from 6.5 to 0 in the reactor with and without fluidic oscillator. Similar to the aeration process, the time of oxygen depleted from water in the gas lift loop reactor is shorter than that for gas lift loop reactor without fluidic oscillator due to higher mass transfer coefficient $k_La$. Similarly to aeration process the improvement caused by fluidic oscillator was enhanced at lower gas flow rate.

Worden (1998) studied behaviours of substantially smaller microbubbles, and found that the mass transfer response was inherently transient. It is because that in the beginning, when the difference between the C* and the $C_L$ is the largest, the gas transfer occurs at maximum velocity. As time passes, the gas concentration in water increases and the driving force decreases which gradually results in a lower gas transfer rate. Likewise, for $O_2$ removal coefficient from the liquid phase, the gap between the $C_L$ and zero is diminishing. The mass transfer rate was mainly affected by the driving force at the later stage of the experiment as the reduction of driving force due to a very low DO.

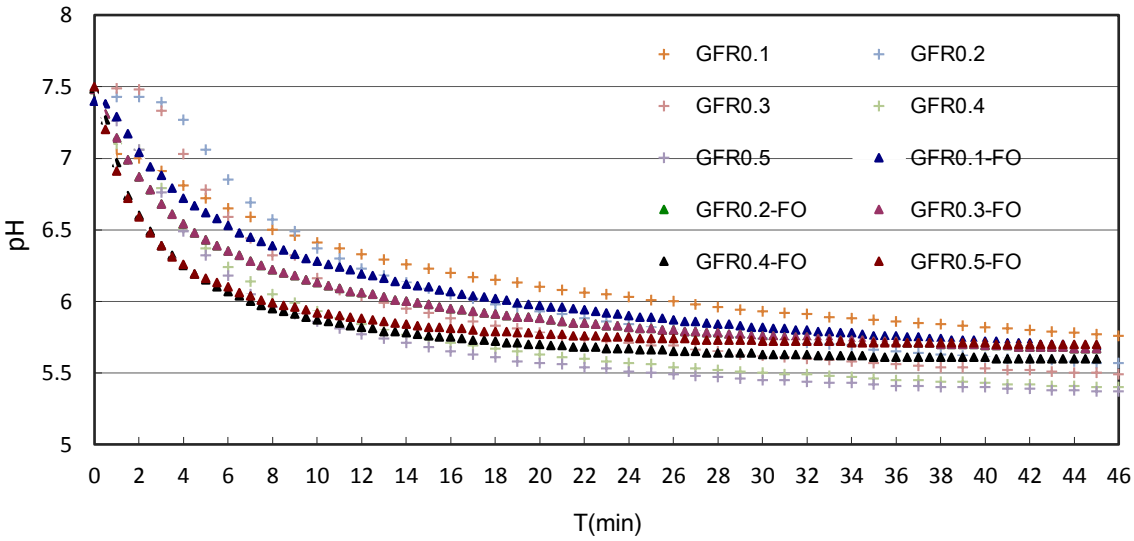


**Figure 4.8** Time-dependent pH in water as a function of concentration of dissolved $CO_2$

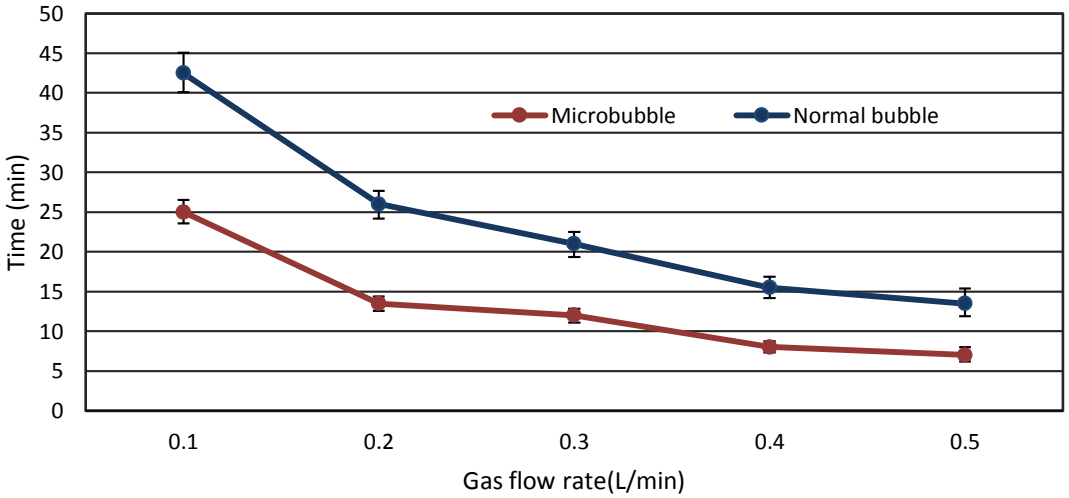


**Figure 4.9** DO depletion time in gas lift loop reactor under different gas flow rate

The effect of microbubble on dissolution of carbon dioxide and stripping-out of oxygen for ALB was further demonstrated in Fig.4.10 and Fig.4.11, which indicate variation of volumetric oxygen removal coefficient and volumetric $CO_2$ transfer coefficient with gas flow rate respectively. Since the mass transfer rate is typically proportional to the interface area exposed per unit volume and the difference between gas saturation concentrations and gas concentration in the bulk liquid. The higher interfacial area and greater concentration driving force, the more gas transfer from gaseous phase to liquid phase is. Thus, it is observed that the overall $O_2$ removal coefficients ($K_La$) estimated for microbubbles were enhanced by around 70% compared with using fine bubble when the gas flow rate was relatively low. In both cases, the variation of $K_La$ exhibited an increasing trend with increasing the gas flow rate. Moreover the improvement of mass transfer efficiency for ALB achieved by microbubble was becoming more evident with the gas flow rate elevated. Similarly, the values of $CO_2$ mass transfer coefficient for microbubble showed the massively higher than that in ALB without the microbubble generations system. The explanation for this phenomenon was the similar to DO removal course.

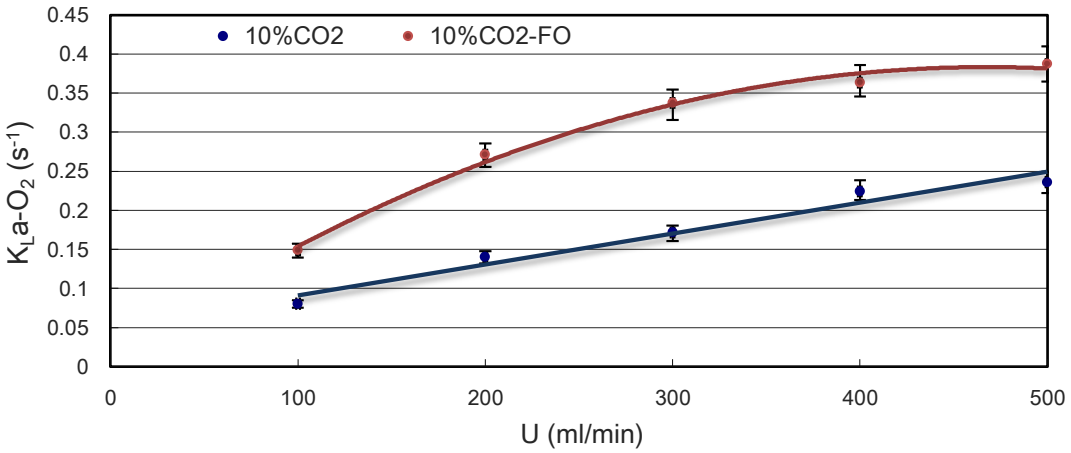


**Figure 4.10** Volumetric oxygen removal coefficients ($k_La$) as a function of the specific gas flow rate

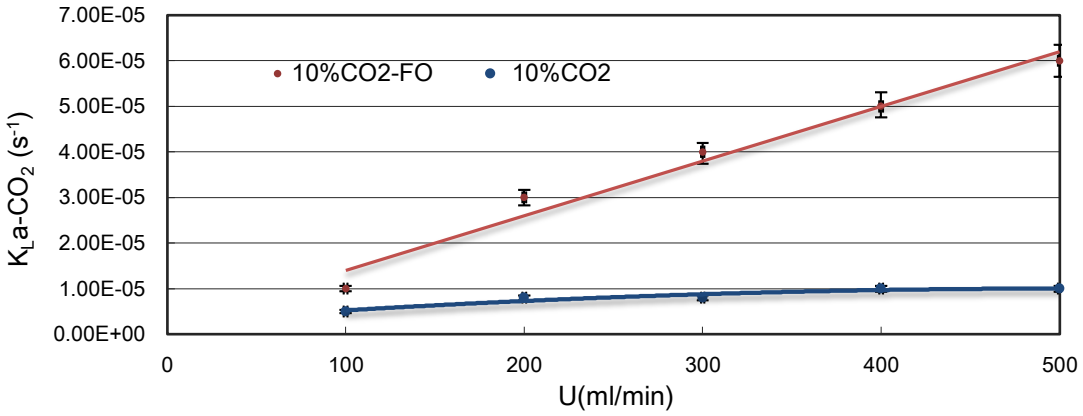


**Figure 4.11** Volumetric CO2 transfer coefficient (kLa) as a function of the specific gas flowrates

## 4.7 Simulation of ALB with COMSOL Multiphysics version 4.1

### 4.7.1 Bubbly Flow Equations

The bubbly flow interface is suitable for macroscopic modelling of mixtures of liquids and gas bubbles. The physics interface between liquid and gas solves for the averaged volume fraction occupied by each of the two phases, rather than tracking each bubble in detail. It also assumes two different velocity fields, one for each phase. A Comsol Multiphysics model was built to simulate the circulation and mixing of the bioreactors with and without fluidic oscillator, which were applied in the subsequent experiments. It's based on the bubbly flow model provided by COMSOL Multiphysics CFD module package. This bubbly flow model is a simplification of the two-fluid model, related to the following assumptions:

1. The gas density is negligible compared to the liquid density.

2. The motion of the gas bubbles relative to the liquid is determined by a balance between viscous drag and pressure forces

3. The both phases share the same pressure zone

4. A large bubble (heterogeneous flow pattern) usually moves faster than a small bubble, which resulted in breakup and coalescence. As the gas-liquid flow is assumed to be homogeneous (bubbly flow), break-up and coalescence are not considered. (Kommareddy and G.anderson, 2004; Zhang et al., 2006).

Based on these assumptions, the sum of the momentum equations for the two phases gives a momentum equation for the liquid velocity, a continuity equation, and a transport equation for the volume fraction of the gas phase.

Momentum equation: The momentum transfer equation is derived as

$$\phi_1\rho_1\frac{\partial u_1}{\partial t}+\phi_1\rho_1 u_1\cdot\nabla u_1=-\nabla p+\nabla\cdot\left[\phi_1(\mu_1+\mu_T)\left(\nabla u_1+\nabla u_1^T-\frac{2}{3}(\nabla\cdot u_1)\mathbf{I}\right)\right]+\phi_1\rho_1\mathbf{g}+F \quad (4\text{-}21)$$

Where, **u** denotes velocity (m/s), $p$ pressure (Pa), $\phi$ phase volume fraction ($m^3/m^3$), $\rho$ density ($kg/m^3$), **g** the gravity vector ($m/s^2$), **F** any additional volume force ($N/m^3$), $\eta_l$ dynamic viscosity of the liquid (Pa s), and $\eta_T$ turbulent viscosity (Pa s). The subscripts "l" and "g" denote quantities related to the liquid phase and the gas phase, respectively. The right side of the above equation respectively show pressure difference, gravity force, stress and the ensemble averaged momentum exchange between the intra-phase forces. The pressue is shared between the phases.

The continuity equation is

$$\frac{\partial(\rho_l\phi_l+\rho_g\phi_g)}{\partial t}+\nabla\cdot\left(\rho_l\phi_l u_l+\rho_g\phi_g u_g\right)=o \quad (4\text{-}22)$$

The equation for the transport of the volume fraction of gas is

$$\frac{\partial\rho_g\phi_g}{\partial t}+\nabla\cdot\left(\rho_g\phi_g u_g\right)=-m_{gl} \quad (4\text{-}23)$$

Here $m_{gl}$ is the mass transfer rate from gas to liquid ($kg/(m^3\ s)$).

For low gas volume fractions (($\phi_g$<0,1) it is in general valid to replace the continuity equation, Equation 4-22, by

$$\nabla\cdot u_l=0 \quad (4\text{-}24)$$

The Bubbly Flow model solves for $\mathbf{u}_l$, $p$, and $\bar{\rho}_g=\rho_g\phi_g$, the effective gas density. The gas velocity $u_g$ is the sum of the following velocities:

$$u_g=u_l+u_{slip}+u_{drift} \quad (4\text{-}25)$$

Where $u_{slip}$ is the relative velocity between the phases, and $u_{drift}$ is an additional contribution when you include a turbulence model.

Mass Transfer and Interfacial Area

It is possible to account for mass transfer between the two phases by specifying an expression for the mass transfer rate from gas to liquid $m_{gl}$ ($kg/(m^3\ s)$).

The mass transfer rate typically depends on the interfacial area between the two phases. An example is when gas dissolves into the liquid. In order to determine the interfacial area, it is necessary to solve for the bubble number density (that is, the number of bubbles per volume) in addition to the phase volume fraction. The Bubbly Flow interface assumes that the gas bubbles can expand or shrink but not completely vanish, merge, or split. The conservation of the number density n ($1/m^3$) then gives

$$\frac{\partial n}{\partial t} + \nabla \cdot \left(n u_g\right) = 0 \qquad (4\text{-}26)$$

The number density and the volume fraction of gas gives the interfacial area per unit volume ($m^2/m^3$):

### 4.7.2 COMSOL Model Simulation for the Liquid Circulation and Mixing in Airlift Loop Bioreactor

Regarding as the parameter setting of reactor walls and draft tube, no slip was used for the liquid phase while “no gas flux” was used for the gas phase.

$$u_1 = 0,\ n(\Phi g\ ug)=0$$

For the diffuser bubbling surface, no slip was set for liquid with “gas flux” for gas. The top liquid surface used “gas outlet” as gas boundary conditions. These imply gas leaving the reactor at $u_g$ with no other constraint at the boundary. For the liquid phase, slip boundary conditions were used.

$$u_1 n = 0$$

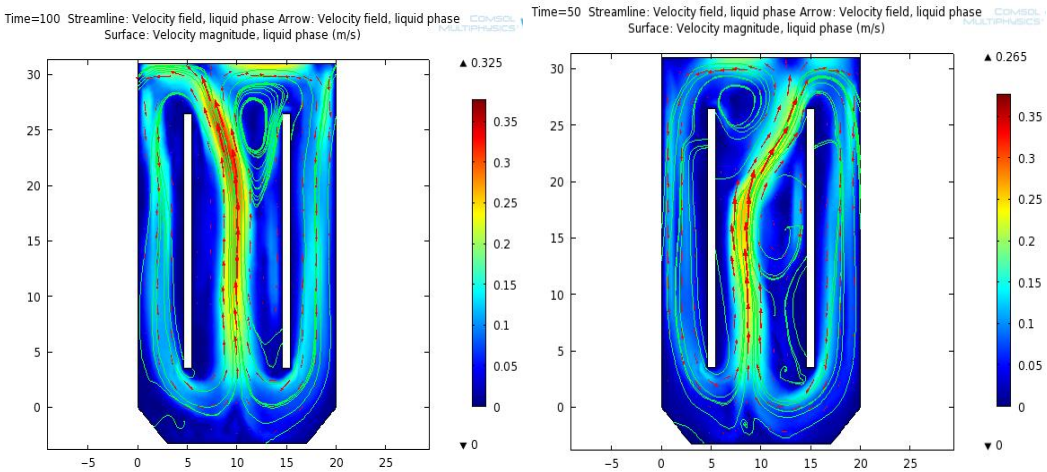

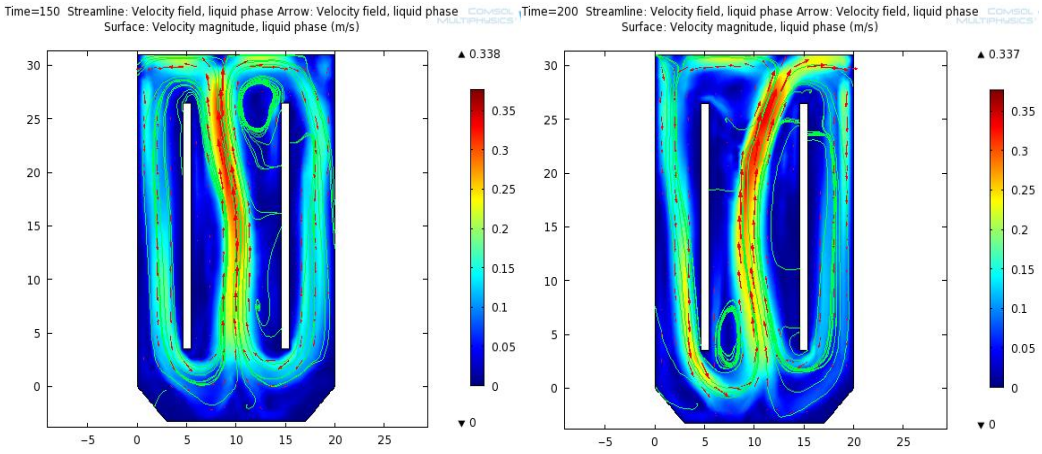


**Figure 4.12** Velocity profiles in the ALB with fluidic oscillator predicted by the CFD model. Velocity magnitude of the liquid phase is shown, while streamlines depict fluid structure. Simulation times are 50, 100, 150, and 200 s.

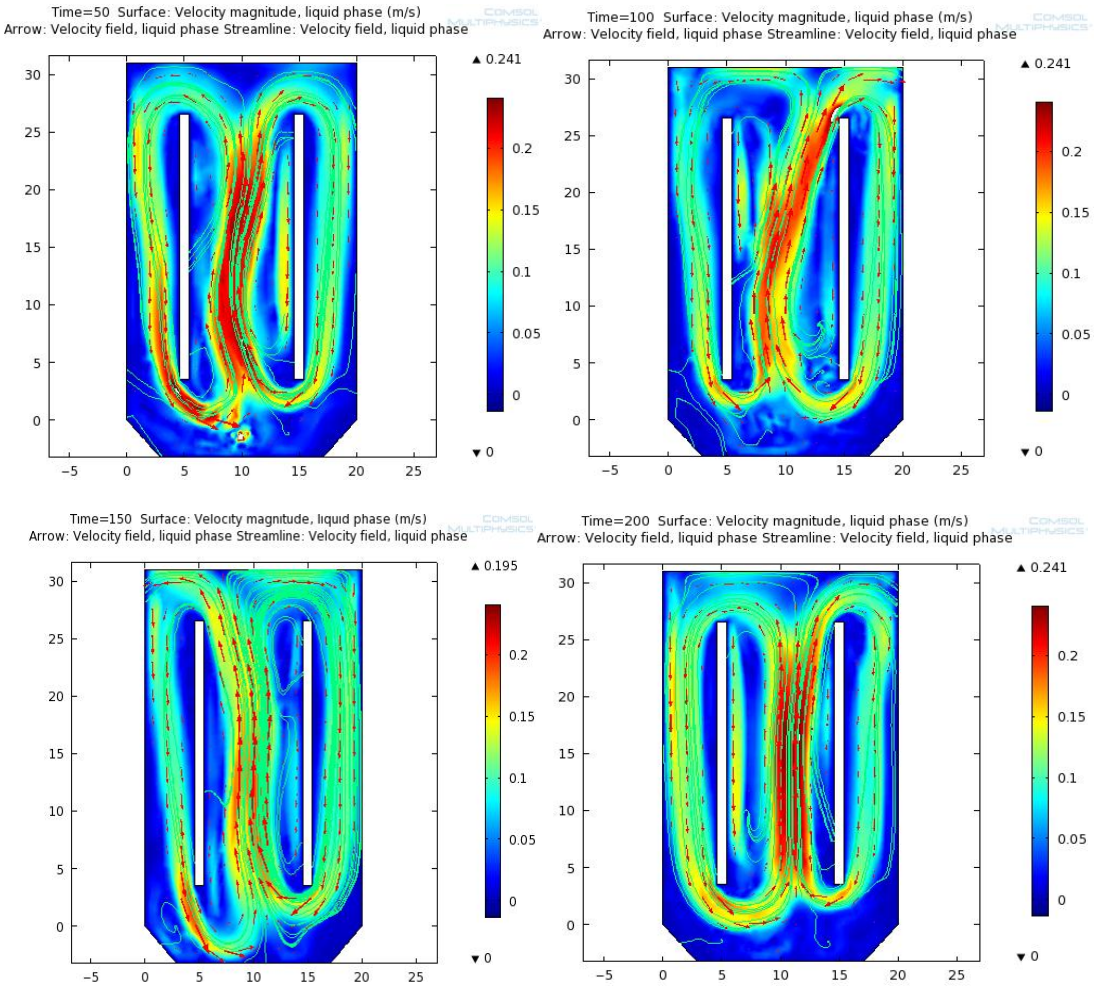


**Figure 4.13** Velocity profiles in the ALB without fluidic oscillator predicted by the CFD model. Velocity magnitude of the liquid phase is shown, while streamlines depict fluid structure. Simulation times are 50, 100, 150, and 200 s.

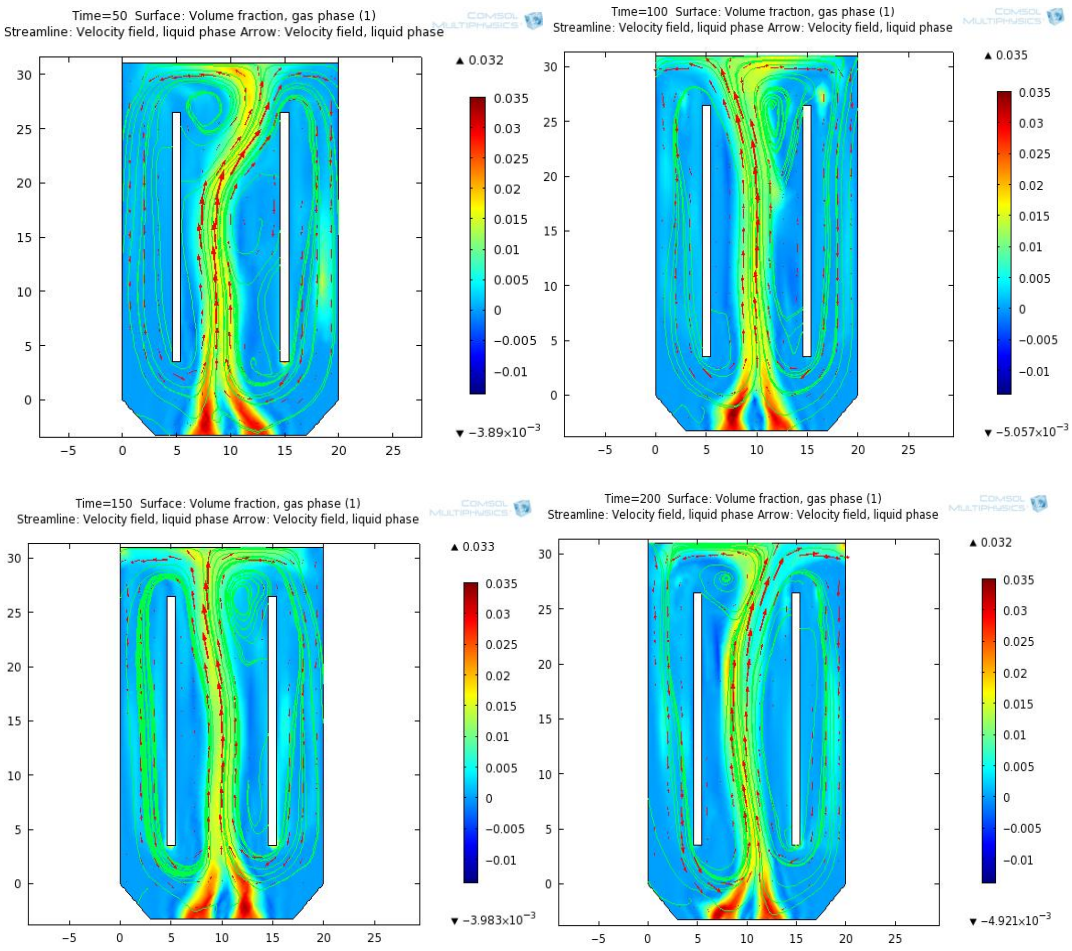


**Figure 4.14** Volume fraction, gas phase in the ALB with fluidic oscillator predicted by the CFD model. The volume fraction of the gas phase is shown, while streamlines depict fluid structure. Simulation times are 50, 100, 150, and 200 s.

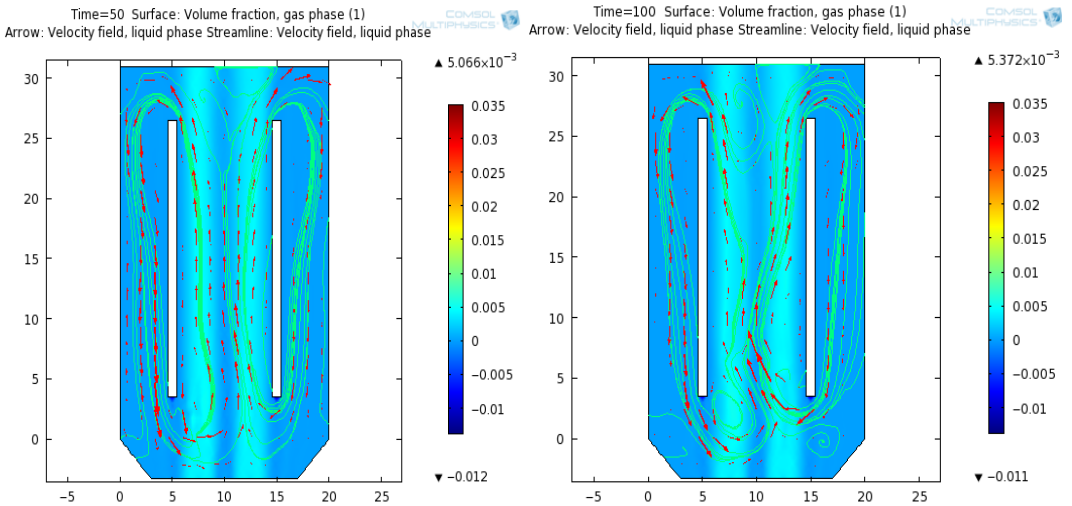

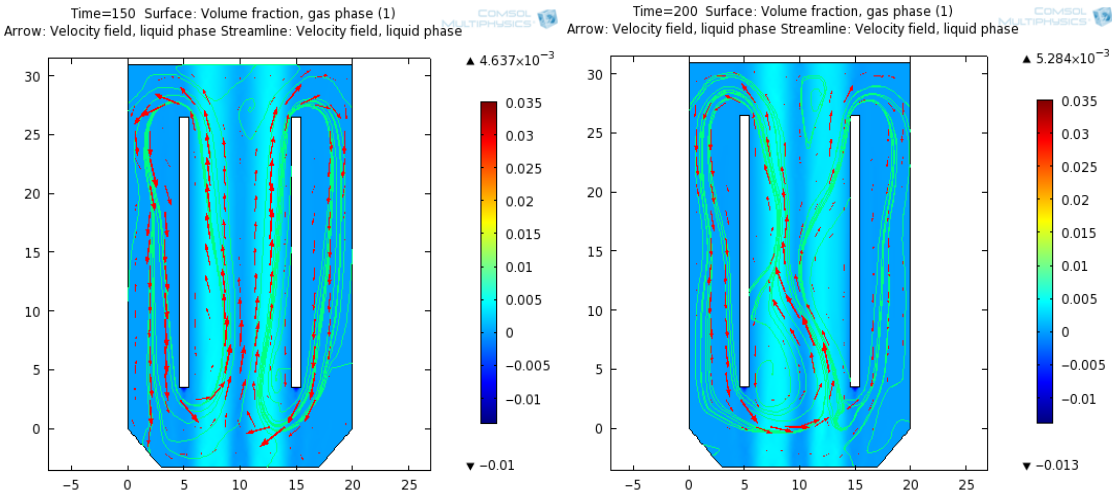


**Figure 4.15** Volume fraction, gas phase in the ALB without fluidic oscillator predicted by the CFD model. The volume fraction of the gas phase is shown, while streamlines depict fluid structure. Simulation times are 50, 100, 150, and 200 s.

The airlift loop bioreactor is characterized by global mixing induced by its draft tube and bubbles rising in the aerated region. The reactors applied in this study were designed for the partial nitrification process in the following study. In order to examine the inner physical motion of the ALB, based on the geometry of airlift loop bioreactor used in the mass transfer experiments, the models of the circulation and mixing in the ALB with different aeration system were built by using COMSOL Mulitphysics.

These Computational models of ALB with and without fluidic oscillator were built at gas flow rates of 0.7Lmin$^{-1}$. Average bubble size calculated from the measured bubble size distribution was used in the model, that is, microbubbles with diameter 311.87μm and fine bubbles with diameter 995 μm.

As can be seen in the Fig 4.12 and Fig4.13, velocity fields for the computational domain with time are shown. The maximum velocity is detected in the center of rising region. The velocity magnitude in this area is much higher than that in the down-comer as expected. A main liquid recirculation loop is generated by the rising bubbles around the suspended baffle promoting vertical mixing. The flow spreads at the top surface reducing the liquid velocity above the baffle, while liquid returning via the down-comer region rejoins through the gap between the baffle and the diffuser. Vortices are created at several points within the ALB where flow turns around solid boundaries. The vortexes formed on top of the baffle or bottom of the baffle at different time. Study of vortex positions with time suggests that this vortex moves downward into the dead

space below the diffuser periodically. However, it can be clearly seen that the region below the diffuser is poorly mixed due to flow separation. Compared the models (Fig4.12) of ALB with fluidic oscillator to the models of ALB without fluidic oscillator (Fig4.13) at the same time point, it is noted that both airlift loop bioreactors achieve homogeneous circulation and mixing, higher liquid velocity in the rising region lower in the downcomer. However the greater velocity magnitude distribution and better mixing pattern were detected in the ALB with fluidic oscillator, compared to the ALB without fluidic oscillator. This crucial feature is very significant and favorable for the partial nitrification process. The Fig 4.14 and Fig4.15 show that the volume fraction of the air distributed in the ALB at the different time was more concentrated in the rising region than that in the down-comer region which means the higher DO concentration presenting in rising region. Like the velocity profiles, the comparison between Fig 4.14 and 4.15 further confirmed that the higher mass transfer and more homogeneous mixing were attributed to the microbubble. Based on the models of velocity magnitude and volume fraction of air, it was apparent the ammonia oxidising bateria for the partial nitrification will recirculate with the liquid streams, more than that, the time staying in the low DO zone would be longer than in the high DO zone. As mentioned in section 2.3.3, DO concentraions exert a significant influence on the activities of AOB and NOB. Therefore, this design, i.e. alternate of low DO concentraion and high DO concentration, contributes to inhibiting and washing out NOB microorganism from the system without affecting the acitivities of AOB microoganism. As is shown in the Fig 4.12 and Fig4.14, microbubble ,which has much higher surface area to volume ratio and longer residence time, devoted the higher velocity magnitude and air volume fraction in the airlift reactor with fluidic oscillator ,which enable the ALB to save more engergy and oxygen comsumption in aspect of the nitrogen removal. The mircobubbles with average size of 311.87μm injected into the bioreactors were much smaller than fine bubble. The gas hold-up in the draft tube of those bioreactors equipped fluidic oscillator is increased. Therefore higher pressure differences are generated, which leads to higher liquid velocity. In the present study the performance of deoxygenation for ALB were not investigated by COMSOL. Nevertheless according to computational models of aeration performance for ALB, it was reasonably concluded that, in the deoxygenating process, the higher velocity of liquid and higher mass transfer efficiency could be also obtained by using microbubbles in the gas lift loop bioreactor. Likewise these benefits are favourable to enhancing the performance of Anammox process in terms of granule

sludge formation and activity of Anammox bacteria. Finally it should also be noted the asymmetric flow structure (recirculation/separated flow region) and wavy flow path indicate that the transient flow structure should not settle down to a steady state.

## 4.8 Conclusions

Based on above observations, it was possible to conclude that using microbubbles instead of fine bubble dramatically enhanced the mass transfer efficiency in the gas lift loop bioreactor. In the oxygenating process the mass transfer coefficient $K_La$ were impressively elevated by 38.9% by using fluidic oscillator to produce microbubble. In the deoxygenating process the improvement for mass transfer of oxygen removal was surprisingly as high as 70%, meanwhile the enhancement was also found in mass transfer from $CO_2$ phase into liquid phase. The performance of the gas lift bioreactor with fluidic oscillator and without fluidic oscillator were modelling respectively by using COMSOL Multiphysics. The results further confirmed that the finer mixing and higher mass transfer inside bioreactor were obtained by introduction of fluidic oscillator. The alternation of low DO concentration in downcomer region and high DO concentration in rising region provided a favorable operating condition for the partial nitrification process. Besides the deoxygenating study in a gas lift loop bioreactor with fluidic oscillator flushing with mixture gas of $10\%CO_2/N_2$ provided a novel concept for implementation of Anammox process. Better mixing effects, higher oxygen removal rates and pH adjustment with the aid of $H^+$ produced by dissolving $CO_2$ would not only ensure a potential better anaerobic conditions for the growth of Anammox bacteria but also save more energy and operating costs.

# Chapter 5. The Effect of Microbubble Aeration System on Partial Nitrification Process (PN)

## 5.1 Introduction

The operational costs of the conventional nitrification–denitrification nitrogen removal process are to a great extent related to the oxygen and organic matter requirements. Recently some novel processes have been developed to reduce these costs. Due to cost-savings in aeration as well as in the form of no need for the addition of organic carbon source compared to the conventional nitrification–denitrification, the combination of the partial nitrification and Anammox is regarded as a promising approach of removing nitrogen from wastewater with a low C/N ratio and a large quantity of ammonium (Feng et.al; 2007).

Nitrite accumulation or partial nitrification has been reported in the literature for decades. However, many challenges were faced during the development of stable and efficient partial nitrification technology, such as inhibition on NOB activity and the effort to save energy, etc. The development of an effective operational strategy for the partial nitrification technology is important to further advance this technology and its popularity. The first introduction of microbubble aeration system into partial nitrification not only contributes a potential oxygen saving and energy saving approach and also enhances the capacity and stability of this novel biological nitrogen removal process.

So far, microbubble produced by fluidic oscillator has been successfully employed in different areas such as flotation separation, biogas production and algal biofuels production due to its outstanding benefits, however there has been no report on the application of microbubble in the biological nitrogen removal process. There are a lot of factors influencing the performance of partial nitrification such as pH, dissolved oxygen (DO), temperature, free ammonia (FA) and nitrous acid (FNA) concentrations and inhibitory compounds, in which the DO concentrations are believed as the most important parameter as well as the most difficult to control for partial nitrification. Therefore a better partial nitrification process could be closely related to the effective aeration system. This study investigated the effect of microbubble aeration system on the performance of sequencing batch airlift loop bioreactor (SBAB) with operating

partial nitrification. A broad range of operating parameters and factors has been examined experimentally in this chapter which are essential for increasing the activity of target bacteria and avoiding interferential species. Two groups of bacteria, namely ammonia-oxidizing bacteria (AOB) and nitrite-oxidizing bacteria (NOB) are involved in nitrification. Chemolitho-autotrophic AOB microorganisms are responsible for the rate-limiting step of nitrification in a wide variety of environments, making them important in the global cycling of nitrogen. Characterization and identification of the bacterial populations in an engineered system which have been considered to be a "black box", has been made possible by using non-cultivation based techniques, such as, polymerase chain reaction (PCR), real-time PRC (QPCR) (Sinha, 2007).

## 5.2 Objectives

The first objective of this work was to evaluate the long-term effects of microbubble aeration system on the partial nitrification activity. To this end, over 200-day experiment was run under different conditions. Furthermore, the morphology of involved bacteria from both air lift bioreactor was assessed by scanning electron microscope (SEM) and Transmission Electron Microscope (TEM). The next objective was to evaluate the effects of microbubble on the growth and activity of target bacteria (including ammonium oxidising bacteria and nitrite oxidising bacteria) by molecular biological method. PCR and Real-time PCR were employed to quantify the different bacteria. These experiments were focused on the effects of microbubble on the capacity and efficiency of the treatment as well as the physical and genetic properties of the biomass.

## 5.3 Materials and Methods

### 5.3.1 Experiment Setup

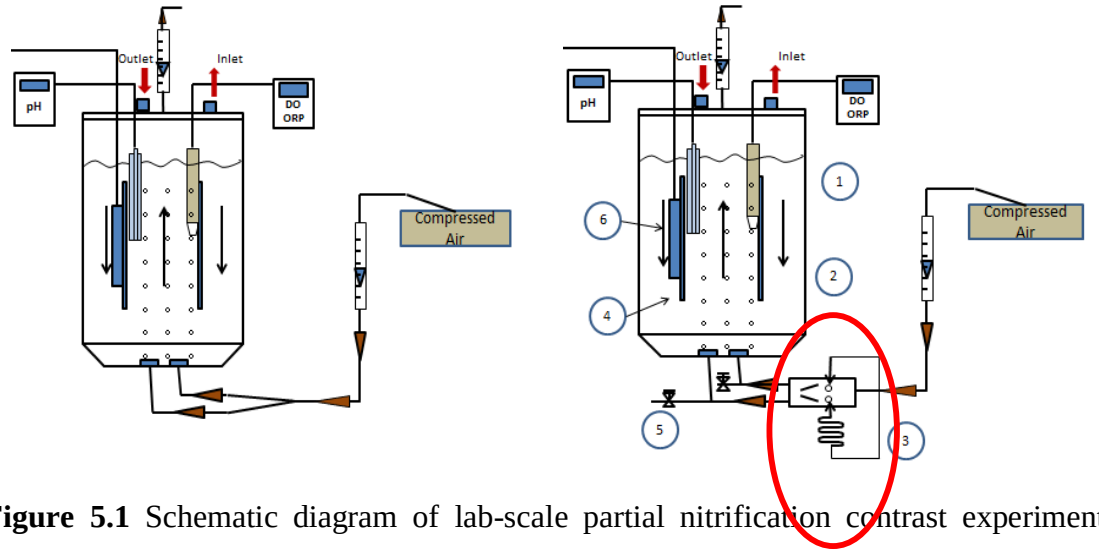


**Figure 5.1** Schematic diagram of lab-scale partial nitrification contrast experiments with and without Fluidic Oscillator (red circle): 1. DO&ORP meter; 2. Sequencing batch airlift loop reactor; 3. Microfluidic oscillator; 4 Baffle; 5. Bleed off ; 6. Aquatic heater

The reaction potential of the reactor depends on the reaction rate and reaction time. In the bioreactor, the reaction rate depends on the activity of microorganism and biomass. The biological activity is subject to the genetic characteristics of microbe usually counting on breeding. Biomass is subject to the ability of the growth rate and the capability of biomass retention for the bioreactor. Generally optimizing the nutritional and environmental conditions are applied to promote biological growth whereas improving the sludge sedimentation performance and optimizing the bioreactor structure are most accepted to accumulate organisms.

In the previous study, different bioreactors, such as membrane bioreactor (MBR sequencing batch reactors (SBR), continuous stirred-tank reactor (CSTR), and ALB were successfully employed in the biological wastewater treatment process. The MBR combines conventional biological treatment processes with membrane filtration to provide an advanced level of solids and bacteria removal. On the other side the disadvantages of the MBR are membrane fouling, higher energy consumption and high cost of membranes, etc. CSTR is also had been widely adopted in the respect of biological nitrogen removal for its continuous operation, good control, simplicity of

construction and low operating (labour) cost. And yet the problems, which CSTR encountered with, are lowest conversion per unit volume, poor agitation as well as low biomass retention. SBR that effectively compete with conventional activated sludge systems (MBR,CSTR), is mostly used in the field of biological wastewater treatment because of the potential capital cost savings, operating flexibility and control, in addition, the most important is equalization, biological treatment and clarification can be achieved in a single reactor vessel.

In this study, combining the advantages of both sequencing batch reactors and airlift loop bioreactor (mentioned in 4.2), a novel bioreactor, sequencing batch airlift loop bioreactor (SBAB) with fluidic oscillator was built and employed. Apart from the benefits of both reactors (SBR&ALB) mentioned above, sequencing batch airlift loop bioreactor (SBAB) strengths the mixing effect, which is a weakness of SBR. The high biomass retention brought by SBR increases the nitrogen loading ability. These complementary advantages achieve the optimization of the partial nitrification system. The microbubble produced through oscillation of air flow attached to activated sludge circulates in the bioreactor so as to largely increase the contact between the bacteria and medium. Higher oxygen mass transfer efficiency of microbubble plays a key role in respect of improving the conversion rate from ammonium to nitrite. Base on the potential superiorities mentioned above, the effect of microbubble aeration systems, on the performance of the partial nitrification process was in depth investigated.

Two sequencing batch airlift loop bioreactor (SBAB) with a working volume of 5 L, made from plexiglass, were used in this study. As shown in fig.5.1, the bioreactor equipped with the microbubble aeration system was defined as PN-SBAB with FO and an identical bioreactor with fine bubble aeration system was marked as PN-SBAB without FO. A constant compressed airflow for aeration was provided to the reactors through two rectangle ceramic diffusers with 20 microns pore size located at the bottom of the reactor.

### 5.3.2 Operation Strategies for PN-SBAB

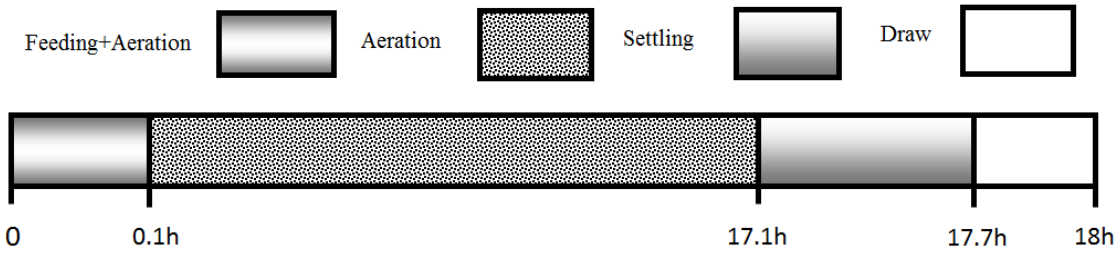


**Figure 5.2** A cycle of batch experiment of partial nitrification

The SBAB was initially operated in a short start-up period (15 days) when a high temperature and a low DO level were applied to enhance the growth of AOB, and short HRT and high free ammonia (FA) concentrations inhibited the growth of NOB. An aquatic heater was used to maintain temperature of bioreactors at 30 ◦C. A continuous aeration (CA) strategy was applied with an airflow rate of 0.7 l air $min^{-1}$. The $NH_4^+$–N concentration in the reactor was gradually increased from 30$mgL^{-1}$ to 100$mgL^{-1}$ by manually replacing all of the supernatant with the feed during the settle phase.

After 15-day start-up period, two SBRBs were started to carry out the partial nitrification process simultaneously. The complete mixture inside both reactors was achieved by using the circulation of air flow in the reactor. The temperature was controlled at 30 ℃, 25 ℃ and room temperature respectively by using an aquatic heater during different period. Different lengths of feedback loop of fluidic oscillator were also applied to the partial nitrification process.

Both bioreactors were operated in cycles of 18 hours distributed in four periods: mixed filling phase (6 min), aeration mixing phase (17 hours), settle phase (36 min) and draw phase (18 min) (Fig 5.2). The samples of influent and effluent were collected from filling phase and drawing phase respectively. Different parameters such as $NH_4^+$-N, $NO_2^-$N, $NO_3^-$N, pH and temperature were monitored every each cycle using the method described in Chapter 3. No purge phase was conducted as such, although suspended solids were washed out from the system through the outflow. The data were measured and recorded every day. Repeated experiment was conducted every other day to make sure the accuracy of measurement and average value was recorded. If the value of data deviated beyond 3% of the expected result, the measurement was repeated for 3 times. The same method was also applied in Chapter 6. Non-settable fractions for each reactor are different due to the application of different aeration systems. This section will be

discussed later. Both bioreactors were fed with a synthetic autotrophic medium described in Section 3.4. Then the concentrations of ammonium of the influent were stepwise increased (Table 3.4). The strategy for achieving conversion of 50% ammonium in both cases was to fix an influent ammonium to bicarbonate molar ratio approximately equal to the stoichiometric value of 1:1 according to Galı´, (2007).

To successfully run Anammox process, the influent for the Anammox process must be composed of $NH_4^+$-N and $NO_2^-$-N in a ratio 1:1~1.32, therefore only a partial nitrification of ammonium to nitrite is required. The modifications of parameters (temperature, ammonium concentration, pH and solid retention time) allow bioreactors to achieve this partial nitrification with a final effluent composed by $NH_4^+$-N and $NO_2^-$-N at the right stoichiometric ratio. Chemolithophic ammonia oxidising bacteria use either carbon dioxide or bicarbonate ions as their carbon source for cell growth (Shuler and Kargi, 1992). Inorganic carbon (IC) in its bicarbonate form can be used as a carbon source for these nitrifiers. Hence, a suitable IC/$NH^+_4$-N ratio will be crucial for the stability and efficiency of the PN process. Partial nitrification is alkali-consuming process. According to Eq (2-4), oxidising 1 mol $NH_4^+$-N produces 2 mol $H^+$. Production of $H^+$ causes the drop of pH in the bioreactor, which will stop the proceeding of ammonia oxidation. In the autotrophic bioreactor system the alkalinity depends on the content of $HCO_3^-$. Based on these principles it is concluded that the key to obtain partial nitrification resides in the bicarbonate/ammonium ratio. The molar stoichiometric relationship for the complete ammonium oxidation must be 2 mol$HCO_3^-$/mol $NH_4^+$. Therefore, to provide 50% ammonium oxidation, ammonium and bicarbonate should be present in a molar ratio of 1:1 (Galı´, 2007). The equal ratio of $HCO_3^-$/$NH_4$ in different wastewater stream, such as reject water, results in a natural pH decrease when approximately 50% of $NH_4^+$ is oxidised and the reaction will stop. As a result, if the wastewater has not this relationship, the pH would have to be controlled in the process.

$$NH_4^+ + 1.5O_2 \rightarrow NO_2^- + H_2O + 2H^+ \text{ (nitrification, by AOB)} \quad (2\text{-}4)$$

The operational strategies to prevent the oxidation of the excess of nitrite to nitrate by oxygen in two reactors were mainly dependent on low DO concentration (<1mg$L^{-1}$), high temperature control, short HRT and inhibition of FA and FNA. Converting approximately 50% of $NH_4^+$-N to $NO_2^-$-N is hinged on the ratio of $HCO_3^-$/ $NH_4^+$, therefore the value of pH were not real-time controlled but measured every day. The details of SBAB operational conditions were shown in the table 5.1

**Table 5.1** The operating strategy for both partial nitrification systems

| Reactor | Periods | Days | DO ($mgL^{-1}$) | Temperature | HRT | Length of feedback loop | NH4+-N ($mgL^{-1}$) |
|---|---|---|---|---|---|---|---|
| SBAB with FO | I | 145 | 0~1 | 30◦C | 0.75d | 30cm | 200~1400 |
| | II | 37 | 0~1 | 25◦C | 0.75d | 30cm | 180~1400 |
| | III | 30 | 0~1 | Room temperature | 0.75d | 30cm | 165~900 |
| | IV | 20 | 0~1 | 30◦C | 0.75d | 20cm | 400~900 |
| SBAB without FO | I | 145 | 0~1 | 30◦C | 0.75d | __ | 200~1400 |
| | II | 37 | 0~1 | 25◦C | 0.75d | __ | 180~1400 |
| | III | 30 | 0~1 | Room temperature | 0.75d | __ | 165~900 |

### 5.3.3 Activated Sludge Inoculation

In this study the both reactors were inoculated with return activated sludge collected from Woodhouse Mill sewage treatment plant of Yorkshire water in Sheffield, UK which employed the A/O process. The sludge seeding for each PN reactor was started by first mixing 1L sedimentary fresh activated sludge with 4L synthetic wastewater. The seeding sludge was a mixture of heterotrophic organisms capable of oxidizing carbonaceous compounds and denitrification, autotrophic nitrifying organisms with low nitrite accumulated rate. The average concentrations of mixed liquor suspended solids (TSS) and mixed liquor volatile suspended solids (VSS) in the reactor were 5000 $mgL^{-1}$ and 4200 $mgL^{-1}$, respectively.

### 5.3.4 Enrichment of Ammonia Oxidizing Bacteria (AOB) in both PN-SBABs

The first 15 days were defined as the start-up period for the partial nitrification. At the early stage of enrichment, the emergence of large amounts of foam during the aeration process was observed in both bioreactors. The explanation for these phenomena is that in order to maintain survival heterotrophic bacteria in the raw sludge degraded or endogenously degraded the organic matter residing in inoculation sludge. In addition, due to different bacterial species contained in the sludge, with the single inorganic ammonium media feeding, the irrelevant species were gradually eliminated except autotrophic aerobic nitrifiers, which take inorganic ammonia as real substrate.

Consequently the biomass decreased and the foam disappeared correspondingly. The inner of SBAB changed into the inorganic environment. The sludge turned to be light in color.

The main product of partial nitrification is nitrite rather than nitrate for conventional nitrification. It is considered if the accumulation of nitrite in effluent is over 50%, the partial nitrification process was successful start-up.

Calculation of nitrite accumulation ratio (NAR) was calculated according to the following equation:

$$\mathrm{NAR\%} = \frac{\mathrm{NO_2^- - N}}{\mathrm{NO_2^- - N + NO_3^- - N}} \times 100\% \quad (5\text{-}1)$$

Both SBABs were operated partial nitrification process with the same operational strategies. The reactor was operated at 30 ℃, and the DO value was regulated within 0~1mgL$^{-1}$ by controlling the aeration rates rate at 0.7mgL$^{-1}$. Influent $NH_4^+$-N concentrations increased gradually from 20 to 400 mgL$^{-1}$; the accumulations of $NO_2^-$-N elevated with the concentration of influent $NH_4^+$-N increasing, from 0.13% to 94.92% and 0.03% to 96.23% for PN-SBAB with FO and PN-SBAB without FO respectively. While the effluent $NO_3^-$-N concentration showed a slight decreasing. These observations suggested that the start-up of partial nitrification processes were successful. AOB dominated over NOB in both SBABs .It should be noticed that the accumulation of $NO_2^-$-N for PN-SBAB with FO reached above 80% on the seventh day which is earlier than the eleventh day for PN-SBAB without FO. However from the 12$^{th}$ day the NAR for two reactors attained and remained above 90%

**Table 5.2** Accumulation rate of $NO_2^-$-N during cultivation in SBAB-FO

| Days (d) | Effluent $NH_4^+$-N (mgL$^{-1}$) | Effluent $NO_2^-$-N (mgL$^{-1}$) | Effluent $NO_3^-$-N (mgL$^{-1}$) | Accumulation of $NO_2^-$-N % |
|---|---|---|---|---|
| 1 | 0.073907 | 0.0306 | 22.1 | 0.13% |
| 3 | 0.193425 | 0.306 | 26.1 | 1.2% |
| 5 | 0.227573 | 64.0764 | 27.7 | 69.81% |
| 7 | 0.056833 | 123.8535 | 27.2 | 81.99% |
| 9 | 0.184888 | 186.66 | 27.7 | 87.07% |
| 11 | 0.381239 | 282.744 | 21.7 | 92.87% |
| 13 | 0.338554 | 302.022 | 19.9 | 93.82% |
| 15 | 0.048296 | 383.418 | 20.5 | 94.92% |

**Table 5.3** Accumulation rate of $NO_2^-$-N during cultivation in SBAB-without FO

| Days (d) | Effluent $NH_4^+$-N ($mgL^{-1}$) | Effluent $NO_2^-$-N ($mgL^{-1}$) | Effluent $NO_3^-$-N ($mgL^{-1}$) | Accumulation of $NO_2^-$-N % |
|---|---|---|---|---|
| 1 | 1.46286 | 0.003979 | 10.4761 | 0.03% |
| 3 | 1.5351 | 0.024488 | 18.1 | 0.13% |
| 5 | 2.8896 | 45.915 | 30.85 | 59.81% |
| 7 | 2.3478 | 70.47953 | 21.08 | 76.97% |
| 9 | 2.5284 | 29.53865 | 20.57 | 58.94% |
| 11 | 2.709 | 104.074 | 19.05 | 84.52% |
| 13 | 6.321 | 203.8626 | 13.7 | 93.70% |
| 15 | 11.9196 | 342.5259 | 13.39 | 96.23% |

## 5.4 Result and Discussion

The influent with appropriate $NO^-_2$-N/$NH^+_4$-N ratio of around 1:1.32 is the key factor to successfully operate Anammox process. The partial nitrification as pretreatment of Anammox is responsible for oxidising half influent ammonium to nitrite meanwhile preventing the further oxidation from nitrite to nitrate, so as to achieve the desired $NO^-_2$-N/$NH^+_4$-N mixture severing as influent of Anammox. In order to obtain the optimum effluent with lower oxygen and energy consumption the microbubble aeration system were first introduced into partial nitrification process.

In order to restrict the nitrification process at the stage of the oxidizing ammonia to nitrite different approaches were wildly used by researchers:

1. Control of the dissolved oxygen concentration at low level to avoid the oxidation of nitrite to nitrate due to the higher affinity of the ammonia oxidizing bacteria for oxygen than that of nitrite oxidizing bacteria (Garrido et al., 1997).

2. To control the concentration of ammonia in the liquid media to inhibit the nitrite oxidation according to the findings of Anthonisen et al. In this case the adaptation of the bacteria to the operational conditions is another problem.

3. Selection of a population based on the different growth rates of AOB and NOB, which is the general mechanism used in the partial nitrification process. This process is carried out in a sequencing batch airlift loop bioreactor with desirable operational

conditions to favour the growth of ammonia oxidizers and to washout the nitrite oxidizers (van Dongen et al., 2001).

### 5.4.1 The Effect of Microbubble on Long-term Global Performance of the Partial Nitrification (PN) Process in Airlift Loop Bioreactor (ALB)

The purpose of this section is to demonstrate the effect of microbubble aeration system on the long-term performance of partial nitrification through evaluating and comparing the differences of the treatment capability, effluent compositions and stability of performance between PN-SBAB with fluidic oscillator and the other one without fluidic oscillator.

Partial nitrification processes were conducted over 140 days in two lab scale identical design airlift loop bioreactor, one of them equipped with fluidic oscillator. The temperatures were kept at 30 ℃. The DO concentrations were controlled under 1 $mgL^{-1}$ by regulating the air flow rate at 0.7$lmin^{-1}$ to favour $NO^{-}_{2}$-N accumulation as well as to inhibit $NO^{-}_{3}$-N production. The both reactors were fed with synthetic wastewater with a $HCO^{-}_{3}/NH^{+}_{4}$ ratio of round 1. The components of influent and effluent were analysed each operational cycle.

Since the main target of the partial nitrification process is to obtain stable effluent with appropriate $NO_2^-$-N/$NH_4^+$-N ratio of around 1:1.32 to fit the subsequent Anammox process, the accumulation of AOB and limitation-inhibition-washout of NOB is the critical point for maintaining stable partial nitrification. Several process parameters, including dissolved oxygen (DO) concentration, temperature, hydraulic retention time (HRT), substrate concentration, and inhibitors, have been found to inhibit or washout NOB selectively . In this study controlling low DO concentration and short hydraulic retention time (HRT) closed to 0.75d were applied as an essential operational strategy to realize long term stable partial nitrification processes in both SBABs.

The contrast experiments were carried out simultaneously during the period I, and the overall performance is illustrated in Fig. 5.3 and 5.4. The $NH_4^+$-N concentrations in the influent were increased step by step from 100$mgl^{-1}$ on day 1 to 1400 $mgl^{-1}$ on day 146. As shown in Fig. 5.3, during the whole operational period I, the PN-SBAB with FO were carried out a stable and satisfactory partial nitrification process with half of ammonium in the influent oxidized to nitrite as well as small amount $NO_3^-$-N detected

in the effluent. However it is clearly found in Fig 5.4 that the partial nitrification process conducted in the SBAB without FO was stably maintained for around 110 days followed by disabled performance of PN process. From day 110 on the activity of ammonia oxidizing bacteria (AOB) in the SBAB without FO was obviously inhibited caused by the elevation in the influent substrate concentration. When the inlet $NH^{+}_{4}$-N concentrations are over 900mg$L^{-1}$ the SBAB without FO is not able to handle this high load ammonium which deteriorated the function of AOB to oxidize half ammonium to nitrite. By comparison there was no inhibition observed in the SBAB with the microbubble aeration system even the ammonium concentration in the influent is up to 1400mg$l^{-1}$. This inhibition was reversible and the partial nitrification performance in SBAB without FO was recovered when the inlet ammonium concentration was diminished. In terms of the stability of PN performance in two bioreactors, PN reactor with FO exhibited more steady and desired effluent with pH ranging from 7.5-6 whereas there is noticeable fluctuation in the effluent $NH^{+}_{4}$-N and $NO^{-}_{2}$-N concentrations from PN-SBAB without FO, which was companied by instability in pH values.

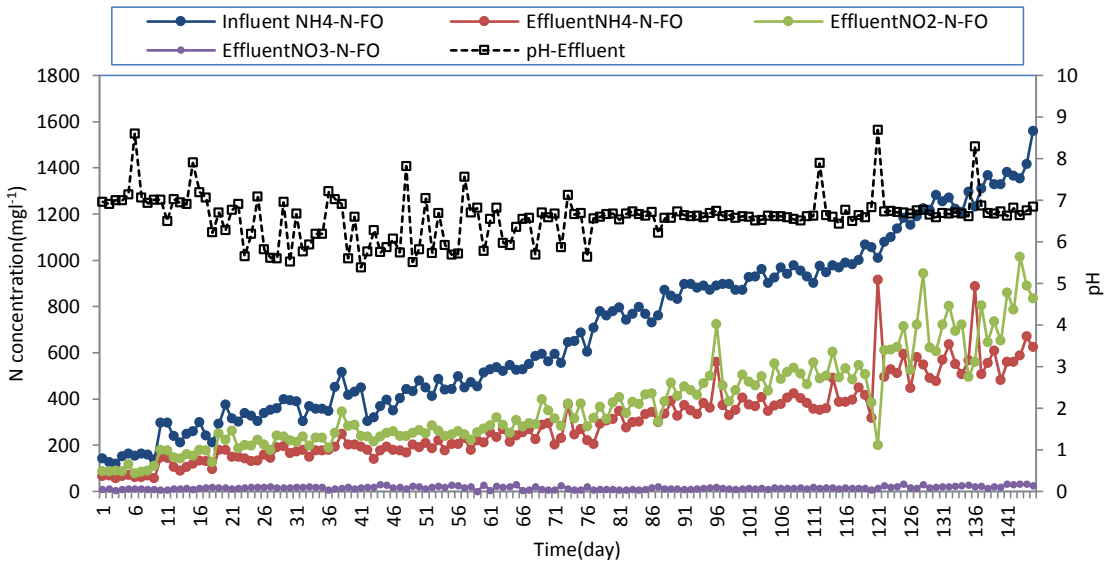


**Figure 5.3** Influent and effluent concentrations of nitrogen compounds for PN process in SBAB with fluidic oscillator

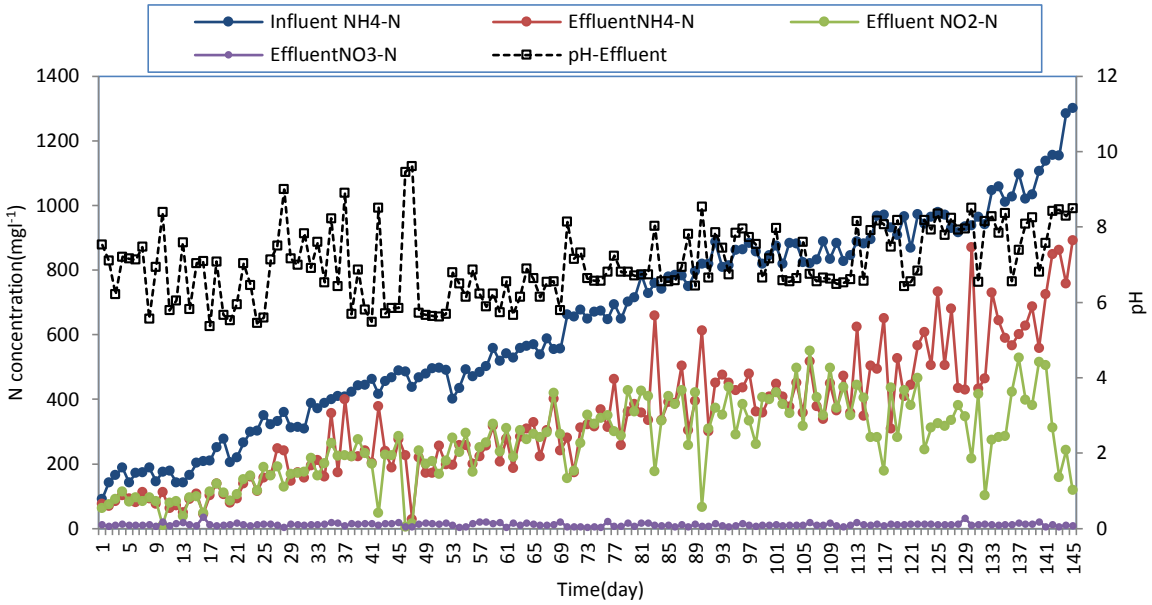


**Figure 5.4** Influent and effluent concentrations of nitrogen compounds for PN process in SBAB without fluidic oscillator

Fig 5.5 shows a more obvious difference of the features of the effluent from both PN bioreactors. The following research in chapter 6 demonstrated that the influent ratio of $NO^{2}$-N/$NH^{+}_{4}$-N between 1-1.5 is able to guarantee a successful performance of Anammox process. Therefore the suitable range of ratio of nitrite to ammonium and theoretical ratio 1.32 were marked in Fig 5.5. As the experiments progressed nitrite buildup was improved with the increase of ammonium concentration in both PN-SBABs. In the initial 20 days the effluent $NO_2^-$-N/$NH^{+}_{4}$-N ratio in PN-SBAB with FO fluctuated between 1.1 and 2; thereafter this ratio stabilized at 1.3±0.2 until the end, which fell in the suitable rang for Anammox reaction ratio. The instability in the early stage is attributed to the low substrate concentration which is prone to be converted to nitrite and nitrate. In the case of PN-SBAB with the normal bubbler aeration system, the effluent $NO_2^-$-N/$NH^{+}_{4}$-N ratio was mostly maintained at around 1.1±0.2 which is lower than that in PN-SBAB with FO. However it is noticeable that the very low effluent $NO_2^-$-N/$NH^{+}_{4}$-N ratios presented from time to time throughout the whole operational stage. There were three main reasons to explain this phenomenon: firstly the fine bubbles caused the inhomogeneous distribution of substrates in the bioreactor; secondly low oxygen mass transfer rate led to very low DO concentration closing to 0.1 causing the inhibition on the activities of AOB; thirdly, the resistance of PN-SBAB without FO to the $NH_4$-N load shock is weak compared to PN-SBAB with FO. Meanwhile as depicted show in Fig5.6 the effluent $NO^{-}_{3}$-N concentrations never exceeded 35mg$L^{-1}$ in PN-

SBAB with FO and 30mgL$^{-1}$ in PN-SBAB without FO respectively except 35.74mgl$^{-1}$ on day 19. In this study, the DO concentration was limited by controlling the airflow rate at low level, which was manipulated as the main operational strategy. Wiesmann (1994) demonstrated that NOB had high specific growth rates at DO concentrations above1.8 mgL$^{-1}$ and were likely to accumulate $NO_3^-$ -N under sufficient oxygen supply. Chung et al. (2005) reported that nitrite oxidation was restricted under low oxygen conditions. Here, with the DO concentration in our reactor restricted less than 1mgL$^{-1}$, $NO_3^-$-N production was limited to a negligible amount and the increment in $NO_2^-$-N accumulated was steady. It is observed in Fig5.7 that a similar evolution of nitrite accumulation ($NO^-_2$-N/($NO^-_2$-N+$NO^-_3$-N)) reached and kept over 90% during the period I. This fact further confirmed the growth of NOB was successfully depressed at very low DO levels in both PN systems.

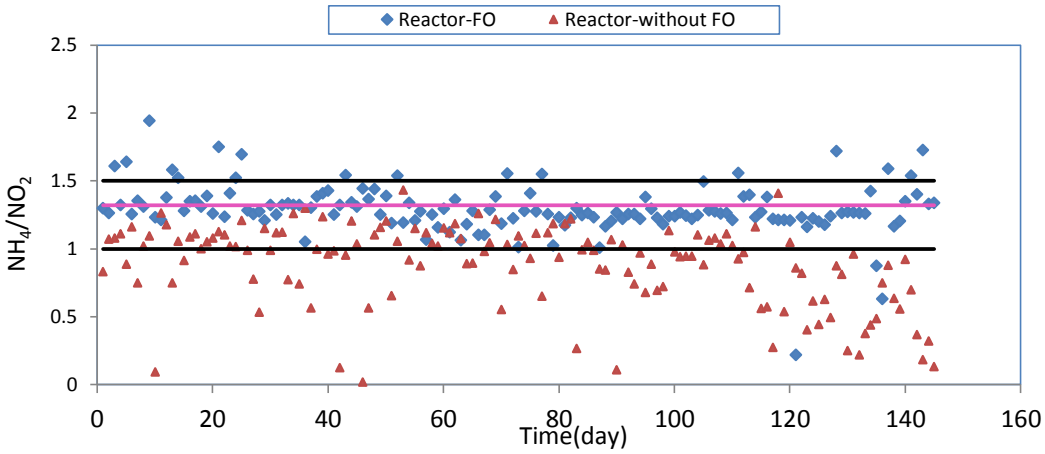


**Figure 5.5** Comparison of effluent $NO_2^-$-N/$NH^+_4$-N ratio in both PN-SBABs

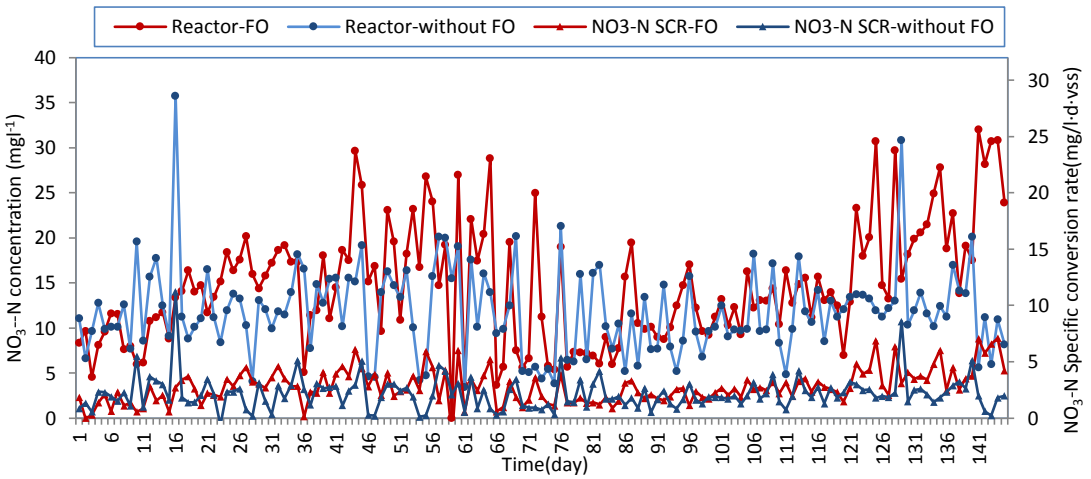


**Figure 5.6** Comparison of $NO^-_3$-N concentration of effluent and $NO^-_3$-N specific conversion rate in both SBABs

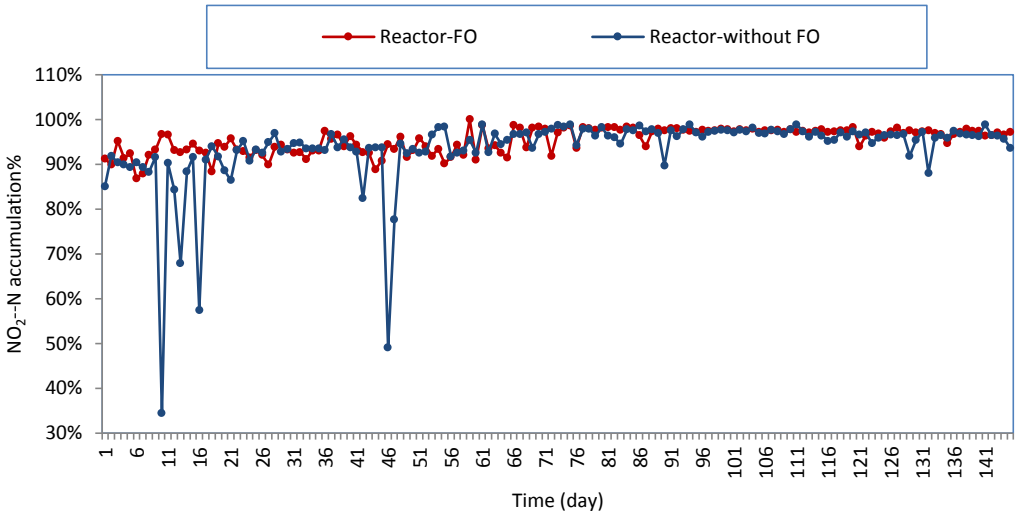


**Figure 5.7** $NO_2^-$-N accumulation rate with microbubble or fine bubble aeration

Because AOB have a lower oxygen half saturation constant than NOB, the activity of NOB can be inhibited by controlling DO at low concentration (commonly lower than 1mg$L^{-1}$). Contradictorily low DO concentration tended to cause low activity of AOB, sludge bulking and the increasing nitrous oxide production. Fig 5.8 and Fig5.9 illustrate the differences of evolution of ammonia conversion rate and evolution nitrate production rate in both PN-SBABs during the operation period I. A more stable and slightly higher specific nitrogen conversion rate was achieved in PN-SBAB with FO compared with PN-SBAB without FO during the first 110 days. However, as the ammonia concentration was increased specific ammonia conversion rate of AOB was dramatically decreased 40% in the bioreactor with fine bubble aeration system. On the contrary the activity the AOB in the reactor with the microbubble aeration system were not affected and kept fairly high level. In terms of specific nitrate production rate, the activity of NOB for both bioreactors were not significantly affected by the increase of ammonia in the influent and always remained at low levels throughout the entire operational stage which indicated NOB did not have sufficient growth potential and were gradually washed out from the system. Due to the higher oxygen mass transfer in PN-SBAB with FO the nitrate produced rate was slightly higher than that in PN-SBAB without FO (Fig 5.9). The energy and growth of AOB was weaker than that of AOB in PN-SBAB with FO. In this case, we can infer that the AOB worked better with the microbubble aeration system during the whole operation stage I.

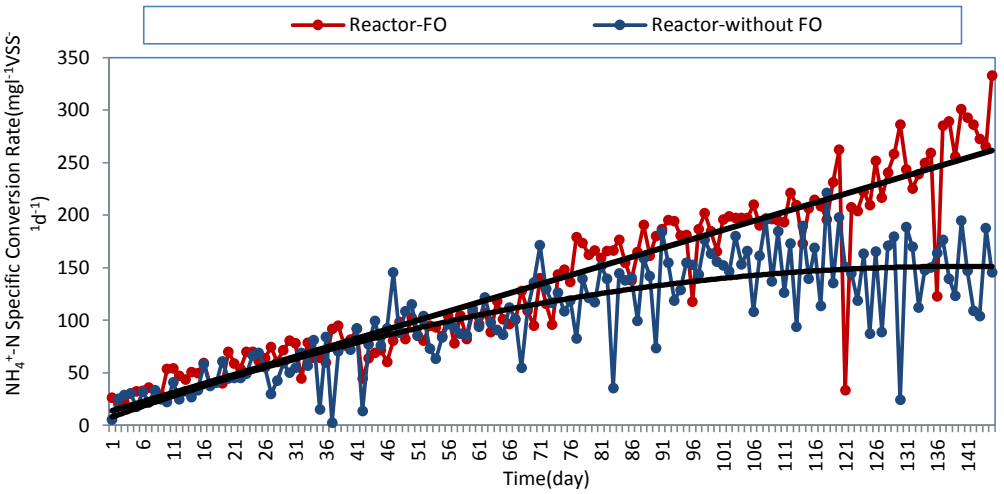


**Figure 5.9 (a)** Variations of ammonium conversion rate in both SBABs

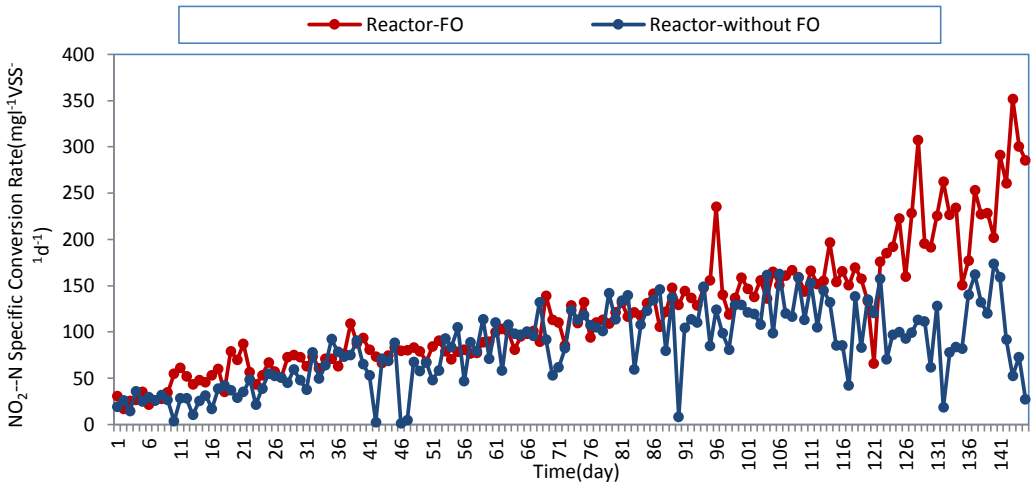


**Figure 5.9** (b) Variations of nitrite conversion rates in both PN-SBABs

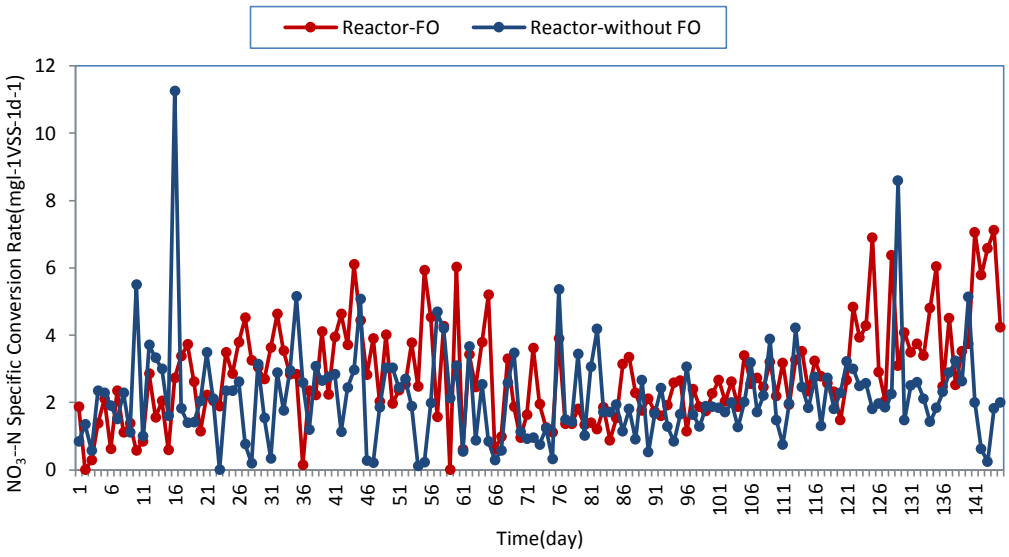


**Figure 5.9** (c) Variations of nitrate production rates in both PN-SBABs

According to the analysis above, it is obvious that higher and more stable treatment capacity was achieved in the bioreactor with the microbubble aeration system. In the present study both PN-SBABs were operated under same operating conditions except the aeration system, hence, it is an undeniable fact that the characteristics of microbubble contributed to the excellent performance of PN-SBAB with FO.

The excellent performance of PN-SBAB can be attributed to the following reasons: Firstly under the circumstance of limiting oxygen, high mass transfer efficiency offered adequate dissolved oxygen for AOB activities, which effectively avoided the inhibition caused by low DO (generally <0.1 $mgL^{-1}$). Secondly, based on the conclusion in Chapter 4, the better mixing condition resulting from the microbubble aeration system enhanced the contact area between AOB and nitrogen substrate which is favor of the diffusion of ammonium into bacterial cell. In addition the uniform distribution of substrate avoided local excessive substrate concentration causing inhibition. Thirdly, in the sense of bubble size, the collision between bigger size bubble and floc sludge tended to increase detachment of biomass and decreased the settleability of biomass, as a result the fractured sludge might be washed out gradually.

Furthermore, hydrodynamic shear force existing in all biological wastewater treatment systems as a result of aeration or liquid fluidization played an important role in microbial attachment and cell self-immobilization processes. The response of microbial cells to varying shear strength was reported by Liu (2005) in terms of sludge particle size, settling properties, cell surface hydrophobicity, and metabolic behavior. A higher cell surface hydrophobicity, larger floc size, lower sludge volume index (SVI) and higher production of exopolysaccharides were observed when shear strength was increasing in the certain range. Even though the lower sludge production rate were investigated as well under such condition, its negative effect on the accumulation of biomass was overwhelmed by the combined positive influences of the other factors. Actually the biomass accumulation for a complete autotrophic system is more dependent on the retention ability of the bioreactor. Finally Liu came to the conclusion that at certain levels higher shear strength is likely to exert a favorable influence on the cell attachment, leading to the growth of settable biological flocs which is in agreement with the observation by the other authors (Arrojo et al., 2006; Chang et al., 1991; Chen et al., 1998;). As we already know, fluid pattern and higher fluid velocity related to microbubble in the SBAB with FO contributed the higher hydrodynamic shear stress. In

this study, since very lower air flow rate was applied to control low discovered oxygen concentration it is assumed that the shear stress did not exceed the suitable rang to exert the negative influent on the biomass.

### 5.4.2 The Effect of Microbubble Aeration System on the Cycle Performance of the Partial Nitrification

In order to study the phenomenon occurring during the cycle of partial nitrification process, a typical cyclic performance analysis was carried out on day 50 with operational temperature of 30℃. The concentrations of each compound have been monitored during specific cycles in both PN- SBABs, sampling the reactors every each hour in all cycle long. The effect of microbubble on the performance of PN cycle was investigated through real-time monitoring of the three major parameters: OPR, dissolved oxygen concentration (0.1–1 $mgO_2\ L^{-1}$) and pH.

The batch experiments were performed respectively in two PN-SBABs with different aeration systems to evaluate the capacity of each bioreactor to achieve 50% partial nitrification under the same operating conditions. Fig 5.10 and 5.11 showed the behaviours of two PN systems with and without fluidic oscillator, respectively. It was observed in both bioreactors that $NH_4^+$-N concentrations decreased from $860mgL^{-1}$ to around $390mgl^{-1}$ with the elapsed time under aerobic condition and there was a corresponding increase in $NO^-_2$-N concentrations from $20mgL^{-1}$ to around $490mgL^{-1}$. The decrease of pH was caused by the reduction of alkalinity and the acid production during oxidation from $NH_4^+$-N to $NO_2^-$-N. After completion of 50% ammonia oxidation, alkalinity was depleted and the ammonia oxidation was stopped. The point marked with a red circle in pH profile represented the end of half ammonia oxidation process and it was known as the 'ammonia valley'. As shown in Fig 5.10 and Fig 5.11, two PN systems took 12h and 17h respectively to achieve this end point. It is noticed that the ammonia break point in the profile of ammonia concentration did not present with ammonia valley simultaneously but anterior to ammonia valley. This valley point was usually adopted to optimize partial nitrification system. At the end of aeration phase, around 50% ammonia was converted to nitrite, half ammonia remaining in the system to obtain the requested effluent. The $NO^-_3$-N concentration was constantly kept very low level about $50mgl^{-1}$ and $55.1mgl^{-1}$ respectively in two PN systems. The higher nitrate

concentration detected in PN-SBAB with fluidic oscillator was explained as a result of over aeration and higher oxygen mass transfer thanks to microbubble characteristics. Through comparing the results shown in Fig5.10 and Fig 5.11, it appears that the real cycle duration time (12 hours) of partial nitrification in PN-SBAB with fluidic oscillator is shorter than the one (17hours) in PN-SBAB without fluidic oscillator. The same observations can be made from Fig 5.12 representing the evolution $NO^-_2$-N/$NH^+_4$-N ratio with time. The suitable $NO^-_2$-N/$NH^+_4$-N ratio of 1:1.3 for subsequently Anammox process was reached faster in the bioreactor profiting with microbubble aeration.

For the combination process of partial nitrification and Anammox, two aspects are essential in the partial nitrification step. Firstly NOB must be continuously suppressed, and secondly the nitrite/ammonium molar ratio produced must be about 1.32 based on the Anammox reaction equation. Even though, after ammonia valley point, the aeration was still working in PN-SBAB with FO, the $NO^-_2$-N/$NH^+_4$-N ratio did not change with time which indicated the alkalinity control is also a robust and effective strategy to achieve partial nitrification when the other conditions changed. In terms of nitrate produced, an unremarkable increasing in nitrate concentration was depicted in Fig5.10 over the aeration period. The possible reasons for this fact were low DO concentration, very limited NOB existence in the partial nitrification system and inhibition of high FA&FNA concentrations.

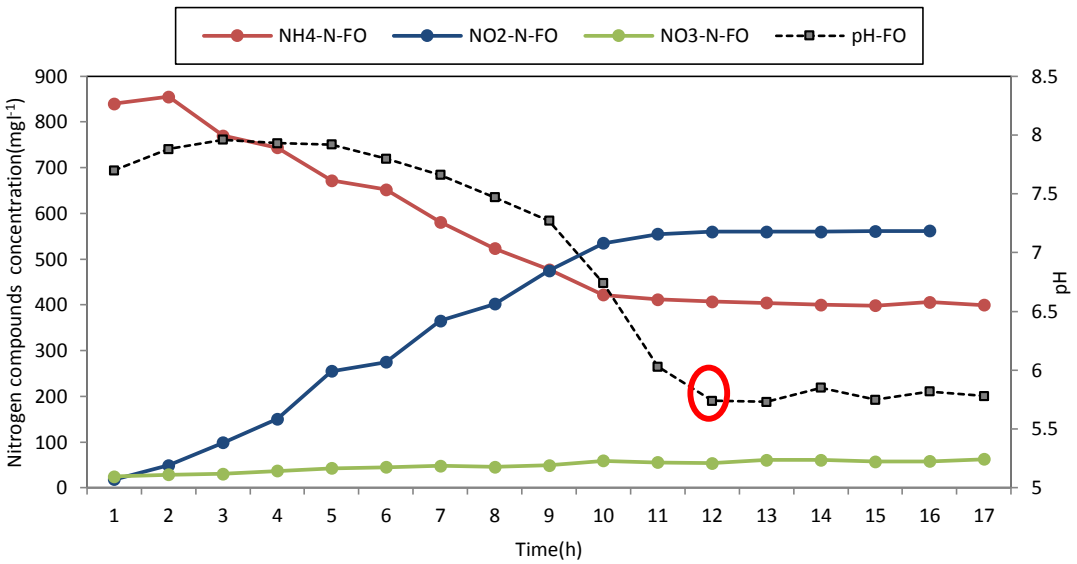


**Figure 5.10** Typical profiles of ammonium, nitrite, nitrate concentrations and pH in a cycle of PN-SBAB with FO

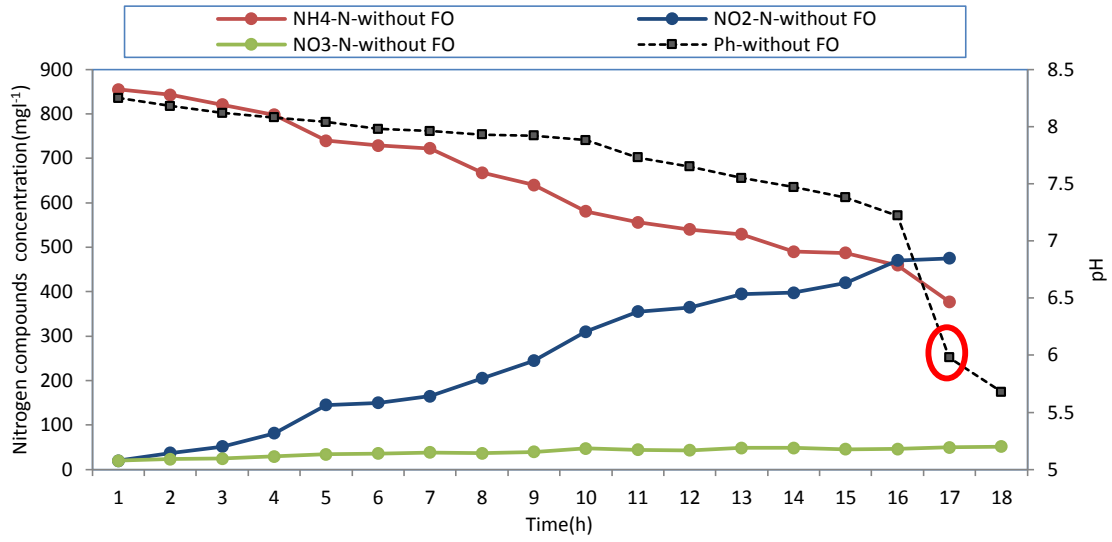


**Figure 5.11** Typical profiles of ammonium, nitrite, nitrate concentrations and pH in a cycle of PN-SBAB without FO

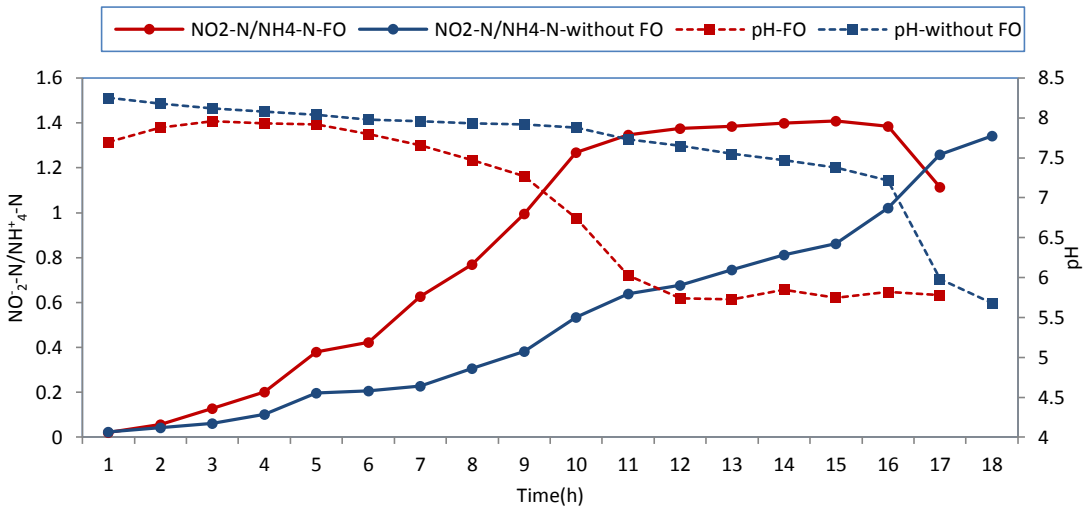


**Figure 5.12** Time course of $NO^-_2$-N/$NH^+_4$-N ratio in cycle of PN-SBABs

During cycle experiment, typical variations of nitrate concentrations and control parameters including DO, pH and ORP are shown in Fig5.13 and Fig 5.14. The initial rise in the pH curve was caused by carbon dioxide stripping from the system (Ra et al., 1998). Based on nitrification reactions equation, the pH value decreased in the course of converting ammonia to nitrite because there was hydrogen ion produced. During the process of nitrite converted to nitrate, there was no hydrogen ion produced. Therefore, pH stopped deceasing or started to ascend due to $CO_2$ stripping when nitration was completed. In this experiment no elevation in pH was found over the entire aeration period which suggested the nitrate production was restrained very well in SBAB with

FO. In both PN systems DO concentrations were remained at very low level, less than 1mg$L^{-1}$ and sharply ascended over 6mg$L^{-1}$ after the completion of ammonia oxidation. A break point named as "DO break point" showed in DO profile (Pavšelj et al., 2001). Throughout the entire cycle performance DO concentration in PN-SBAB with FO was always slightly higher than that in PN-SBAB without FO due to the higher oxygen mass transfer by using microbubble. Through detecting these break points (generally "ammonia valley" in pH profile), the duration of aerobic could be controlled stably, which was favourable to achieving high ammonia removal efficiency and avoiding the further transformation from nitrite to nitrate. Similar to the results from Fig 5.13, the ammonia valley on the pH profile for the microbubble aeration system showed up distinctly earlier than that for the normal bubble aeration system. Unlike the Fig5.10 the break point for DO presented with ammonia valley on the pH profile at the same time. These facts lead to the conclusion that the application of microbubble aeration system dramatically reduces the operating time for nitrogen removal process as well as saves more energy and oxygen.

It was necessary to state that using 'aeration-time-control' as operational strategy was beneficial for the nitrite accumulation and the growth of dominant AOB over NOB. Extended aeration encouraged the transition of partial nitrification to complete nitrification, thus in order to improve the performance of the directors, aeration was supposed to be stopped as soon as detecting the ammonia valley on the pH profile in PN-SBAB with fluidic oscillator. Since the DO concentrations were very low throughout the partial nitrification stage some people doubted the denitrification reaction would take place leading to loss in nitrite in the reactor. Our PN-SBABs experienced very long term operation under inorganic environment which is impossible to supply the organic carbon source for the growth of denitrification bacteria; therefore the disturbance from denitrification was neglected.

ORP reflects the variations in DO concentration and the activity of oxidizers and reducers. Besides DO and pH, ORP is also a very important indicator to examine the performance of the partial nitrification system and optimize the operation conditions. Especially, in the case of very low DO concentration (close to zero), the ORP is better to indicate the end point of oxidizing reaction in the PN system. Fig 5.14 shows us the higher ORP in PN-SBABs with FO was measured compared with the PN-SBABs without FO. As nitrification from the nitrite to nitrate was effectively inhibited in both

bioreactors, the observed ORP revealed that the stronger ammonia oxidation taking place in PN-SBAB with FO resulted in a shorter time operation cycle. The ORP break point correspondingly emerged at the end of ammonia oxidation.

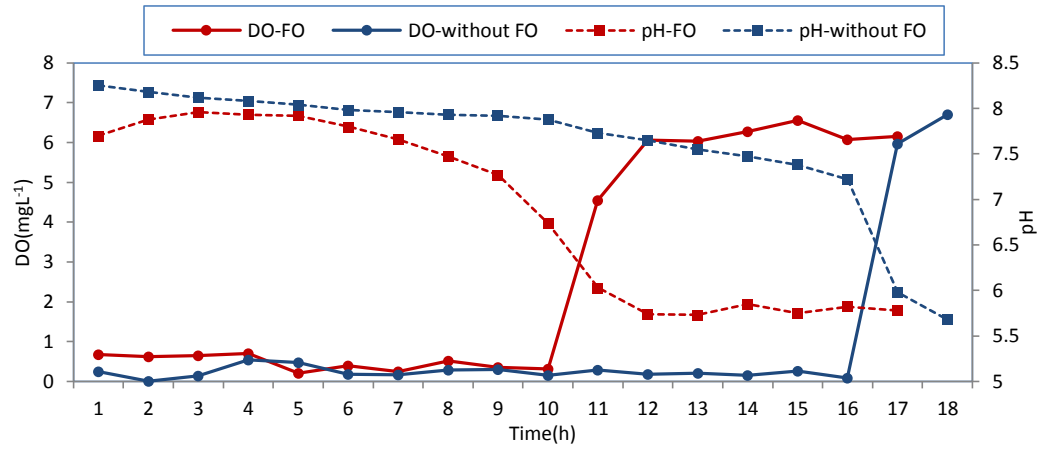


**Figure 5.13** Profile of DO and pH in typical SBAB cycle with and without fluidic oscillator

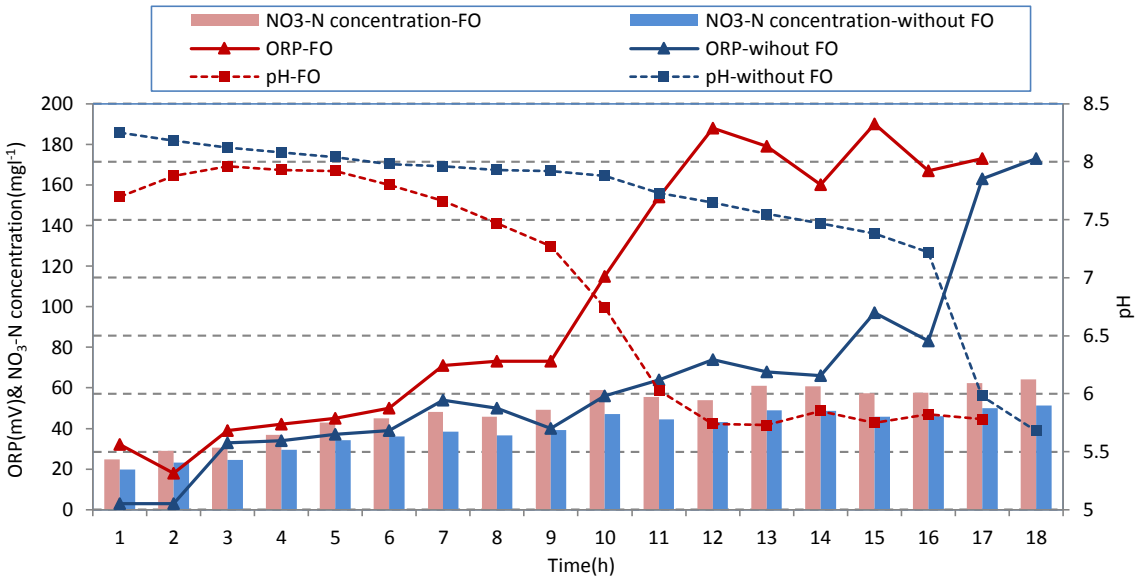


**Figure 5.14** Profile of $NO^-_3$-N, ORP and pH in typical SBAB cycle with and without fluidic oscillator

$NH^+_4$-N depletion was getting quicker by using a microbubble aeration system, corresponding to the elevated partial nitrification speed. Fig5.15 demonstrated the specific ammonia conversion rate speeded up in PN-SBAB with FO. It is true that the higher DO concentration accelerates the nitrification speed. In the suitable range of DO concentration, the higher DO concentration contributes to higher efficiency of the partial nitrification process. We already proved the microbubble undoubtedly brought

higher $K_l a$ value under the same conditions compared with normal size bubble. Moreover, the $NO^-_2$-N production seemed to be earlier benefited from the DO concentration increased than $NO^-_3$-N production. This phenomenon can be explained by that NOB has a less affinity for oxygen than that of AOB as a result of their different oxygen saturation levels: 1.1 mg $O_2$ $L^{-1}$ for NOB and 0.3 mg $O_2$ $L^{-1}$ for AOB (Wu et al., 2007). Admittedly, the nitrate production rate correspondingly increases when NOB exposed to the higher DO concentration (Fig 5.16). While this increase was negligible when DO concentrations dropped back in the desirable range of DO for partial nitrification very soon and little NOB presented in the PN system.

At the end of aeration period, DO concentration in PN-SBAB with FO is sharply increased to over 6mg$l^{-1}$ but the nitrate production rate was not sped up as expected. The $NO^-_3$-N specific conversion rate still remained at the same or lower level. It is explained that the combined influence of high FA /FNA concentration and deficiency of carbon source for NOB growth played the main role to suppress the activity of NOB.

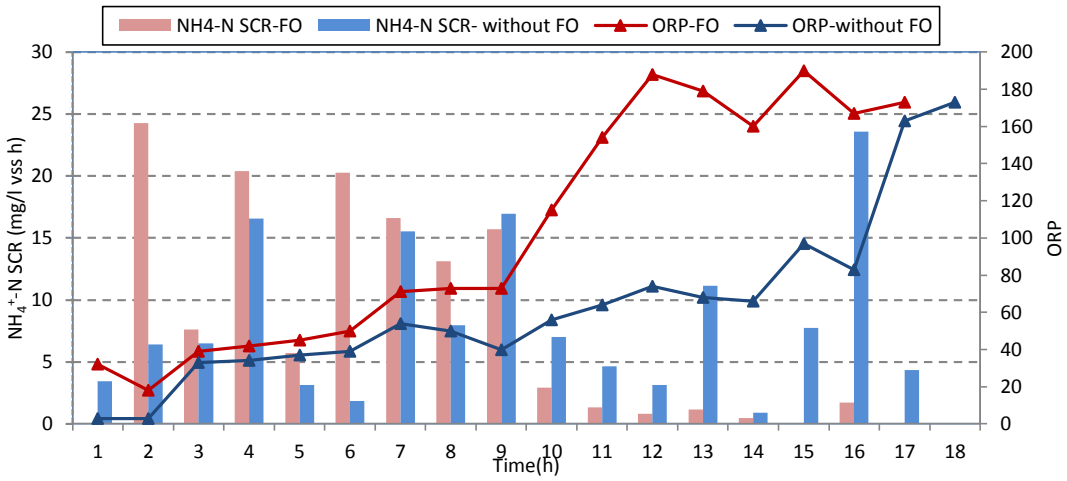


**Figure 5.15** Variation of $NH_4^+$-N specific conversion rate with time in both PN-SBABs

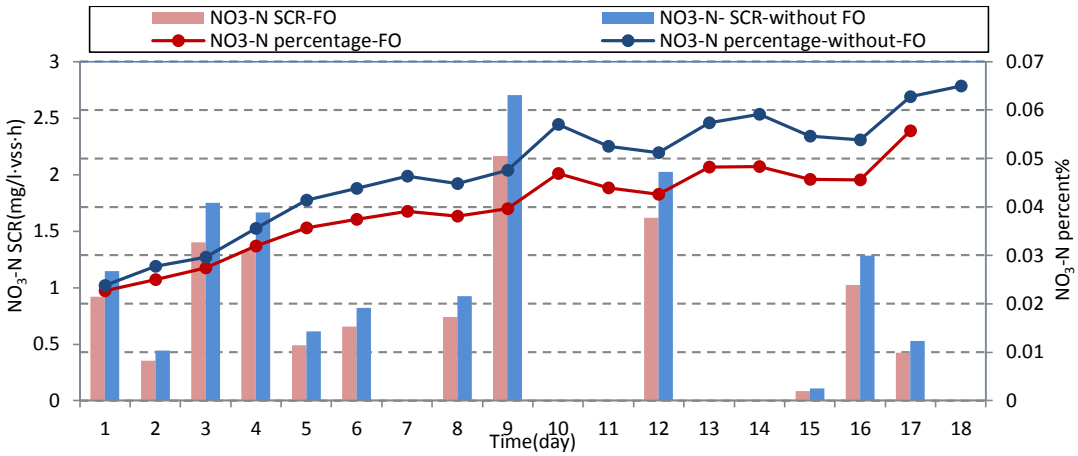


**Figure 5.16** Variation of $NO_3^-$-N specific conversion rate with time in both PN-SBABs

Oxygen uptake rate, whose measurement can be understood as a direct indicator of biological activity, has been used for investigating the effect of microbubble on the AOB activities in two PN-SBABs. Since the small quantity of nitrate produced in the process was taken into account, it was assumed that the oxygen consumption in both PN-SBABs is due solely to AOB activity and OUR would then be a good indicator of AOB performance. It can be seen in Fig 5.17 that the comparison between the oxygen uptake rates (OUR) under different aeration systems shows the higher activities of AOB microorganism were found by using microbubble aeration system. In PN-SBAB with FO, the values of OUR were established between 0.65~0.69 $mgO_2/L \cdot min$ during the ammonia oxidation stage. This value for normal bubble aeration system declined to 0.42~0.51 $mgO_2/L \cdot min$, 30% reduction. The value of OUR in PN-SBAB with FO progressively decreased to around 0.15 $mgO_2/L \cdot min$ when IC was depleted, indicating the oxidation of nitrite to nitrate was hardly occurred. The curve pattern of OUR almost fits with evolution of pH. The break points showed up in two OUR curves when half ammonium oxidation is finished. From this observation it can be concluded that the biological activity reduction was related to inhibition factor or inorganic substance limitation.

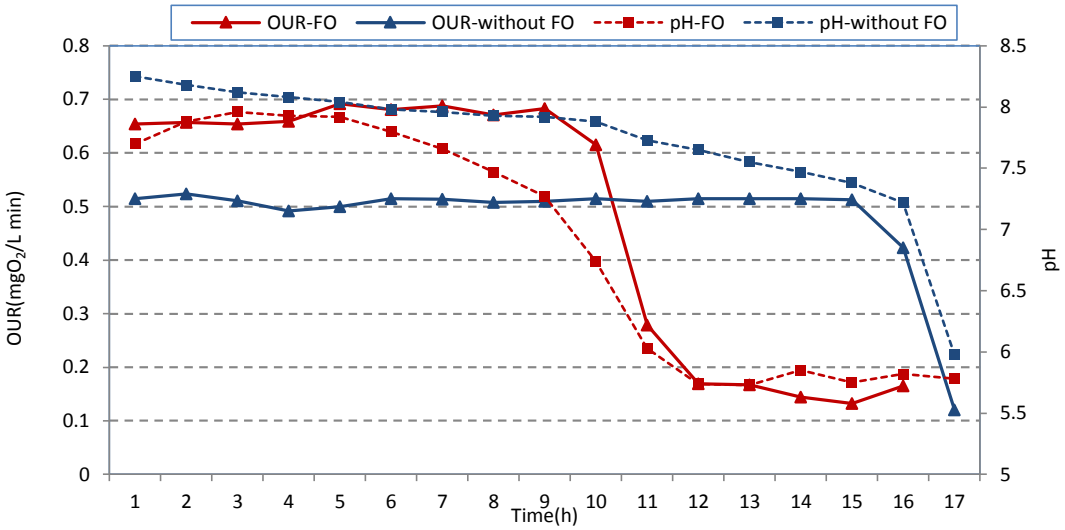


**Figure 5.17** Cycle profile evolution of OUR in both PN-SBABs

### 5.4.3 The Influence of Nitrogen Loading Rate on (NLR) on the Performance of PN-SBABs with Different Aeration Systems

The nitrogen loading rate in the field of biological wastewater treatment is an essential indicator to evaluate the capacity of different nitrogen removal processes. The performance of partial nitrification (i.e., ammonium conversion rate and nitrate production rate) was evaluated as a function of the ammonium loading rate (Fig. 5.18 and Fig 5.19). The specific ammonium conversion rate in both PN-SBABs gradually was increased with the ammonium loading rate increasing, while nitrate production rate did not exhibit the similar tendency with specific $NH_4^+$-N conversion rate curve during the whole range of the ammonium loading rate but mostly fluctuated from 0 to 7mg-N (l vss d) $^{-1}$. Nitrite accumulation ranged from 86% to 97%±1% in the case of NLR less than 0.75 kg-N $m^{-3}day^{-1}$ followed by remaining at 97%±1% in PN-SBAB with FO, which is more stable and slightly bigger than that in PN-SBAB without FO (Fig5.18). As can be seen in the Fig 5.19 it is illustrated that nitrate specific production rate was mostly controlled under around 7mg-N $l^{-1}vss^{-1}d^{-1}$ and 5.5mg-N $l^{-1}vss^{-1}d^{-1}$ respectively in both bioreactors by high FA and low DO concentration. It is, however, noticed that the specific ammonium conversion rate in PN-SBAB without microbubble aeration system stopped increasing when the ammonium loading rate was over 1.23 kg-N $m^{-3}day^{-1}$ and inhibition on activity of AOB represented whereas the specific ammonia oxidation rate in PN-SBAB with FO were not disturbed at all as NLR increasing, on the contrary enhanced by higher NLR. The nitrogen loading capacity for the PN system with the

microbubble aeration system reached up to 2.08kg-N $m^{-3}day^{-1}$ comparable to 1.23 kg-N $m^{-3}day^{-1}$ in PN system with normal bubble aeration system.

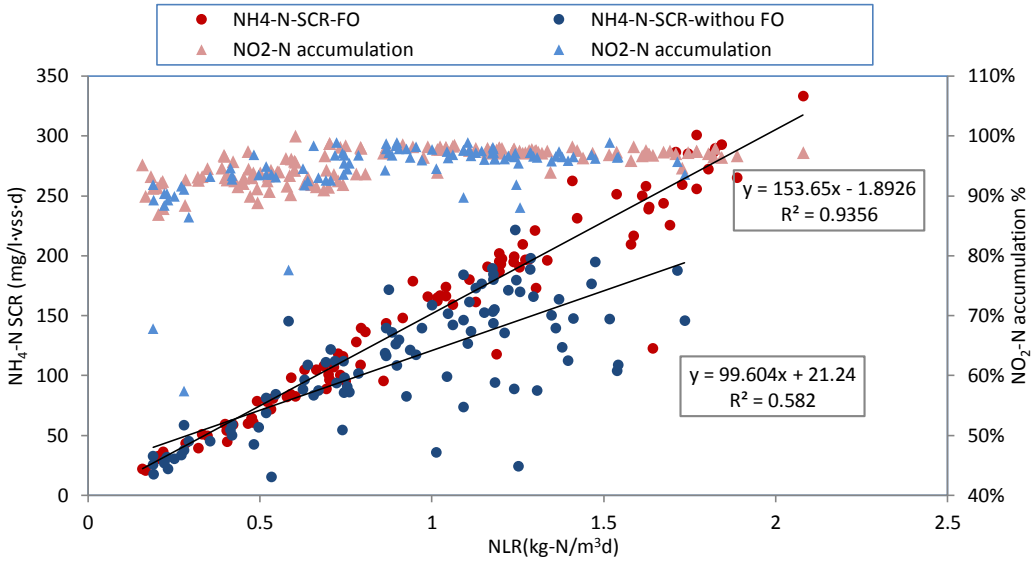


**Figure 5.18** Specific ammonia conversion rate and nitrite accumulation rates were related to ammonium loading rate

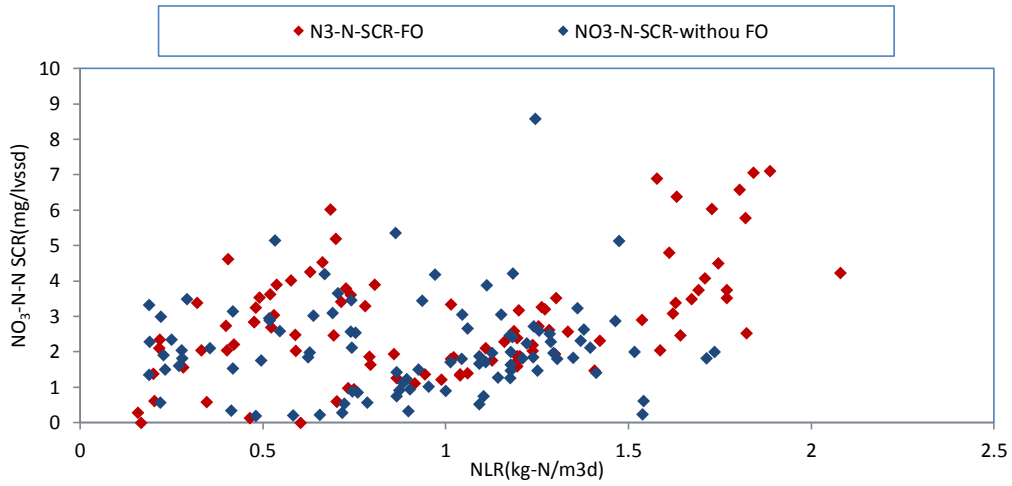


**Figure 5.19** Specific nitrate conversion rate was related to ammonium loading rate

Fig5.20 and Fig5.21 show the variations of the effluent with NLR increasing in both PN-SBABs. NLR was enhanced gradually in both PN-SBAB by increasing the substrate concentrations. During the entire operational period I, the PN-SBAB with FO exhibited an acclimating and stable performance. In this period, the AOB in the reactor gradually adapted to these cultural conditions. Various influent substrate concentrations, ranging from 100 to 1188 $mgL^{-1}$ $NH^{+}_{4}$-N, were added to the bioreactor during this period and the NLR increased from 0.18 to 2.08kg-N/m3/day. A suitable $NO^{-}_{2}$ -N/$NH^{+}_{4}$ -N effluent

ratio of 1.3 ± 0.2 was maintained. Two unstable points presenting on day 123 and day 168 in the profile is due to the aeration failure. The $NO_3$-N concentration in the effluent was getting lower and more stable with the NRL increasing. In the first 112 days the PN-SBAB without FO showed an unstable partial nitrification process. From day 113 to the end of the experiment, the effluent $NO^-_2$ -N/$NH^+_4$ -N ratio was decreased sharply to below 1. The partial nitrification was deteriorated however this inhibition is reversible by decreasing the NRL. These results come to conclusion that the microbubble aeration system improved the capacity of SBAB for treating the high loading nitrogen by more than 65% and also enhanced adaptability of SBAB to $NH_4$-N shock load, compared to the normal bubble aeration system.

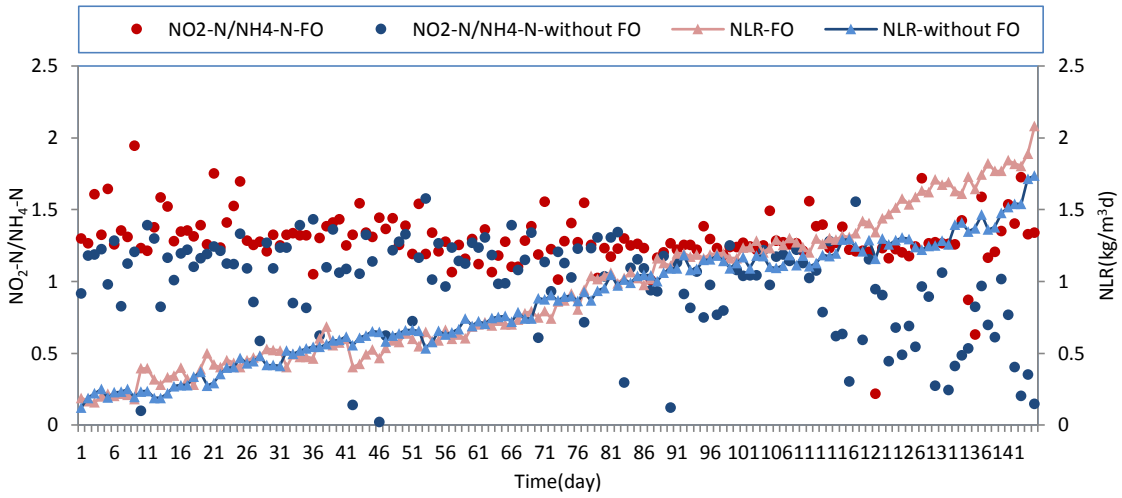


**Figure 5.20** Time course of $NO_2$-N/$NH_4$-N and NLR in both PN-SBABs

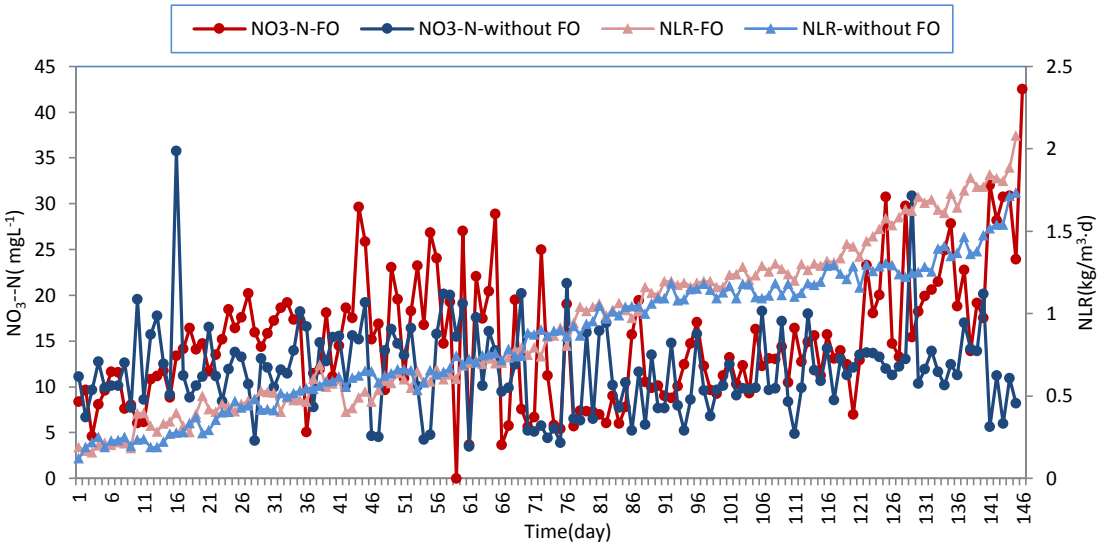


**Figure 5.21** Time course of nitrate concentration in effluent and NLR in both PN-SBABs

### 5.4.4 The Influence of FA, FNA on the Performance of both PN- SBABs with Different Aeration Systems

In the PN process, FA and FNA are the true substrates for ammonia oxidizing bacteria (AOB) and nitrite oxidizing bacteria (NOB). It is well known that Nitrosomonas are inhibited by concentrations of free ammonia over 10 mg$NH_3$-N $L^{-1}$ while Nitrobacter are inhibited by values of only 0.1–1.0mg$NH_3$-N $L^{-1}$ (Anthonisen et al., 1976). Therefore, partial nitrification could be obtained by maintaining levels of free ammonia in the reactor which caused only inhibition on the nitrite oxidizing bacteria (NOB) population. While the inhibition on Nitrobacter bacteria was initiated at concentrations of FNA between 0.22 and 2.8 $mgL^{-1}$. Mosqura-Corral et al. (2005) reported that inhibition on AOB took place when FNA concentrations were higher than 0.2 $mgL^{-1}$. However, both AOB and NOB were able to acclimatize to high FA concentrations with NOB acclimatization to FA concentrations as high as 22 $mgL^{-1}$ (Turk and Mavinic, 1989; Villaverde et al., 2000). The other researchers also reported that partial nitrification could be achieved at FA levels of about 20 $mgL^{-1}$ (Qiao et al., 2008) while Peng and Zhu (2006) reported stable PN operation obtained at FA concentration as high as 50 $mgL^{-1}$. It is evident that the reported threshold inhibition values of FA on NOB have been somewhat inconsistent until now. This fact demonstrated the inhibition of FA and FNA on partial nitrification to a large extent depends on the operating condition and acclimatized biomass.

The concentrations of $NH_3$ and $HNO_2$ were calculated at the operational temperature 30 ℃ from the $NH_4^+$-N, $NO_2^-$-N concentrations and the pH in the bulk liquid using Eqs. (5-2) and (5-3) according to the expressions proposed by Anthonisen et al. [1976]:

$$C_{NH_3} = \frac{C_{NH_4}}{\frac{6344}{(\frac{e^{\frac{}{T+273}}}{10^{pH}}+1)}} \quad (5\text{-}2)$$

$$C_{HNO_2} = \frac{C_{HNO_2}}{10^{pH} e^{\frac{-2300}{T+273}}} \quad (5\text{-}3)$$

Fig5.22 a shows us the time course of influent FA concentration in both PN-SBABs during the whole operational period I. The both influent FA concentration represented increasing tendency with the influent ammonium concentration. During the first 70 days, the both influent FA concentrations fluctuated, accompanied with significant changes in

the pH. In the following operational period, pH was getting stable and the influent FA concentrations were approximated 160 $mgL^{-1}$ and 120 $mgL^{-1}$ under two different aeration systems, respectively.

Fig5.23 illustrates the variation in effluent FA concentrations in both PN-SBABs during the entire operational period I. The effluent FA concentration in both reactors represented the similar variation pattern. In the first 70days FA concentration generally fluctuated between 0.03$mgL^{-1}$ and 1.84$mgL^{-1}$ in SBAB with FO and between 0.02$mgL^{-1}$ and 2.0$mgL^{-1}$ in SBAB without FO, respectively. From day 70 to day 116 there is evident leap on the profile of outlet FA concentration and then the effluent FA concentration maintained at about $1.3 \pm 0.2 mgL^{-1}$ steadily as a result of high influent ammonium concentration as well as the stable pH in the effluent. It is also observed that some very high effluent FA concentrations emerged in two PN systems due to the aeration system malfunction which inhibited the activity of nitrifiers in the bioreactors. Thereafter the FA concentration in the SBAB with FO kept increasing to 3$mgL^{-1}$ whereas in the SBAB without FO the FA concentration became very unstable.

The effluent FNA concentration variations with time in both PN-SBABs were depicted in Fig 5.24. Compared with the effluent FA concentration profile in Fig 5.23 there is a similar trend in the variations of FNA concentration within the operational period which is an unstable stage in first 70days followed by stable stage. During the stable operational period the FNA concentration (0.003mgl-1~0.99mgl-1) in PN-SBAB with FO was detected slightly higher than that (0$mgl^{-1}$~0.8$mgl^{-1}$) in the PN-SBAB without FO as a result of high ammonia conversion rate obtained by the microbubble aeration system. The stability of FNA in SBAB with FO is remarkable better than that in SBAB without FO.

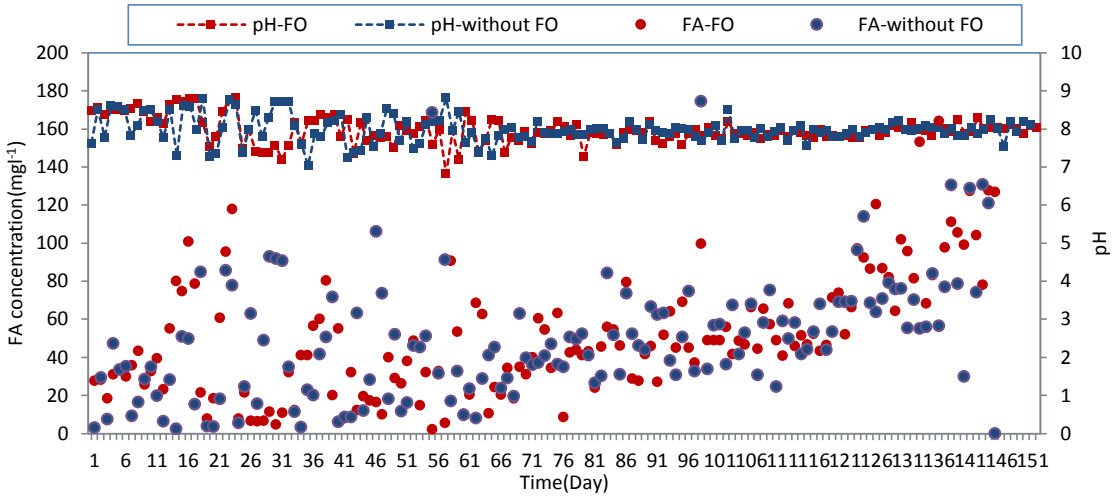


**Figure5.22** Evolution of influent free ammonia concentration and pH in both PN-SBABs along the operational period I

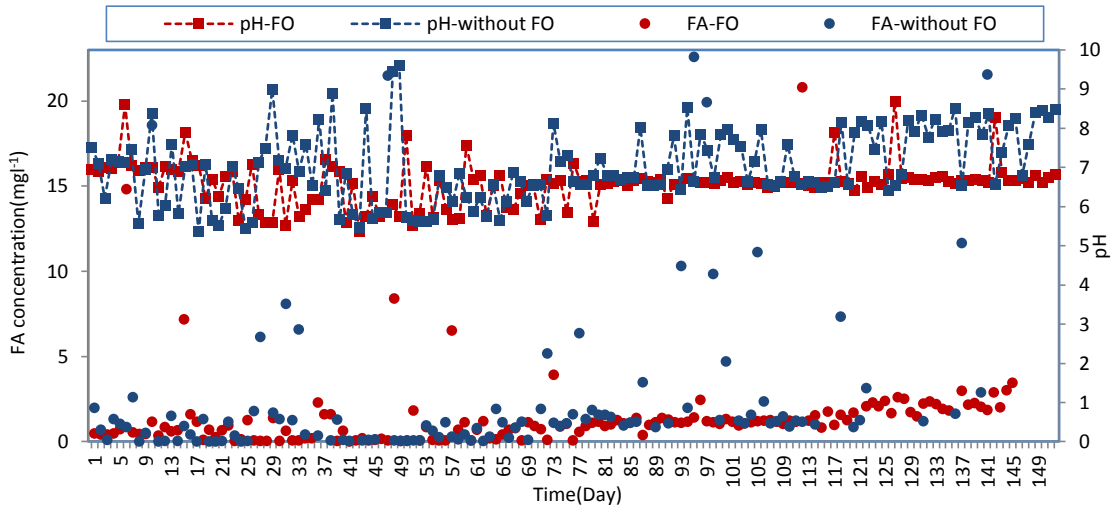


**Figure 5.23** Evolution of effluent free ammonia concentration and pH in both PN-SBABs along the operational period I

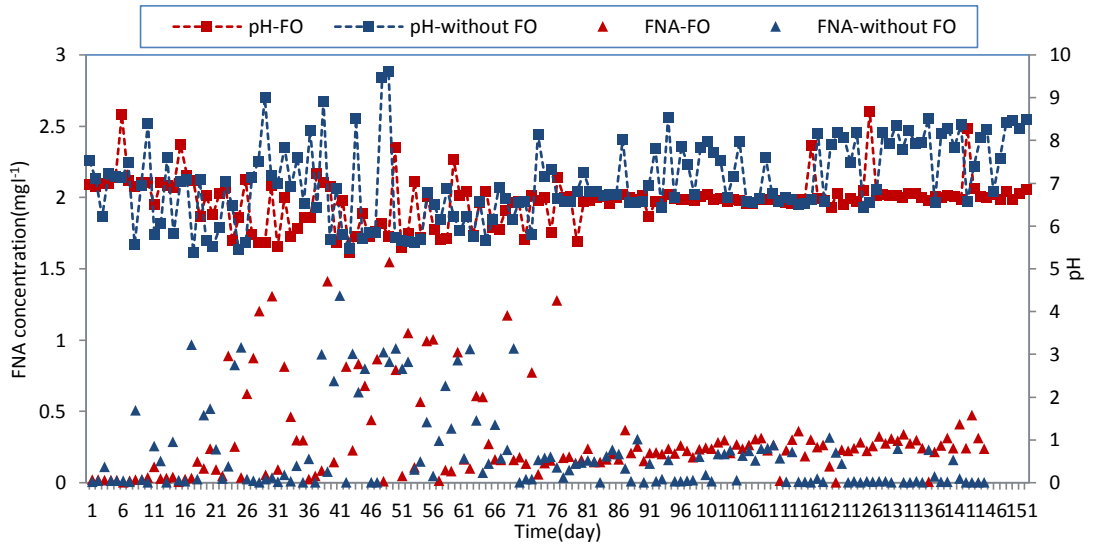

**Figure 5.24** Evolution of effluent free nitrous acid concentration and pH in both PN-SBABs along the operational period I

In this study the influent ammonium concentration was gradually increased. In the earlier stage the low substrate concentration resulted in the low FA and FNA concentration leading to low inhabitation while unstable pH caused fluctuations in both FA and FNA concentration. In the follow-up operational period the concentration of ammonium and nitrite played the primary role in the determination of the FA and FNA. In addition, long term operation acclimatized the active sludge to the high FA and FNA concentrations, which guaranteed a better activity of AOB. According the inhibition theory of Anthonisen, the FA concentrations detected in both SBABs were much higher than the threshold of inhibitory concentration of $1mgl^{-1}$for NOB, thus, the growth and activity of NOB were consequently inhibited, as shown in Fig5.25 The average specific $NO_3$-N conversion rates were restricted below 2.804 mg $gvss^{-1}$ $d$ and 2.18 mg $gvss^{-1}$ $d$ respectively in two SBABs whereas the primary AOB microorganisms gradually acclimatized to the high FA concentration and efficiently converted ammonium to nitrite. The combined effect of inhibition of FA, the short HRT and low DO concentration contributed to the washout of NOB from two PN systems. Interestingly, very high influent FA concentrations, outdistancing the threshold of inhibitory concentration of $50mgl^{-1}$for AOB ever reported, were detected in both PN systems however, during the entire operational period no FA inhibition of AOB was observed in PN-SBAB with FO, even though the FA concentration reached $160mgl^{-1}$. As can be seen in the Fig 5.26 the specific ammonium conversion rate was increased with the FA concentration elevated. Until the final operational day, the inhibitory concentration was not being reached. Nevertheless this threshold was increased to $85mgl^{-1}$ in the PN-SBAB without FO. It is suggested that the tolerance of AOB to high FA concentration under the microbubble aeration system is definitely stronger than that under a fine bubble aeration system.

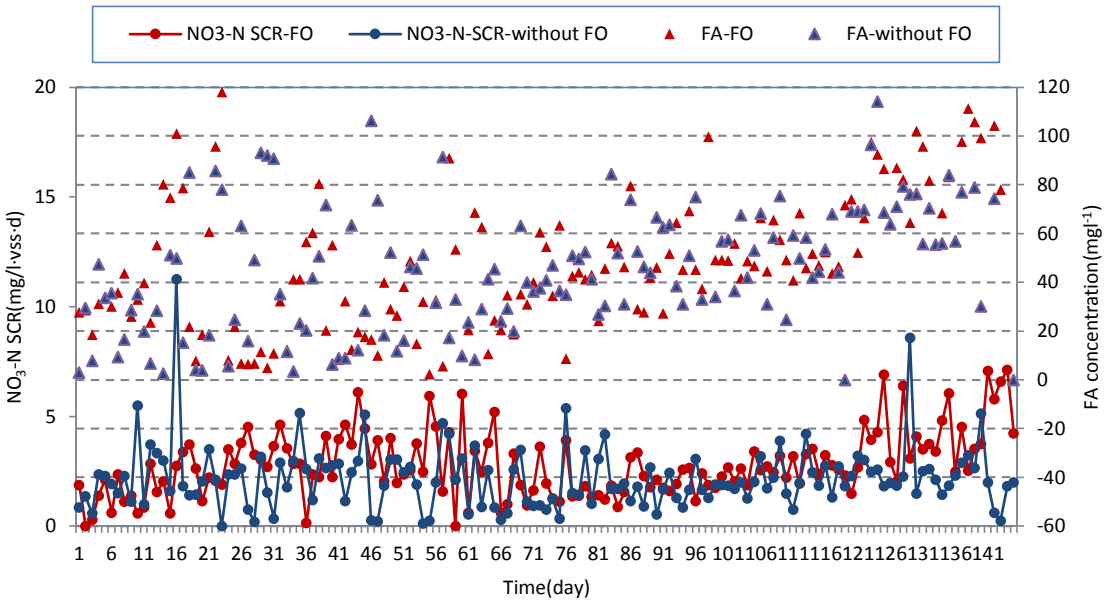


**Figure 5.25** Profile of influent free ammonia concentration and specific $NO_3^-$-N conversion rate in both PN-SBABs along the operational period

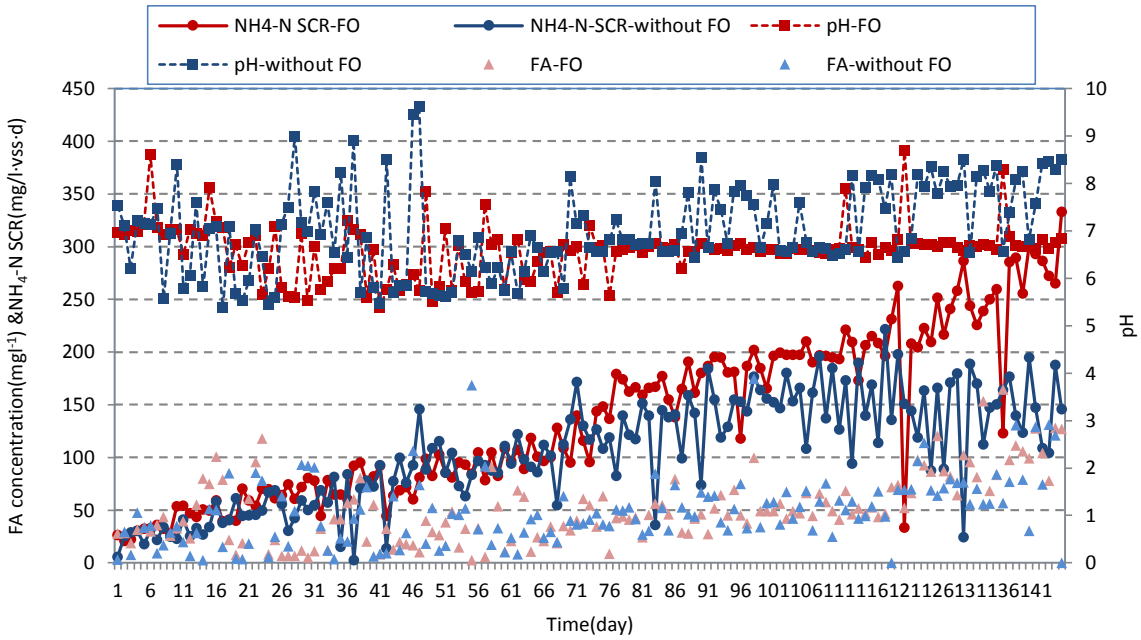


**Figure 5.26** Profiles of influent free ammonia concentration and specific $NH_4^+$-N conversion rate in both PN-SBABs along the operational period

The further relationship between specific $NH_4^+$-N conversion rate and FA concentration as well as between specific $NO^-_3$-N conversion rate and FA concentration in both PN systems were analyzed in Fig5.27&Fig5.28. As shown in Fig5.27, no obvious difference in specific ammonia conversion rate between two PN systems, when FA concentration was lower than 85mgL$^{-1}$. This fact indicated that the activities of AOB in

the bioreactors were not evidently inhibited by the FA concentration as high as 85mgL$^{-1}$ although the initial FA concentrations were considered to initiate inhibition on AOB were 20mgl$^{-1}$ in PN-SBAB with FO and 10mgl$^{-1}$ in PN-SBABs without FO, respectively. In comparison with the completely inhibitory FA concentration of 85mgL$^{-1}$ on AOB in SBAB without FO, this value under the microbubble aeration system was increased to 160mgL$^{-1}$ due to higher activity of AOB and stronger tolerance of AOB to the high FA concentration. Fig5.28 revealed that $NO^-_3$-N specific production rates were mostly suppressed under 6mg/l ·vss d and 5 mg/l ·vss d respectively in both PN-SBABs systems. Similarly, the long term operation under condition of high FA concentrations caused acclimation of NOB and increased inhibition thresholds of FA concentration on NOB. Free ammonia could affect NOB anabolism but it was not expected to be the main factor affecting the nitrite oxidation capacity of the bioreactors (Fux, 2004; Blackburne et al., 2008). Hence the different selective factors were already chosen to obtain long-term stable operation, in which suitable DO concentration and low HRT were essential control factors.

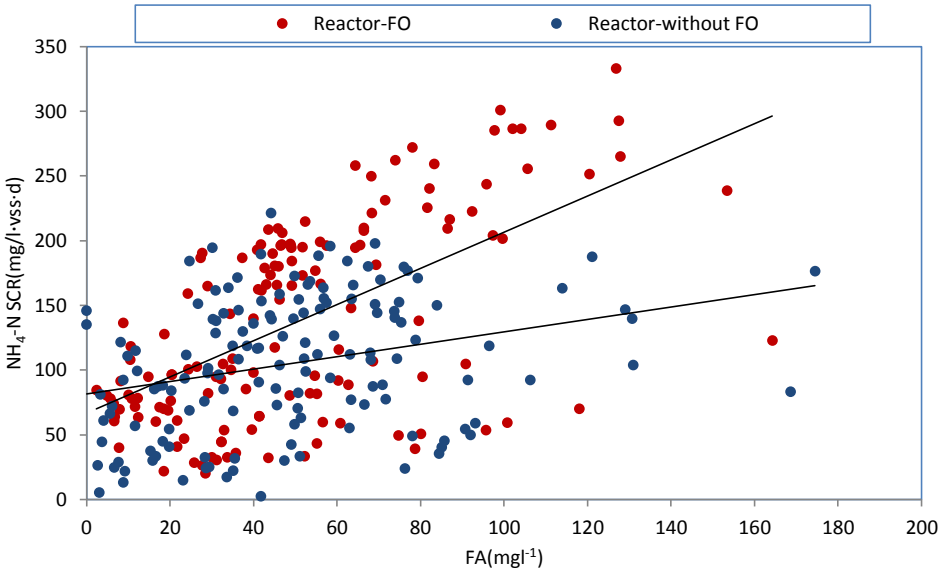


**Figure5.27** The relationship between NH4+-N SCR and Free ammonia concentration in both PN-SBABs

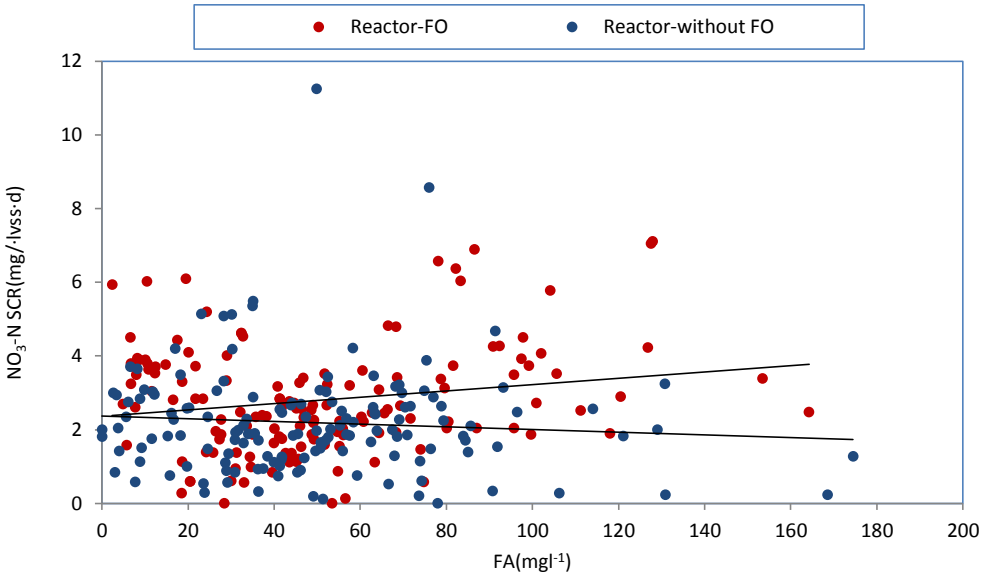


**Figure 5.28** The relationship between $NO_3^-$-N SCR and Free ammonia concentration in both PN-SBABs

### 5.4.5 The Influence of Temperature on the Performance of PN-SBAB with FO

It is well known that biological reaction rates increase with increasing temperature within the physiologically allowable range. Nitrification reaction obeys the Arrhenius law and thus, nitrification proceeds better in a warmer seasons or climates. Knowles et al. (1965) reported increases in ammonium and nitrite oxidation rates by 2.6× and 1.8×, respectively, for every 10℃ increase in the physiologically relevant range. The maximum growth rate of *Nitrosomonas* is significantly lower than that of *Nitrobacter* in the temperature range of 10–20 ℃, however, at a temperature >20 ℃ the growth rate of *Nitrosomonas* bacteria will surpass that of *Nitrobacter*.

The time profiles of the nitrogen compounds concentrations , effluent $NH_4^+$-N/$NO_2^-$-N ratio and nitrite accumulations under the three tested temperatures: room temperature(19~21 ℃), 25 ℃ and 30 ℃, are illustrated in Fig 5.29 & Fig 5.30. It was can be seen that as the temperature was decreased, the average $NO_2^-$-N accumulation ratio in effluent gradually dropped from 92.5% at 30 ℃ to 85.6% at room temperature companied by higher $NO^-_3$-N concentration in the effluent. At 30 ℃ the effluent $NO^-_2$-N/$NH^+_4$-N ratio was ranging from 1.1~1.4 which just met the requirement for Anammox influent. The similar pattern of the effluent $NO_2$-N/$NH_4$-N ratio was detected in the bioreactor at 25 ℃ with stronger fluctuation whereas for room temperature the ratios of $NO_2$-N/$NH_4$-N in the effluent were mostly closed to 1 which was lower than the bound of appropriate $NO^-_2$-N/$NH^+_4$-N ratio required to operate a stable Anammox

process. As described in Fig 5.29 and Fig 5.30, with the increase of the inlet $NH^{+}_{4}$-N concentration, the outlet $NO_3$-N concentration was slightly increased under different temperatures. The highest effluent $NO_3$-N concentration was detected in the bioreactor at room temperature which was 57mg$L^{-1}$ accounting for 1.7% of total nitrogen compounds in the effluent comparable with 0.5% for 30 ℃ and 1.1% for 25 ℃. It should be noticed that even though lower $NH_4^+$-N concentration was added into the partial nitrification system at room temperature higher $NO_3$-N concentration was obtained in the effluent, which was in agreement with conclusion of Hellinga et al. (2007).

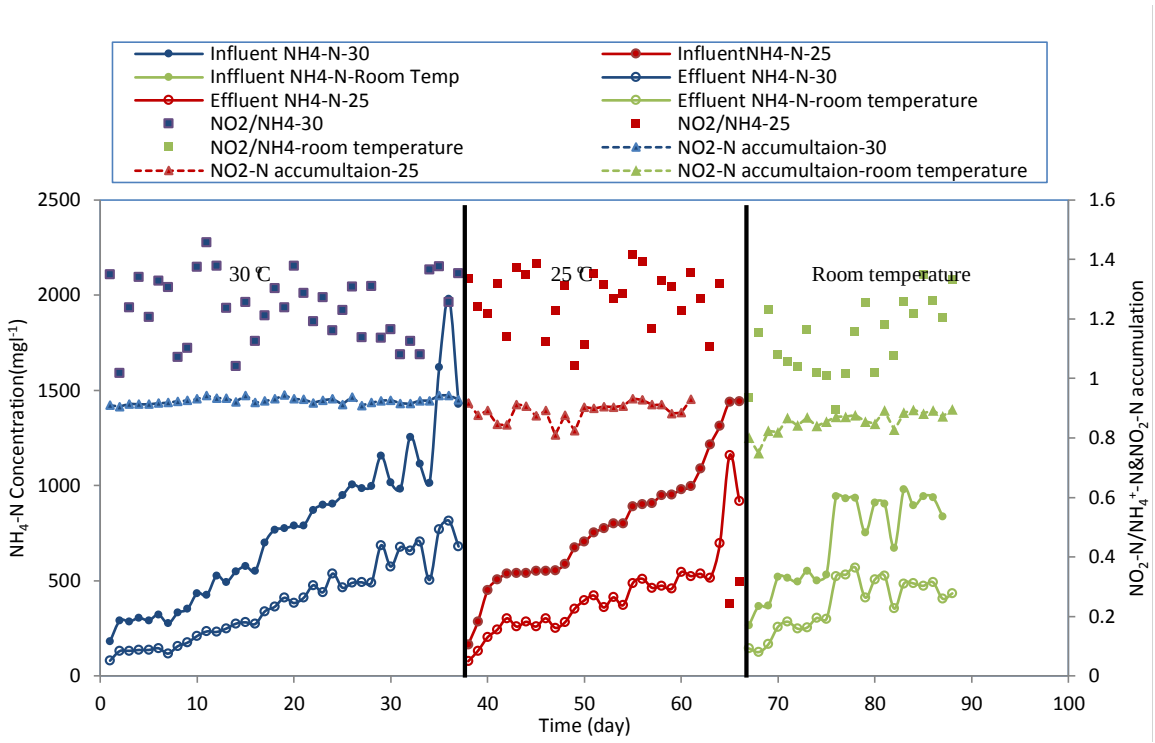


**Figure 5.29** Variation of influent ammonium concentration and nitrite accumulation with time under different temperature in PN-SBAB with FO

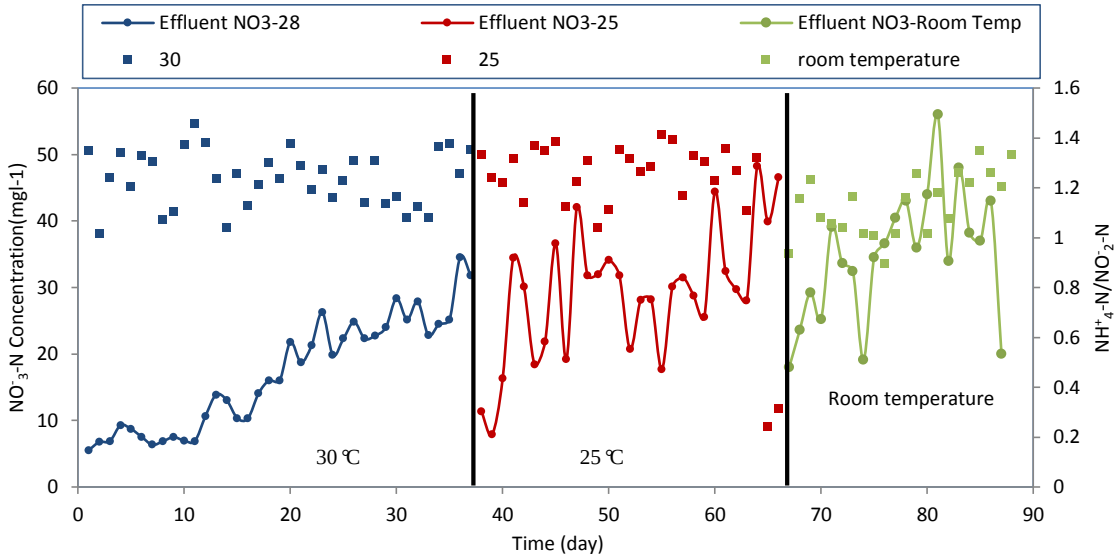


**Fig 5.30** Variation of nitrate concentration and nitrite accumulation with time under different temperature with FO

Based on Eq5-2, the FA concentration is affected by temperature, pH and concentration of ammonium. The results of FA obtained under different test temperatures were shown in Fig 5.31 which illustrated that FA concentration mounted with temperature increasing in accordance with the experienced equation of FA. High FA concentration is prone to exert inhibiting effect on ammonia oxidation, however, according to data obtain in this study, it is evident that the influence of temperature is not sufficient to elevate the FA concentration to the inhibitory rang. Thus it is reasonable concluded that pH and ammonium concentration were essential factors controlling the FA concentration.

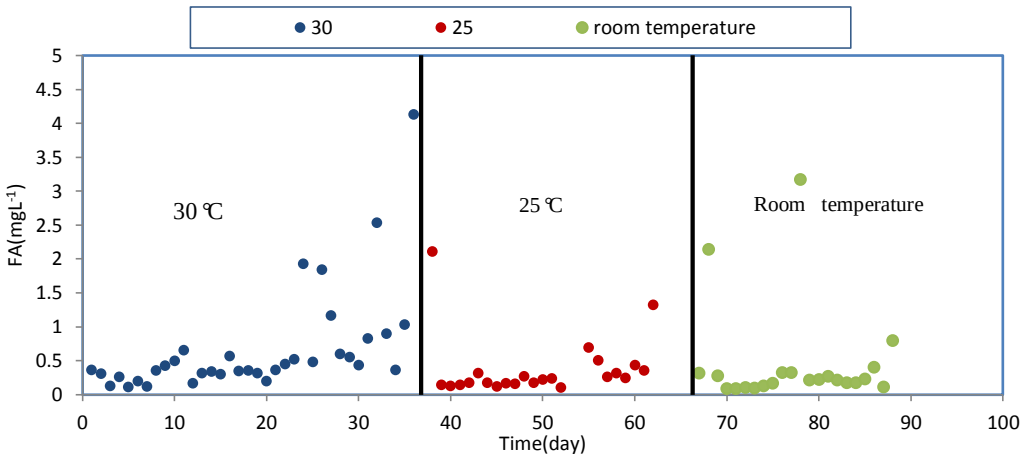


**Figure 5.31** Evolution of FA concentrations under different test temperature in PN-SBAB with FO

The substrate is generally used by involved bacteria as element for cell synthesis therefore the specific ammonia conversion rate and specific nitrate conversion rate reflect the growth rate of AOB and NOB respectively in the partial nitrification system. The Fig5.32 shows the relationship between specific nitrogen compounds conversion rate and temperature which indicates the specific ammonium conversion rate by AOB was significantly higher than the specific nitrate production rate by NOB when test temperature is over 18℃ in addition the disparity between both grow rates is growing with temperature increasing. Some researchers reported the maximum specific growth rate of AOB is lower than that of NOB in a temperature range of 10–20 ℃ (Knowles, 1965; Qiao, 2010). In the present study the reasons for this inconsistent fact is attributed to the long term suitable operation for the PN system which maximally inhibited and washed out NOB, leading to the optimum AOB accumulation. The dominant role of AOB in PN system at room temperature overwhelmed effect of the higher specific growth rate of little amount of NOB. Furthermore, since different factors such as reactor configuration, hydraulic residence time (HRT) and effluent concentrations have also played an important role in AOB activity, the solo role of low temperature is not enough to deteriorate the partial nitrification performance with the microbubble aeration system. This fact is of great significance to spread this new technique because it offers valued evidence for the feasibility of running partial nitrification process in a cold environment. As can be seen in Fig 5.23, an exponential increase of the specific ammonia oxidation rate with temperature was observed in PN-SBAB with FO, which was similar and consistent with the results obtained by other authors (Yang, 2007; Guo et al, 2010).

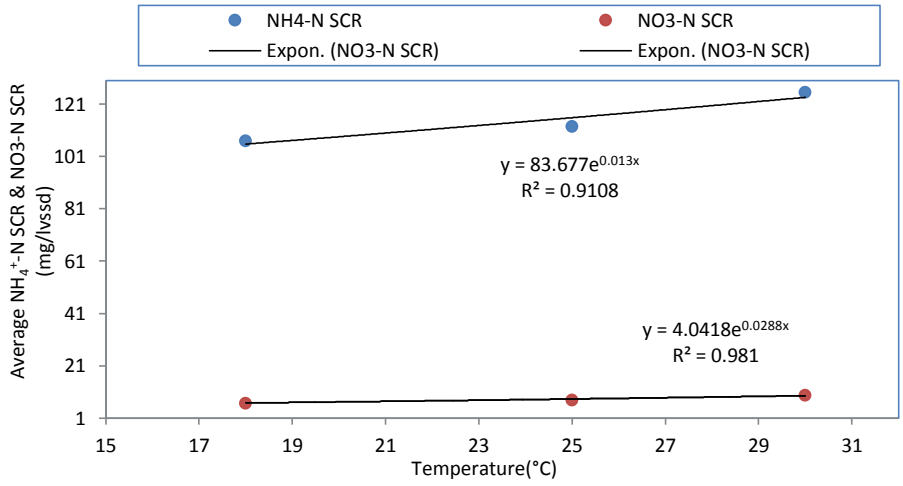

**Figure 5.32** Effect of temperature on the average specific ammonia oxidation rate and specific nitrate conversion rate in SBAB with microbubble aeration system

Optimizing the nitrifying bacteria community was a crucial step in achieving reliable partial nitrification. The partial nitrification process can be rapidly established while AOB becomes the dominant bacteria and NOB is gradually washed out from the system. As noted in this study, partial nitrification could be maintained stably at different temperatures due to the optimization of the nitrifying bacterial community. Certainly, the temperature in the bioreactor should be maintained at 30℃ instead of at lower temperature in order to achieve high efficiency and more stable partial nitrification process in a short-term operation.

### 5.4.6 The Influence of Length of Feedback Loop on the PN-SBABs

As we mentioned in Section 2.5.2 the microbubble is induced by impulse air flow with high frequency. Theoretically, the size of microbubble is related with the frequency caused by a feedback loop, the higher the frequency the smaller bubble size. Therefore the length of feedback loop seemed to be an essential part in a fluidic oscillator for controlling the bubble size small enough. Up to now, nevertheless, the influence of the length of feedback loop on the microbubble size has not been studied in depth and reported. In this study influence of feedback loops with two different lengths on the partial nitrification system was investigated. The feedback loops with 30 centimeters and 20 centimeters were employed to explore the influence of frequency of impulse air flow on partial nitrification in SBAB. Two SBABs were inoculated with the same amount of enriched biomass from the previous PN-SBAB with the microbubble aeration system. The temperature was controlled at 30℃. The same continuous aeration strategy was applied at an air flow rate of 0.7l $min^{-1}$ to guarantee the DO concentration felling in the suitable range for partial nitrification. Contrast experiments were carried out for 20 days under the same conditions and the results were shown as follows.

According the principle of design of fluidic oscillator, higher frequencies of the oscillation in the fluidic oscillator chamber caused by shorter feedback loop are responsible for the smaller size bubbles and more continuous airflow. They both contribute to supply higher oxygen-liquid mass transfer, homogenous calculation and higher shear stress in the bioreactor. It is proved that higher mass transfer efficiency

improved the activity of biomass with lower oxygen required. Lau (1993) reported that higher physic shear forced will cause the better biomass retention through decreasing the sludge volume index (SVI). Fig 5.33 illustrated the global performance of two PN-SBABs with feedback loop of different length. As can be seen in the Fig 5.33, both PN-SBABs were performed the satisfactory and stable partial nitrification performances with perfect effluent characterized by very low nitrate concentration and suitable $NO_2$-N/$NH_4$-N ratio. Moreover the variation curves of effluent with time in both bioreactors displayed strikingly similar pattern, especially in nitrate concentration. This similarity is caused by bubble sizes of semblable micron scale order in both bioreactors.

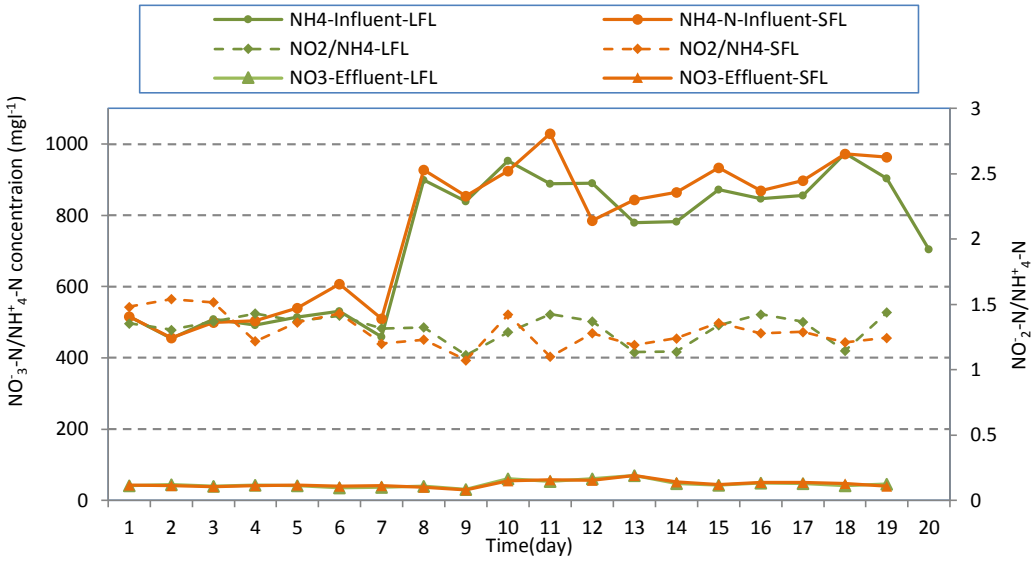


**Figure 5.33** Variation of Nitrogen compounds in influent and effluent during 20days PN operation with different length feedback loop

Since there is no obvious difference observed in the global behaviors between the PN-SBAB with long feedback loop (LFL) and the one with a short feedback loop (SFL) the cycle performance of both PN-SBAB were further investigated shown in the following figures. Fig5.34 a and b show the evolution of nitrogen compounds measured in both bioreactor during one cycle under the same operating conditions. It appears that the long cycle duration of 15h is observed in the PN-SBAB with LFL whereas PN-SBAB with SFL only took around 12hours to accomplish the half ammonia oxidation. The similar observations can be found from Fig5.35 and Fig5.36 representing the evolution on pH, DO and ORP. When pH met the ammonia valley point, DO had the breakpoint and the ORP knee point at 15 h and 12h in different bioreactors respectively. After valley point in the pH profile, chemical analyses showed the completion point of half removal of

ammonia and therefore indicated the end of partial nitrification. Not only valley point but also the break point in the curves of DO and ORP could indicate the end completion of nitrification. However DO value was somehow believed to be more convenient and reliable for the control of partial nitrification.

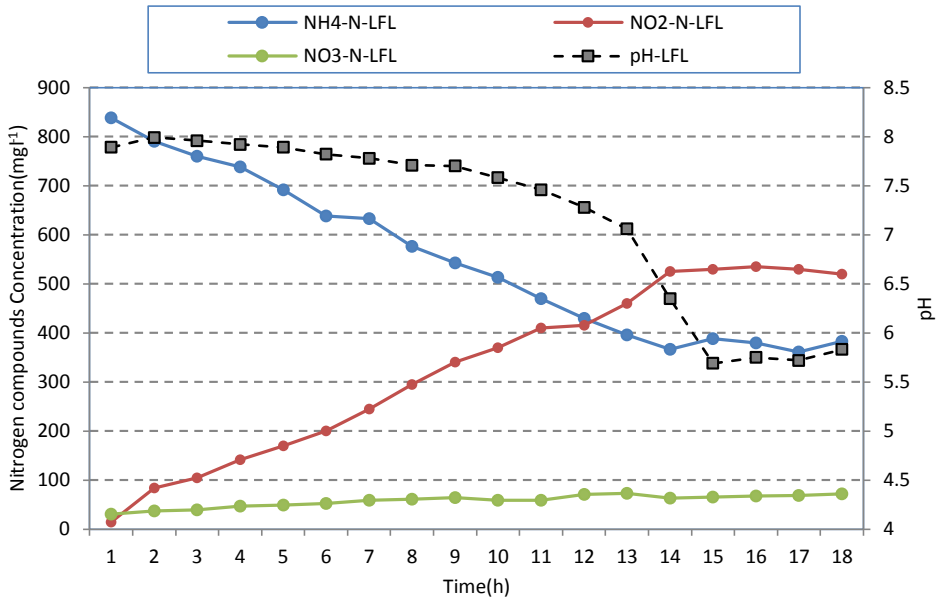


**Figure 5.34** (a) Typical profiles of ammonium, nitrite, nitrate concentrations and pH in a cycle of PN-SBAB with long feedback loop

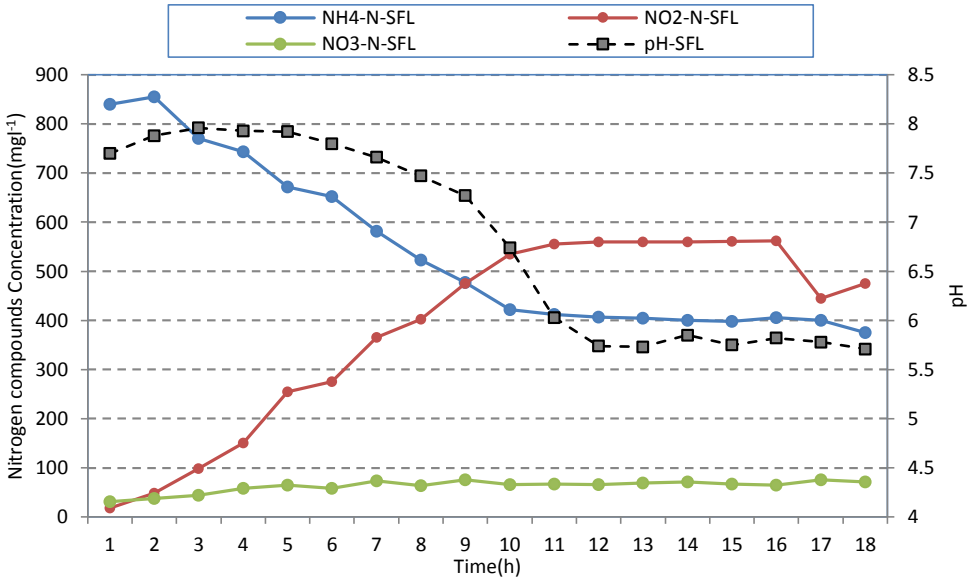


**Figure 5.34** (b) Typical profiles of ammonium, nitrite, nitrate concentrations and pH in a cycle of PN-SBAB with short feedback loop

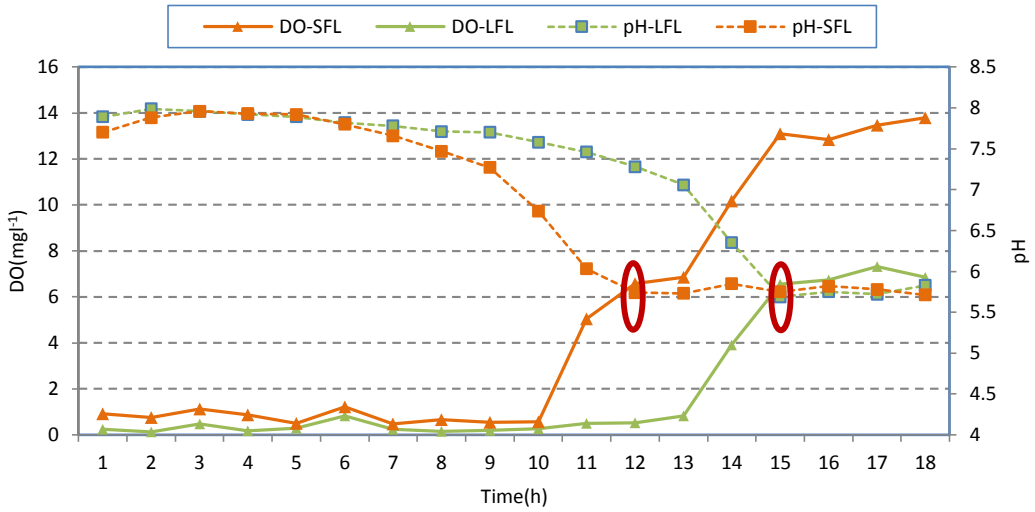


**Figure 5.35** Typical profiles of ammonium, nitrite, nitrate concentrations and pH in a cycle of PN-SBAB without feedback loop of different length

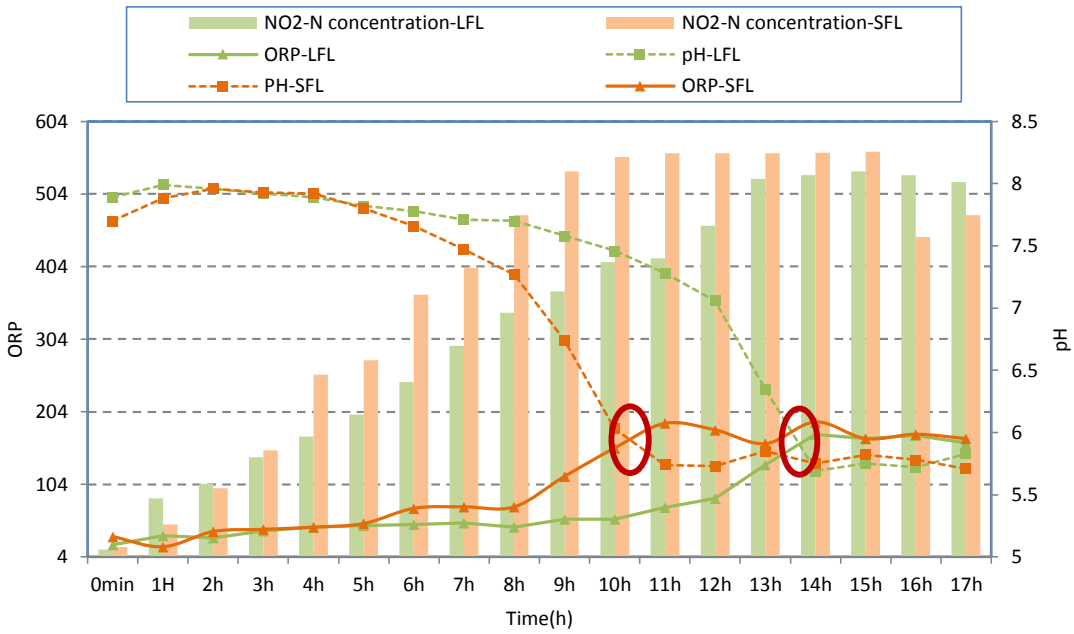


**Figure 5.36**Time course of ORP in cycle of PN-SBABs

From combined analyses of the nitrogen species and the real-time operational parameters detected above, it was clear that the application of short feedback loop shortened the duration of aeration benefiting from smaller microbubble and better mixing. After emergence of the ammonia valley point on the pH profile of PN-SBAB with short feedback loop, aeration need to be prolonged to 15 hours to accomplish half ammonia oxidation for PN-SBAB with long feedback loop, 20% increasing in time, indicating saving 20% operation time and 20% energy consumption compared to application long feedback loop.

### 5.4.7 Biomass Characteristics

The bubble size exerts significant influence on the biomass growth and setteability as a result of the different shear stress brought by different bubble size. Due to the fact that nitrifying bacteria vulnerability to being washed out of the reactor by intense aeration, improvement of physical properties was considered as the one of the alternative solutions, leading to effective bacterial retention in the bioreactor. The changes of physical properties of sludge were monitored to assess biomass characteristics involved in both PN-SBAB systems equipped with different aeration system. All the measurements were repeated more than three times and the average valued were recorded. If the difference between the first two measurements was over 3%, more measurements were conducted to eliminate the systemic error.

The TSS of the sludge taken from both PN-SBABs throughout 126 days experiment covering three different temperatures employed were analysed shown in Fig5.37, Fig 5.38 and Fig 5.39. The biomass concentrations at the beginning of stage at 30℃ were set at 1.93mgl$^{-1}$ in two reactors. As the experiment progressed there were increasing trends in the TSS in both PN systems. At the end of the experiment with operational temperature of 30℃ the TSS concentrations were examined to be 3.26mgL$^{-1}$ and 3.02mgL$^{-1}$ in two PN systems, respectively. During the early period, the TSS in PN-SBAB without FO represented decreasing tendency due to loss of biomass with effluent. This fact was ascribed to poor settle ability related to fine bubble aeration system and lower growth rate of biomass relevant to lower activity of AOB due to lower tolerance to the nitrogen load rate shock. Through analyzing variation of the TSS concentration along time at 25℃ and ambient temperature (Fig 5.37, Fig3.39) respectively, the results showed a concussive trend during the whole operational stage II and III. The initial TSS concentrations for each PN system under different operational temperatures were around 5mgL$^{-1}$. Two peaks of TSS concentration for 25℃ and one for room temperature were found in the TSS profile, respectively. The different numbers of peak emerging under different operational temperature might be caused by the different frequency of sample collection. As discussed in Section 5.4.5 the activity of ammonia oxidizing bacteria, as the dominant population in the PN system, declined with temperature decreasing. Based on measured biomass concentration in the effluent we estimated the SRT were about 35 days for PN-SBAB with FO and 25 days for PN-

SBAB without FO. The biomass growth rate in the early stage could not catch up with the rate of biomass washed out from system, therefore, the biomass concentration consequently declined. Throughout the entire experiment it is clearly observed that the TSS concentrations in PN-SBAB with FO were consistently surpassing that in PN-SBAB without FO. This superiority in TSS concentration was concluded to result from the higher biomass growth rate and enhanced settle ability in the PN system with the microbubble aeration system. The results shown in Fig 5.40 confirmed once again that the higher efficiency of the partial nitrification process was achieved at 30 ℃ rather than low temperature. Even though the lowest initial TSS concentration was applied in the experiment with operational temperature of 30 ℃, after same operation time, the disparity among the final TSS concentrations under different temperatures was reduced rapidly. Hence in order to optimize the nitrifying bacteria community, the microbubble aeration system and high temperature are crucial operational strategy.

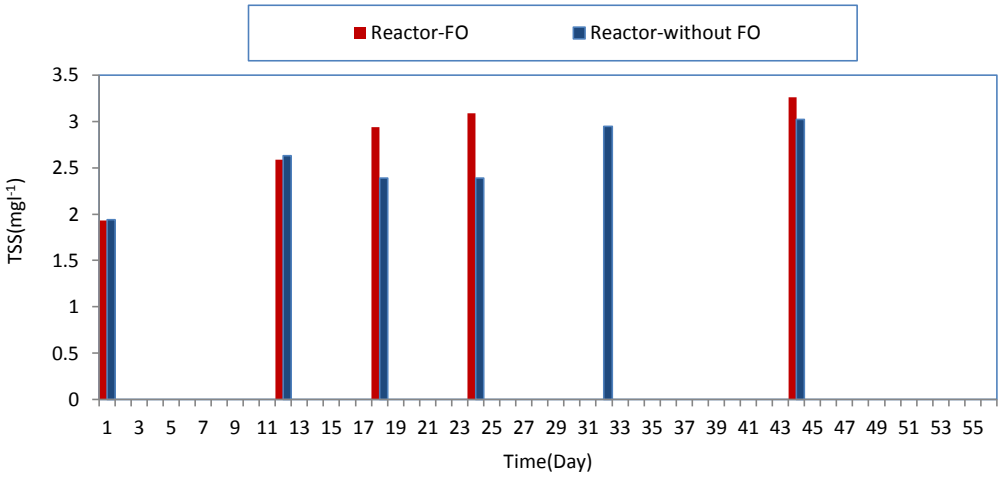


**Figure5.37** Time courses of volatile suspended solids TSS at 30 ℃

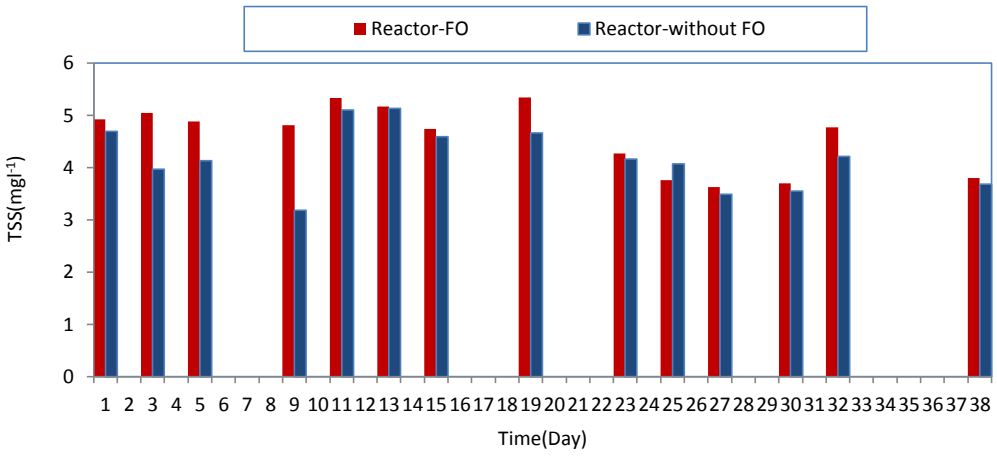


**Figure5.38** Time courses of volatile suspended solids TSS at 25 ℃

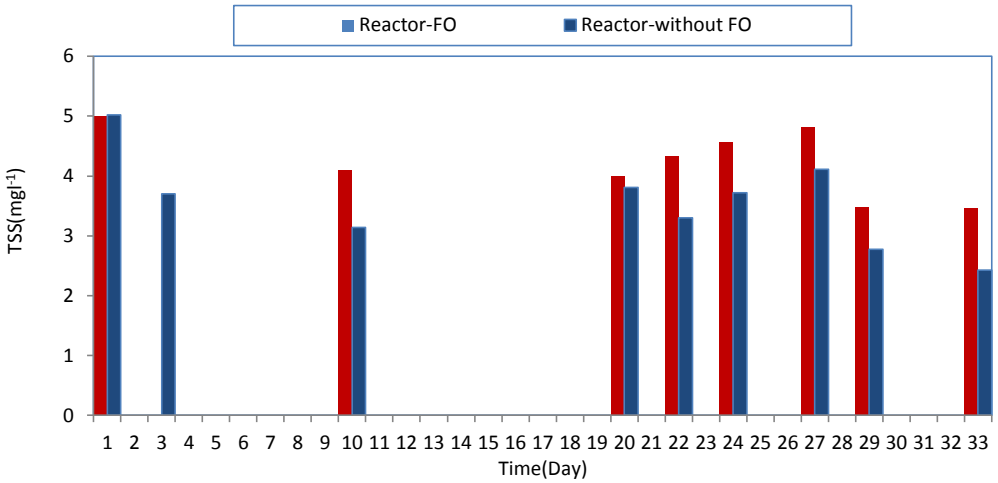


**Figure 5.39** Time courses of volatile suspended solids TSS at ambient temperature

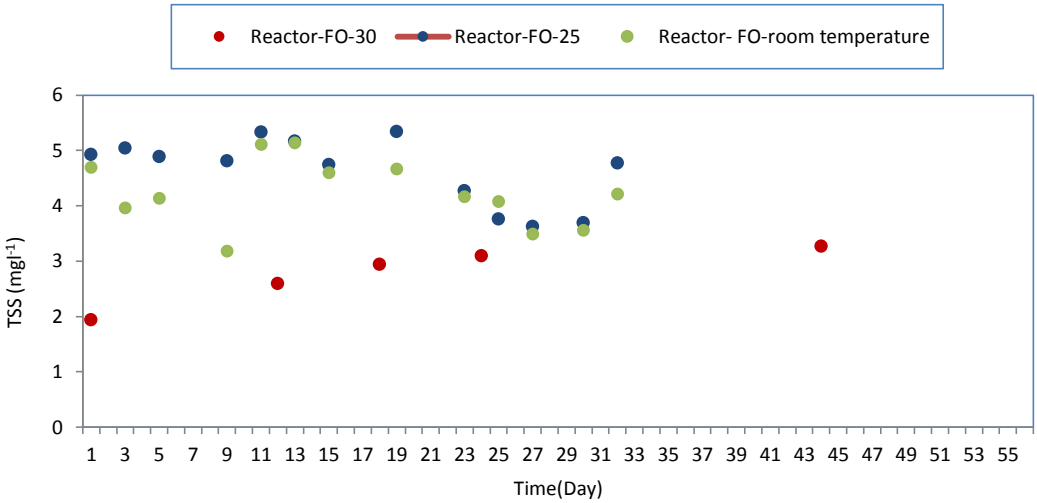


**Figure 5.40** Time courses of volatile suspended solids TSS at different temperature in PN-SBAB with FO.

DO deficiency was believed to be one of the most frequent causes responsible for the most filamentous bacteria proliferation in activated sludge processes (Zhang et al, 2011). Therefore, the effect of bubble size on sludge settleability was visually investigated. Fig 5.41 illustrated the variations of settle properties in two PN systems on the different operational dates which indicated better settle ability always appeared in the PN-SBAB with FO during the entire operational period.

The initial sludge volume index (SVI) value of the sludge in both PN-SBABs was 117mL/g. After 30 days of operation, SVI decreased to lower than 100 ml/g in both PN reactors indicating the improvement of sludge settling properties. The low SVI value was likely to be due to the increase in sludge density, as nitrifiers often form cell

aggregates in enrichment cultures. During the following 20 days' operation the SVI decreased gradually to 76ml/g and 92 ml/g respectively in both PN reactors, which manifested an excellent settle characterises was obtained in the PN system with the microbubble aeration system. No clear relationship between DO concentration and SVI could be found in this study; there was only a trend towards lower SVI value at higher DO concentrations. It is out of question that smaller microbubbles make contribution to high oxygen mass transfer to the liquid phase increasing the DO concentration. Therefore better solid-liquid separation was established in the PN-SBAB with FO. This result was consistent with the report that the turbidity of supernatant in reactors with low DO was higher than that with high DO (Wilen and Balmer, 1999)


Day 1 (20 min) Day 7 (20min)


Day25 (20 min) Day 40 (20 min)

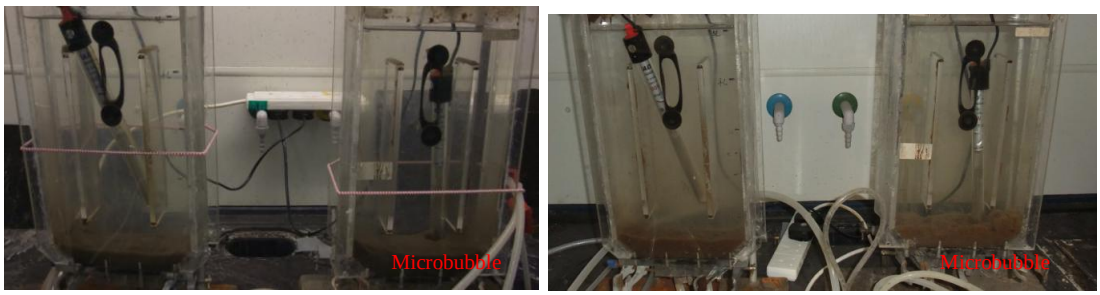


Day 45 (10 min) Day 70 (5min)

**Figure 5.41**Time course of settlebility in both PN-SBABs

## 5.5 Microorganism analysis of Partial Nitrification Systems by TEM and SEM

### 5.5.1 Morphology Observation of Nitrifiers by TEM

During the Period I, the microbial composition and cell structure involved in both partial nitrification systems with different aeration system were investigated by transmission electron microscope for the purpose of evaluation of influence of bubble size on microbial cell structure.

Fig 5.42 and Fig 5.43 show the transmission electron microscope (TEM) photograph of nitrifying bacteria found in both PN-SBABs. From the point view of morphology of cell, despite of different aeration system applied, it is obvious the rod-shaped cells and fat rod-shaped cells dominated the microbial community, some of which characterized by single flagellum or multiple flagella. Morphology of the straight rod cells were coincided with *Nitrosomonas* or *Nitrobacter* genus and the viroid cells to the *Nitrosovibrio* genus (Watson et al., 1989). But later PCR analysis proved that *Nitrobacter* were not detected in both PN systems.

In the PN-SBAB with fine bubble aeration system, the cellular structure of some microbes was ruptured (Fig 5.43 c), which was probably caused by the collision between sludge particles or between bigger size bubble and cells aggregate. In the other partial nitrification system the ruptured cell was hardly detected, thus it is reasonably deduced that this phenomenon was highly likely to be resulted from collision between big size bubble and cells aggregate.

Although a lot of AOB-like cell were found in both partial nitrification system, it is not sufficient to identify these bacteria as ammonia oxidizing bacteria because of the presence of NOB, therefore the following QPCR were performed to further classify the microorganism involved.

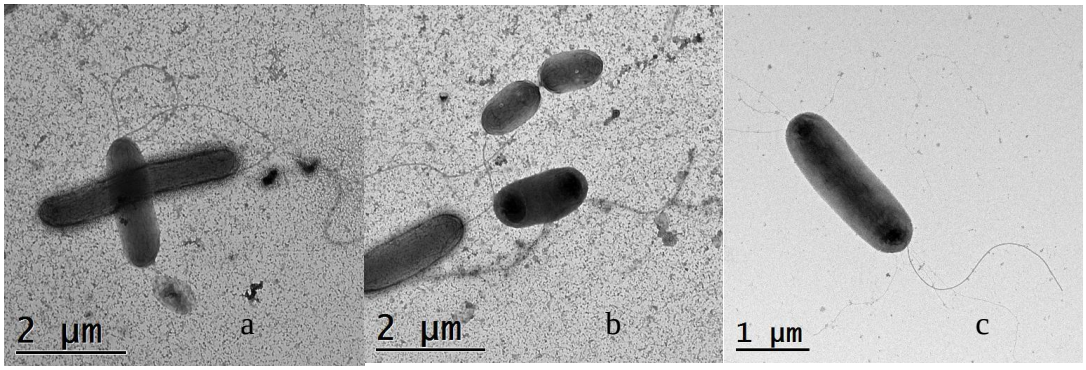


**Figure5.42** TEM (transmission electron microscope) photograph of nitrifying bacteria in PN-SBAB under condition of microbubble aeration

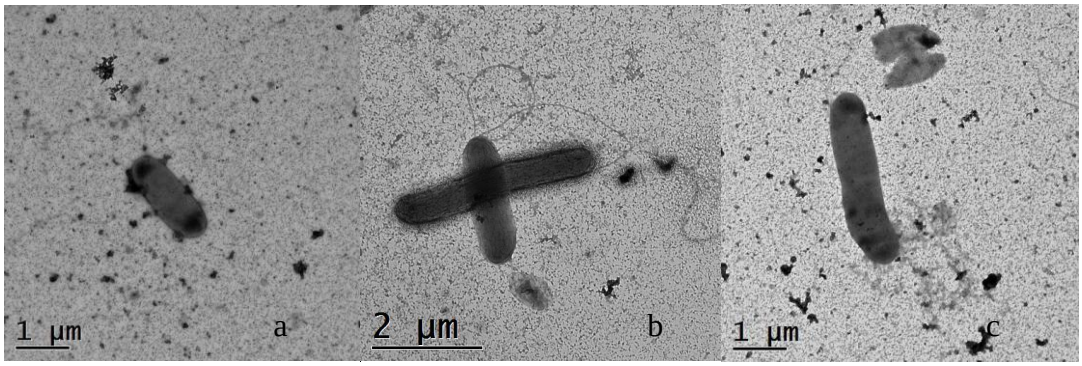


**Figure 5.43** TEM (transmission electron microscope) photograph of nitrifying bacteria in PN-SBAB under condition of fine aeration

### 5.5.2 Morphology Observation of Nitrifiers by SEM

The morphology and structure of the floc sludg were observed in more detail using SEM. Culture sludge on day15 and enriched sludge on day 65 and day 120 at operational temperature of 30 ℃ was taken from both PN-SBAB with fluidic oscillator and PN-SBAB without fluidic oscillator for SEM examination. Images taken from the culture sludge on day 15 showed that the biomass was covered with some substance and the shape of the bacterial cluster could not be identified properly (Fig. 5.44a, b). After 50 days operation, thick clusters of different sizes were observed and distributed all over the samples (5.45 a) in SBAB with FO. The aggregates consisted of different morphology of cells including the straight rod, curved rod and short rod, respectively; while in the SBAB without microbubble generations system(5.45b), clusters of small rod-shaped cells were not obvious compared to the former and occupied area out of the total viewed area seemed to be smaller than that in SBAB with fluidic oscillator. On day 120, the thicker cluster with spherical cells and fat rod-shaped cells (*Nitrosomonas* and

*Nitrosococcus* genus are rod-shaped to spherical cells; the only nitrifiers which has a curved rod shape is *Nitrosovibrio* genus according to table 2.1) were observed and became the dominant population structure over filamentous and other forms in SBAB with microbubble generation system (Fig.5.46a); meanwhile the aggregates dominated by bigger fat rod cells were gradually formed in SBAB with fine bubble aeration system. Nevertheless, these clusters of bacteria could not be identified as *Nitrosomonas* or *Nitrosococcus* genus by SEM viewing alone and so the PCR technique was carried out.

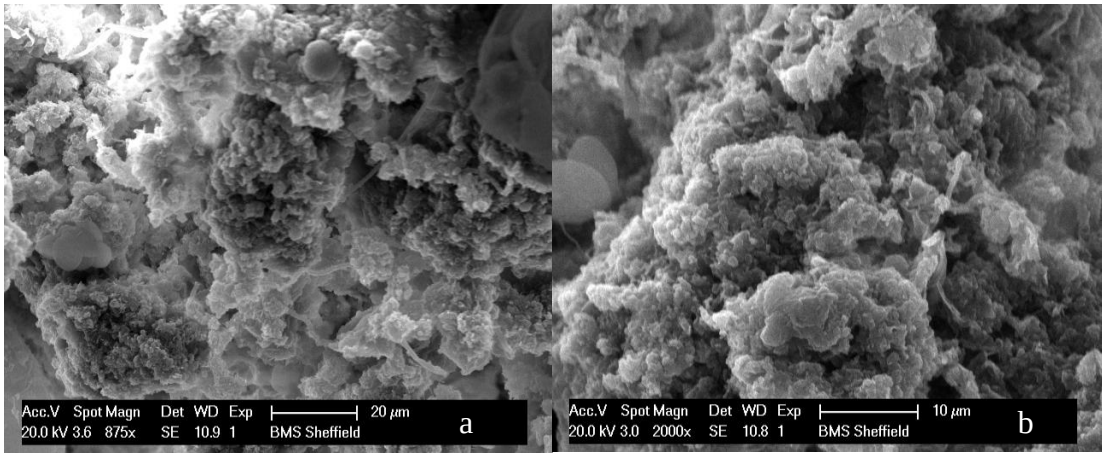


**Figure 5.44** SEM pictures taken from both PN-SBABs on day 15 (a: PN-SBAB with FO; b: PN-SBAB without FO)

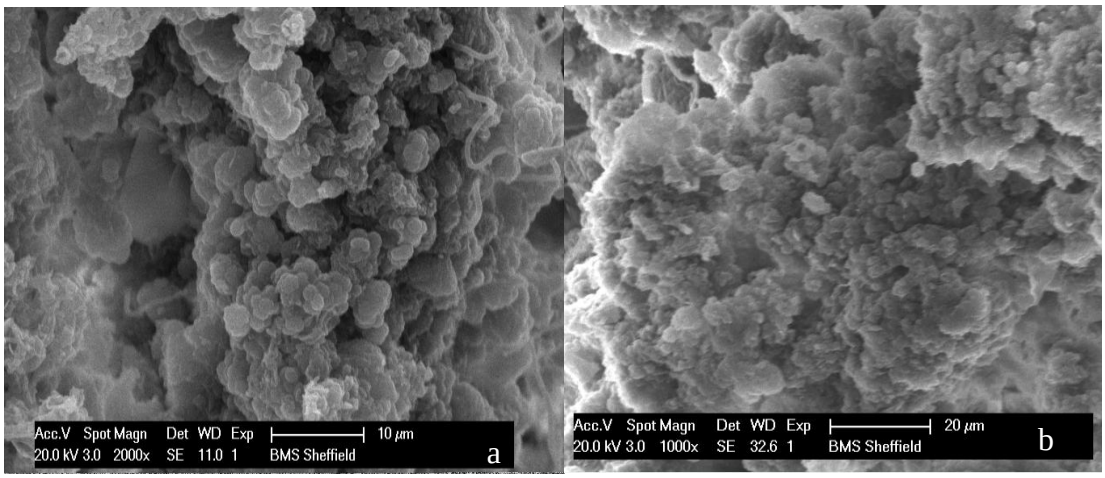


**Figure 5.45** SEM pictures taken from both PN-SBABs on day 65 (a: PN-SBAB with FO; b: PN-SBAB without FO)

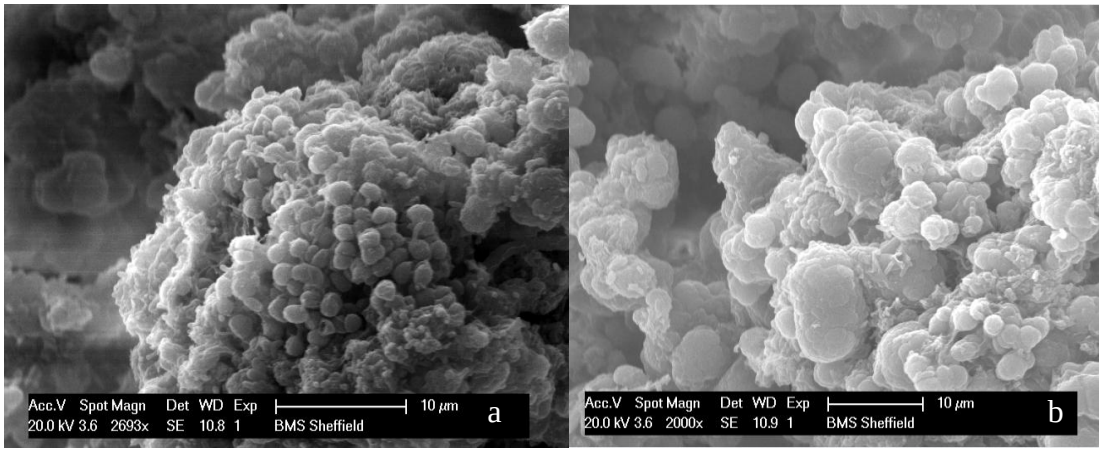


**Figure 5.46** SEM pictures taken from both PN-SBABs on day120 (a: PN-SBAB with FO; b: PN-SBAB without FO)

After the experimental period I, both PN-SBABs were inoculated with the same amount of extra fresh sludge and continuously carried out a new round of partial nitrification at different temperatures. Fig 5.47 and Fig 5.48 describe that the optical microscopic observation of the sludge aggregates on day 30 in period II and day 30 in period III respectively. It seemed to indicate that no evident differences in morphology and structure of the floc sludge between 25℃ and room temperature could be visually observed from the SEM observations. However, through comparing two partial nitrification systems with different aeration mode, it is illustrated that the thicker and uniform structure aggregated microorganisms with smaller cell (less than 10μm) was formed in SBAB with the microbubble aeration system.

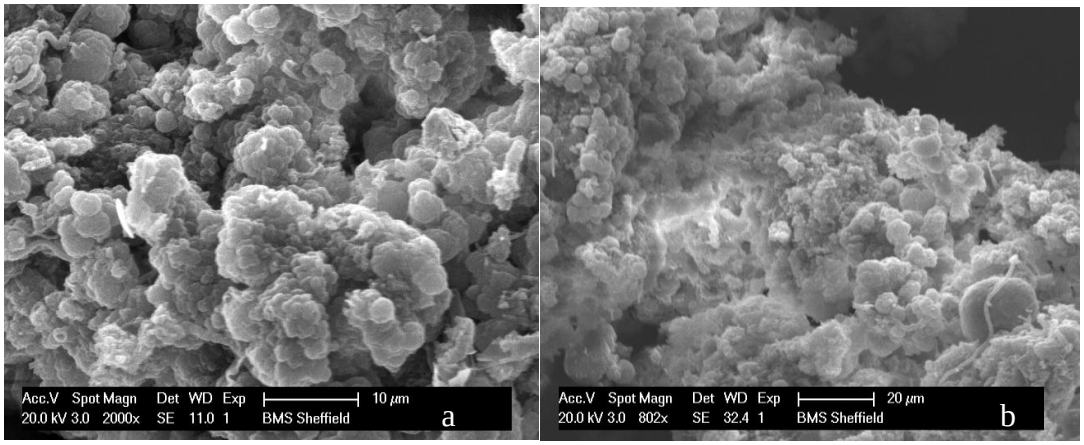


**Figure 5.47** SEM pictures taken from both PN-SBABs at 25 ℃ on day 30 (a: PN-SBAB with FO; b: PN-SBAB without FO)

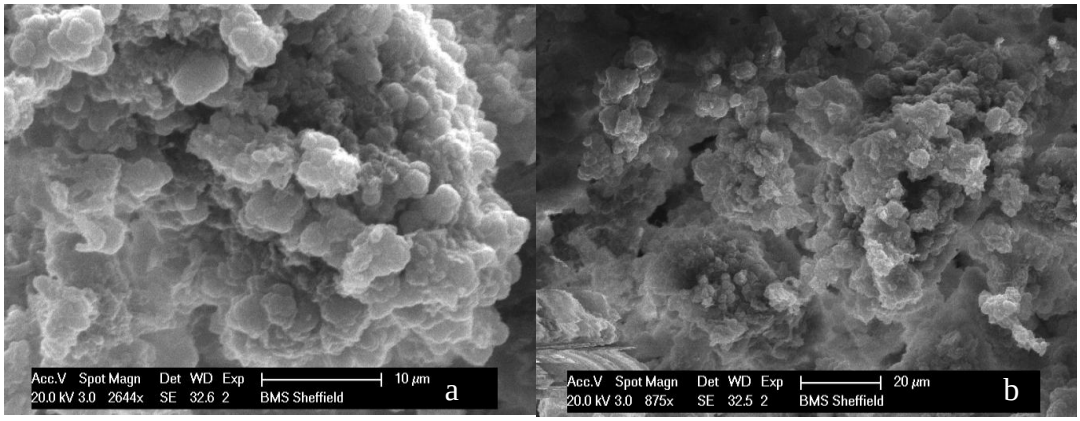


**Figure 5.48** SEM pictures taken from both PN-SBABs at room temperature day 30 (a: PN-SBAB with FO; b: PN-SBAB without FO)

## 5.6 Microbial Community Analysis of in the Partial Nitrification Systems

The evolution of anammox biomass was assessed by QPCR. Besides distinct difference in performance between PN-SBAB with FO and PN-SBAB without FO, the results (Fig 5.49) of relative abundance of AOB species illustrated that the bacteria community structure contribute to better partial nitrification in PN-SBAB with FO. As can be seen in Fig 5.49 under different temperature conditions or different stage, *Nitrosomonas europaea* are always dominant AOB species in all systems, ranging from 17% to 91% of total AOB and hinting their robust and importance during partial nitrification process. *Nitrosomonas cryotolerans* also exist under either condition with less population from 5% to 44%. Surprisingly, no *Nitrobacter* were found throughout the experimental period though nitrate was detected in the effluent from both bioreactors. Further data analysis revealed the potential origin of nitrate, where nitration function gene (*nxrA*) was present at some stage ( P3(0.08%), P5(1.1%) and P6(0.7%)). The outcome of QPCR further confirmed the operational strategies such as lower DO concentration, short HRT, higher FA and FNA etc. applied in the present study satisfactorily supressed the growth of NOB bacteria, probably forcing the horizontal gene transfer of *nxrA* from NOB to AOB or other species for nitrite utilization. Another possibility might be derived from the inappropriate primer design due to various nitration pathways and relative metabolic genes. According to the result of *nxrA* proportion, it is evident the partial nitrification system with microbubble generation system contain higher percentage of nitrification

function gene *nxrA*, which might be attributed to higher dissolved oxygen concentration in this PN system cause by higher mass transfer of microbubble.

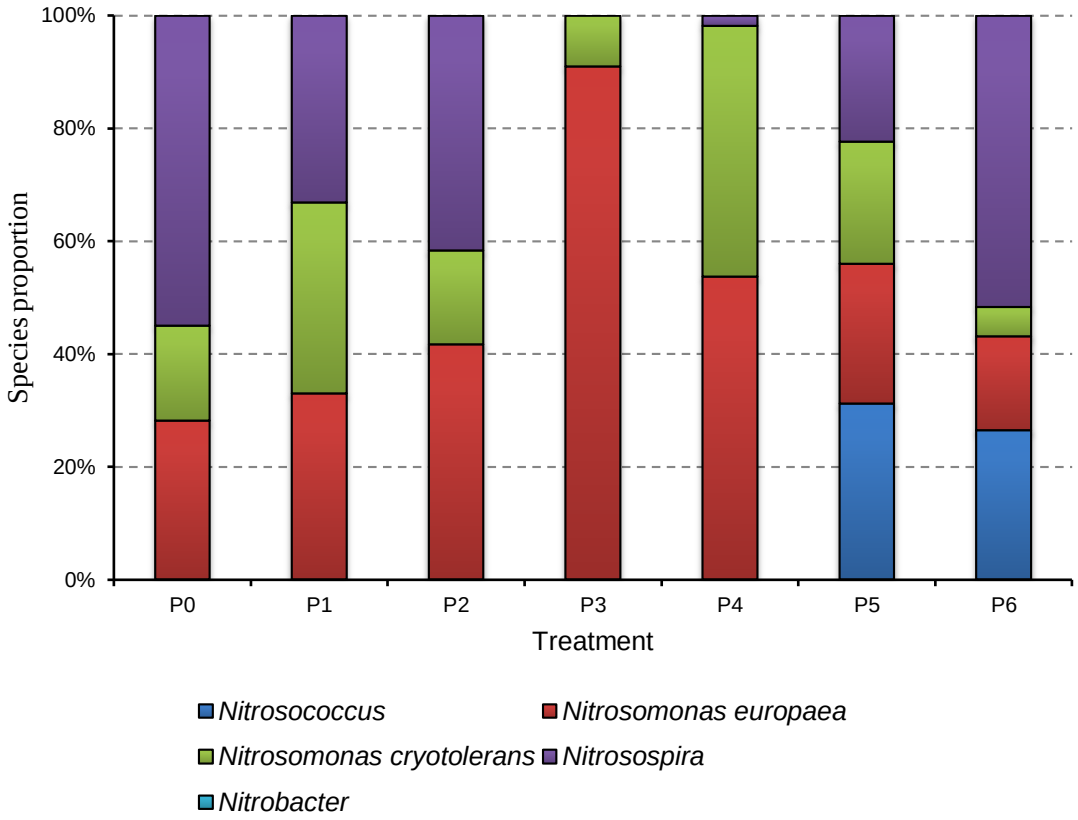


**Figure 5.49** Relative abundance of respective AOB and NOB species. P0: Inoculum samples; P1, P2 : sludge samples from PN-SBAB with FO and PN-SBAB without FO at 25℃. P3, P5: sludge samples from PN-SBAB with FO at early and final stage; P4,P6: sludge samples from PN-SBAB without FO at early and final stage

Looking into specific treatment with respective aeration conditions at different operation stage, similar conclusion was drawn that the population of functional groups is highly related to the performance of SBAB. Temperature shows significant impact on the growth rate of AOB, where the optimal temperature (30$^{o}$C) results in higher AOB intraspecific level (14.4% under 25$^{o}$C while 22.4% under 30$^{o}$C, Figure 5.50A). Nevertheless, the effect of temperature on community structure is limited since the relative abundance of *Nitrosomanos europaea*, *Nitrosomanos cryotolerans* and *Nitrosospira* remained stable, although *Nitroscoccus* can be only observed under 30$^{o}$C. In the meanwhile, obvious population enhancement occurred during the operation period, as shown in Figure 5.50B, that AOB proportion increased from 1.7% at initial

stage to 22.4% at final stage with microbubble aeration, whereas from 11.% to 17.3% with normal bubble aeration respectively.

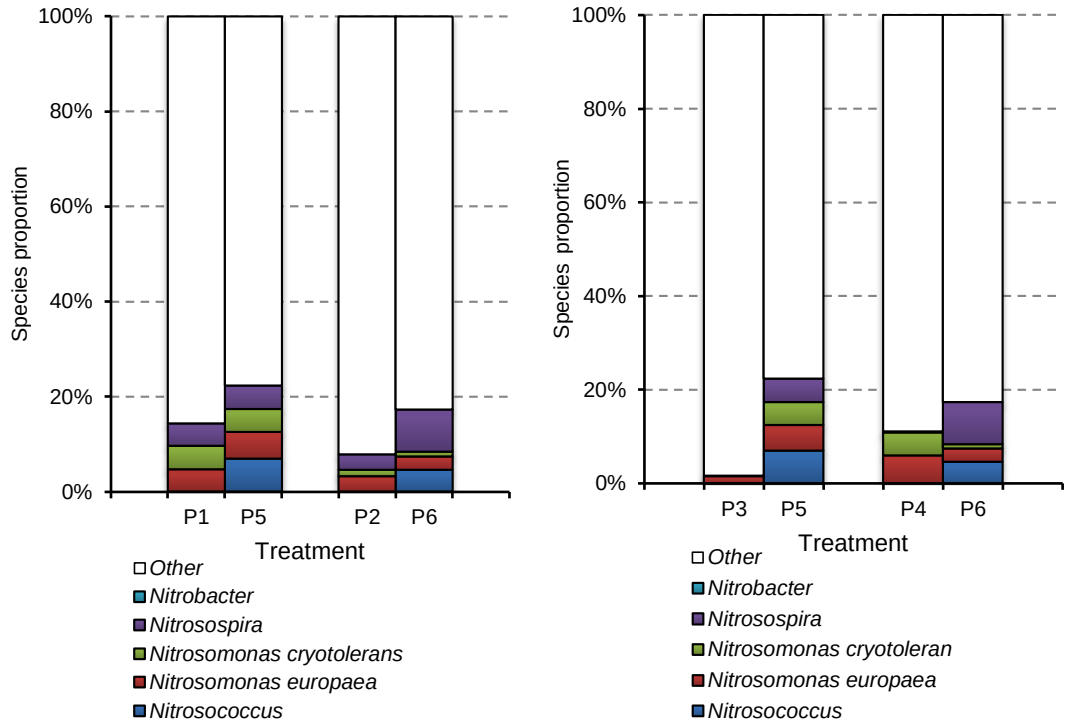


(A) (B)

**Figure 5.50** Dynamic population change of AOB and NOB species in different systems. (A) Trends under different temperature (25 ℃ for P1 and P2, while 30°C for P5 and P6); (B) Trends at different operation stage (early stage for P3 and P4, while final stage for P5 and P6).

# Chapter 6. Study of Anammox Performance Flushed with $CO_2$ rich Gas by using Microbubble Generation System

## 6.1 Introduction

The anaerobic ammonium oxidation (Anammox) process is a novel, cost-effective and low energy consuming alternative to the conventional nitrogen removal processes (Hellinga et al., 1998). Anaerobic ammonium-oxidizing (Anammox) bacteria belonging to the order Planctomycetales convert $NH_4^+$ -N directly to nitrogen gas ($N_2$) using nitrite ($NO_2^-$-N) as the electron acceptor (van de Graaf et al., 1996). This process could be applied for the treatment of wastewater contained high ammonium and low organic material, such as sewage sludge digester liquor, livestock wastewater, and power plant wastewater (Yamamoto et al., 2008). However, the application of the Anammox process to pilot-scale plants is limited by stringent metabolism conditions and extremely slow growth rate (0.072/d at 32 ℃) and low biomass yield of the Anammox bacteria (0.13 g dry weight/g Amm-N oxidized) (Chamchoi and Nitisoravut, 2007; Trigo et al., 2006; Third et al., 2005). Additionally, maintaining a long-term stable Anammox process needs large quantities of finance invested due to the complex and stringent operating conditions for the Anammox biomass, such as high operating temperature, strictly anaerobic environment, very narrow range of operational pH and appropriate inlet $NH_4^+$ -N/ $NO_2^-$-N ratio. Since nitrite is rarely detected in typical wastewater (Jetten et al., 1997) the partial nitrification provides the sufficient nitrite as electron acceptor for Anammox bacteria (Cho et al., 2011). In order to improve Anammox biomass retention, some more recent technologies successfully employed including the use of Sequencing Batch Reactors (SBR) (Dapena-Mora et al., 2004a) and membrane reactors (Trigo et al., 2006) etc. Tsushima et al., (2007) reported that to promptly established Anammox reactors, appropriate seeding sludge or starter cultures must be selected and used, and sufficient amounts of Anammox bacteria must be efficiently retained in the bioreactors. Zhang et al., (2010) proved that the use of a biomass carrier is very important for the attachment of slow growing Anammox sludge so as to avoid the bacteria being washed out in the effluent. Since the Anammox biomass can grow forming granules, it is important to have favourable conditions for granulation in order to obtain a stable Anammox population. The up-flow anaerobic sludge blanket (UASB) reactors and

mechanical stirring were investigated and demonstrated to improve granulation of anaerobic biomass caused by higher shear force. (Arrojo et al., 2006)

The previous study has verified the introduction of microbubble aeration system not only improved the performance of the partial nitrification system and accumulation of biomass but also made the PN-SBAB more time saving and energy saving. Take account of the higher mass transfer and higher shear stress produced by microbubble, the microbubble generation system were first introduced into the Anammox process as a gas exchange regime to investigate how much improvement of treatment performance of Anammox process can be obtained in gas lift loop bioreactors.

It is well known that the Anammox bacteria are very sensitive to pH variation. Both too high and too low values of pH will deteriorate the Anammox system through inhibiting the activity of bacteria or killing them. Thus, in the previous research, real-time control of pH in bioreactor is regarded as essential and indispensable for conducting a successful Anammox process. In this study pH control system was replaced by flashing acid gases to achieve cost effective and stable Anammox process. As we all know that the stack gas usually consists of mostly nitrogen (more than 2/3) derived from the combustion and carbon dioxide ($CO_2$), which makes the survival environment of the human being in danger. In this study the mixture of $N_2$/10%$CO_2$ (simulating composition of stack gas) was injected into the Anammox system to remove the oxygen, accordingly anaerobic condition produced. The high mass transfer owned by microbubble potentially removes the oxygen from bioreactor more effectively and more thoroughly in comparison with fine bubble aeration system. The behaviours and stability of Anammox system under different operational conditions were observed for optimization of Anammox system. The morphology of Anammox bacteria from different systems were observed and compared in order to achieve the further knowledge of the influence of the shear force on the granulation and bacteria growth. Characterization and identification of the bacterial populations in an engineered system which have been considered to be a "black box", has been made possible by using non-cultivation based techniques, such as, polymerase chain reaction (PCR), real-time PRC (QPCR).

## 6.2 Objectives

In this study we tried to (i) seeking for the feasibility of continuously flushing mixed gas of 10%$CO_2/N_2$ into bioreactor as oxygen exchange regime and pH control strategy to realize the satisfactory Anammox operation instead of a pH control system. (ii) Investigate the potential of the Anammox process for ammonium removal in gas lift loop bioreactor equipped with fluidic oscillator. (iii) Evaluate the characteristics of Anammox sludge and quantify the divers bacteria involved from different Anammox system with SEM&TEM and DNA analysis.

## 6.3 Materials and Methods

### 6.3.1 Experiment Setup

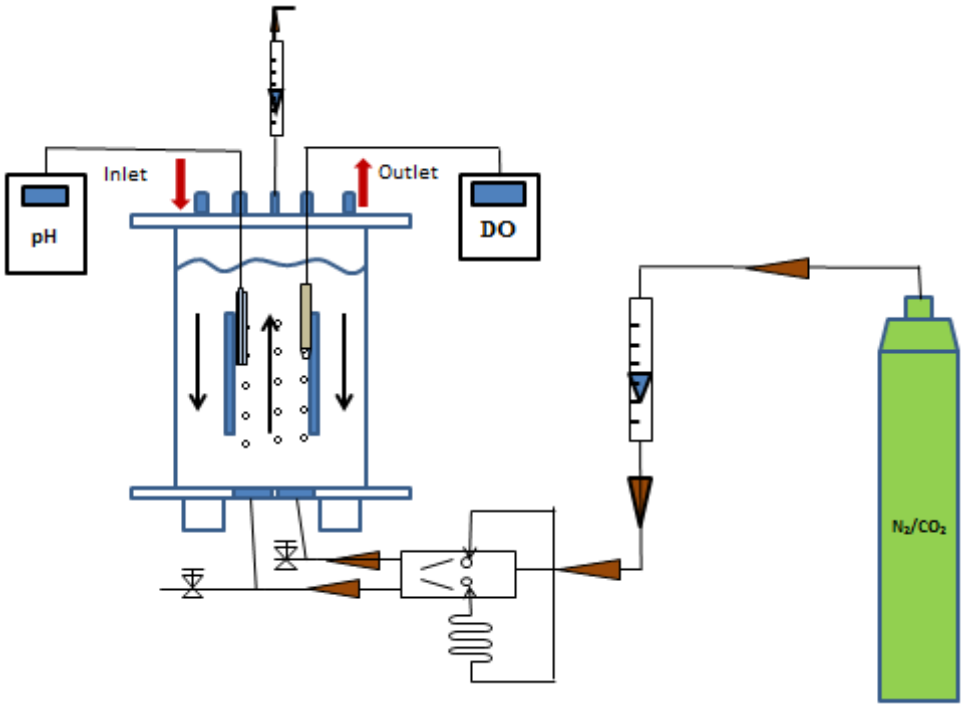


A

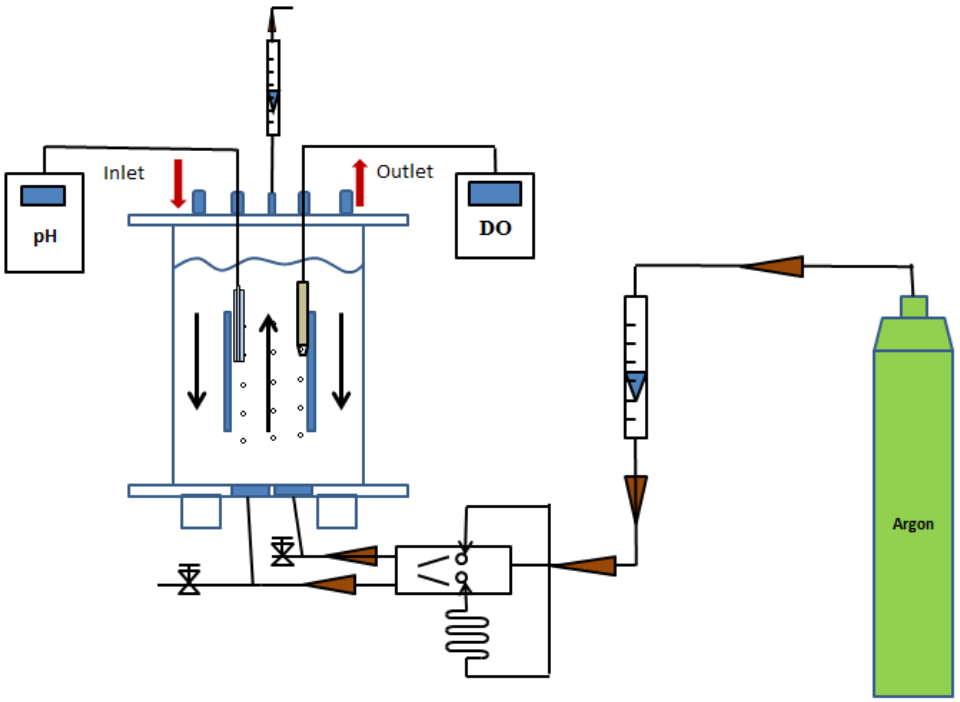


B

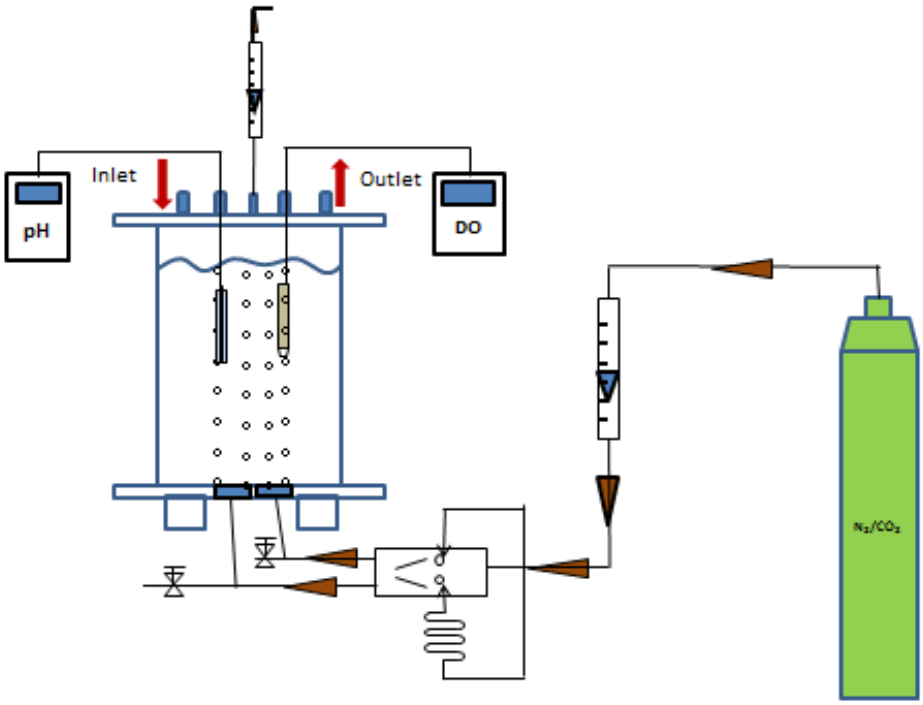


C

**Figure.6.1** Schematic diagram of lab-scale Anammox experiments: A) Anammox sequencing batch gas lift loop bioreactor (SBGB) with Fluidic Oscillator with mixture of $CO_2/N_2$injected; B) Anammox sequencing batch gas lift loop bioreactor (SBGB) with

Argon injected; C) Anammox sequencing batch bioreactor (SBR) with fluidic oscillator with mixed gas of $CO_2/N_2$ flushed.

Due to the slow growth rate of the Anammox bacteria, minimizing the wash-out of biomass from the reactor by improving its retention is regarded as the most important for designing the reactors used to carry out the ANAMMOX process. In order to achieve this aim, different types of reactors were developed such as fixed bed reactor, fluidised bed reactor, gas-lift reactor or sequential batch reactors (SBR), etc. (Sliekers et al., 2003, Strous et al., 1997, 1999; Fux et al., 2002; Van Dongen et al., 2001).

Different reactors designed for Anammox process and their capacity previously reported by other authors were summarized and compared in table 6.1. It is clear that the SBR and Gas lift loop bioreactor showed the higher NLR compared with the others. It is, however, noticed that the four SBR presented different performances shown in Table 6.1. These results should be interpreted carefully due to the large differences in the biomass concentrations presenting in the different reactors, which resulted in the different values of Specific Nitrogen Loading Rate (SNLR) treated. The higher the biomass concentration, the higher the amount of nitrogen removed. (Dapena-Mora, 2004)

**Table 6.1** The operation of different Anammox reactors (Dapena-Mora, 2004)

| Reactor | Inlet | NLR | Specific activity (g g-1 per day) | $NH^+_4$-N (gl-1) | $NO^-_2$-N (gl-1) | Reference |
|---|---|---|---|---|---|---|
| Fixed bed | Synthetic medium | 1.1 | | 0.84 | 0.84 | Strous et al. (1997) |
| Fluidised bed | Synthetic medium | 1.8 | 0.18 | 0.84 | 0.84 | Strous et al. (1997) |
| Fluidised bed | Sludge digester Effluent | 1.5 | 0.15 | 2.1 | 0.84 | Strous et al. (1997) |
| SBR | Synthetic medium | 1.0 | 1.3 | 0.3 | 0.40 | Strous et al. (1998) |
| SBR | SHARON effluent | **2.4** | 0.3 | 0.42 | 0.42 | Fux et al. (2002) |
| SBR | SHARON effluent | 0.7 | 0.8 | 0.55 | 0.6 | Van Dongen et al. (2001) |
| Gas-lift | Synthetic medium | **2.0** | 1.15 | 0.9 | 1.10 | Dapena-Mora(2004) |
| SBR | Synthetic medium | 0.75 | 0.65 | 0.375 | 0.375 | Dapena-Mora(2004) |

The experimental setups are schematically depicted in Fig 6.1. Two types of bioreactor configurations were selected to carry out the Anammox process: sequencing batch gas-lift loop bioreactors (SBGB) and sequencing batch reactor (SBR). Similarly with the

PN-SBAB, two identical sequencing gas lift loop cylindrical bioreactors (SBGB) with a working volume of 3.2 L, made from plexiglass, were applied in the present study. One of the SBGBs was equipped with fluidic oscillator to investigate the contribution of microbubble to the performance of Anammox process. In addition the sequencing batch reactor with the same working volume was equipped with fluidic oscillator as well in the experiment to investigate the effect of difference configurations of bioreactor on the Anammox process.

### 6.3.2 Anammox Sludge Inoculation

The enriched Anammox sludge collected from full-scale One-Step Anammox reactors located in the Netherlands were provided by Paques, The Netherland. The biomass generated in the One-Step Anammox process is of a granular nature, and has a typical red colour caused by specific enzymes.

- Biomass yield: 0.05 kg VSS/kg N
- Conversion rate: 1 kg N/kg VSS d
- Min. doubling time: 11 days (biomass retention is important!)

Each bioreactor was inoculated with the same amount of concentrated enriched anaerobic ammonium-oxidising granular sludge. Due to the strictly anaerobic conditions applied the activity of AOB presenting in the seeding sludge were effectively inhibited in three bioreactors through continuously flushed with the mixture of $N_2$/10%$CO_2$ or Argon . The initial concentration of biomass in the bioreactors was about 35.1 g TSS $L^{-1}$. Anammox biomass has a very high affinity for the substrates ammonia and nitrite. As previously reported, they can be reversibly inhibited by oxygen and irreversibly by nitrite and phosphate (Strous et al., 1999).

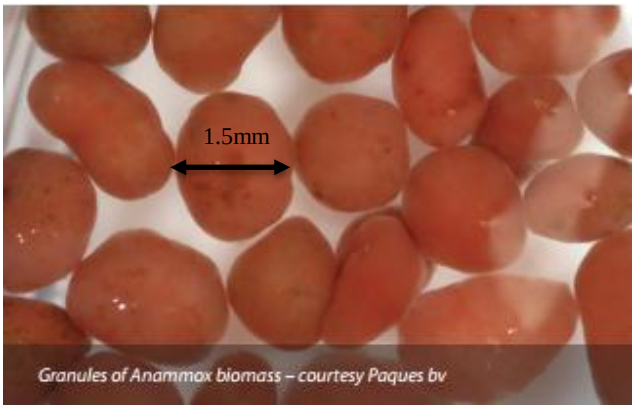


**Figure 6.2** The Anammox granular sludge from Paques (Driessen and Reitsma, 2011)

### 6.3.3 Operational Strategy

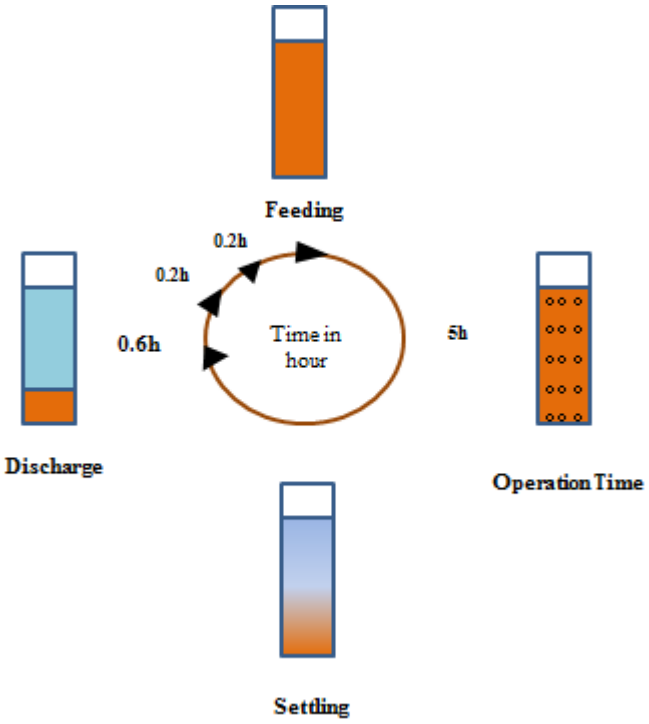


**Figure 6.3** The 6 hours cycle operation of a batch experimental of Anammox: (1) mixed anaerobic feeding period; (2) anaerobic operation period; (3) settling period; (4) discharge period

Since the bioreactors were inoculated with enriched Anammox sludge with high activity start-up period was saved in this study. The activities of ammonia oxidizing bacteria in the inoculum were inhibited due to the anaerobic conditions and AOB were washed out gradually with effluent.

The temperature of liquid inside bioreactors was maintained at 32 ℃ by using a water bath heat-treatment, which was referred to be the suitable temperature for ANAMMOX cultivation (Kim et al., 2006). To prevent light penetration and the growth of phototrophic microorganisms, all of the directors were entirely covered with a black shade. All bioreactors were operated in a sequencing batch experiment mode (Fig6.3). As the HRT changed during the experiment period, the duration time of the batch experiment was shortened from 7 hours to 5 hours. Each cycle comprised four phases: during the first phase the reactor was continuously fed in complete mixed conditions during 12 min; in the second phase anaerobic ammonia oxidizing reaction was conducted with continuously injecting the mixture of $N_2$/10%$CO_2$ or Argon at flow rate

of 0.4Lmin$^{-1}$ as oxygen exchange regime and mixing strategy; the third phase of settling lasted 36 min; and finally the fourth phase of effluent withdrawal of 12 min was applied. This cycle experiment corresponded to HRT 6h. During the whole operational period HRT were decreased step by step from 5h to 7h. The operational pH ranged between 7.0 and 8.0 without control. All of the directors were fed with a synthetic autotrophic medium described in Section 3.4. The stoichiometric ratios of ammonium to nitrite in the influent remained at around 1.4±0.2 close to the reported ratios required for the Anammox process (Strous et al., 1998). Then the concentrations of ammonium and nitrite in the influent were stepwise increased (Table 3.5)

The experiment was divided into two periods. In period I (day 1–60), three sequencing batch gas lift loop bioreactors (SBGB) with working volume 3.2L were carried out Anammox process in parallel, two of them equipped with fluidic oscillator to produce microbubble. Three bioreactors were simultaneously inoculated with the same amount of Anammox sludge stored in the fridge at 4℃. The Anammox system was fully started up as soon as inoculation, which suggested storing Anammox sludge at 4 ℃ is able to maintain activity of biomass for short term. In order to obtain strictly anaerobic conditions two Amox-SBGBs including the one without fluidic oscillator were continuously flushed with mixed gas of $N_2$/10%$CO_2$ at a flow rate of 0.4Lmin$^{-1}$and the other Amox-SBGB with fluidic oscillator was injected with Argon instead with the same flow rate through the ceramic diffuser at the bottom of the SBGB.

Taking into account of the potential of dissolved $CO_2$ to adjust the pH in a suitable range for the Anammox process, during the entire operational period I, pH control system was absent for all Amox-SBGBs used in this experiment. The performances of three different Anammox systems were investigated respectively and were pairwise compared. The influence of microbubble on the behaviours of Amox-SBGB was analysed through comparing with the fine bubble generation system. The triple functions of the mixed gas of $CO_2$/$N_2$ on the performance of Anammox process i.e. deleting the oxygen from system, mixing and pH adjustment were also observed and compared with the effect of using argon to obtain anaerobic conditions for Anammox process. In period II (day 60– 90), two types bioreactors SBGB and SBR, which were both installed with the same microbubble generation system, were employed to conduct the Anammox process in parallel with similar operational strategies as used in Period I. Both Anammox systems were flushed with mixed gas $CO_2$/$N_2$ to achieve a required

environment for Anammox process with HTR of 7hours. The effects of different reactor configuration on Anammox process were studied through comparing the nitrogen removal efficiency of Amox-SBGB with FO and that of Amox-SBR with FO.

In the choice of gases, inert gas Argon instead of $N_2$ was selected to deplete oxygen from control Anammox system and to compare with the performance of reactor flushed with mixture gas $CO_2/N_2$. This experimental design was based on the following reasons: 1) Argon was the most common gas in the lab-scale research of Anammox. Therefore Argon makes this research more comparable and more convincing compared with other similar research;

2) From a safety perspective, Argon is inert gas and easily operated in the lab;

3) $N_2$ was one of the products of Anammox reaction. Theoretically more $N_2$ in the reactor would hinder the reaction proceeding towards right hand side according to the Anammox equation Eq2-14. Hence the Argon exerts less influence on the performance of the Anammox process. Therefore, compared to $N_2$ Argon is better choice in this research.

### 6.3.4 Analytical Procedure

Sampling of the influent, effluent of the different bioreactors was conducted every day during entire operational period. The samples were prepared by filtering through 42 μm filter paper (Whatman), prior to analysis. The Nitrogen transformations were studied through the analyses of $NH^+_4$-N, $NO^-_2$,-N $NO^-_3$-N and ANAMMOX biomass development was determined indirectly by the VSS and TSS estimations. The various analytical techniques adopted to carry out in the present study are represented in Chapter 3. Free ammonia (FA) and free nitric acid (FNA) concentrations were calculated according to5-2 and 5-3. The effect of FA and FNA on the Anammox process was also studied.

Batch experiments were performed in each bioreactor in one cycle on the day 20 in period I. The oxygen was removed from the mixed liquor by flushing with Argon gas or mixture of $N_2$/10%$CO_2$ respectively. The samples were collected and measured every each hour in terms of concentration of $NH^+_4$ -N or $NO^-_2$ –N and $NO^-_3$ –N. Meanwhile the pH was monitored online as well.

Stability is one of the most important indicators of bioreactor performance as the application of a bioreactor highly depends upon its stability. Therefore, the performance

of Anammox process in different bioreactors were investigated based on a stability evaluating system established by Jin et al., (2008). In the present study three instability indices i.e. coefficient of variation ratio, coefficient of range ratio and coefficient of regression function derivative were used to assess the stability of Anammox bioreactors.

**Coefficient of variation ratio**

The coefficient of variation ratio (CVR) is defined as

$$CVR = \frac{CV_2}{CV_1} \qquad (6\text{-}1)$$

Where, $CV_1$ and $CV_2$ are the coefficients of variation in the operational parameter and the performance parameter, respectively.

$$C_{V1} = \sqrt{(N-1)^{-1}\sum(x_i - \bar{x})^2/\bar{x} \times 100} \qquad (6\text{-}2)$$

$$C_{V2} = \sqrt{(N-1)^{-1}\sum(\rho_i - \bar{\rho})^2/\bar{\rho} \times 100} \qquad (6\text{-}3)$$

Where: N is the number of samples, $x_i$ and $\rho_i$ influent TNLR and effluent substrate concentration, $\bar{x}$and $\bar{\rho}$ the arithmetic mean value of $x_i$ and $\rho_i$ respectively.

**Coefficient of range ratio**

The coefficient of range ratio (CRR) is defined as follows.

$$CRR = \frac{CR_2}{CR_1} \qquad (6\text{-}4)$$

where, $CR_1$ and $CR_2$ are the coefficients of the operational and the performance parameter range, respectively.

Coefficient of range (CR) is another index measuring the dispersion of a data set.

$$C_{RI} = (x_{max} - x_{min})/\bar{x} \qquad (6\text{-}5)$$

$$C_{RI} = (\rho_{max} - \rho_{min})/\bar{\rho} \qquad (6\text{-}6)$$

**Coefficient of regression function derivative**

The above instability indices are based on discrete data. If the independent variable X represents the operational parameter and dependent variable Y represents the performance parameter, there is correlation between X and Y: Y = f(X) by regressing $y_i$. The regression function derivative ($D_{RF}$) (Eq. (6-7)) reflects the influence of disturbance in the reactor performance parameters.

$$D_{RF} = \frac{dY}{dX} = \lim_{\Delta X \to \infty} \frac{\Delta Y}{\Delta X} \quad (6\text{-}7)$$

Since, $D_{RF}$ is a time-dependent parameter, therefore mean value of $D_{RF}$ were introduced in the study. A dimensionless instability index, coefficient of RFD, is defined as follows.

$$C_{RFD} = \overline{D_{RF}} \times (\frac{\bar{x}}{\bar{\rho}}) \quad 6\text{-}8$$

Based on Eq6-8 the smaller $C_{RFD}$ is, the higher the stability of the reactor is.

## 6.4 Result and Discussion

### 6.4.1 The Effect of $CO_2$ Rich Mixed Gas and Argon on the Performance of Anammox Process

Autotrophic anaerobic ammonium oxidation (Anammox) is a biological process in which Planctomycetetype bacteria combine ammonium and nitrite to generate nitrogen gas under anaerobic environment. The Anammox reaction is easily inhibited by oxygen. It is no doubt that the anaerobic condition is one of the key factors for the successful start-up and stable operation of Anammox process. The influence of oxygen on the Anammox process has been investigated by some researchers and different results were obtained. Very low oxygen levels (>0.04 mg $L^{-1}$) reversibly inhibit (Strous et al., 1998) the Anammox activity. Although Liu et al. (2008) verified that the possibility of cultivating Anammox consortium in the presence of DO will lead to substantial savings of energy and resource in the industrial application, most researches considered that the consuming ammonium and nitrite through the Anammox activity is only possible under strict anoxic conditions (Jetten et al., 2001).

The most widely used methods for maintaining the strictly anaerobic condition in Anammox system is to vigorously flush the $N_2$ or inert gases such as argon into the bioreactor for removal of the dissolved oxygen. Besides, a promising strategy to avoid the DO influence is to enrich some particular oxygen-consumed bacteria for creating the Anammox's anaerobic niches (Liu, 2008). The Anammox bacteria are very sensitive to the change of pH value. As we all know along the Anammox reaction proceeding the pH in the bioreactor was increased due the $H^+$ consumed, hence for all above approaches the real-time pH control system is indispensable for start-up or stable operation of Anammox process. As a result the operating cost for Anammox will be

very high, which is also an important issue to restrict the industrial application of this technology. A potential solution to this problem was proposed in the present study. The rich $CO_2$ mixed gas (10%$CO_2$/$N_2$) instead of traditional $N_2$ and argon was first applied in the Anammox process as operational strategy to deoxygenate the bioreactor and control the pH of Anammox system. $CO_2$ acting as the main contributor to global environmental issues of green effect was mostly released from industrial plant and vehicle exhaust, in which the flue gases with $CO_2$ concentrations of typically 3 to 13 Vol% and depleted $O_2$ is possibly collected and injected into Anammox bioreactor. On this basis we adopted mixed gas of 10%$CO_2$/$N_2$ simulating the content of $CO_2$ in real stack gas to remove oxygen as well as adjust pH, thus the pH control system was saved in this study.

Two identical sequencing batch gas lift loop bioreactors (SBGB) were carried out Anammox process for 63 days under the same operating conditions, except one of them flushed with Argon gas while the other one flushed with a mixture of 10% $CO_2$/$N_2$.

The treatment performance for both Anammox sequencing batch gas lift loop bioreactors (Amox-SBGB) are shown in Fig 6.4. Throughout the experiments, the NLR in each bioreactor was increased stepwise from initial 0.53 kg-N $m^{-3}d^{-1}$ to 4.93 kg-N $m^{-3}d^{-1}$ and from 0.73 kg-N $m^{-3}d^{-1}$ to 5.3kg-N $m^{-3}d^{-1}$ respectively by increasing the influent nitrogen concentration and reducing the HRT from 7 hours to 5 hours.

The Amox-SBGB with $CO_2$/$N_2$ injected showed slightly unstable performance during the first 31 days followed by very stable nitrogen removal behaviour due to the shorter HRT (5 hours) applied and enrichment of Anammox culture, as depicted in Fig 6.4. The nitrogen removal rate (NRR) steadily increased with increasing the NLR up to 4.338kg-N $m^{-3}d^{-1}$ above which it decreased. The maximum NRR of 4.0 kg-$Nm^{-3}day^{-1}$ was obtained during this period under the conditions of a NLR of 4.34 kg-$Nm^{-3}day^{-1}$ and a HRT of 5 h on day 60. Stable total nitrogen removal efficiencies were maintained above 80% and the maximum nitrogen removal efficiency as high as 97.8% were obtained on day 8. As the HRT was decreased from 7 hours to 5 hours the NRR of Amox-SBGB with mixed gas injected did not exactly follow the increasing trend of NRL which showed a more significant elevation. Compared with the performance of Amox-SBGB with flushing $CO_2$/$N_2$, the Amox-SBGB with Argon injected exhibited very disappointing treatment performance. As can be seen in Fig6.4, likewise, during the entire experimental period, the NLR was raised stepwise from 0.73 kg-N $m^{-3}d^{-1}$ to 5.3

kg-N $m^{-3}d^{-1}$ as a result of increasing influent substrate and shortening HRT. During the first 37 days, the nitrogen removal rate (NRR) in the Anammox system decreased and then dramatically fluctuated from 0.32 kg-$Nm^{-3}day^{-1}$ to 1.6 kg-$Nm^{-3}day^{-1}$ meanwhile the total nitrogen removal efficiency declined gradually from 85% to around 10%. From day 38 until the end of the experiment the NRR was remained approximately at the half of the NRL, nevertheless the observed fluctuation on NRR was mainly attributed to the unstable NRL. Consequently the average total nitrogen removal efficiency was recovered to the 50.3% with an unstable tendency, far lower than the average value of 88% obtained by the other Anammox system. In this case it is evident that a significant loss (up to 90%) of Anammox activity was observed when pH control system was not employed. The failure of the bioreactor could be ascribed to the fact that the pH was increased along the proceeding of the Anammox reaction or other possible biological nitrogen removal reaction i.e. denitrification and exceeded the optimal range of 6.7-8.3 for Anammox bacteria (Strous, 2000).

The values of pH in both Amox-SBGBs were monitored for 63 days. The evolutions of pH of influent and effluent throughout the operation period in both Amox-SBGB were described in Fig 6.5. In the case of mixture of 10%$CO_2/N_2$, the pH of effluent mostly ranged from 7.11 to 7.82. Even though the values of pH occasionally presented over 8 the whole range of effluent pH always fell in the range from 7.11 to 8.21 which is favorable to Anammox process. Compared with the pH of effluent, the influent pH showed slightly higher stabilizing in the scope from 7.5 to 8.1. Since the Anammox is an acid consuming biological process, pH should have increased along the Anammox reaction proceeding. The decrease on the pH in this Anammox system was attributed to the $H^+$ generated by the reaction between $H_2O$ and dissolved $CO_2$. In the case of argon employed, due to no pH adjusting or no supplement of $H^+$, the alkalinity accumulated in Anammox process caused the effluent pH significantly increasing from 8 to 8.9 which surpassed the upper limit of pH for Anammox process. The high pH was responsible for the deterioration of Anammox activity. From day 41 a pH control system was added to the Anammox system with argon flushed and yet the treatment performance of bioreactor was not fully recovered according to the result of total nitrogen removal efficiency shown in Fig 6.4.

Besides establishing an anaerobic environment in the reactor, it is clear that, even under condition of absence of pH control system, the mixed gas of 10%$CO_2/N_2$ can act as a

buffer to regulate the pH of the medium in order to maintain high Anammox activity in the reactor. Furthermore Anammox autotrophs utilize dissolved carbon dioxide or bicarbonate stemming from the mixture of $CO_2/N_2$ for cell biosynthesis with a slow growth rate (doubling time 11 d) (Jin et al., 2008; Wang et al) resulting in hydrazine and hydroxylamine as intermediary metabolites (Chamchoi and Nitisoravut, 2007). Strous et al. (1999) documented that the inhibition from high $NO_2$-N concentrations could be overcome by addition of hydrazine. The addition of dissolved inorganic carbon (IC) source is very likely to accelerate the decomposition rate of hydroxylamine, leading to the accumulation of hydrazine (Yang et al., 2010). Thus the extra IC is beneficial to enhance the capability of treatment of Anammox bioreactor.

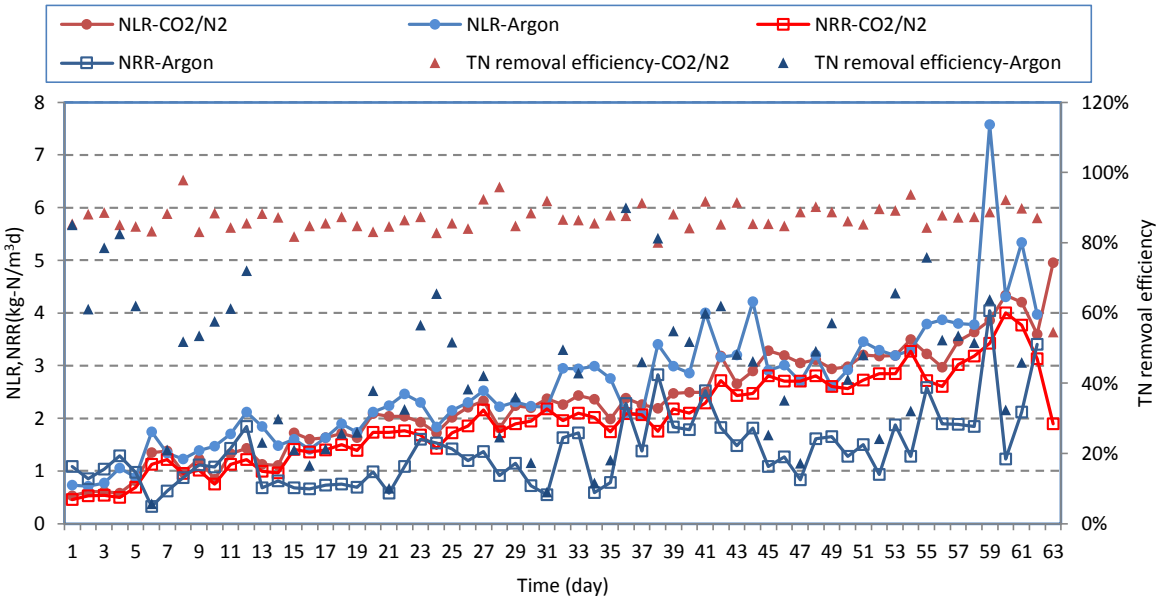


**Fig.6.4** The global performance of Amox-SBGBs with flushing CO2/N2 or Argon in terms of NLR NRR and TN removal efficiency

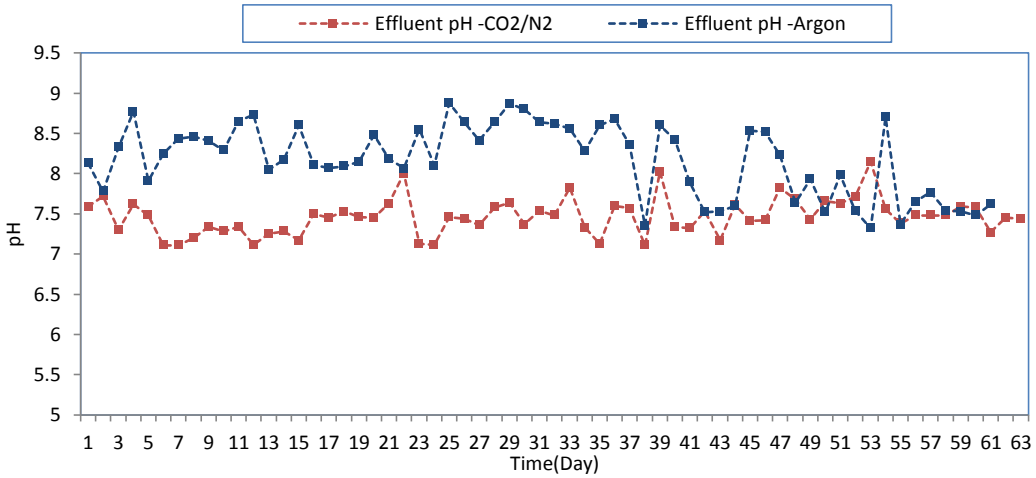


a

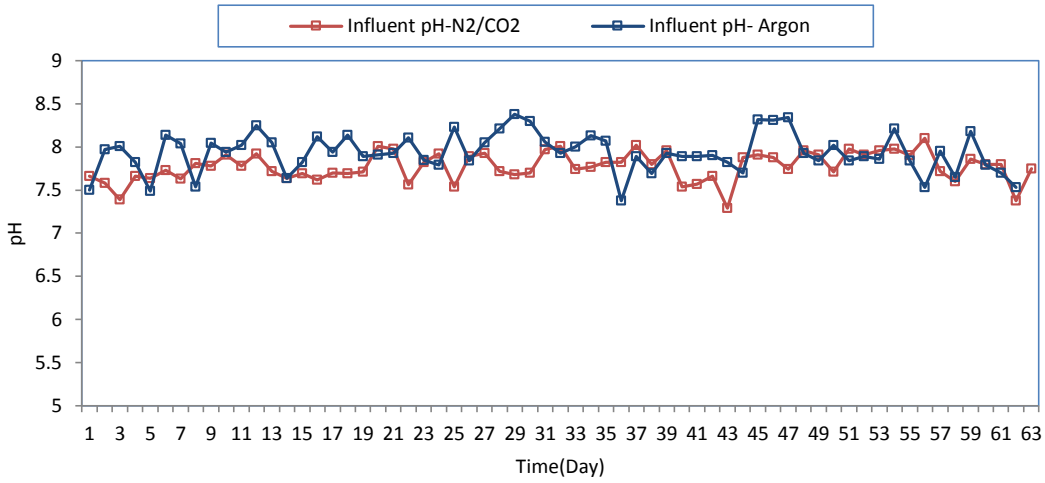


b

**Figure 6.5** The time course of pH value in both Amox-SBGBs: a Effluent pH; b Influent pH

In order to test whether Anammox reaction is the only reaction of biological nitrogen removal taking place in both Amox-SBGBs, the variation of nitrogen compounds concentration i.e. $NH_4^+$-N, $NO_2^-$-N and $NO_3^-$-N were further investigated.

The treatment performances of the Anammox reactors in terms of various nitrogen compounds as well as the nitrogen removal rates are shown in Fig. 6.6. As can be seen in Fig 6.6 (a) and (b), the influent ammonium concentrations and nitrite concentrations were gradually increased in both Amox-SBGBs and maintained the stoichiometric ratio relationship around 1:1.32 for Anammox. In the Amox-SBGB with mixture of $CO_2/N_2$ the average ammonium removal efficiency remained around 96.8% and the nitrite removal efficiency was surprisingly around 98.9% during the entire experiment, in addition during a lot of operational periods these removal efficiencies impressively reached up to 1; whereas for the Amox-SBGB with argon flushed the average removal efficiencies of ammonium and nitrite were declined to 19.6% and 70.7% respectively. From the point view of the effluent quality it is exhibited in Fig 6.6 (a.b) that the concentrations of ammonium and nitrite were mostly lower than 10 $mgL^{-1}$ in Amox-SBGB with mixture of $CO_2/N_2$ flushed. These values observed in SBGB with argon flushed were fluctuated from 36 to 345$mgl^{-1}$ and from 0$mgl^{-1}$ to 178$mgl^{-1}$ respectively. Fig 6.7 (c) describes the evolution of nitrate concentration in the effluent throughout the operational period in both Amox-SBGBs. Careful observation of 6.7 (c) shows that the nitrate concentrations presenting in the effluent from Anammox systems with mixture

of $CO_2/N_2$ flushed were maintaining persistently lower than 56.8mgL$^{-1}$ with average production efficiency of 0.126 ($NO^-_3$-N/$NH^+_4$-N) while interestingly the outlet nitrate concentration in the Amox-SBGB with flushing argon were mostly closed to 0 mgL$^{-1}$. Through examining the nitrogen compounds in the effluent from the former it is demonstrated that most ammonium and nitrite were simultaneously removed from the system along with the production of nitrate. The reported reaction ratios of $NO^-_2$ –N to $NH^+_4$-N and $NO^-_3$-N to $NH^+_4$-N for anammox reactions were 1.32 and 0.26 according to Eq. 2-15. In this case the average reaction ratio of 1:1.38:0.088 was achieved slightly different from the theoretical value which suggested that substantial Anammox biomass accumulated and was dominant in the bioreactor. In addition, there is one possible reason to explain the varying stoichiometric reaction ratio obtained experimentally, which is heterotrophic denitrification bacteria and Anammox bacteria coexisting in this Amox-SBGB. Therefore a part of nitrate produced and nitrite in the medium were grabbed by denitrifying bacteria to produce $N_2$ using decayed organisms as organic carbon source. In the case of the Amox-SBGB with flushing argon it was observed that the over 90% ammonium and 30% nitrite still remained in the effluent which means the most Anammox activity was lost. Surprisingly, nearly all nitrate and most nitrite were removed from the system but the effluent ammonium concentration basically remained at the initial concentration. This was probably attributed to two reasons: deterioration of Anammox activity occurring and denitrification bacteria cultivation in the system.

In general, denitrification occurs only where oxygen, a more energetically favourable electron acceptor, is depleted, and bacteria respire nitrate as a substitute terminal electron acceptor to generate $N_2$. Optimum pH values for denitrification are between 7.0 and 9. Temperature affects the growth rate of denitrifying organisms and the denitrification rate increases with temperature until it reached 40 ℃. Denitrification is also an alkalinity producing process.

Denitrification generally proceeds through some combination of the following intermediate forms:

$$NO_3^- \rightarrow NO_2^- \rightarrow NO + N_2O \rightarrow N_2\,(g)$$

The complete denitrification process can be expressed as a redox reaction:

$$2\,NO_3^- + 10\,e^- + 12\,H^+ \rightarrow N_2 + 6\,H_2O,\ \Delta G^0 = -333\ \text{kJ/mol} \quad (6\text{-}10)$$

Including the following four redox reactions

1. $NO_3^-$ reduced $NO_2^-$: $2NO_3^- + 4H^+ + 4e^- \rightarrow 2NO_2^- + 2H_2O$ (6-11)
2. $NO_2^-$ reduced NO: $2NO_2^- + 4H^+ + 2e^- \rightarrow 2NO + 2H_2O$ (6-12)
3. NO reduced $N_2O$: $2NO + 2H^+ + 2e^- \rightarrow N_2O + H_2O$ (6-13)
4. $N_2O$ reduced $N_2$ : $N_2O + 2H^+ + 2e^- \rightarrow N_2 + H_2O$ (6-14)

Another important aspect for denitrification is the requirement for organic carbon source; that is, the presence of sufficient organic matter to drive the denitrification reaction.

There is no doubt that the bioreactor with argon flushed failed to consume the ammonium and nitrite by means of Anammox process due to the high pH resulting in the irreversible inhibition on the Anammox bacteria. At the same time, the operating conditions in this bioreactor had met the environmental requirement for the enrichment of the denitrifying organisms; hence the heterotrophic denitrification culture gradually adapted to the environment of Amox-SBGB with flushing argon and accumulated to play an increasingly important role which was to effectively removal nitrate and nitrite from the system and leave ammonium behind. Due to the high biomass inoculation 35.1$gL^{-1}$, deterioration enriched Anammox biomass produced a great number of the decayed bacteria providing the adequate organic carbon source for the denitrification bacteria growth.

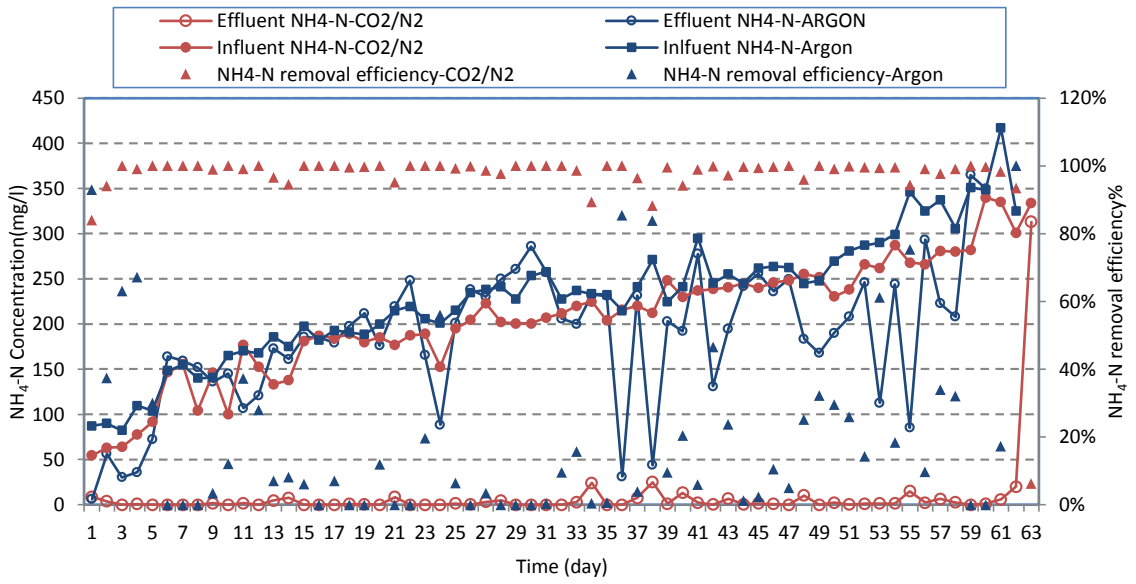


a

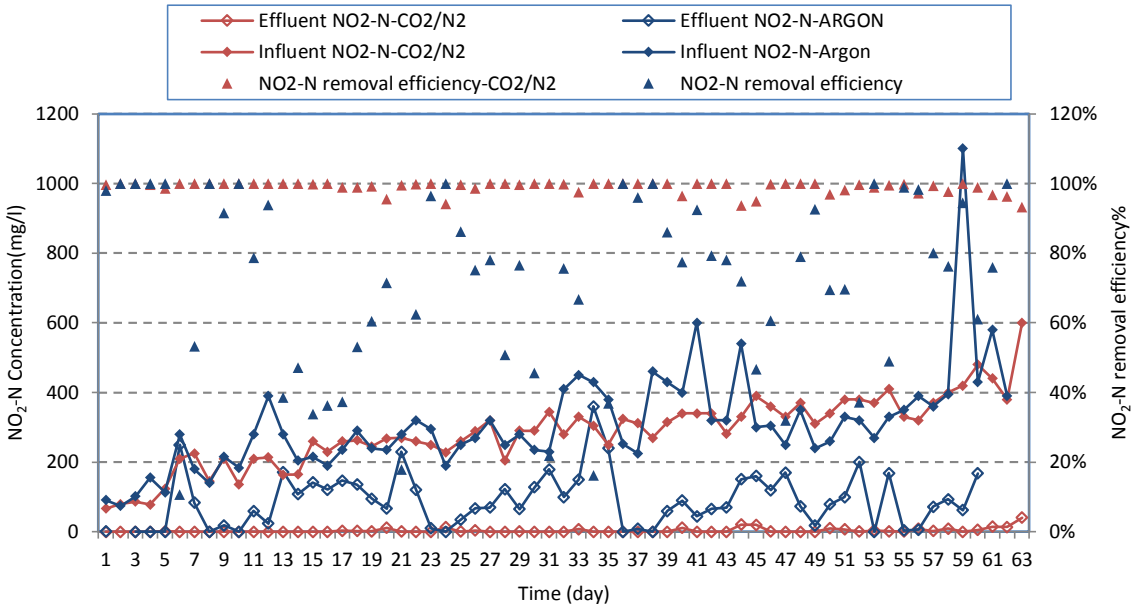


b

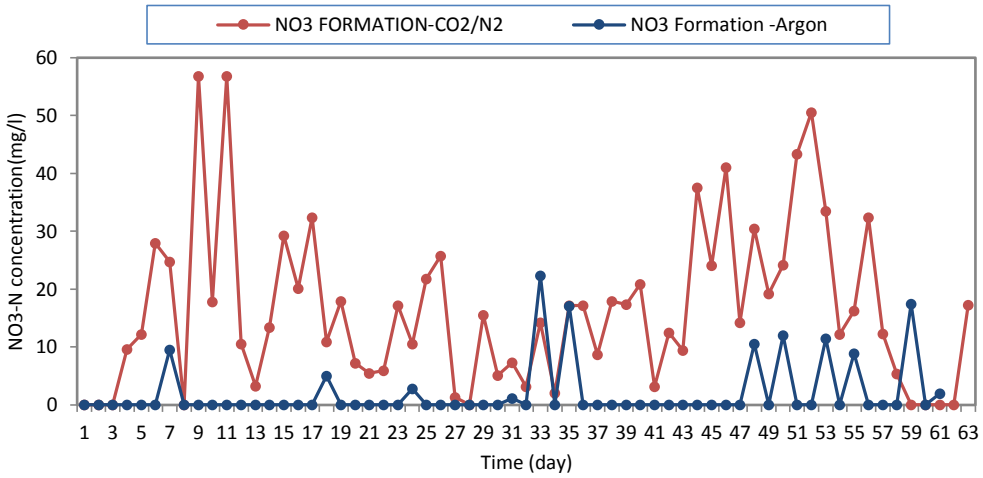


c

**Figure 6.6** Evolution of nitrogen compounds in both Amox-SBGBs during the operational period: a) ammonium concentration and ammonium removal efficiency; b) nitrite concentration and nitrite removal efficiency; c) nitrate concentration

As depicted in Fig 6.7, a steady and high conversion rate of ammonium and nitrite were achieved during the operating stage in Anammox system with a mixture of $CO_2/N_2$ flushed. These conversion rates were gradually increased with the NLR mounted until NLR reached 4.95 kg-$Nm^{-3}d^{-1}$. While in the case of argon, the loss of Anammox activity and the growth of denitrifying organisms resulting from the increasing of pH decreased the conversion rate of ammonium closed to zero and maintained very unstable the nitrite conversion rate ranging from 0.1 to 3.5 kg-$Nm^{-3}d^{-1}$.

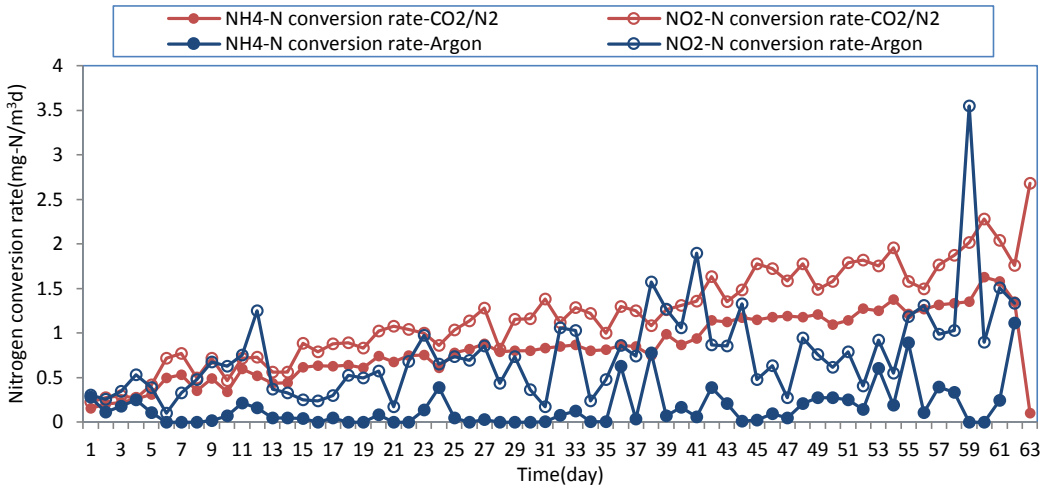


**Figure 6.7** Evolution of nitrogen compounds conversion rate in both Amox-SBGBs

Based on the analysis above, it was concluded that the application of the mixture of $CO_2/N_2$ on the Anammox system as operational strategy to keep the anaerobic condition was regarded as a promising and effectively measure to carry out the satisfactory Anammox process. Compared to the inert gas the advantages of mixed gas of $CO_2/N_2$ are as follows: a satisfactory and more effective treatment performance of Anammox were obtained; the capability of automatic controlling the values of pH in proper range saved an additional device for pH adjusting in the Anammox system followed by minimizing operation cost; feeding the Anammox bacteria with more $HCO^-_3$ enhanced cell synthesis as well as avoiding the lack of inorganic carbon source; continuously flushing mixed gas $CO_2/N_2$ means less greenhouse gas emissions. However, it was disappointing that the Amox-SBGB with argon flushed without pH adjusting device lost over 90% Anammox activity and was shifted to breed denitrifying microorganism , which was not our target culture.

### 6.4.2 The Effect of Microbubble Generation System on Performance of Anammox process

The purpose of this study is to investigate the improvement of the nitrogen removal performance of the anaerobic ammonium oxidation (Anammox) process and the microbial community that enables the Anammox system to function well, by using the microbubble generation system to inject the gas mixture of 10%$CO_2/N_2$ into Anammox sequencing batch gas lift loop bioreactor (Amox-SBGB). A gas lift loop bioreactor with a novel fluidic oscillator was used to conduct the Anammox process compared with the

one with the normal bubble generation system. Both bioreactors were fed with synthetic inorganic wastewater composed mainly of $NH_4^+$-N and $NO^-_2$-N and operated for 63 days under the same operational conditions but different bubble generation systems.

According to the previous research, the NRR of conventional biological nitrogen removal was generally less than 0.5 kg-N $m^{-3}$ $day^{-1}$ (Jin et al., 2008), whereas for Anammox process, as high as 5 kg-$Nm^{-3}day^{-1}$ was obtained by a number of researchers using different reactors such as upflow biofilter, upflow anaerobic sludge blanket (UASB) reactor and gas-lift reactor (Sliekers et al., 2003; Imajo et al., 2004; Isaka et al., 2007; van der Star et al., 2007; Tang et al., 2009a). There are three main aspects contributing to the improvement of the Anammox process performance. Firstly, the bioreactors should have high-quality sludge retention for sufficient biomass accumulation (good settlebility). Secondly, the microbial communities should aggregate well as granular sludge or biofilms for optimum metabolic activity. Finally, the substrate requirements for Anammox bacteria should be satisfied simultaneously avoiding substrate inhibition, especially nitrite inhibition (Strous et al., 1999; Isaka et al., 2007; Tsushima et al., 2007; Tanget al., 2010).

The overall nitrogen removal performance of Amox-SBGB with fluidic oscillator and Amox-SBGB without fluidic oscillator is depicted in Fig.6.8. Throughout the operation period, NLR was increased by increasing the influent substrate concentration stepwise as well as reducing HRT from 7 hours to 5 hours in both Amox-SBGBs. During the first 22 days, NLR of both Amox-SBGB was elevated from 0.5 kg-N $m^{-3}$ $day^{-1}$ to 2.1 kg-N $m^{-3}$ $day^{-1}$ and 2.03kg-N $m^{-3}$ $day^{-1}$ that corresponded to HRT of 7 h; the NRR was enhanced to 1.49 kg-$Nm^{-3}day^{-1}$ and 1.48kg-$Nm^{-3}day^{-1}$ respectively. In this period the total nitrogen removal efficiency in the Amox-SBGB with fluidic oscillator stabilized above 90% in comparison with 80% in Amox-SBGB without fluidic oscillator. From day 23 to day 44 the HRT was shortened to 6 hours. The nitrogen removal performances of Amox-SBGB with FO also showed a steadily enhanced trend, in which the NRR was increased as the NLR increasing and the highest total nitrogen removal efficiency reached 96% on day 27. However the nitrogen removal performance in Amox-SBGB without FO was disturbed by the fluctuated NLR, as a result the efficiency of nitrogen removal dropped to below 80% several times. The NRR in SBGB with FO was always higher than that in SBGB without FO. Since day 45 the NLR was continuously increasing in both bioreactors and the HRT was further reduced to 5h. It is

clear that the performance of nitrogen removal in Amox-SBGB with FO was tending to be more stable until the NLR was increased to over 5 kg-$Nm^{-3}day^{-1}$ the decline of Anammox performance presenting. The inhibition caused by high substrate concentration decrease the activity of Anammox bacteria. In Amox-SBGB without FO this inhibition emerged earlier on day 59 meanwhile the total nitrogen removal efficiency was declined to 37%. Interestingly, since day 45, it should be pointed out that subsequent attempts made to increase NLR of both reactors did not significantly improve NRR, which indicated that there was a limitation to enhance the nitrogen removal rate by only increasing the influent nitrogen concentration at a fixed HRT.

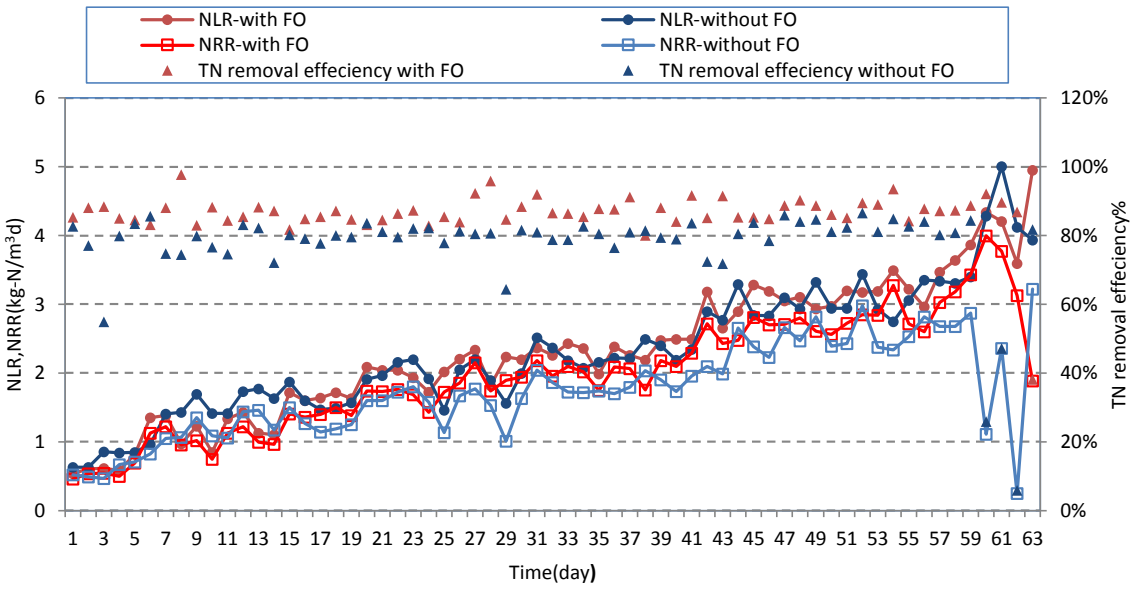


**Figure 6.8** The global performance of Amox-SBGB with and without microbubble generation system in terms of NLR NRR and TN removal efficiency

The treatment performance of both Amox-SBGB systems was further analysed in terms of various nitrogen compounds i.e. $NH_4$-N, $NO_2$-N and $NO_3$-N as well as the nitrogen compounds removal rates during the operational period. As can be seen in Fig 6.9 and Fig 6.10, the influent ammonium concentrations and nitrite concentrations were gradually increased in both Amox-SBGBs with maintaining the stoichiometric ratio relationship for Anammox. In the Amox-SBGB with FO the average ammonium removal efficiency remained around 96.8% and the nitrite removal efficiency was surprisingly around 98.9% during the entire experiment; in addition during a lot of operational period these removal efficiency impressively reached up to 1; while in the Amox-SBGB without FO the average removal efficiency of ammonium and nitrite was around 90% and 96% respectively and sometimes the unstable performance decreased

the removal efficiency to 65.9% and 69.7% respectively on ammonium and nitrite. From the point view of the effluent quality it is exhibited in Fig 6.9 and Fig6.10 that the concentrations of ammonium and nitrite were mostly lower than $10mgL^{-1}$ in Amox-SBGB with FO. This valued observed in SBGB without FO fluctuated from $0mgL^{-1}$ to $69mgL^{-1}$. As ammonium concentration was increased to $340mgL^{-1}$ the ammonium removal rate declined in SBGB with FO whereas the deterioration of ammonium removal took place in Amox-SBGB without FO when the ammonium concentration was around $280mgL^{-1}$. This is probably due to the toxicity of the increment of substrate or possibly an accumulation of unknown by-products derived from the Anammox reaction (Tsushima, 2007). Similarly the nitrite removal efficiency fluctuated due to the high substrate concentration presenting in the influent of Amox-SBGB without FO, however this decrease was not significant. The nitrite removal from the Anammox system with FO were not disturbed by the substrate concentration which indicated substrate inhibition threshold was not reached yet in Amox-SBGB with FO. Kimura et al. (2010) pointed out that the Anammox activity decreased by 37% when the influent $NO^-_2$–N concentration was 430 $mgL^{-1}$. The results obtained in our study differ from their results. As mentioned above, neither a $NO^-_2$–N concentration of 600 mg-N $L^{-1}$ in Anammox system with the microbubble generation system, nor a $NO^-_2$–N concentration of 490 $mgL^{-1}$ in Amox-SBGB without FO had an obvious inhibitory effect on the Anammox activity in this study. The deterioration of nitrite removal was detected after day 60 when an abrupt elevation occurred in the effluent nitrite concentration. The similarity of the evolution of nitrite removal efficiency and the variation of ammonium removal in both Anammox systems illustrated the Anammox activity dominated nitrogen removal but higher tolerance to the high TN concentration shock belongs to the Amox-SBGB with FO. According to the above analysis, there might be a possibility that the denitrification bacteria coexisted with the Anammox bacteria to consume some nitrite and nitrate. It is clear that the decline of the treatment performance in both Anammox systems was caused by the high substrate concentration; however, the inhibition thresholds in different Anammox systems were different, obviously higher inhibition threshold under condition for the microbubble generation system. One possible solution reported by Tsushima (2007) to eliminate the inhibition caused by high substrate concentration or unknown by-product is to shorten HRT, as result the unknown by-products derived from Anammox reaction, which possibly cause self-inhibition of Anammox bacterial activity, were washed out at shorter HRTs.

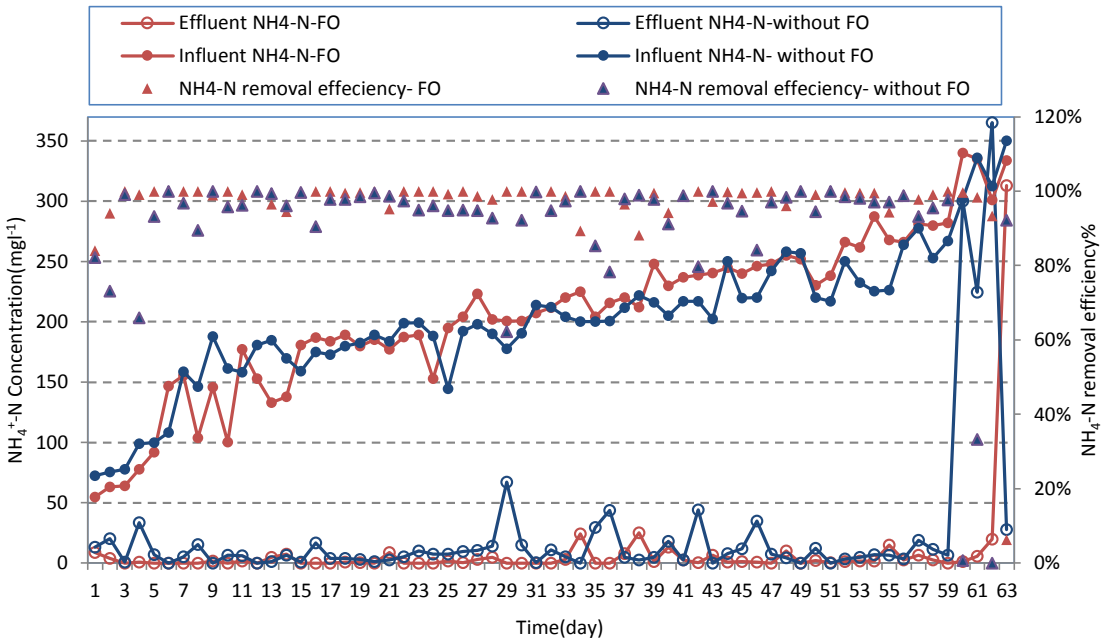


**Figure 6.9** Evolution of ammonium concentration and ammonium removal efficiency during operation period of both Amox-SBGB with and without microbubble generation system

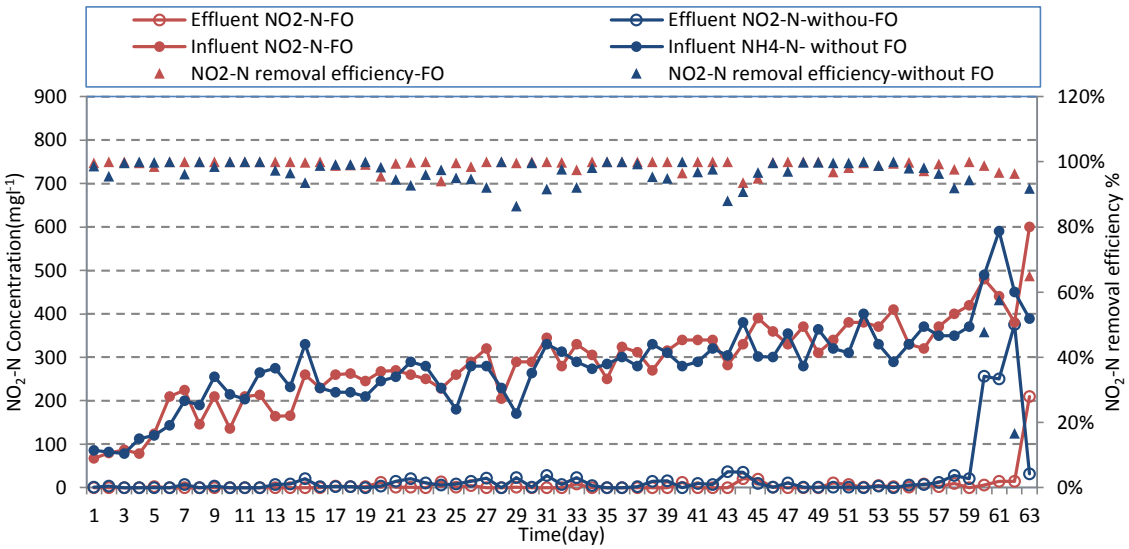


**Figure 6.10** Evolution of nitrite concentration and nitrite removal efficiency during operation period of both Amox-SBGB with and without microbubble generation system.

According to the stoichiometry of Eq 2-15, consuming one mole ammonium could produce 0.26mole nitrate in the Anammox process which is generally ignored due to trace amounts. Fig 6.11 described the evolution of nitrate concentration in the effluent and nitrate production rate efficiency throughout the operation period in both Amox-SBGBs. Careful observation of Fig 6.11 shows the higher nitrate concentration

presenting in the effluent from Anammox systems without FO maintaining persistently lower than 56.8mgl$^{-1}$ with average production efficiency of 0.126 ($NO_3$-N/$NH_4$-N) while in the Amox-SBGB with FO outlet nitrate concentration had a fluctuation most between 0 and 50.57 mgL$^{-1}$ with average produced rate of 0.082. By examining the similarities and differences of evolution of nitrate in both Anammox systems it was observed that the nitrate production was not increased with the NRL mounting but slightly decreased as the HRT shortened. Furthermore the nitrate production efficiency was lower than 0.26 as the stoichiometric relationship of the Anammox reaction expected. There is one possible reason to explain this phenomenon, which is heterotrophic denitrification bacteria and Anammox bacteria coexisting in both Amox-SBGB systems. Therefore part of nitrate produced was grabbed by denitrification bacteria to produce $N_2$ using the organic carbon source from decayed organisms.

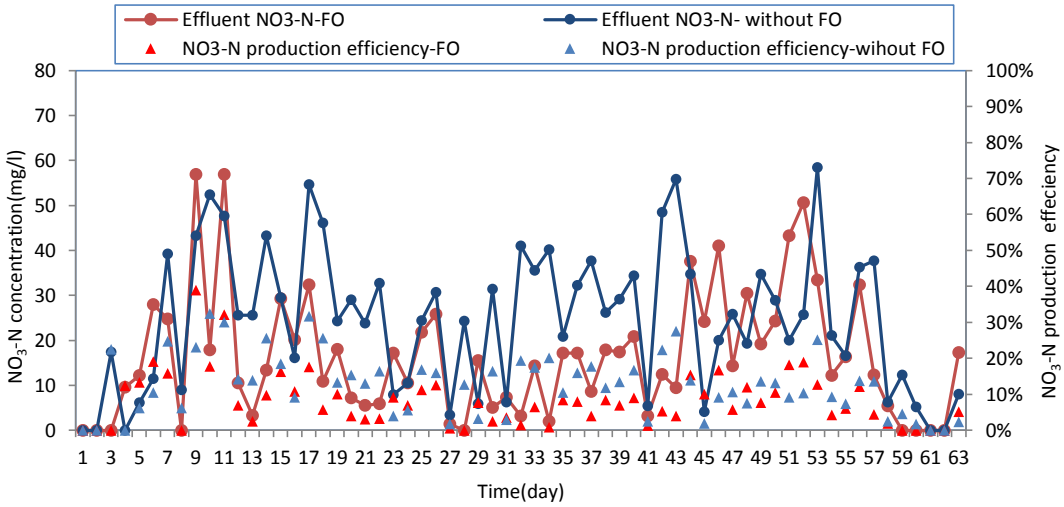


**Figure 6.11** Evolution of nitrate concentration in the effluent and nitrate production rate ($NO_3$-N/ $NH_4$-N) efficiency during operation period of both Amox-SBGB with and without microbubble generation system.

Biodiversity is not only beneficial to the growth of bacteria but also favorable to the interoperability of different bacteria (Zhang et al., 2011). In order to verify the hypothesis of biodiversity in both Amox-SBGBs, the ratio of the $NO^-_2$-N removal rate and $NO^-_3$-N production rate to $NH^+_4$-N removal rate were investigated. The essential characteristic of the Anammox process is the simultaneous transformation of $NH^+_4$-N and $NO^-_2$-N to $NO_3$-N at a given proportion; therefore the ratio among their conversion rates can be used as the main criterion for estimating the Anammox reaction's state. The ratios of nitrite conversion to ammonia conversion as well as the ratios of nitrate

formation to ammonia conversion for both Anammox systems are shown in Fig. 6.12. The reported reaction ratios of $NO^-_2$ –N to $NH^+_4$-N and $NO^-_3$-N to $NH^+_4$-N for Anammox reactions were 1.32 and 0.26 according to Eq. 2-15. In the case of Amox-SBGB with FO, the experimental result shown in Fig6.12 (a) demonstrated that the removal ratio of $NO^-_2$-N to $NH^+_4$-N was 1.38 corresponding to the reaction ratio of $NO^-_3$-N to $NH^+_4$-N of 0.088, which is far below the reported value of 0.26. Similarly the values of two ratios were obtained as 1.4 and 0.132 in Amox-SBGB without FO (Fig 612(b)). In this study, the fact, that the removal ratio of $NO^-_2$-N to $NH^+_4$-N was slightly higher than the theoretical value of 1.32 and the reaction ratio of $NO_3$-N to $NH_4$-N was far lower than theoretical value of 0.26, implies that the presence of anaerobic heterotrophic bacteria was considered as a contributor to the increment in nitrite consumption and the reduction in nitrate formation under anaerobic conditions in both Anammox systems. Since the bioreactors were fed with inorganic synthetic wastewater the reasonable approach for the heterotrophic denitrification bacteria to obtain organic carbon source is released chemical oxygen demand (COD) from granule sludge. Zhang (2011) reported the presence of AOB in the Anammox system due to lower removal ratio $NO^-_2$-N to $NH^+_4$-N of 1.09 obtained. The continuously mixed gas $CO_2/N_2$ flushing promised DO lower than 0.05mg$L^{-1}$ throughout the operational time in an experimental cycle, however at the beginning of the operational period low DO existing in the influent might cause very little AOB growth on the surface layer of the Anammox granule. Taking into account of a higher ratio of $NH_4$-N removal to $NO_2$-N removal and the ideal anaerobic condition in the Amox-SBGBs, the effect AOB on the treatment performance of Amox-SBGB generally was ignored in this experiment.

Based on the above view, we can conclude that the simultaneous existence of denitrifiers and Anammox in the microbial community of the bioreactor played an important role in the effective nitrogen removal process. A comparison between reaction ratios ($NH_4$:$NO_2$:$NO_3$≈1:1.38:0.088) for Amox-SBGB with FO and reaction ratios ($NH_4$:NO2:$NO_3$ ≈ 1:1.4:0.132) for Amox-SBGB without FO illustrates a possibility of more denitrifiers or higher denitrifiers activity taking place in the former. As a result the produced $NO^-_3$-N was grabbed by heterotrophic bacteria as substrate to generate $N_2$, thus to some extent the total nitrogen removal efficiency was improved by the biodiversity in the Anammox system. Ruscalleda et al. (2008) considered that Anammox bacteria could simultaneously coexist with denitrifiers and play an important

role in treating wastewater with high quantities of slowly biodegradable organic carbon, such as digested liquor and landfill leachate. Consequently, a slight proportion of denitrifiers would have a positive impact on the nitrogen removal. Therefore the treatment performance of the Anammox system with the microbubble generation system was improved by higher Anammox activity as well as higher denitrification.

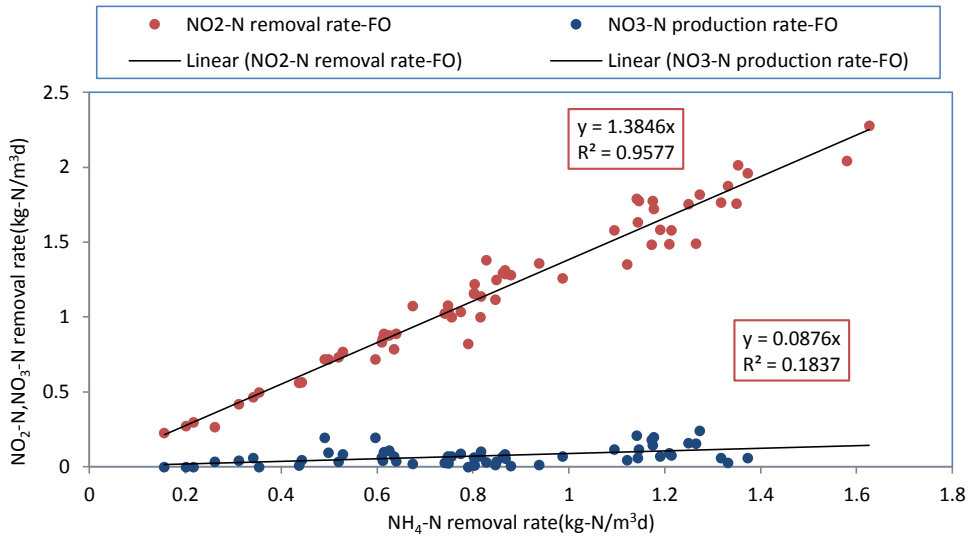


a

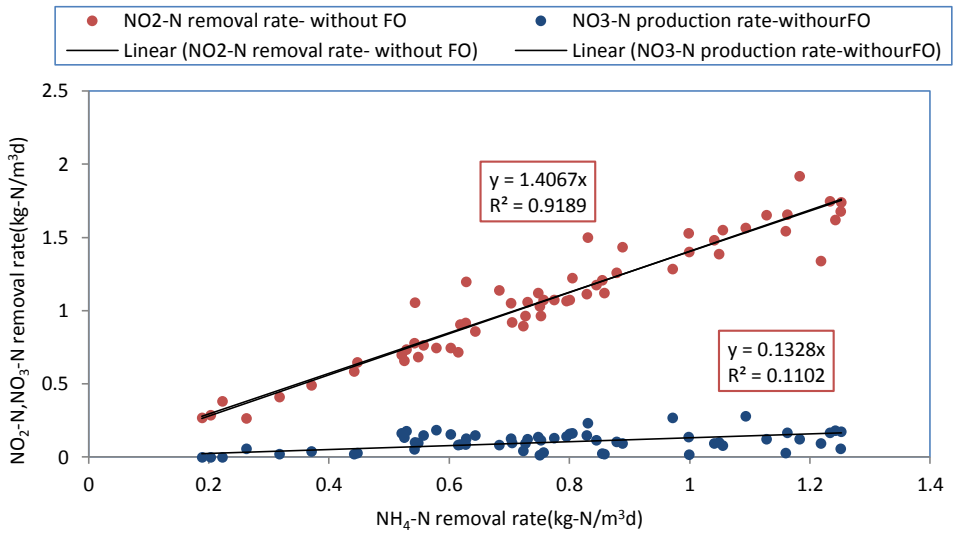


b

**Figure 6.12** $NO_2$-N removal and $NO_3$-N production with respect to $NH_4$-N removal for Amox-SBGB with FO (a) and Amox-SBGB without FO (b).

The results obtained during the operation period indicated that the Anammox bacteria are very sensitive to changes of the pH values as it was previously observed by Aktan (2012). The presence of high substrate concentrations and pH value may cause free ammonia and nitrous acid inhibition at high temperature environments. The pH value in the system affects the Anammox activity due to its effect on the $NH_3/NH_4^+$ and

$HNO_2/NO_2^-$equilibrium; $NH_3$ and $HNO_2$ being inhibitory compounds for Anammox bacteria. Previously, Waki et al. (2007) presumed that FA concentrations of 13–90 $mgL^{-1}$ could negatively affect the performance of the Anammox process. Aktan (2012) also reported that Anammox bacteria in the middle port of reactor upon acclimation can tolerate FA concentrations as high as 150 $mgL^{-1}$. However, up to date only few studies focused on the free nitrous acid inhibition in the Anammox process. Strous et al. (1999) showed that nitrite inhibition was independent of pH over the relatively narrow range of 7.0 and 7.8 and the activities of enriched Anammox culture was completely inhibited by FNA at a very low concentration of 6.0 $\times 10^{-3} mgL^{-1}$. Meanwhile, Egli et al. (2001) showed that the Anammox activity at a constant nitrite feeding level was completely inhibited at pH 6.0 and 6.5, and optimal at higher pH (7.5 and 8.0), which suggests that Anammox system lost its activity completely at a higher FNA concentration of $0.04 mgL^{-1}$. Admittedly different inhibition thresholds of FA and FNA to repress Anammox process were achieved under different operating conditions.

In the present study the both reactors were operated for 90 days under different inlet substrate concentrations. The pH of effluent and influent throughout the operation period in the reactors are presented in Fig. 6.13. It is apparent from these data that the pH in both Amox-SBGB with not pH control system fluctuated in a range between 7 and 8 thanks to flushing mixed gas of $10\%CO_2/N_2$ into Anammox system. The $H^+$ is consumed in both Anammox and denitrification processes. As a result, the neutralization reaction of $HO^-$ and $H^+$ produced by dissolved $CO_2$ tended to maintained the pH at the appropriate level. The stronger fluctuation of pH in the effluent from Amox-SBGB without FO reflected that unstable Anammox performance.

The time courses of free ammonia and free nitric acid during the study period, calculated from Eqs. (5-2) and (5-3), is indicated in Fig. 6.14. Through analyzing the evolution of the FA concentration in both reactors it was noticed that FA concentration in both Anammox systems had a tendency of increase from 1.4 to $27.7 mgL^{-1}$ and from 1.7 to $41.7 mgL^{-1}$ respectively as the influent concentration mounted. Nonetheless the FA in the Amox-SBGB with FO was mostly higher than that in the other Anammox system but varied within a narrower range. Based on the result obtained by Aktan there was no significant inhibition caused by FA in Amox-SBGBs with FO because FA concentration is lower than the inhibition threshold $150 mgL^{-1}$. In the final stage the FA concentration in Amox-SBGB without FO was sharply increased to $40 mgL^{-1}$ and the

conversion rate of ammonium and nitrite shown in Fig 6.15 remarkably decreased. The high FA might be related to the decrease in nitrogen removal efficiency. From the point view of FNA there were two peak values of FNA concentration, 0.027 $mgL^{-1}$on day 34 and 0.0298 $mgL^{-1}$ on day 62 in Amox-SBGB with FO whereas in the other Anammox system the FNA started to increase dramatically from day 57. As can be seen in Fig 6.15 during the whole experiment, the Amox-SBGB with FO was conducted stable Anammox process with increasing NRR and no evidently inhibition of FA or FNA were detected. In contrast with the Anammox system with FO, the SBGB without FO exhibited deteriorative nitrogen conversion when FNA concentration sharply mounted. This decline of Anammox performance was attributed to the inhibition of FNA due to the concurrence of the sharp elevation of FNA concentration. Furthermore the fact that the first appearance of high FA in SBGB without FO did not interfere with the treatment performance of the bioreactor also proved the high FA concentration in this study lower than the complete inhibitory threshold of FA concentration. Therefore the inhibition effect caused by high FNA was considered to be the primary reason responsible for the unstable Anammox performance. The high FA concentration at second time might aggravate suppression on the activity of Anammox bacteria and thereby increasing toxicity to the Anammox bacteria.

In addition, Strous et al. (1999) documented that the inhibition from high FNA concentrations could be overcome by addition of hydrazine. Hydroxylamine, nitric oxide, and hydrazine were intermediates in the Anammox reaction and the production of these intermediates was continuous. The addition of dissolved IC is very likely to accelerate the decomposition rate of hydroxylamine, leading to the accumulation of hydrazine (Yang et al., 2010). One of the advantages of the microbubble is a high mass transfer efficiency which induced the more $CO_2$ dissolved in the liquid phase in the Amox-SBGB with FO consequently leading to more $HCO^-_3$ product. These addition inorganic carbon sources were applied to alleviate the inhibition of FNA which is able to explain that the Anammox system with microbubble can tolerate higher FNA concentrations.

The higher conversion rate of ammonium and nitrite during the stable operating stage is evident in the Anammox system with microbubble generation system (Fig 6.15). The lower nitrate conversion rate shown in this system was because of the fact that higher denitrification activity was involved in the nitrate consumption.

Based on these, it was deduced that the application microbubble on the Anammox system not only enhanced the Anammox performance and coexisting denitrification activity but also strengthened the tolerance of bioreactor to higher substrate concentrations compared with the Anammox system with fine bubble generation system.

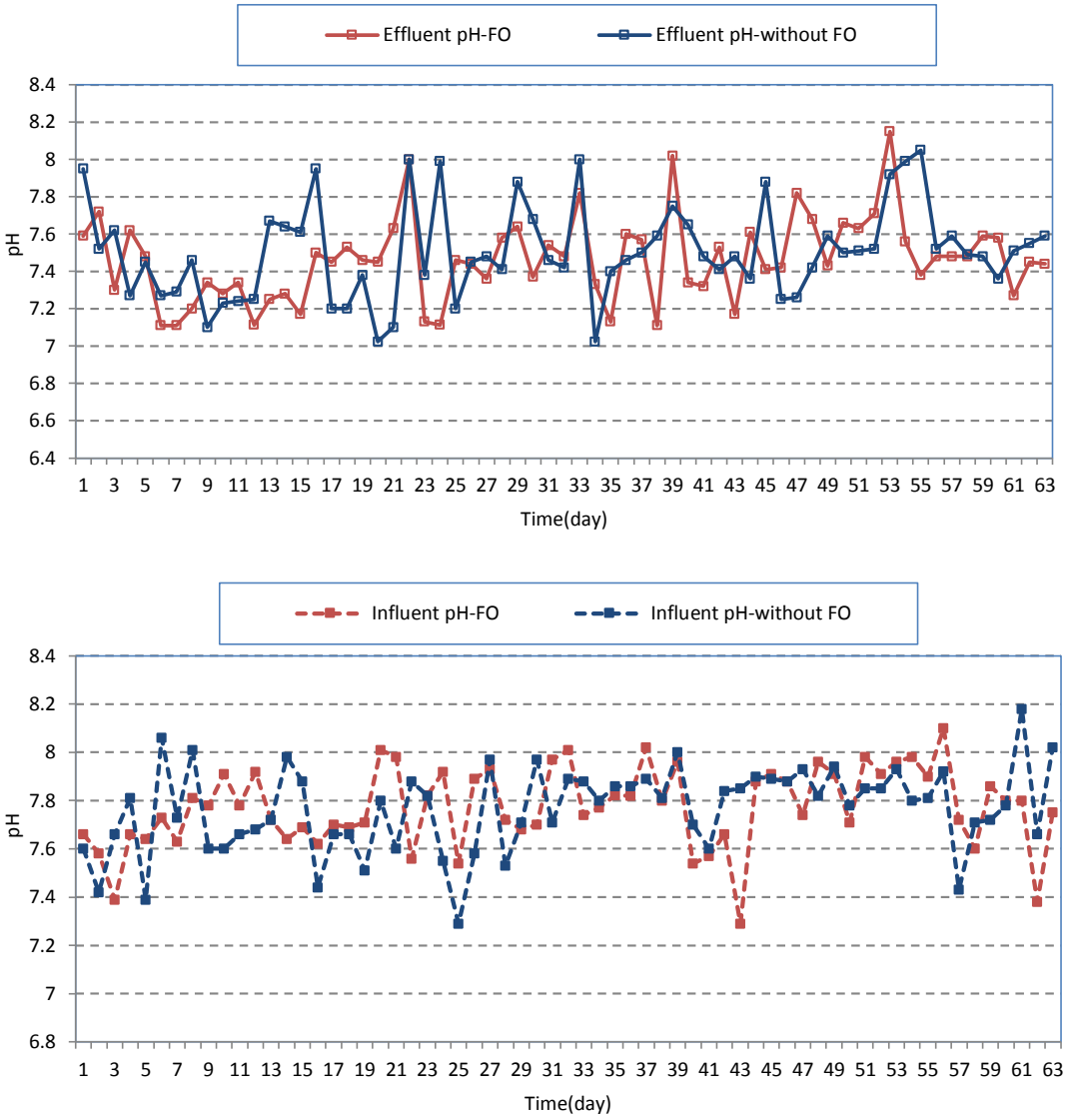


**Figure 6.13** The time course of pH value in both Amox-SBGBs with and without FO: a) Effluent pH; b) Influent pH

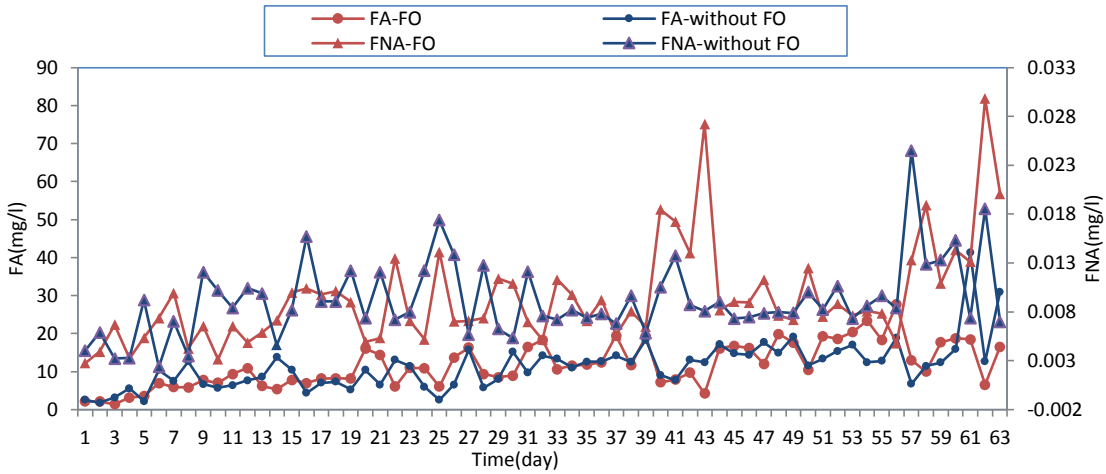


**Figure 6.14** The time course of FA and FNA in both Amox-SBGBs with and without FO

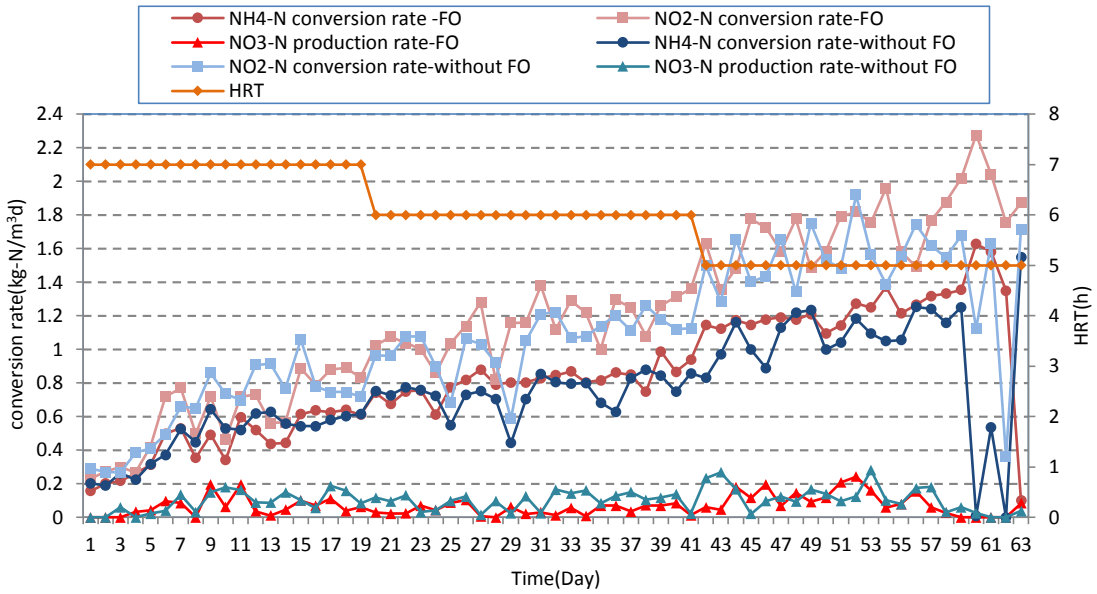


**Figure 6.15** Evolution of nitrogen compounds conversion rate in both Amox-SBGBs with and without FO.

Stability is another essential indicator to evaluate the treatment capacity of bioreactor. Stability is regarded as the resistance of the performance parameters (e.g. substrate conversion percentage, effluent substrate concentration) change to operational parameters (e.g. inflow rate, influent substrate concentration) variation. If a slight disturbance in inflow rate or influent substrate concentration results in alteration of the effluent substrate concentration enormously then the system is judged as sensitive. From statistics point of view, the dispersion of data can reflect the extent of change and

some indices measuring the dispersion are supposed to assess the stability. （Jin et al., 2007)

In Amox-SBGB with FO, the influent $NH^+_4$-N and $NO^-_2$-N concentration were raised from 54.6 to 340mg$L^{-1}$ and from 67 to 580mg$L^{-1}$, respectively. The nitrogen loading rate was elevated from 0.5 to 4.9kg-N$m^{-3}d^{-1}$. As a result the total nitrogen removal efficiency fluctuated from 80.1% to 97.8%. In Amox-SBGB without FO, the initial influent $NH^+_4$-N concentration was increased from 72.2 to 350mg$L^{-1}$, while $NO^-_2$ -N from 85.5 to 590mg$L^{-1}$, accordingly, the total nitrogen loading rate was enhanced from 0.63 to 5.0 kg-N/$m^3$d. The total nitrogen removal efficiency ranged from 0.5% to 86.7% for this Anammox system. The instability indices i.e. coefficient of variation ratio, coefficient of range ratio and coefficient of regression function derivative for the both bioreactors are summarized in Table 6.2. As we expressed in Section 6.3.3, CVR and CRR are the ratios of the dispersion of performance parameter to the operational parameter, and denote how closely the performance parameter change correlates with operational disturbance. Therefore smaller are the values of instability indices, the more stable is the reactor performance, as well as CRFD. After a comparison of the tolerance to substrate concentration shock Amox-SBGB with FO was regarded as a more stable operational system than Amox-SBGB without a microbbubble generation system.

**Table 6.2** Instability indices of both Amox-SBGB with and without FO under substrate load sock

| Reactor | CVR | CRR | CRFD |
|---|---|---|---|
| **SBGB-FO** | 3.81 | 5.81 | 1.28 |
| **SBGB-NO FO** | 5.69 | 6.45 | 3.22 |

Through comparing treatment performance of both bioreactors during the operating period of 63days, it is evident that the Amox-SBGB with FO was carried out an Anammox process with higher nitrogen removal efficiency, more stable operation and more tolerance. Generally, the total biomass and their biological activity in the bioreactor, as major factors, contributed to the optimum performance of the Anammox processes. As we have discussed before microbubble applied to inject mixed gas 10%$CO_2/N_2$ into bioreactor has some desirable features such as higher mass transfer efficiency, higher shear stress and velocity magnitude, which all can change the reaction

of inner bioreactor and properties of granular sludge. Firstly in the Anammox system only $CO_2$ and $O_2$ took part in the gas-liquid mass transfer so that partial $CO_2$ was dissolved into the water and dissolved oxygen was removed by undissolved mixed gas $CO_2/N_2$. The reaction between $CO_2$ and $H_2O$ will produce $HCO_3^-$ and $H^+$, which are regarded as carbon source and reactant for Anammox reaction (based on Eq 2-15). The higher mass transfer brought by microbubble can enhance the production of $HCO_3^-$ and $H^+$ in the liquid phase, thus according to the mechanism of the reaction, the reaction equilibrium can be driven toward the right side of the equation. Moreover the addition IC can strengthen the tolerance of Anammox bacteria to the high FNA.

Secondly, the shear force was considered as a key factor that influences the formation, structure and stability of biomass aggregates in aerobic conditions (Kwok et al., 1998; Liu and Tay, 2002). It was reported in the previous literature that the higher shear force resulting from hydraulics or particle–particle collision could exert positive influence on the properties of biomass aggregates and on the system efficiency (Chang et al., 1991; Chen et al., 1998; Gjaltema et al., 1997) while absence of granulation at weak shear force has been reported (Alphenaar et al., 1993; O'Flaherty et al., 1997; Arcand et al., 1994). In the present study, due to the same operational condition applied, the different shear stress on both Anammox systems were mainly determined by the hydraulic pattern (such as velocity of the liquid) caused by different bubble size, suggesting smaller bubbles corresponding to higher shear stress. On one hand higher shear force enhanced the formation of anaerobic granules and the granule compactness so that settling property of the sludge was improved during the operational period. The retention ability of the biomass could ensure abundant sludge volume in the reactor, which is of primary importance to provide the foundation for high-rate nitrogen removal and stable performance. On the other hand, a higher shear stress decrease of the size of the biomass granules (Chisti, 2000), which should benefit the substrate diffusion (Van Benthum et al., 1997) and improve the activity of the biomass placed in the inner cores of the granules with a consequent increment of SAA.

$$NH_4^+ + 1.32NO_2^- + 0.066HCO_3^- + 0.13H^+ \rightarrow 1.02N_2 + 0.26NO_3 + 0.066CH_2O_{0.5}N_{0.15} + 2.03H_2O \quad (2\text{-}15)$$

Thirdly, another drawback of the Anammox process is its relatively high sensitivity to its substrates, especially nitrite (Strous et al., 1999; Guven et al., 2005). For this reason the obtaining good mixing conditions inside the bioreactor is required to avoid the presence of punctual high concentrations of nitrite or ammonia in the medium. This

better mixing can be achieved by means of high liquid velocity caused by the recirculation of the mixed gas microbubble.

Last but not the least, the application of microbubble on the Anammox system could achieve the desirable anaerobic environment faster than the fine bubble after feeding stage. More homogeneous mixing in the Amox-SBGB with FO is favour to avoid incompletely anaerobic environment which suppressed the activity of Anammox culture.

Throughout the entire operational period the influent $NH^+_4$-N/$NO^-_2$-N ratio of both Anammox systems was not stable, ranging from 0.95 to 2.07 (Fig 6.16). The influent $NH^+_4$-N/$NO^-_2$-N molar ratio could play a vital role in obtaining efficient nitrogen removal in this study. In addition, since the denitrification reaction presented in both Anammox system causing variation of the optimal ratio, the effects of a wider range of molar ratio of ammonium to nitrite on the treatment performance of both Anammox systems was investigated.

Fig. 6.17 showed the nitrogen removal efficiency at different influent $NH^+_4$-N/$NO^-_2$-N molar ratios. As described in Fig 6.17(a) the optimum influent $NH^+_4$-N/$NO^-_2$-N molar ratios ranged from 1.40~1.48, corresponding to the nitrogen removal efficiency at around 95%. The lower or higher influent $NH^+_4$-N/$NO^-_2$-N ratio resulted in instability and decline in the treatment performance of Amox-SBGB with FO. By comparing with Amox-SBGB with FO, the total nitrogen removal efficiency varied from 79.8% to 86.5% by increasing the influent $NH^+_4$-N/$NO^-_2$-N molar ratio from 0.64 to 1.33 (M/M) in the Amox-SBGB without FO (6.17(b)). Subsequently the total nitrogen removal efficiency stabilized at 86±1% in the range of $NH^+_4$-N/$NO^-_2$-N from 1.33 to 1.62 followed by decrease of treatment capacity. Strous et al. (1999) previously reported that the best $NH^+_4$-N to $NO^-_2$ -N ratio for the Anammox process was 1:1.32. The results of the present study showed that the Anammox processes could proceed efficiently and successfully under different ranges of influent $NH^+_4$-N/$NO^-_2$-N ratio due to the application of different bubble sizes. If the ratio was experiencing wide variation and deviated greatly from the suitable ratios, the Anammox process would be inhibited. On the other hand, when the influent TN concentrations were low, the variation of influent $NH^+_4$-N/$NO^-_2$-N ratio would have relatively small effect on reactor performance.

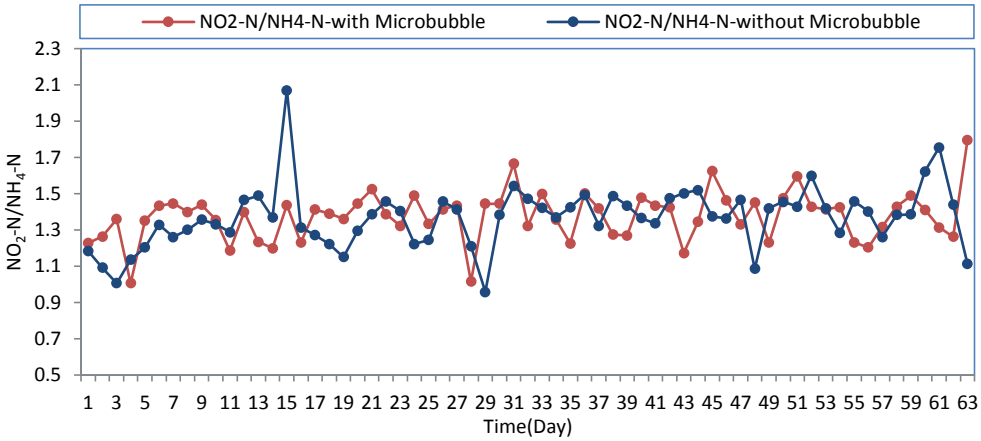


**Figure 6.16** The time course of influent $NH^{+}_{4}$-N/$NO^{-}_{2}$-N ratio of both Anammox systems

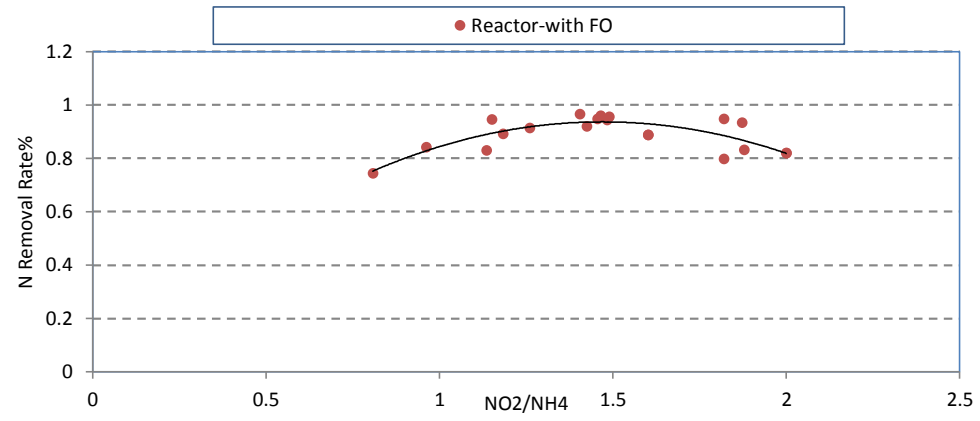


a

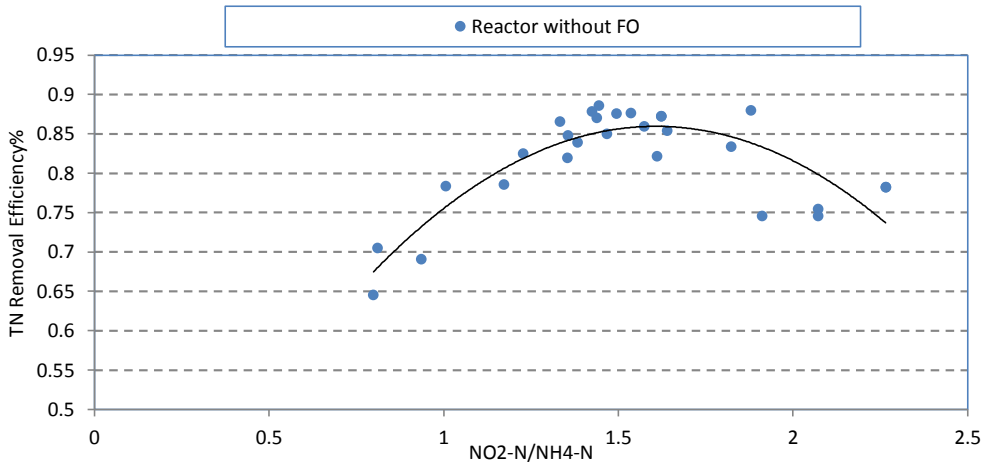


**b**

**Figure 6.17** The influence of influent ratio of $NO_2$-N/$NH_4$-N on the nitrogen removal efficiency in Amox-SBGB with FO (a) and Amox-SBGB without FO (b)

### 6.4.3 The Study of Performance of Anammox Process in Bioreactors with Different Configurations

It is considered that a more efficient and stable Anammox bioreactor must be characterized by the successful cultivation of slow growing bacteria with complete biomass retention, high reactor loading, low sludge production, production of Anammox bacterial suspension as free cells or aggregates with high growth rate (Trigo et al., 2006; Van der Star et al., 2008; Yuan et al., 2008).

In the second experimental period the SBR and SBGB both equipped with fluidic oscillator were employed to carry out parallel Anammox processes (Fig6.1 A, C). Each reactor was inoculated with same amount enriched Anammox biomass stored in fridge at 4 ℃. The temperatures of liquid inside reactors were maintained at 32±0.5 ℃ by using water area. The both reactors were flushed continuously with mixture of 10%$CO_2$/$N_2$ as an operating strategy to keep anaerobic conditions and adjust the pH inside. The HRT was fixed at 7hours.

The crucial distinction between the configuration of SBR and SBGB lies in baffled vessel residing in the latter which divides bubble columns into four distinct sections with different flow characteristics (discussed in Section 4.2). In other words fluid circulation was generated as a result of hydrostatic pressure difference in a defined cyclic pattern through channels built specifically for this purpose while the SBR was simply designed as bubble column without internal fluidic circulation. Beyond all doubt this difference of structure exerts influence on the liquid shear stress, mass transfer efficiency, mixture of inside reactor, the formation of granular etc., which might change the treatment performance of the Anammox bioreactor.

Two lab scale Anammox reactors viz sequencing batch reactor (SBR) and sequencing batch gas lift loop bioreactor (SBGB) were compared for their capacity and stability based on NLR, nitrogen removal efficiency and the established criterion(CVR, CRR, CRFD) against the substrate concentration shock.

The both reactors performances were monitored for 35 days during which the applied NLRs were progressively increased by increments of influent substrate concentration to evaluate the maximum nitrogen load to be treated. The nitrogen removal performance of SBR and SBGB is depicted in Fig6.18. Throughout the SBGB' operation, the NLR was

increased from 0.97 kg-$Nm^{-3}day^{-1}$ to 5.26 kg-$Nm^{-3}day^{-1}$ that corresponded to HRT of 7 h; the NRR was enhanced from 0.90 kg-N $m^{-3}$ to 4.13 kg-N $m^{-3}day^{-1}$ with the NLR of 4.71 kg-$Nm^{-3}day^{-1}$ during which a stable nitrogen removal efficiency was obtained at around 90% with a little fluctuation. A significant deterioration in Anammox activity occurred on day 34 due to inhibition of influent high substrate concentration of 1329 $mgL^{-1}$. Therefore the maximum TN removal rate of 4.13 kg-N $m^{-3}$ $day^{-1}$ and maximum NLR of 4.71 kg-N $m^{-3}$ were obtained during this phase with maximum TN removal efficiency of 94%. The effluent pH (7.2–7.7) was lower than that in the influent (7.66–8.04) (Fig6.19), due to the acidity produced by dissolved $CO_2$ which neutralized the alkalinity produced in Anammox process. No matter the effluent pH or influent pH was in favour of the Anammox process.

The nitrogen removal performance of SBR also showed a similar trend when the influent substrate concentration was progressively increased during the first 34 days. In this stable operational period, the initial NLR of 0.95kg-$Nm^{-3}day^{-1}$ was stepwise elevated to 4.19 kg-$Nm^{-3}day^{-1}$, as result the NRR was raised to 3.38 kg-$Nm^{-3}day^{-1}$ on day 32 during which the steady total nitrogen removal efficiency varied from 0.55 to 0.85. Thereafter, further increasing the influent substrate concentration to 1172$mgL^{-1}$ caused the nitrogen removal performance of SBR to decline to 28%. Compared to the SBGB, maximum NRR and maximum NLR in SBR were 3.38 kg-N $m^{-3}$ $day^{-1}$ and 4.19 kg-N $m^{-3}$ $day^{-1}$ during this phase with maximum TN removal efficiency of 85%. As shown in Fig6.19. Throughout the entire experiment, the variation of effluent pH and fluctuation of influent pH always fell in the range of 7-8.3 which is required by Anammox microorganism.

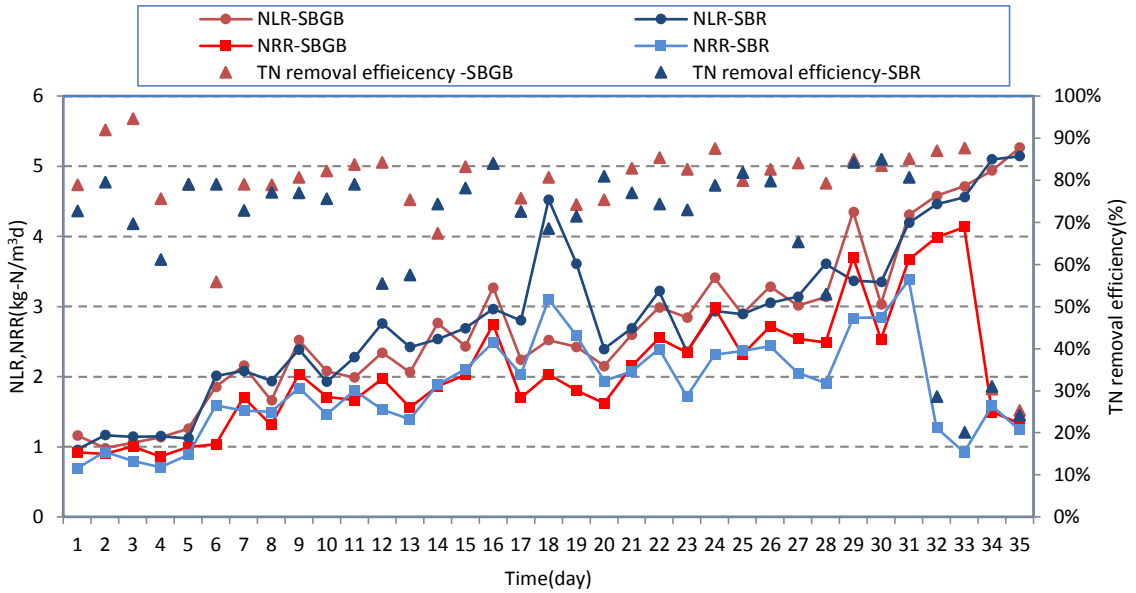


**Figure 6.18** The global performance of SBGB and SBR in terms of NLR NRR and TN removal efficiency

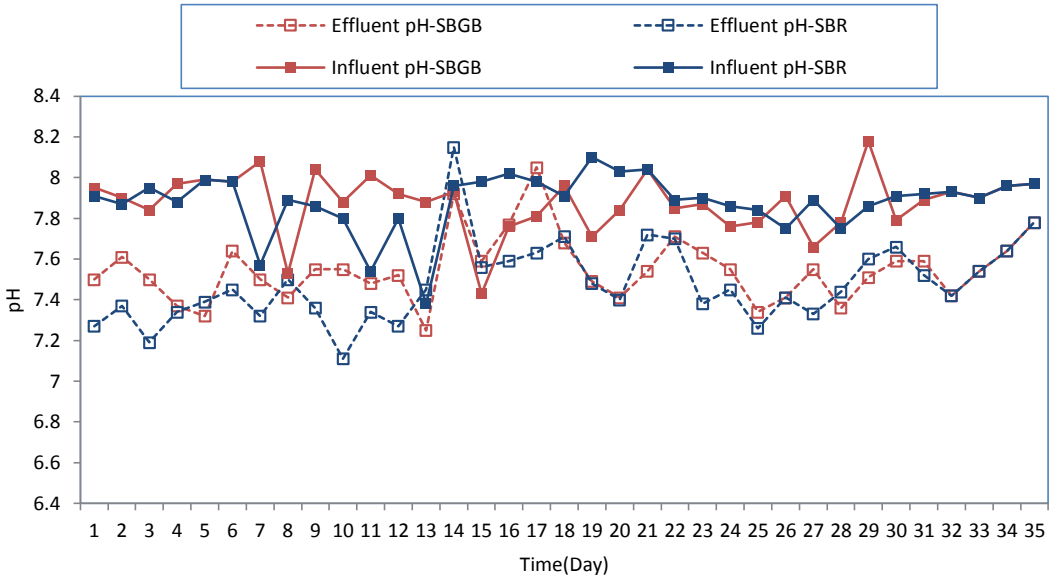


**Figure 6.19** The profile of pH in the effluent and influent in both Anammox systems

Fig. 6.20-6.22 show the results of the influent and effluent concentration of nitrogenous compounds as well as the nitrogen compounds removal efficiency. The influent ammonium concentration was gradually increased for both reactors as described in Materials and Methods section. During the first 34 days the average ammonium removal efficiency was as high as 94.94% in SBGB when the effluent ammonium concentration varied from 0 to 36mgL$^{-1}$; while Anammox activity significantly decreased to 19% when the TN concentration was over 1329mgL$^{-1}$ (influent ammonium

concentration, 559mgL$^{-1}$). Likewise, in the stable operational stage, the average ammonium removal efficiency was around 81% for SBR, during which the effluent ammonium concentration fluctuated between 0 and 108mgL$^{-1}$, until day 32 a evident loss of ammonium removal efficiency was observed (influent ammonium concentration, 467mgL$^{-1}$;).

It is demonstrated that nitrite removal efficiencies of both the reactors are presented in Fig6.21. For SBGB, the nitrite was depleted with the removal efficiency higher than 96.8% and the average effluent nitrite concentration was about 9.0 mg L$^{-1}$ when the influent nitrite concentration was no more than 748mgL$^{-1}$. But it further mounted to 770 mgL$^{-1}$ accumulation of nitrite presented in the effluent with a sharp decrease in nitrite removal efficiency to 43.9%. By contrast, it was evident that the nitrite removal efficiency of SBR remained at around 92% with average effluent nitrite concentration increased to 31.9mgL$^{-1}$. The decease of nitrite removal emerged earlier than SBGB when influent nitrite concentration was incremented to 790mgL$^{-1}$.

The nitrate production fluctuated from 0 to 59mgL$^{-1}$ in SBGB and from 0 to 72mgL$^{-1}$ in SBR respectively and it was counted in total nitrogen removal. The stoichiometric ratios of ammonium conversion, nitrite removal and nitrate production (Fig 6.23) were 1:1.6:0.16 for SBR and 1:1.5:0.08 for SBGB close to the previously reported ratios (Section 6.4.2), which suggested that Anammox biomass dominate the bioreactor. Based on this result, it also draws the conclusion that that the heterotrophic denitrification took place in both reactors without exception.

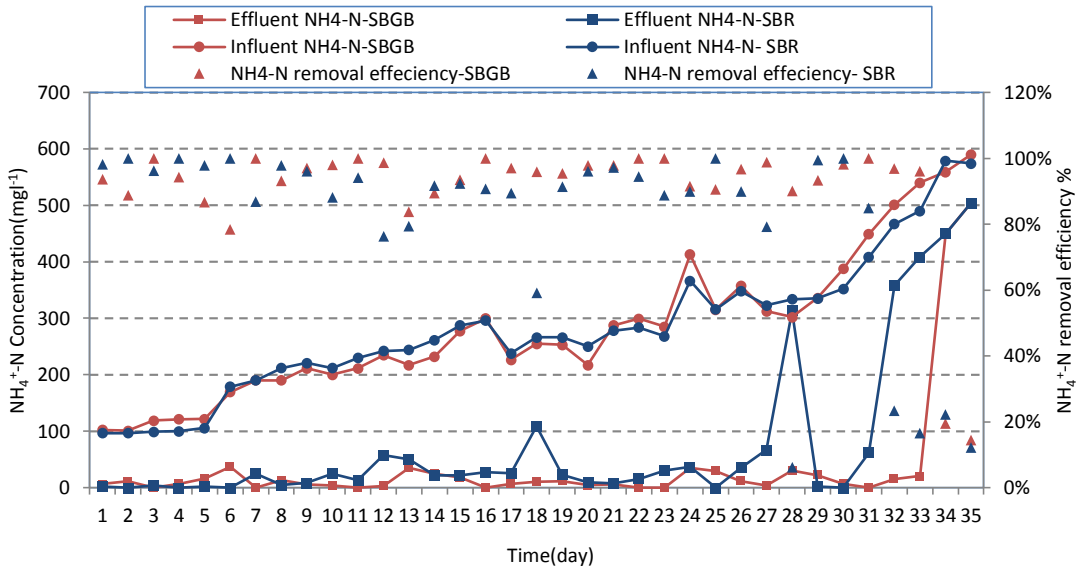

**Figure 6.20** Evolution of ammonium concentration and ammonium removal efficiency of both SBGB and SBR during operation period

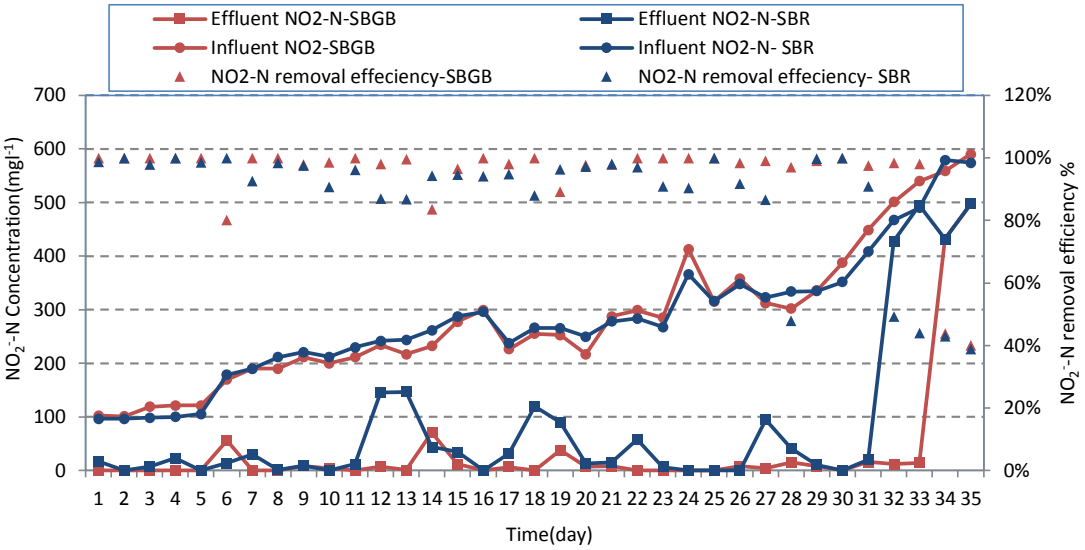


**Figure 6.21** Evolution of nitrite concentration and nitrite removal efficiency of both SBGB and SBR during operation period

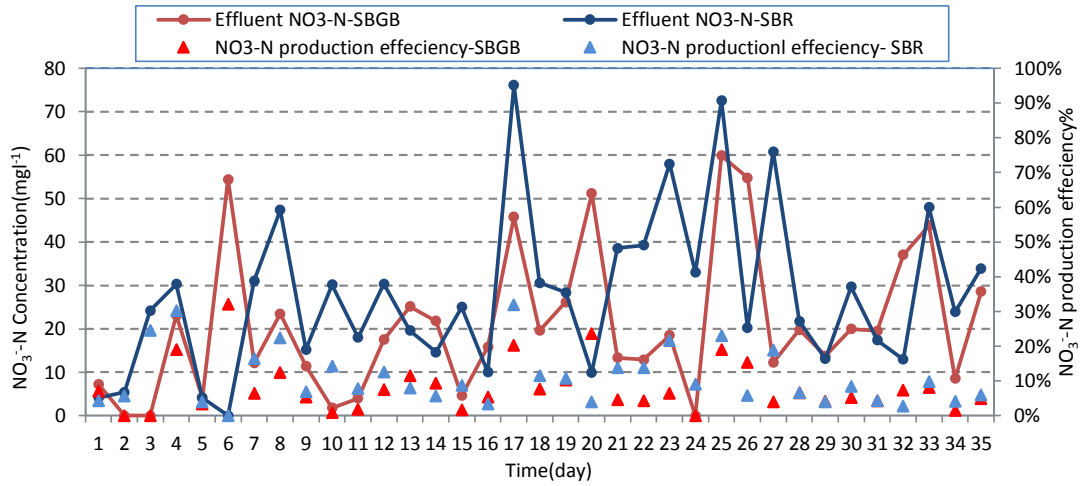


**Figure 6.22** Evolution of nitrate concentration in the effluent and nitrate production rate ($NO^{-}_{3}$-N/ $NH^{+}_{4}$-N) efficiency of both SBGB and SBR during operation period

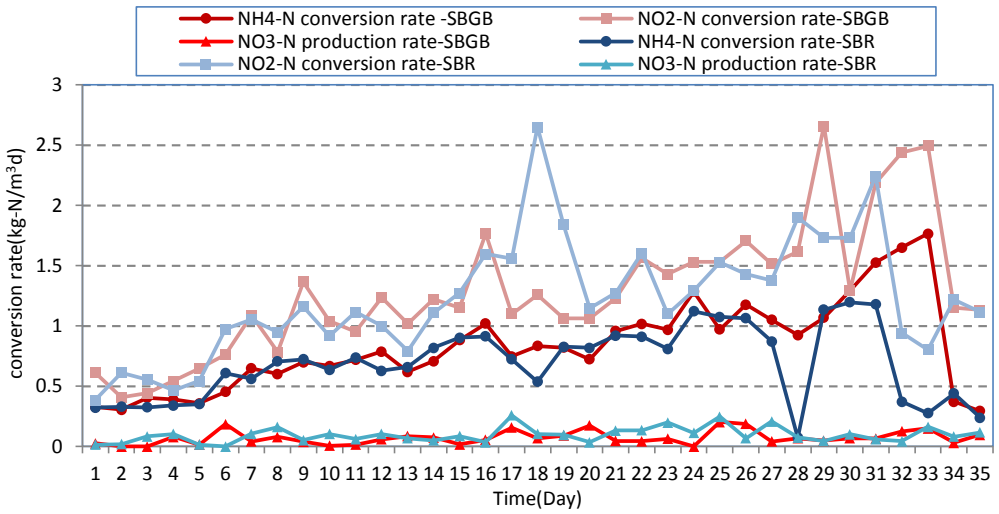


**Figure 6.23** Evolution of nitrogen compounds conversion rate in both SBGB and SBR.

Through investigating the profile of effluent nitrogen compounds concentrations it is easily observed that relative steady nitrogen removal behaviour presented in SBGB. In order to obtain further knowledge regarding to the stability of different type reactors, the instability indices i.e. CVR, CRR and CRFD were calculated and summarize in table 6.3. It is true that smaller values of these indices are the more stable treatment result was achieved. By comparison, the experimental results indicated that the SBGB was performed a more satisfactory Anammox process. Therefore we come to the conclusion that the Anammox process in SBGB showed not only a high-Anammox activity but also high resistance to the high-strength substrate shock, which provided a good foundation for the future works.

**Table 6.3** Instability indices of both SBGB and SBR under substrate load shock

| Reactor | CVR | CRR | CRFD |
|---|---|---|---|
| **SBGB-FO** | 2.28 | 2.48 | 0.567 |
| **SBR-FO** | 2.56 | 2.79 | 1.28 |

According to the investigation of the nitrogen removal performance in two bioreactors with different configurations, it is revealed that two types of bioreactors were successfully carried out the Anammox process whereas higher efficient and more stable treatment performance was observed in SBGB. Excellent treatment results were obtained with average $NH^{+}_{4}$–N and $NO^{-}_{2}$–N removal efficiencies of 94.9% and 96.8%, respectively in SBGB. However under same operational strategy these removal

efficiencies for SBR were 81% and 93% respectively, more than that the maximum treatment capacity (NLR) for SBGB was as high as 4.71 kg-$Nm^{-3}d^{-1}$ compared to 4.19 kg-$Nm^{-3}d^{-1}$ for SBR. The adequate performance of an Anammox in SBGB may be attributed to its unique configuration which provides better contact between Anammox sludge and wastewater and ability to retain the biomass inside the reactor.

The main difference between gas lift loop bioreactor (SBGB) and bubble columns (SBR) (which are also pneumatically agitated) lies in the type of fluid flow, which depends on the geometry of the system. The bubble column is a simple vessel into which gas is injected at the bottom, and random mixing is produced by the ascending bubbles. In the gas lift loop bioreactor, the major patterns of fluid circulation are determined by the unique design of the reactor, draft tube, which divides the reactor into riser, downcomer, base and gas separator (Fig4.1). The riser and downcomer are linked the bottom and the top to form a closed loop. The gas is usually injected near the bottom of the riser. The extent to which the gas disengages at the top, in the section termed the gas separator, is determined by the design of this section and the operating conditions. The fraction of the gas that does not disengage, but is entrapped by the descending liquid and taken into the downcomer, has a significant influence on the fluid dynamics in the reactor and hence on the overall reactor performance.( Merchuk and Gluz, 2002)

In a hydrodynamic sense, column-type gas lift reactor (SBGB) and bubble column reactor (SBR) have very different hydrodynamic behaviours in terms of interactive patterns between flow and microbial aggregates due to the existence of draft tube. The gas or liquid circulation flow pattern in the SBGB can create a relatively homogenous circular flow along the reactor height, and microbial aggregates are constantly subject to such a circular hydraulic attrition. According to the thermodynamics, the evident circular flow could force microbial aggregates to be shaped as regular granules that have a minimum surface free energy, provided those aggregates could be kept in the reactors under given dynamic conditions (Liu and Tay, 2002). It is clear that in a gas lift loop bioreactor the internal loop (draft baffle) can ensure a nearly constant circular flowing trajectory, which creates a more effective hydraulic attrition to microbial aggregates and better mixing conditions for the substrate diffusion. It thus seems reasonable to assume that the homogeneity of the stress forces is the main advantage offered by SBGB which is responsible for the success of shear-sensitive cultures. Admittedly, in SBR, there were some minor and indistinctive circular flows in the

region deviating from the main upflow trajectory which would cause some regional turbulence, as result microbial aggregates move with random flows in all directions. For this reason microbial aggregates are subject to varying localized hydrodynamic shear force, flowing trajectory and random collision. Under such circumstances, the irregular shape and size granules occasionally formed inclined to cause the rupture of the Anammox granules which might be washed out with effluent stream, at last imperilling the Anammox bacteria activity. Moreover the extensive up flow in SBR can result in the evaporation of volatile intermediate compounds such as hydrazine, and interruption of the catabolic cycle. It seems certain that not only the strength of hydrodynamic shear force, but also the interactive pattern between flow and microbial aggregates have effects on the formation of granular sludge. In this aspect, the column-type gas lift loop bioreactor with high ratio of reactor height to diameter can provide an optimal interactive pattern between flow and microbial aggregates for granulation.

Apart from aspects discussed above, the superiority of gas lift loop bioreactor over SBR in terms of mass transfer rated for a given energy input has been demonstrated by Legrys (1978). Therefore the more $CO_2$ was dissolved to enhance the Anammox reaction and keep more strictly anaerobic condition.

### 6.4.4 Batch Experiment of Anammox Process

During the period I, three SBGBs were employed to operate Anammox process with the same operational conditions of HRT fixed at 7 and temperature controlled at 32 ℃, respectively, but the different deoxygenating strategies were applied to achieve the strictly anaerobic environment for Anammox microorganism. In order to conveniently distinguish three Amox-SBGBs were defined as SBGB I, SBGB II and SBGB III respectively, in which SBGB I equipped with microbubble generation system and SBGB II without microbubble generation system were both continuously flushed with mixed gas of 10% $CO_2/N_2$ while SBGB III with installation of fluidic oscillator to produce microbubble was flushed argon to remove oxygen.

In order to study in more detail the process and the conversion of the nitrogen species in the three Anammox systems, batch tests were performed. Three consecutive cycle experiments of each bioreactor were performed and real-time monitored respectively on day 20 of Period I (Fig. 6.24). In this experiment, pH, ammonium, nitrite and nitrate

concentrations were synchronously measured per hour over 3 cycles. The real operation time lasted 6 hours for each cycle.

The time courses of ammonium, nitrite and nitrate concentrations over three cycles at different Anammox systems are shown in Fig. 6.24. As shown it is demonstrated that, at the end of each operational cycle, the concentration of ammonium remained constant and the concentration of nitrite slightly decreased in the Amox-SBGB III flushed with argon. In the other words, Anammox activity suffered from a decrease of nearly 100%, on the contrary the dominant position of heterotrophic denitrification was gradually formed in SBGB III but it remained at very low level. By comparison the stable and efficient Anammox processes were established in both SBGB I and SBGB II. It was observed in both reactors with the different bubble generation systems that ammonium concentrations and nitrite concentrations were stepwise consumed with elapsed time and decreased to $0mgL^{-1}$ simultaneously which suggested Anammox activity was taking dominant status. Careful observation of $1^{st}$ cycle and $3^{rd}$ shows that in the case of microbubble, the end point of Anammox cycle appeared slightly earlier than that in the SBGB II due to the steeper evolution of ammonium and nitrite concentrations. Therefore it seemed that the Anammox activity is higher in SBGB with the microbubble generation system. As shown in Fig 6.24, it is clear that 6 hours cycle seemed to be too long because the finish points for both reactors showed up around at 2 or 3 hours. In order to save more energy and improve the treatment capacity of bioreactors, since day 22, the HRT was shortened and nitrogen substrate concentrations were increased gradually.

From Fig 6.25 it is can be seen that along with consumption of ammonium and nitrite, the nitrate was produced in both SBGB I and SBGB II. After the end of the cycle the nitrate concentration was slightly declined under the action of denitrifying bacteria. The higher nitrate concentrations were mostly detected in SBAB II due to two possible reasons: firstly in the SBAB I higher Anammox activity led to a shorter Anammox reaction time and correspondingly left the denitrifers more time to consume nitrate; secondly higher denitrification activity caused more nitrate depleted from the system in SBAB. Not surprisingly the lowest nitrate concentration (close to zero) was observed in SGBG III thanks to the primary denitrifying bacteria.

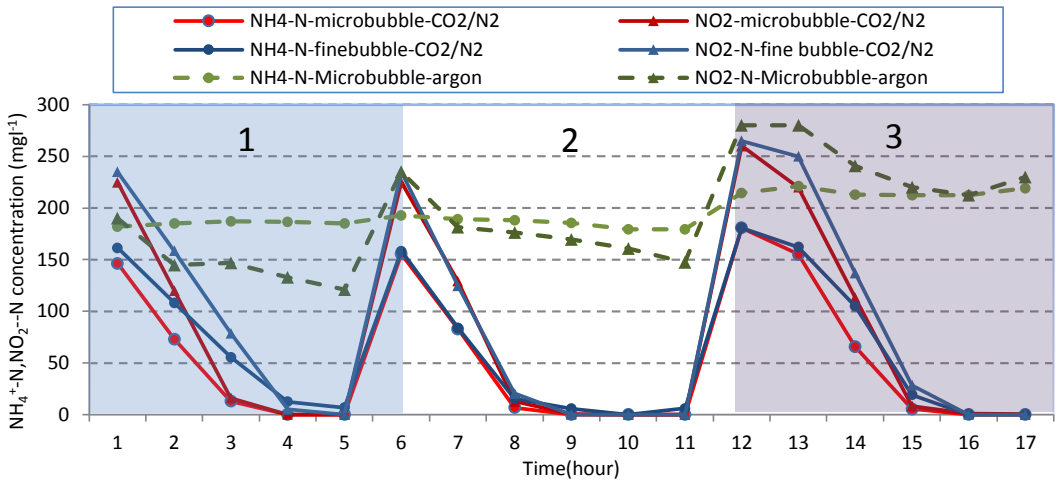


**Figure 6.24** Evolution of nitrogen species over 3 operation cycles: Amox-SBGB-with microbubble of $CO_2/N_2$(I), Amox-with fine bubble of $CO_2/N_2$(II), Amox-with microbubble of argon (III)

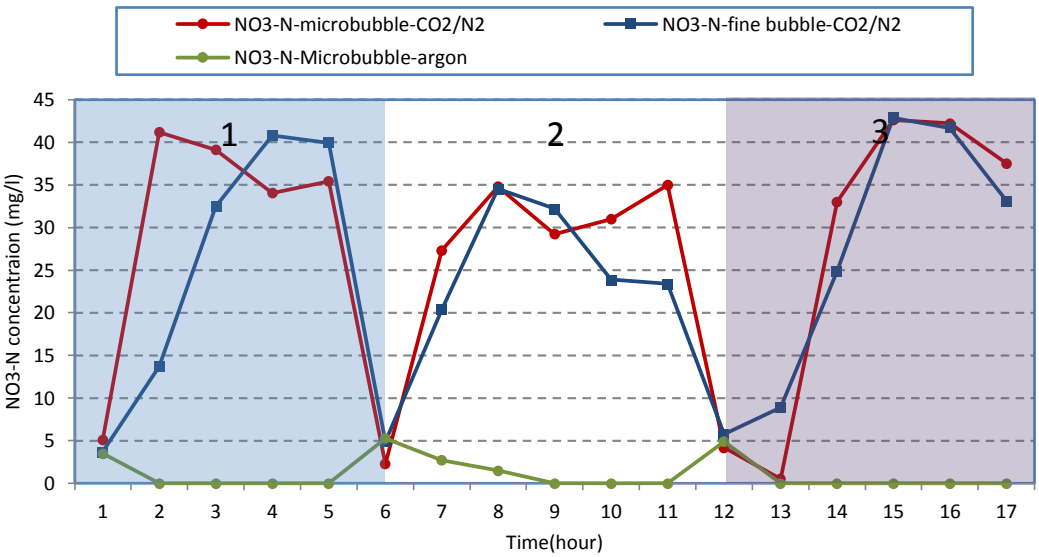


**Figure 6. 25** Time course of nitrate concentration in three Anammox systems over three operation cycles.

Fig 6.26 shows the evolution of nitrogen removal rate and total nitrogen removal efficiency over three operational cycles in three Anammox systems. As described in SBGB I, the nitrogen removal rate was quite high in the first few hours of the operation cycle followed by dramatically decrease because of exhausted nitrogen compounds. Likewise the performance of SBGB II showed the similar variation along with time but lower NRR in first half of the cycle and higher NRR in the second half of the cycle compared to SBGB I. The capacity of SBGB III was totally disabled by the higher pH as depicted in Fig 6.27 while the application of the mixed gas of $CO_2/N_2$ guaranteed the

values of pH for SBGBI and SBGB II could fall in the appropriate range throughout operating cycle. The results of batch experiments further proved that employment of mixture $CO_2/N_2$ and microbubble generation system not only enhance the Anammox activity but also satisfactorily acted as an automatic regulation system for pH and deoxygenating measure.

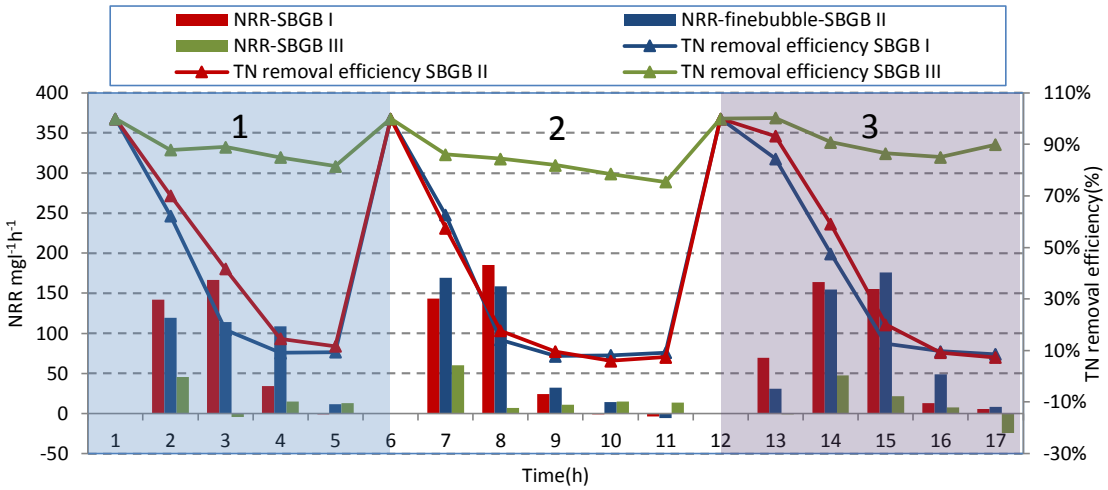


**Figure 6.26** Evolution of NRR in three Anammox systems over three operation cycles

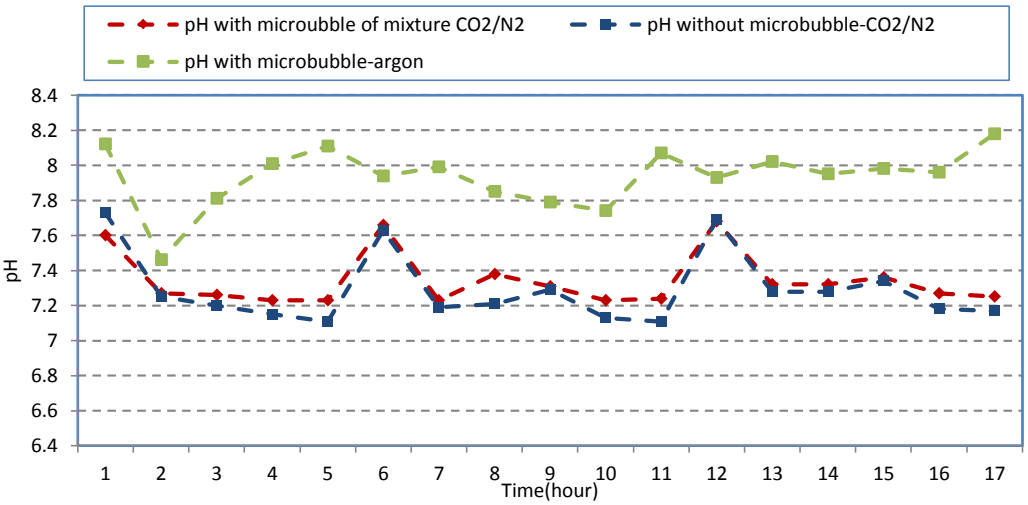


**Figure 6.27** Time course of pH in three Anammox systems over three operation cycles

### 6.4.5 Biomass Evaluation

Since the performance of the Anammox system primarily depends on the characteristics of biomass involved, it is important to have favourable conditions for granulation in order to obtain a stable Anammox population. The granular sludge characterized by good settling property and high activity, plays a pivotal role in the performance of high-

rate bioreactors (Thiele et al., 1990; Franco et al., 2006; Zhang et al., 2008). In this section the properties of the Anammox granules of Amox-SBGB I and Amox-SBGB II in terms of biomass growth, the settling property and diameter distribution were studied.

Fig 6.28 illustrates the development of Anammox biomass in both Amox-SBGBs during the experimental period I. Each bioreactor was initially inoculated with same amount enrich Anammox granule of 400ml, equal to TSS of around $35gL^{-1}$. In view of low growth rate of Anammox bacteria, it is interesting to see during the first 20 progressive increase of the Anammox granules was observed in both bioreactors followed by slightly decline and stability. The explanation for this phenomenon is that relatively high calcium and phosphorous concentrations were included in the mineral medium according to the results of Trigo et al. (2006). Thereafter the calcium and phosphorous concentrations were decrease to $47mgL^{-1}$ and $52\ mgL^{-1}$, thus TSS concentrations were deceased and stabilized at approximately $39gL^{-1}$ and $28gL^{-1}$ respectively in both bioreactors. As shown the VSS/TSS ratios of the ANAMMOX granules in both reactors were in the range of 0.66-0.87 and 0.65-0.75 respectively. Precipitation of lower calcium and phosphorous on the granular circumferences gave rise to the high volatile solids content of the enriched granules in both bioreactors. Additionally, throughout the period I, it is also observed that Amox-SGBG I maintained a higher biomass compared with that in Amox-SBGB II. Taking into account of the very low growth rate of Anammox bacteria, the major retention ability of the biomass I and minor growth of Anammox and denitrifying bacteria were attributed to different biomass in both bioreactors. The same method of sampling and measurement with Chapter 5 was also used here.

A better retention ability of the biomass could ensure abundant sludge volume in the reactor, which is of primary importance to provide the foundation for stable performance (Zhang, 2011). The settling property of the sludge expressed through SVI was regarded as primary contributor to the biomass retention ability in sequencing batch reactor. Fig 6.29 illustrates the time courses of TSS and sludge volumetric index (SVI) in two Amox-SBGBs during the experimental period I. The SVI was consistently lower than $60mlg^{-1}$ throughout the operational period with high concentration of VSS which indicate that both bioreactors sludge had good settling capacity. However, on day 10, SVI in SBGB I was significantly decreased to $7.46mlg^{-1}$, the similar trend presented in SBGB II. This result was explained by that the precipitation of high calcium salts on the

granules could effectively strengthen the density of sludge. Thenceforth, SVI gradually increased because the biomass density decreased due to the fact that the breakage of the granule caused by shear stress and the collision was suspended in the liquid or attached by dinitrogen gas finally being washed out. Along with depletion of the fluffy and less dense sludge, thereby the biomass aggregates occurred again and improved the settling property in both reactors. In the most steady-state, SBGB I showed lower SVI than that in SBGB because the higher hydrodynamic shear stress caused by microbubble promoted the cell aggregates of the sludge instead of destroying its structure, accordingly enhancing the formation of anaerobic granules. This finding is also supported by the report of Liu and Tay (2002), who stated that hydrodynamic shear force promoted the production of extracellular polymeric substrate, which is assumed to play an important role in sludge granulation.

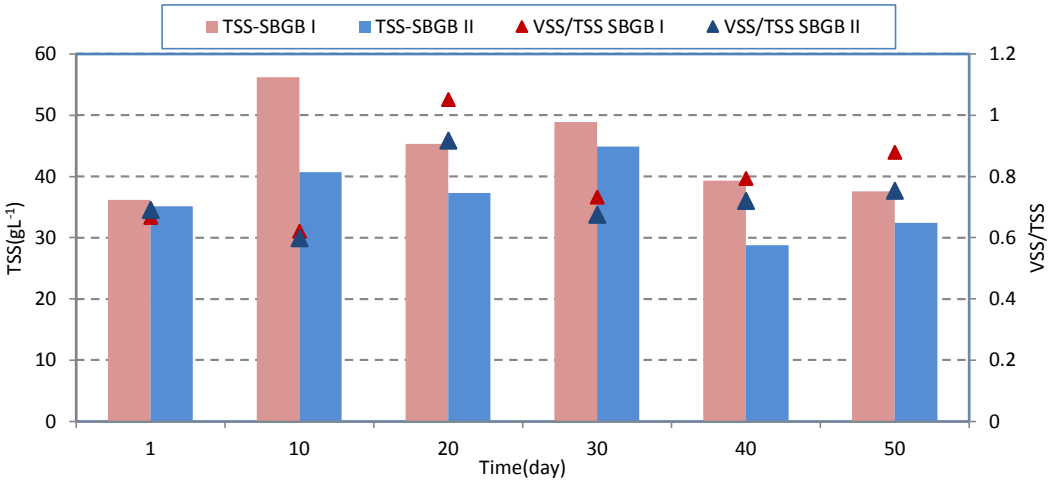


**Figure 6.28** Biomass variations in Amox-SBGB I, II throughout period I

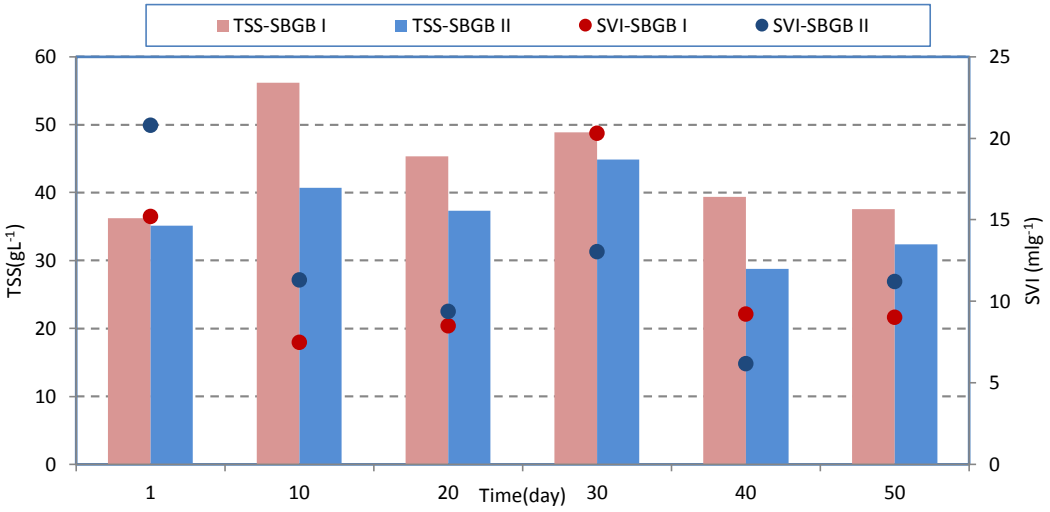

**Figure 6.29** Time course of total suspended solids and sludge volume index in Amox-SBGB I, II throughout the period I.

Specific Anammox activity (SAA) is calculated from the ammonium and nitrite consumption rate divided by the biomass concentration (g VSS $L^{-1}$) (Eq. (6-9)):

$$\mathrm{SAA}\left(\frac{\mathrm{gN}}{\mathrm{gVSS}}\cdot \mathrm{d}\right) = \frac{NRR\left(\frac{gN}{L\cdot d}\right)}{VSS\left(\frac{g}{L}\right)} \quad 6\text{-}9$$

The relationship between Specific ANAMMOX Activity (SAA) and NLR in both SBGBs is illustrated in Fig 6.30. During the stable operation period the SAA of SBGB I exponentially increased with the NLR increasing from 0.026 to 0.08gNVSS$^{-1}$d$^{-1}$ whereas the initial SAA of 0.025 gNVSS$^{-1}$d$^{-1}$ in SBGB II was mounted to 0.126gNVSS$^{-1}$d$^{-1}$ with exponential growth in SBGB II. It seemed that the higher Anammox activity was obtained in SBGB II with the fine bubble generation system. This interesting phenomenon was due to the relative higher biomass with an average of 34.4gVSSL$^{-1}$ in the SBGB I compared to 26.3gVSSL$^{-1}$ in SBGB II. It also explained why the inhibition of Anammox reaction in SBGB II arose with NRL of 3.3 kg-Nm$^{-3}$d$^{-1}$ at the end of experimental period I, while no inhibition was detected in SBGB I under such NRL (Fig 6.8).

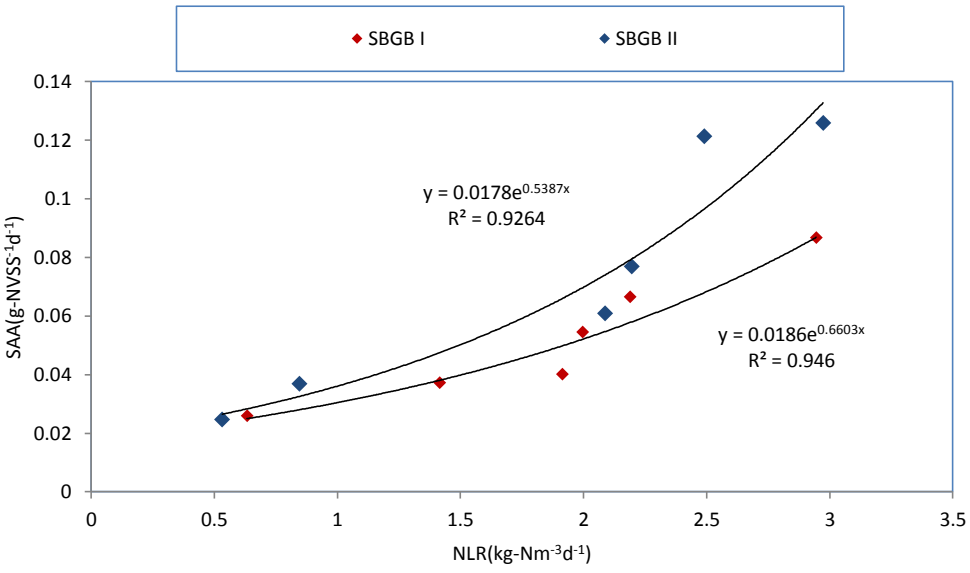


**Figure 6.30** The relationship between SAA and NLR in SBGB I&II during the experimental period I

On day 40 the sludge samples were collected from three Anammox systems to study the effect of the bubble size and different gas on the physical properties of granule sludge.

Fig 6.31 shows appearance shape of the granule. From Fig 6.31 it is can be seen that after 40 days operation, the Amox-SBGB I equipped with microbubble acquired the smaller and more homogeneous size Anammox granule with characteristic red colour. In Amox-SBGB II the Anammox sludge was growing to be bigger and uniform compared with the original inoculation and the colour was carmine very closed to the initial colour, whereas granular sludge in the Amox-SBGB III turned from carmine to brown, in addition serious flotation sludge caused by abundant breakage of sludge is considered to be a serious problem that results directly in a decrease in sludge density as well as sedimentation properties. The hydroxylamine oxidoreductase and hydrazine oxidoreductase are two important enzymes of the Anammox pathway (Tang, 2010). Both of these enzymes are rich in heme c (Klotz et al., 2008; Schmid et al., 2008), which endows the granular sludge with the red colour. The size distribution of the granules were measured (Fig 6.32) at the end of the period I. The large averaged diameter of the granules can be another negative factor for the system stability because granules can break due to substrate limitation by diffusion in the inner zones and a collision between the big size granule and smaller sludge granule, causing the lysis of the cells inside the granule (Van Benthum et al., 1997). Conversely, the smaller granular size contributed to high biomass retention, contact area and the high diffusion of substrate into the sludge granule. In addition smaller granules reduced chance of the particle-particle collisions thereby the breakage was effectively prevented. As we discussed previously the better mixing and hydromantic shear force are beneficial to ensure the better granulation and decreasing the granular size. As expected the Amox-SBGB I which was equipped with the microbubble generation system harvested smaller Anammox granules as well as profited through them.

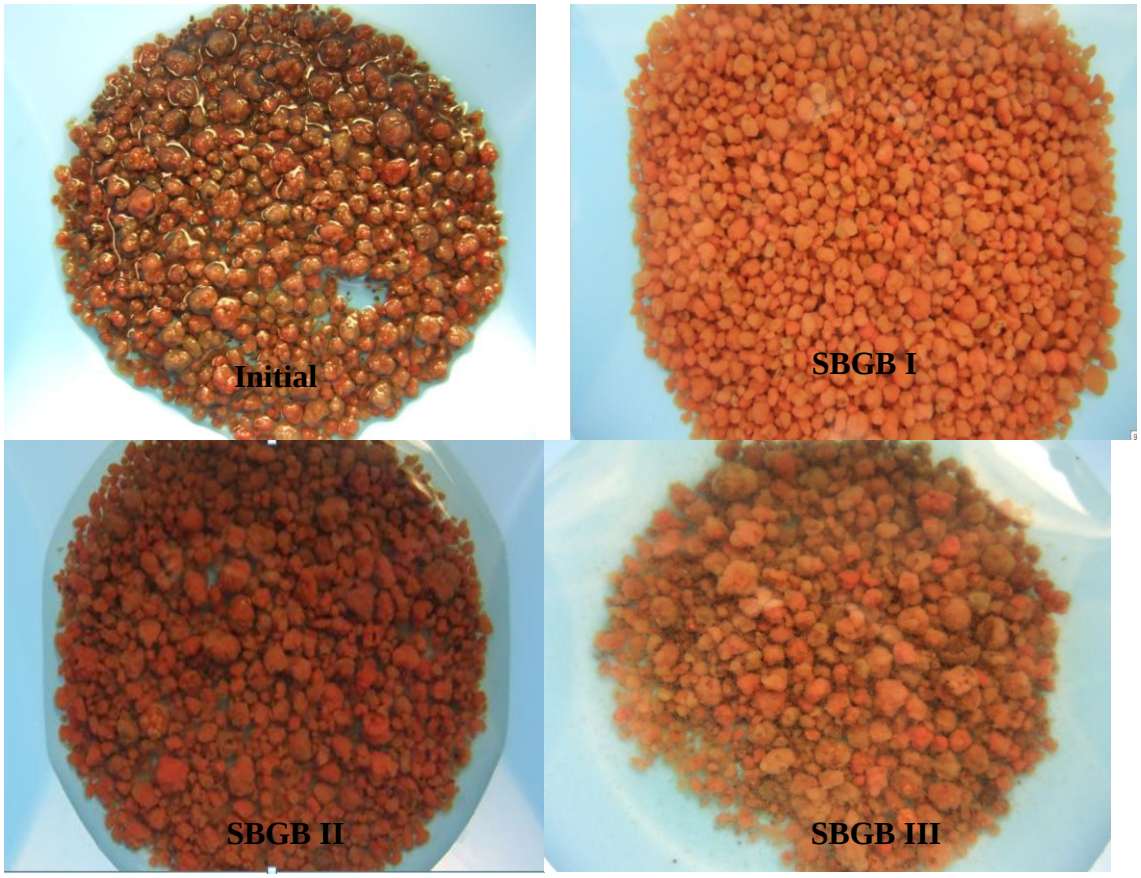


**Figure 6.31** Appearance shape of Anammox granules taken from three Amox-SBGBs and initial inoculated sludge

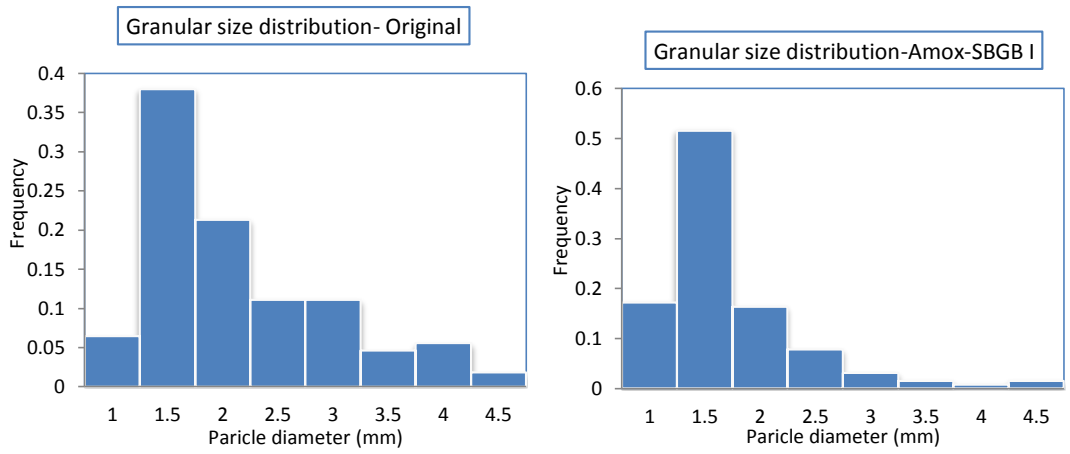

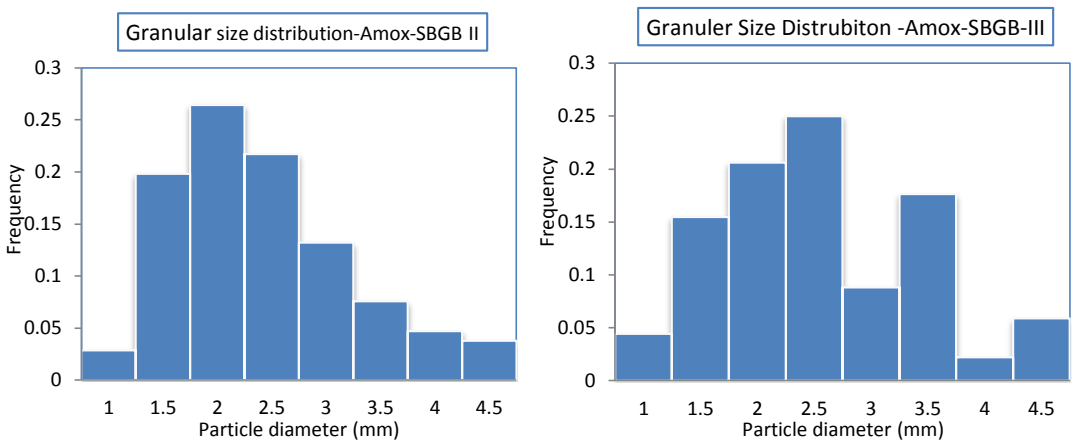


**Figure 6.32** Distribution of granular size at the beginning and at the end from three Amox-SBGBs

## 6.5 Analysis of Microorganism Involved in Anammox systems by TEM and SEM

### 6.5.1 Morphology Observation of Anammox Bacteria by TEM

In order to identify the presence of various microbial populations and reveal the inner structure of Anammox cell in present study TEM was performed on the enriched biomass taken from three Amox-SBGBs in the late experimental period I.

On close inspection, three different cell morphology in both Amox-SBGB I and Amox-SBGB II were detected shown in the Fig 6.33 and Fig 6.34. According to the description for Anammox bacteria in previous study (Schmid et al., 2003; Tang et al., 2010; Lindsay et al., 2001; Kartal et al., 2007)), it is evident in Fig6.33 (a) that this Anammox-like cell displayed typical ultrastructural features of Anammox bacteria: the innermost compartment, named anammoxosome (A), filled with material of moderate electron density and granular texture, but devoid of ribosome-like particles, is surrounded by a single membrane; anammoxsome and riboplasm with ribosome-like particles separated from paryphoplasm at the cell rim by an intracytoplasmic membrane (ICE) shadow area. The paryphoplasm (P) surrounds the rim of the cell. However in Amox-SBGB II Anammox cell (Fig 6.34 a), it seems difficult to distinguish this part.

The Anammox phylotype in SBGB I had a morphological similarity to “Candidatus Brocadia”, while the Anammox phylotype in SBGB II had morphological similarity to “Candidatus Kuenenia” (Tang et al., 2010). In the present study, the morphology and

ultrastructure of the Anammox cells seemed different under the two deoxygenating models. Although the same seed sludge was inoculated and the same operating condition was applied for both reactors, the different hydrodynamic conditions might be a reason leading to the ultrastructure differences of enrichments in both bioreactors, suggesting that the dominant populations in the two reactors enrichments would probably be different.

Besides the dominant Anammox cell it was also observed that two types cell with different morphology co-existed in the Anammox system in SBGB I&II, shown in Fig 6.33 (b, c) and Fig 6.34(b, c). Due to the fact that occurrence of the denitrification process was confirmed in both bioreactors during the stable operational period it could be deduced that some cells were related to the denitrifying bacteria. In previous studies, more than one researcher (Lai, 2008; Domenech, 2009; Lin, 2006) described the denitrifying bacteria as a single flagellum at one pole of the rod-shaped cells, just like cell shown in Fig 6.33(b) and Fig 6.34 (b). The third morphology (Fig 6.33 c and Fig 6.34 c) found in both bioreactors was visually similar with the nitrifying bacteria. Although, based on the results obtained before there was no nitrification activity detected, the possibility of presence of nitrifiers in Anammox consortium could not be completely excluded. It seemed reasonable that the feeding phase of batch cycle encouraged the growth of little nitrifying bacteria which were completely inhibited as song as the oxygen eliminated from the system.

As expected, in the Amox-SBGB III, no Anammox-like cell could be observed instead the denitrifying bacteria with various structures and morphologies gradually changed the microbial consortium (Fig 6.35)

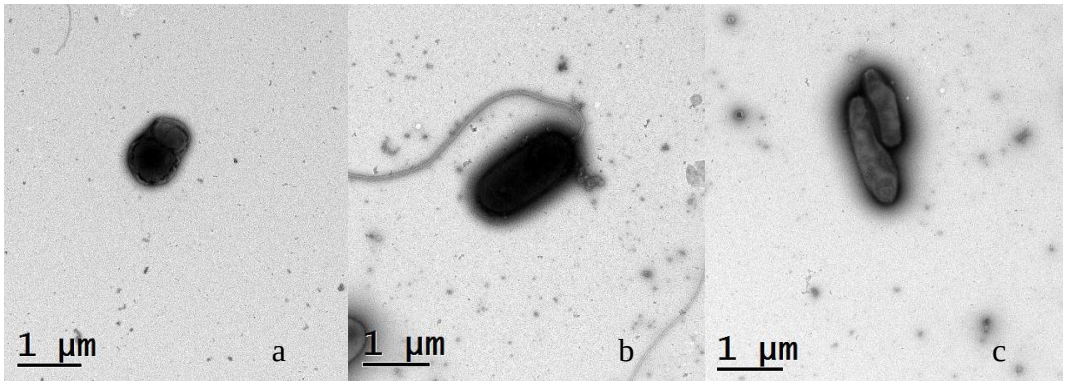

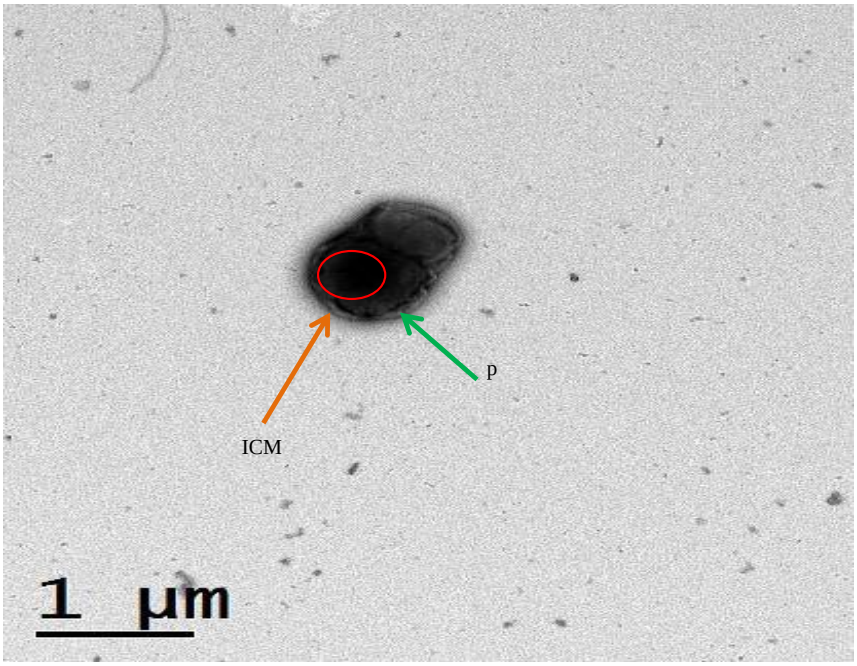


**Figure 6.33** TEM photographs of the granular sludge in Amox-SBGB I

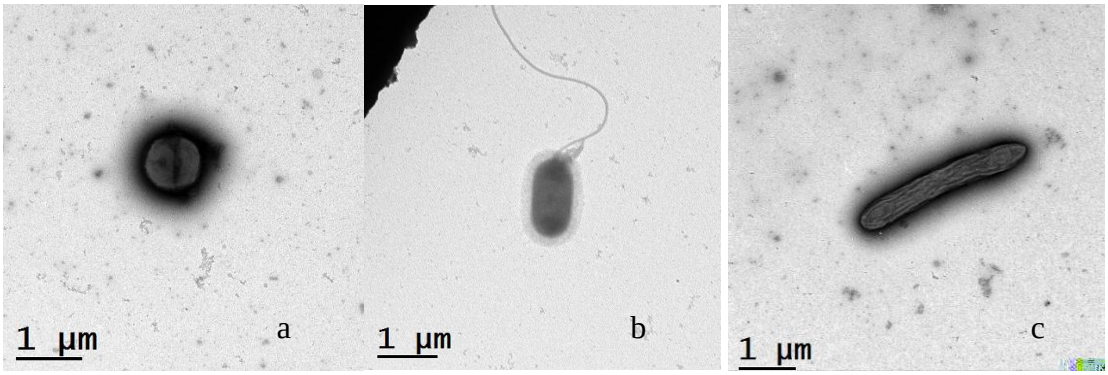


**Figure 6.34** TEM photographs of the granular sludge in Amox-SBGB II

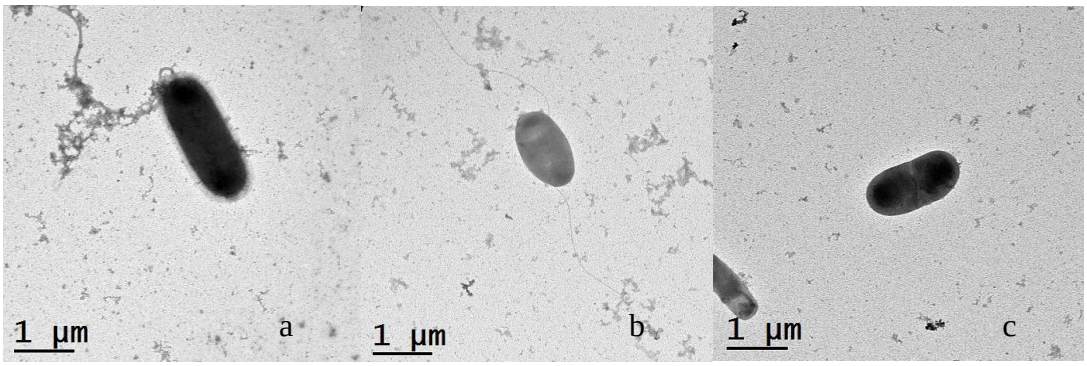


**Figure 6.35** TEM photographs of the granular sludge in Amox-SBGB III

### 6.5.2 Morphology Observation of Anammox Bacteria by SEM

Morphological characteristics of the Anammox sludge developed in three Amox-SBGBs were observed using SEM. Sludge samples on day 10 and day 60 after seeding were collected. As described in Fig6.36, SEM observation revealed that the cultivated Anammox granular sludge (Fig 6.36 b, d) from Amox-SBAB I were aggregated with mostly spherical and elliptical shape with smooth surface and "crateriform structures" (Fig 6.36 a, c), the unique characteristic of Anammox cell. It also observed that other microbes co-existed with cocci bacteria such as filamentous and short-rod bacteria like AOB or denitrifiers. This observation together with monitoring of the Nitrogen transformations reveals the presence of high Anammox activity in this Anammox system, indicating the harmonious coexistence of Anammox bacteria with other microbial populations. Compared with Fig. 6.36 (a), the Anammox biomass in Fig. 6.36(c) seemed to have a higher degree of compactness, which was attributed to the long term cultivation with synthetic wastewater. More spherical shaped bacteria were dominant in Anammox system microorganisms and interference bacteria were gradually eliminated. The shape of Anammox aggregate was changed from irregular aggregate (Fig 6.36 b) to uniformly round aggregate (Fig 6.36 d) with smoother surface but not very evident. Similarly various bacterial morphologies were observed in the Amox-SBGB II, it also indicated a harmony of Anammox culture with other organisms in this system. As can been seen in Fig 6.37 (a, c) the coccoid cells were observed to be dominant in the Anammox enrichment culture on day 60 however the purity and compactness of coccoid cell was not as high as that in Amox-SBGB. It is observed in Fig 6.37(b, d) that the sludge aggregate showed a semblable structure with Fig 6.36(b,c).

During the operational period, hydrodynamic shear stress encouraged the granules to produce uniform morphology. In the bioreactor with microbubble generation system, high shear stress arose, as result the dense structure of the sludge illustrated high contents of extracellular polymer substrates (EPS). Because EPS could bridge two neighbouring cells physically to each other, as well as with other particulates (Schmidt and Ahring, 1994, 1996), aggregates were formed in the bioreactors.

Whereas in Amox-SBGB III with seed sludge from same enriched Anammox sludge, the main types of bacteria were not spherical shaped bacteria anymore but rod shaped (Fig 6.38 a, c) related to pseudomonas and bacillus which were regarded as rod shaped

denitrifying bacteria. In addition the cyst of H. globosa (Fc) is also shown in the red circle (6.38 c), which generally presented in the denitrification system (Mattison et al., 2002). All of these observations proved the truth happened in Amox-SBGB III, which is the Anammox bacteria were inhibited and washouted with effluent; instead the denitrification bacteria arise in Amox-SBGB III. Compared to the first two bioreactors, the undesired condition with high pH denatured granular sludge in this system which caused the sludge flotation threatening the performance of bioreactor.

As coccoid cells were observed to be dominant in the Anammox enrichment culture from the first two bioreactors, a large majority of the microbial community was comprised by Anammox bacteria, further proved by the quantification of QPCR.

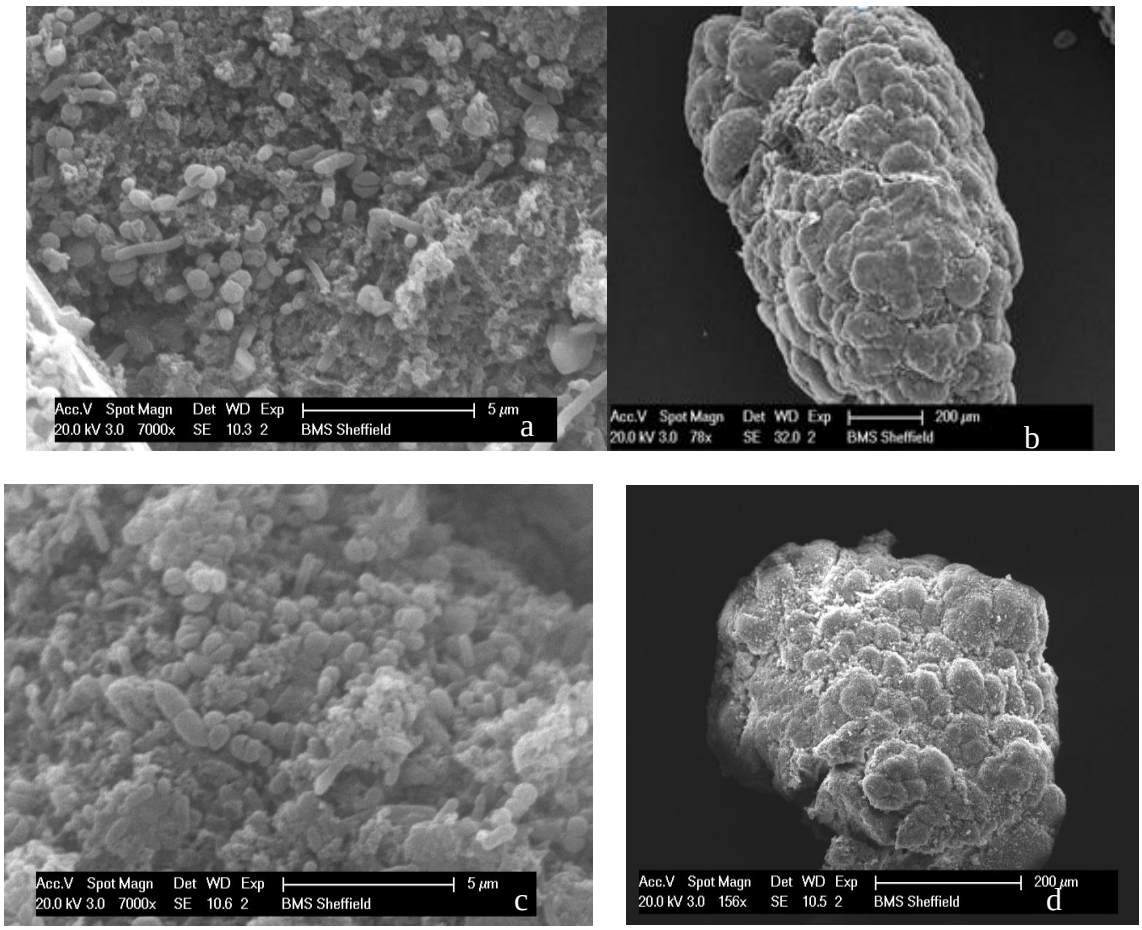


**Figure 6.36** SEM observation of the morphology and structure of the Anammox biomass cultivated sludge on day 10(a, b) and day 60 (c, d) in Amox-SBGB I during period I

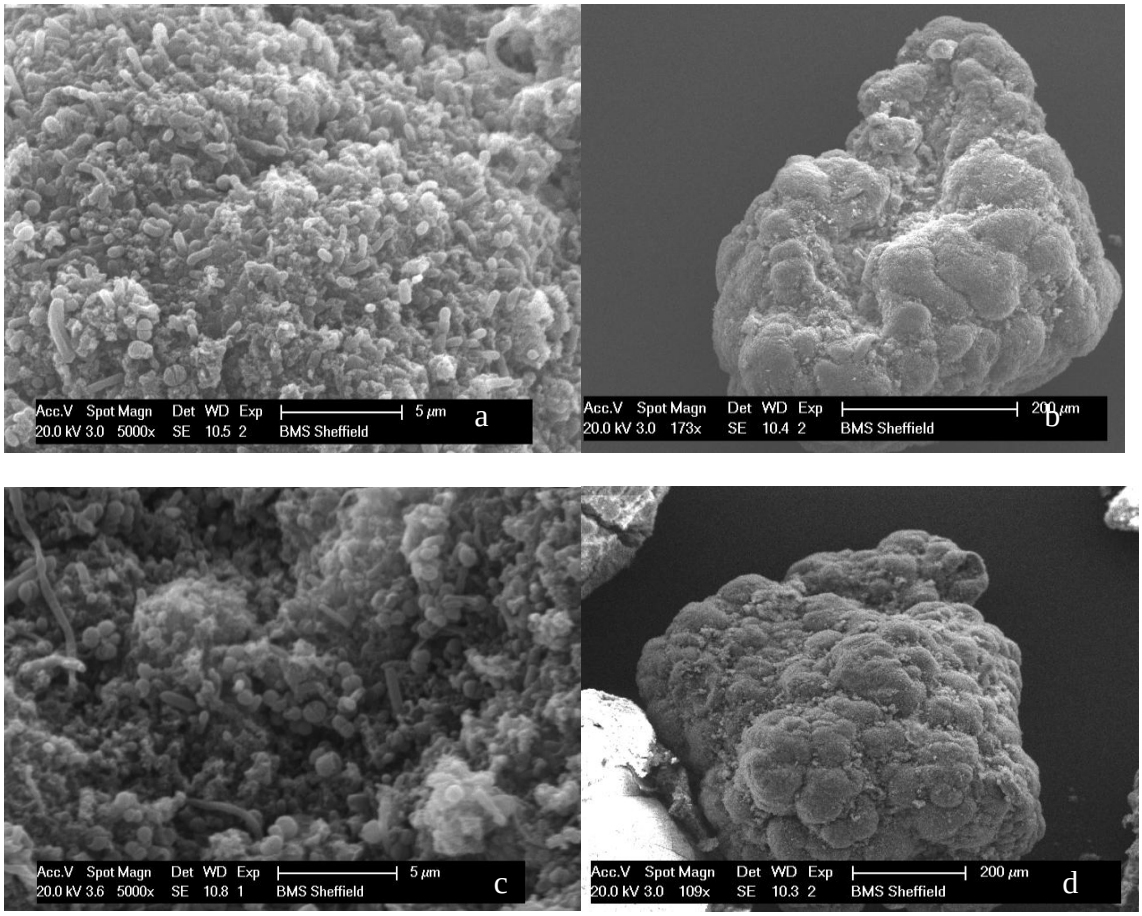


**Figure 6.37** SEM observation of the morphology and structure of the Anammox biomass cultivated sludge on day 10 (a, b) and day 60 (c, d) in Amox-SBGB II during period I Amox-SBGB II

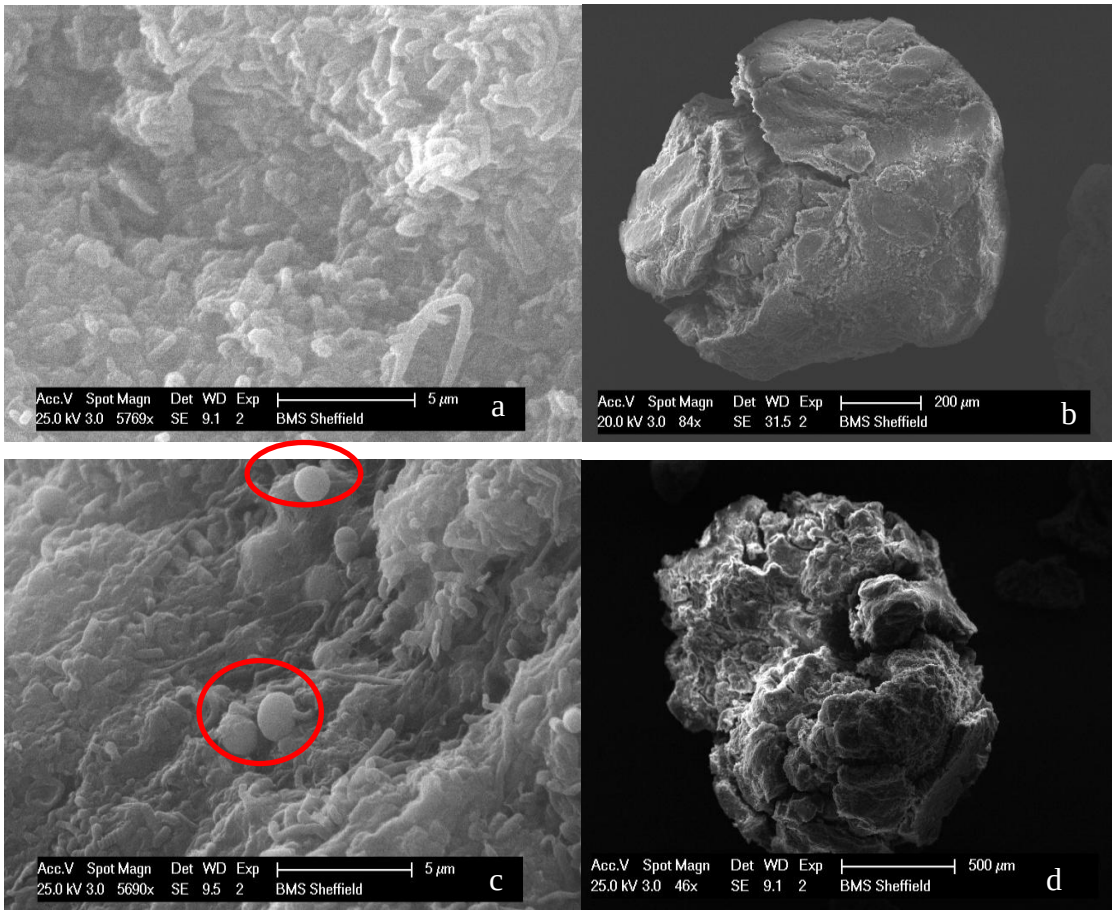


**Figure 6.38** SEM observation of the morphology and structure of the Anammox biomass cultivated sludge on day 30 (a, b) and day 60(c, d) in Amox-SBGB III during period I Amox-SBGB III.

## 6.6 7 Microbial Community Analysis in Anammox Systems

The community structure of Anammox species behaved more stably throughout the entire experimental period when compared with partial nitrification process. Different types of *Plancotymyctales* species has been acclimated and sampled from mature waste water treatment plant, where the anti-shock capability attributed to the inherent stability and adaptation. *Anammox* Group A and D are dominant and contributed 30% to 50% of total anammox population. Though *Anammox* Group C can be hardly found in the original (A1) or final (A6 and A7) sludge source, the meteoric population increase in inoculation stages represents the roles of *Anammox C* in community structure recovery. From the aspect of denitrifying bacteria, they had a constant 20% proportion of all the identified species, indicating that electron acceptor (nitrate) is the limitation factor for

the activities of denitrifying bacteria. Sufficient carbon source from residual metabolites or biomass could effectively form the carbon pool and left the electron chain restricting the performance of denitrifying bacteria. The level of nitrate, which is highly associated with the activity of anammox process, therefore determines the constant relative population ratio of denitrifying bacteria to anammox bacteria.

Using molecular techniques of PCR for amplification of the signal for low density bacteria, at least two well-known anammox species were identified: *Candidatus Kuenenia stuttgartiensis and Candidatus Brocadia fulgida*. (Schmid et al., 2005; Fujii, et al., 2002; Stara et al., 2007).

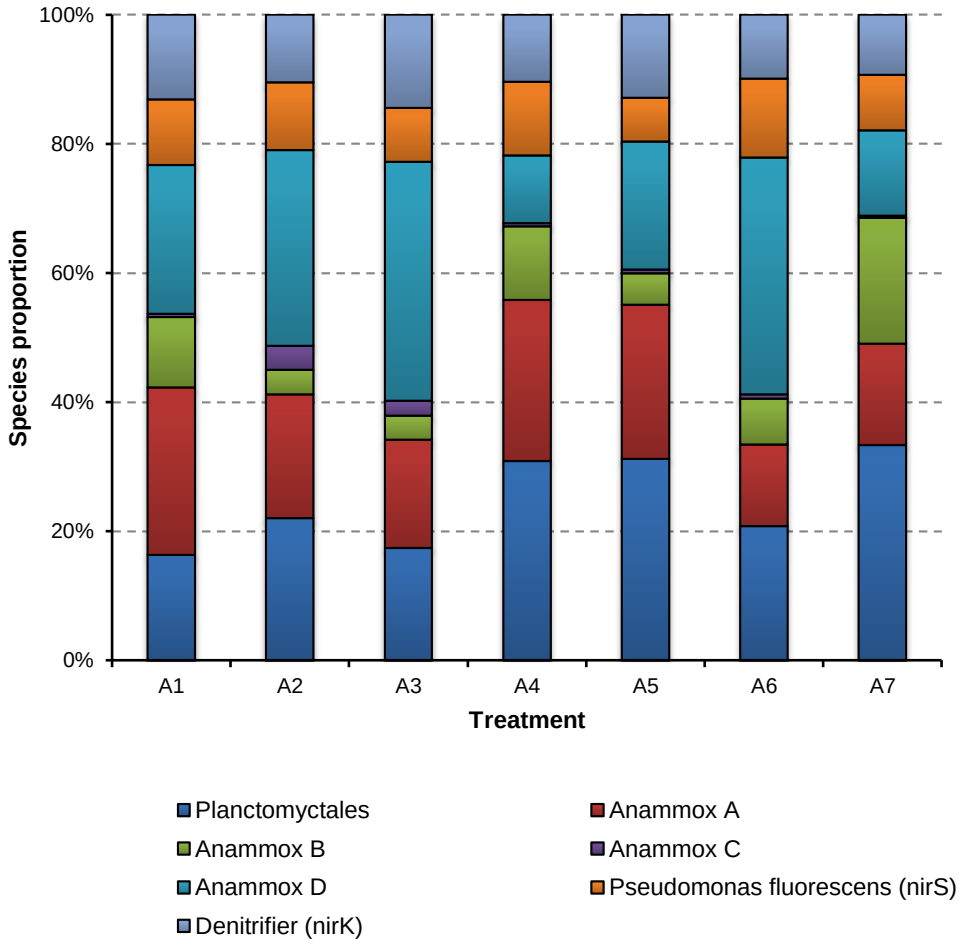


**Figure 6.39** Relative abundance of respective anammox and denitrifying bacteria.A1: Inoculum sample; A2, A4 and A6: Anammox sludge samples from Amox-SBGB without microbubble generation system at early (day 20), middle (day30) and final stage (day60) respectively. A3, A5 and A7: Anammox sludge samples from Amox-SBGB with microbubble generation system at early (day 20), middle (day30) and final stage (day60) respectively.

Distinct communities were observed in different bubble generation system, as shown in Figure 6.40, representing the impacts of sufficient carbon source (bicarbonate) distribution on community structure. Better mass transfer efficiency and bicarbonate distribution were achieved when microbubble was applied, leading to supplement of $H^+$ and $HCO_3^-$ which performs as the dominant role of the most adapted anammox bacteria (Anammox Group D, in Figure 6.40). In addition, the higher shear contributing to the smaller granule size change the substrate diffusion which might exerts influence on the community structure. The granule size and anammox performance therefore were affected with specific characters. Along with the time curve, the microbubble significantly contributed to the robust activity of Anammox bacteria and higher anammox biomass. Throughout the operational period the quantification of Anammox bacteria enrichment in the sludge with percentages of over 60% was achieved in Amox-SBGB under condition of microbubble, with highest percentage of 71.9% at final stage, whereas the high population proportion of 61.9% could only be achieved at the final stage in normal bubble generation system.

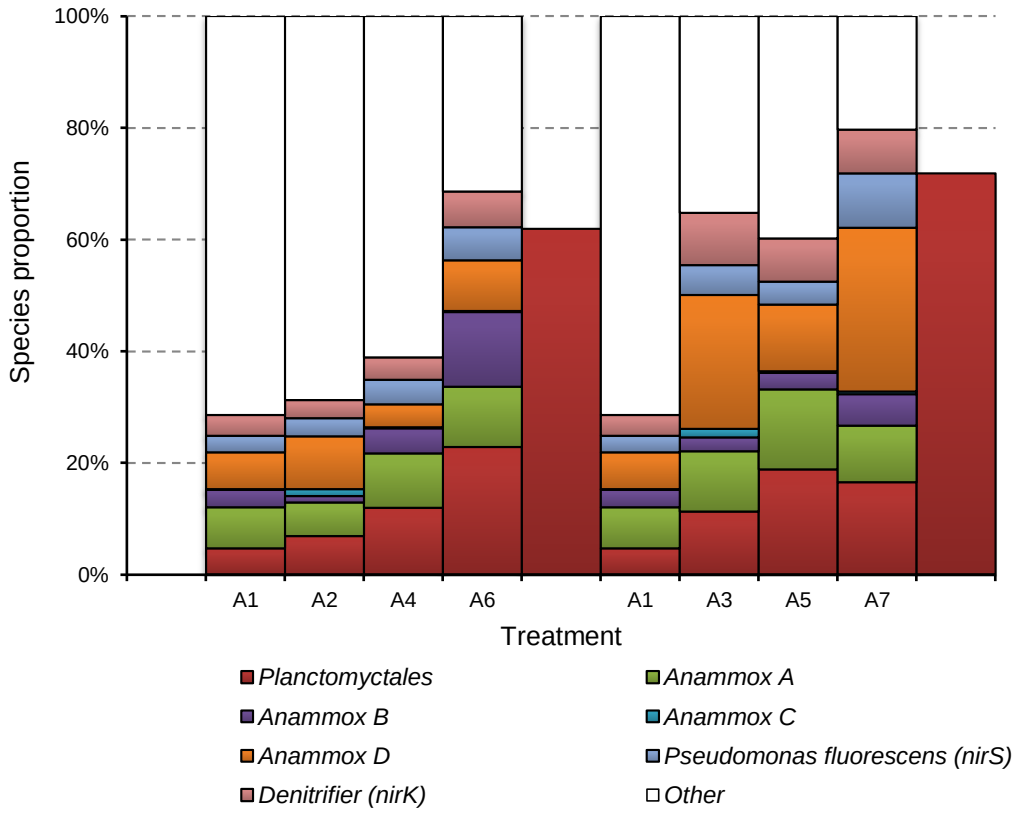

**Figure 6.40** Dynamic population change of anammox and denitrifying bacteria species in different systems. A1: Inoculum sample; A2, A4 and A6: Anammox sludge samples from Amox-SBGB without microbubble generation system at early (day 20), middle (day30) and final stage (day60) respectively. A3, A5 and A7: Anammox sludge samples from Amox-SBGB with microbubble generation system at early (day 20), middle (day30) and final stage (day60) respectively.

# Chapter 7. Kinetics Model for Partial Nitrification-Anammox Process

## 7.1 Introduction

The previous chapters demonstrated the feasibility of enhancing partial nitrification-Anammox process by using sequencing batch gas lift loop bioreactor with microbubble generations system. These studies have focused on novel, autotrophic and cost-effective alternative to the traditional biological nitrogen removal process to understand not only the microbiology of the partial nitrification and anammox process, but also how important to engineer these nitrogen removal processes are. In order to increase the process knowledge and acquire a better understanding of the biological process and more phenomena taking place in the SBGBs process, the kinetic models were developed to describe and simulate the performance of two biological processes. The kinetic model of process was a widely accepted route for describing the performance of biological treatment systems and predicting their performance (Jin et al., 2009) and most important for optimizing operational and environmental factors affecting substrate utilization rates. Therefore, it is possible to optimize reactor performance based on the kinetics study (Ni et al., 2010). Although the kinetic models for complete nitrification and denitrification have been reported previously (Fang et al., 2009; Gao et al., 2010), little attention has been paid to substrate removal kinetics for partial nitrification and Anammox process.

In partial nitrification process, ammonium is oxidized to nitrite by ammonium oxidizing bacteria (AOB) but not further to nitrate by nitrite oxidizing bacteria (NOB) under DO-limiting condition. Recently, models were developed for the membrane-aerated biofilm reactor and sequencing batch reactor with a community consisting of AOB, NOB and hereothrophic bacteria (Matsumoto et al., 2007; Gao et al., 2010). Partial nitrification process does not have the reaction of nitrite to nitrate by control microbial community via operation and is different from denitrification which demands for organic carbon source. Due to these differences, the model and kinetic parameters for partial nitrification was developed. First of all it is necessary to determine the key physiological parameters like the maximum specific growth rate ($\mu_{max}$) for AOB in SBAB, which is no doubt the most critical parameter in the modelling and design of partial nitrification systems, as it plays a dominant role in determining the minimum sludge age (Sozen et al., 1996). Different approaches have been suggested to estimate

the value of $\mu_{max}$ in activated sludge; in general, they involve using activity measurements such as substrate consumption or product formation rates (Sozen et al., 1996; Hunnik et al., 1990). In this study, based on reaction kinetics and Monod model, kinetic models of substrate consumption for the partial nitrification process in airlift loop bioreactor with fluidic oscillator were first built.

For Anammox process, different mathematical models were reported to study the kinetics of this novel nitrogen removal process in the different reactors. For substrate removal kinetics, the modified Stover-Kincannon model and the Grau second-order model were regarded as more applicable than the first-order model. Whereas the Van der Meer and Heertjes model was more applied for the kinetics of nitrogen gas production (Ni et al.， 2010). In the present study substrate removal kinetic model for Anammox process in SBGB with fluidic oscillator were developed based on different mathematical models including Stover-Kincannon model and the Monod model.

The major kinetic parameters including the maximum specific rates and half-maximum rate concentrations were determined by using experimental approaches and kinetic models for partial nitrification and Anammox process in sequencing batch gas lift loop bioreactor with fluidic oscillator were built respectively. Model evaluation was carried out by comparing experimental data with predicted values calculated from suitable models. It was confirmed that these kinetic models can be used to predict treatment performance of partial nitrification and Anammox processes in SBGB with different nitrogen compound loads and various DO concentrations.

## 7.2 Objectives

The main aim of this chapter is to develop, calibrate and validate a kinetic model of partial nitrification and Anammox process in sequencing batch gas lift loop bioreactor with microbubble generation system for the treatment of wastewater with low C/N ratio. Once the models were built, the key parameters of the new models for partial nitrification and Anammox process will be compared with the ones reported by the other authors. Model evaluation was carried out by comparing experimental data with predicted values calculated from suitable models. The kinetic model for partial nitrification process was used to simulate the performance of SBGB with FO under

different conditions and optimization of the operation for the bioreactor were finally achievied.

## 7.3 Model Development for Partial Nitrification Process

### 7.4.1 Materials and Method

The batch experiments for partial nitrification were repeated in the SBABs with FO in this study. The temperature was maintained at 30 ℃ in the reactor. Each cycle of the SBR system consisted of filling, aeration, settling, and decanting stages. The DO concentration in the SBAB was controlled at 0.5 or 3 mg $L^{-1}$, as test required. The synthetic wastewater with $NH_4^+$-N concentrations of 800±50 $mgL^{-1}$ was used to feed the bioreactor. During the operation period, DO, redox potential (ORP), and pH were continuously monitored and recorded. Biomass, or total suspended solids (TSS), in SBAB with FO was maintained at 3.8 $gTSSL^{-1}$ and wastewater samples were analyzed for $NH_4^+$-N, $NO_2^-$-N, $NO_3^-$N and TSS.

### 7.3.2 Kinetic Model for Partial Nitrification

The kinetic model built for partial nitrification is based on the following assumptions:

(1) The quantity and quality of influent are constant and there is no microorganisms exiting in the influent.

(2) The influent filling is instantaneous, which means that substrate is not degraded by microorganisms during influent filling stage.

(3) The biomass inside of bioreactor is homogeneously mixed during the filling period and operation period.

(4) During partial nitrification process, AOB are not in endogenous respiration phase, i.e., the endogenous-decay coefficient b = 0.

(5) The metabolic characteristics of AOB are stable

(6) A good solid-liquid separation was obtained during settling sage. The activity of AOB stopped during the decant stage

(7) The partial nitrification kinetics is on the basis of Monod equation

*** Monod Equation**

This relationship most frequently used to represent bacterial growth kinetics was developed in the 1940s by the famous French microbiologist Jacques Monod. His original work related specific growth rate of fast-growing bacteria to the concentration of a rate-limiting, electron-donor substrate.

$$\mu = \mu_{max} \frac{S}{K_S + S}$$

$\mu$: specific growth rate due to synthesis ($h^{-1}$)

S: concentration of the rate-limiting substrate (mg $l^{-1}$)

$\mu_{max}$: maximum specific growth rate ($h^{-1}$)

$K_S$ : concentration giving one-half the maximum rate (mg $l^{-1}$)

This equation is a convenient mathematical representation for a smooth transition from a first-order relation at low substrate concentration to a zero-order relation at higher growth rates. At sufficiently high substrate concentrations, according to the Monod equation, the relationship between substrate degradation rate and substrate concentration is 0-order – in other words, cell growth is independent of the substrate concentration and at its maximum value $\mu_{max}$ (Bruce E et al, 2001). A typical Monod constant of 1.0 mg $NH^{+}_{4}$-N $L^{-1}$ at 20 ℃ has been reported stated by Henze et al. (1987).

In the autotrophic partial nitrification system, ammonium is substrate for growth of ammonium oxidizing bacteria. Base on the mass balance, the total change in ammonium content is as follows:

$$\frac{dS_{NH}}{dt} = \left(\frac{dS_{NH}}{dt}\right)_{assimilated} + \left(\frac{dS_{NH}}{dt}\right)_{nitrified} \quad (7\text{-}1)$$

Where the first term in the right hand side of the equation is ammonium assimilated for microbial cell synthesis and the second term indicates the ammonium converted to nitrite. In order to create the inorganic environment for AOB, the organic matters and heterotrophic bacteria had been degraded and washed out from system in the earlier enrichment stage; the ammonium production from degradation of nitrogen-containing organic matter and the $NH_4^+$-N used by the heterotrophic bacteria for assimilation is have been ignored.

The oxidation of ammonium is also taking place in the autotrophic bacteria to synthesize cells in partial nitrification process. The reaction equation is

$$NH_4^+ + 1.382\ O_2 + 1.982\ HCO_3^- \rightarrow 0.018\ C_5H_7O_2N + 0.982\ NO_2^- + 2.927\ H_2O + 1.891\ CO_2 \quad (2\text{-}9)$$

As shown in Eq (2-9), the molar mass of $NH_4^+$-N used for AOB cell synthesis is less than 2% of total $NH_4^+$-N during partial nitrification process. Therefore, to simplify the model, trace amount of the assimilation of $NH_4^+$-N is ignored.

$$\left(\frac{dS_{NH}}{dt}\right)_{assimilation} \approx 0 \quad (7\text{-}2)$$

Substitute Eq 7-2 into Eq 7-1 we obtain

$$\frac{dS_{NH}}{dt} = \left(\frac{dS_{NH}}{dt}\right)_{nitration} \quad (7\text{-}3)$$

Conventional nitrification is the catabolic oxidation of ammonium via nitrite to nitrate by aerobic chemolitho autotrophic ammonium oxidizing bacteria and nitrite oxidizing bacteria, as followed

$$NH_4^+ + 1.05O_2 \rightarrow NO_2^- + 2H^+ + 2H_2O \quad (2\text{-}1)$$

$$NO_2^- + 0.5O_2 \rightarrow NO_3^- \quad (2\text{-}2)$$

In this study the activity of NOB was inhibited by controlling various variables such as FA, FNA, high temperature, low DO concentration and short HRT. In our experiments described in chapter 5, AOB in the partial nitrification process completely out-competed NOB and dominated the SBAB system. Long-term operation demonstrated the nitrate production in the effluent was kept at 1% and nitrite was produced as major nitrification product. Hence, the step of $NO_3^-$-N production can be ignored in the model. We obtain the following equation:

$$\left(\frac{dS_{NO2}}{dt}\right)_{produced} = -\left(\frac{dS_{NH}}{dt}\right)_{nitritated} \quad 7\text{-}4$$

Based on the Monod equation and reaction kinetics, the relationship between the specific growth rate of AOB and concentrations of $NH_4^+$-N and DO is

$$\mu_{AOB} = \mu_A \frac{S_{NH_4}}{K_{S,NH_4} + S_{NH_4}} \cdot \frac{S_O}{K_{S,O} + S_O} \quad (7\text{-}5)$$

Where

$\mu_{AOB}$ is specific growth rate of AOB ($h^{-1}$)

$\mu_A$ is maximum specific growth rate of AOB ($h^{-1}$)

$Ks,_{NH4}$ is half-maximum rate concentration for $S_{NH4}$ for autotrophs ($NH_4^+$-N in mg • $L^{-1}$)

$K_{s,O}$ is half-maximum rate concentration for DO for autotrophs (mg O2 $L^{-1}$)

$S_{NH4}$ is ammonium concentration (mg $NH_4^+$-N $L^{-1}$)

$S_O$ is DO concentration (mg DO $L^{-1}$)

The growth of biomass is related to the substrate degradation. The relationship between growth and ammonium consumption can be expressed as $dS_{NH4}^+$ (consumption of $NH_4^+$-N) and $dX_A$ (increment of AOB biomass) in the following equation:

$$Y_A = \frac{dX_A}{dS_{NH_4}} = -\frac{dX_A/dt}{dS_{NH_4}/dt} = -\frac{r}{v} = -\frac{r/X_A}{v/X_A} = -\frac{\mu_{AOB}}{q_{ammomia}} \quad (7\text{-}6)$$

Where $r = (dX_A)/(dt)$, $v = (dS_{NH4})/(dt)$, $q_{ammonia}$ is specific nitrification rate of ammonium ($h^{-1}$)

Transform 7-6 to get

$$\mu_{AOB} = -Y_A \cdot q_{ammomia} = -Y_A \cdot v/X_A = -Y_A \cdot \frac{dS_{NH_4}}{X_A dt} \quad (7\text{-}7)$$

Merge Eq 7-8 and 7-5

$$\frac{dS_{NH_4}}{dt} = -\frac{1}{Y_A} \cdot \mu_A \frac{S_{NH_4}}{K_{S,NH_4}+S_{NH_4}} \cdot \frac{S_O}{K_{S,O}+S_O} \cdot X_A \quad (7\text{-}8)$$

Assume that the percentage of AOB in biomass of the SBAB is constant during the nitrification process during short operational period, so $M = \frac{X_A}{X}$

Therefore, the partial nitrification kinetic Eq 7-8 can be expressed as followed

$$\frac{dS_{NH_4}}{dt} = -\frac{1}{Y_A} \cdot \mu_A \frac{S_{NH_4}}{K_{S,NH_4}+S_{NH_4}} \cdot \frac{S_O}{K_{S,O}+S_O} \cdot X \cdot M \quad 7\text{-}9$$

In Eq7-9 the concentration of $NH_4^+$-N varies with time during partial nitrification process in the SBAB with FO, where $S_{NH4}$,$S_O$, and are the function of time, which is $S_{NH4}=S_{NH4}(t)$, and $So=So(t)$, $X=X(t)$, and $X$, $Y_A$, $\mu_A$,$K_{S,NH4}$, and $K_{S,O}$, are constant coefficients under certain operational conditions. These kinetic constants can be determined using experimental data from SBAB operation.

### 7.3.3 Determination of Partial Nitrification Kinetic Parameters

When DO concentration ($S_O$) is controlled at a constant level, the term ($S_O$)/($Ks,_O$ + $S_O$) in Eq 7-9 can be regarded as a constant. Because of slow growth of AOB, the amount of AOB in biomass can be assumed to be invariant during the partial nitrification cycle in SBAB. The average concentration of biomass for $X_A$ was used in eq 7-9. Since the amount of AOB does not change over time in the experiment with constant DO, the Eq 7-9 can be simplified as

$$\frac{dS_{NH_4}}{dt} = -A\frac{S_{NH_4}}{K_{S,NH_4}+S_{NH_4}} \quad (7\text{-}10)$$

In which

$$A = \frac{1}{Y_A}\cdot\mu_A \cdot\frac{S_O}{K_{S,O}+S_O}X_A\cdot M \quad (7\text{-}11)$$

The transformation of Eq 7-10 is as follows:

$$\mathrm{dt} = -\frac{\mathrm{K_{S,NH_4}}+\mathrm{S_{NH_4}}}{\mathrm{AS_{NH_4}}}\mathrm{dS_{NH_4}} \quad (7\text{-}12)$$

The integral of Eq 7-12 is as follows:

$$t = \int -(\frac{\mathrm{K_{S,NH_4}}}{\mathrm{AS_{NH_4}}}+\frac{1}{A})\,\mathrm{dS_{NH_4}}$$

$$t = \frac{\mathrm{S_{NH_4}}}{A}-\frac{\mathrm{K_{S,NH_4}}}{\mathrm{A}}\ln \mathrm{S_{NH_4}}+\mathrm{C}$$

$$t = -\frac{1}{A}\left(\mathrm{S_{NH_4}}-\mathrm{K_{S,NH_4}}\ln \mathrm{S_{NH_4}}\right)+C \quad (7\text{-}13)$$

Where A and C are constant, and t represents the time of partial nitrification process. The principle of least-squares method was used to estimate the values of A and C.

In order to obtain maximum specific growth rate and half-maximum rate concentration, we used the following approaches to design batch tests in this study:

(1) Firstly, a high concentration of DO (3 $mgL^{-1}$) was maintained in the reactor so that it is far greater than the saturation constant for DO, while the ammonia concentration was maintained at normal levels .Therefore the partial nitrification rate only varies with the changes of the ammonia concentration. Under this condition, $S_O$ and $K_{S,O}$, therefore, in Eq 7-11, $S_O/(K_{S,O} + S_O) \approx 1$ and $A \approx M \cdot X\ \mu_A/Y_A$. Since the value of M is assumed to be constant, so $\mu_A/Y_A$ can be obtained. During the batch experiment, a constant DO

concentration was maintained to avoid the influence of DO fluctuation on nitrification rate.

(2) In the second test, a low DO concentration and high ammonium concentration were adopted to determine the $K_{S,O}$ for DO. Likewise compared to the very low DO concentration the high ammonium concentration is far greater than saturation constant for ammonium. Thus, bacteria growth was independent from substrate concentration.

During the first batch experiment, DO concentration in the SBAB with FO was maintained constantly at around 3mg $L^{-1}$. Then samples were real time monitored in terms of the concentrations of $NH_4^+$-N, $NO_2^-$-N, and $NO_3^-$-N over operational cycles. For each experiment the data were fitted to Eq. 7-13 using a nonlinear regression module in Original.9 (Fig 7.1); the solution was A =52.36, $K_{S,NH4}$ = 38.54 mg $L^{-1}$, and C = 22.16. The value of $K_{S,NH4}$ is much higher to the empirical value provided by ASM3 (1.0 mg$L^{-1}$, 20 ℃) (Henze et al., 1999)due to high ammonia loading rate and high operational temperature. In the first experiment, DO concentration was maintained at the constant of about 3 mg $L^{-1}$, Under this condition the $S_{S,O}$ is much higher than $K_{S,O,}$ therefore, in Eq 7-11, $S_O/(K_{S,O} + S_O) \approx 1$which was much greater than $K_{S,O}$, so Eq 7-11 can be expressed as

$$A \approx \frac{1}{Y_A} \cdot \mu_A \cdot X_A \cdot M$$

Since the concentration of AOB biomass was assumed to be unchanged, when value M≈20%, the biomass concentration ($X$) was measured as 3.8 g TSS $L^{-1}$, and the observed yield coefficient $Y_A \approx Y_{A,obs}$=0.26mgSSmg$^{-1}NH_4^+$-N. Therefore, it was calculated as $\mu_A$=0.0179 $h^{-1}$. Compared to the maximum growth rate of nitrate autotrophic bacteria of 0.042 $h^{-1}$ reported by ASM3 ($\mu_A$) (Gujer et. Al., 1999), the value obtained in this study was much lower. The lower maximum growth rate of is attributed to the fact that the rate of ASM3 is based on the conventional nitrification process where the major end product is nitrate, and the rate is the overall rate of both AOB and NOB; but the rate obtained in the present study was only from partial nitrification process with nitrite as major product (>95% of ($NO_2^-$-N+$NO_3^-$N)) and basically represented the growth of autotrophic AOB. The result also confirmed that the biomass produced in partial nitrification process is less than that of conventional nitrification process indicating less sludge produced which is a very important advantage of the partial nitrification compared to conventional nitrification.

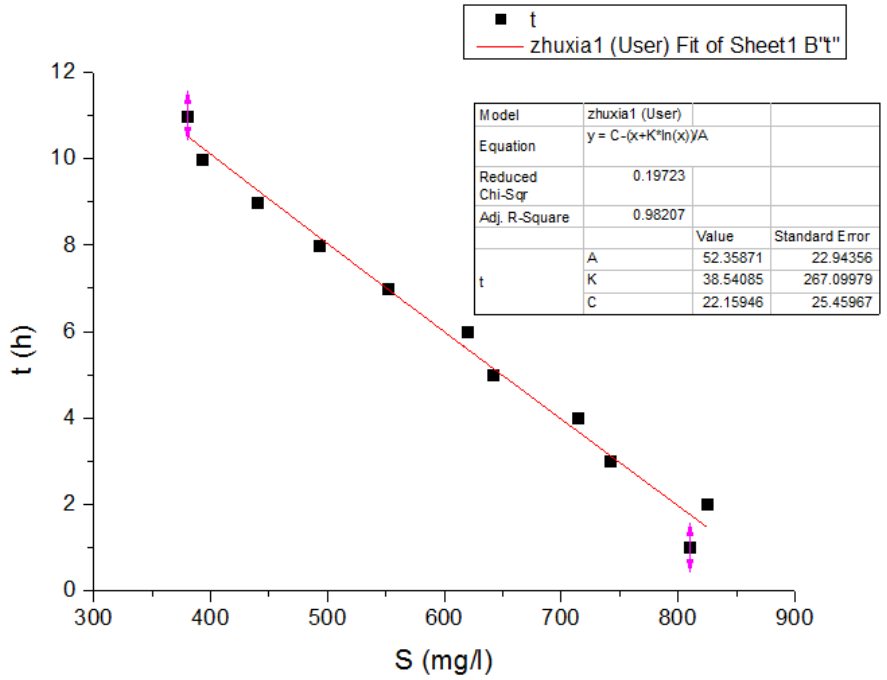


**Figure 7.1** A nonlinear regression module with Origin 9.0 for determining $K_{S,NH4}$

After $\mu_A$ was obtained, the second batch experiment were carried out in order to estimated Ks,o. During this experiment, DO concentration was decreased and then maintained constantly at 0.5 mg $L^{-1}$. Subsequently, the concentrations of $NH_4^+$-N, $NO_2^-$-N, and $NO_3^-$-N were real time monitored. Likewise, in order to determine $K_{S,O}$, using the data of variation of $NH_4^+$-N concentrations *vs.* reaction time (Fig 7.2) as well as $K_{S,NH4}$ obtained in last batch experiment, the values of *A*, and C was estimates as 34.8 and 34.2 under this DO level. According to Eq 7-11 $K_{S,O}$ was calculated to be 0.302 mgDO$L^{-1}$. The calculated value of $K_{S,O}$ is lower than $K_{A,O}$ of 0.31mgDO$L^{-1}$ from PN-SBR system (Gao et.al., 2010) and $K_{A,O}$ of 0.5 mgDO$L^{-1}$ in ASM3, but higher than the half-maximum rate concentration of heterotrophic bacteria ($K_O$ ) 0.1 mgDO$L^{-1}$, 20 ℃) (Henze, 2000). The relatively lower $K_{S,O}$ value than that of ASM3 is likely due to the fact that the biomass in PN-SBAB was dominated with AOB rather than NOB with higher half-maximum rate concentration for DO. The reason for lower Ks,o than that from similar PN system obtained by Gao (2010)was probably attributed to further optimization of the growth of AOB over NOB in PN-SBAB thanks to the microbubble aeration system applied. The DO concentration had greater influence on NOB than on AOB during a nitrification process owning to higher $K_{A,O}$ for NOB than AOB.

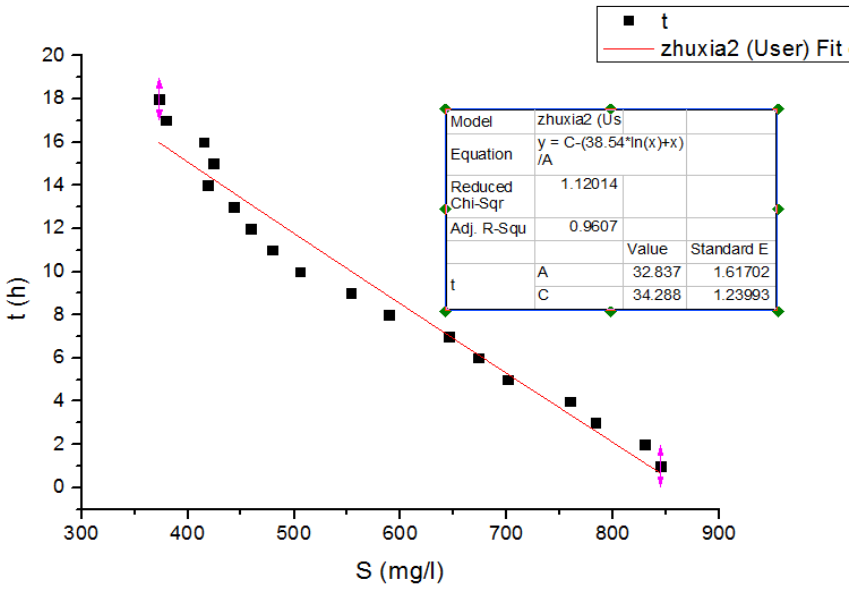


**Figure 7.2** A nonlinear regression module with Origin 9.0 for determining $K_{S,O}$

Substitute $\mu_A$, $K_{S,NH4}$, and $K_{S,O}$ calculated into Eq7-9, and the final dynamic equation of partial nitrification with microbubble generation system was deduced as Eq7-14 through which allowed us to calculated the nitrification rates under different $NH_4^+$-N concentrations and the approximate variation of $NH_4^+$-N concentrations with time in the PN-SBAB with FO.

$$\frac{dS_{NH}}{dt} = -0.069 \cdot \frac{S_{NH}}{38.5+S_{NH}} \cdot \frac{S_O}{0.302+S_O} \cdot M \cdot X \quad (7\text{-}14)$$

In order to validate the kinetic model for PN-SBAB with FO, the experiment under different conditions was conducted and the simulated values obtained through the model were compared with the new measured values. As can be seen in Fig 7.3 it is evident that the simulated values accorded with the observed values on the whole. The estimated values had good correlation with experimental results with the correlation coefficient R = 0.9881, as is shown in Fig 7.4. This suggests that, using the kinetic parameters obtained from experimental data, the kinetic model Eq 7-14 can be used to simulate the partial nitrification process in PN-SBAB.

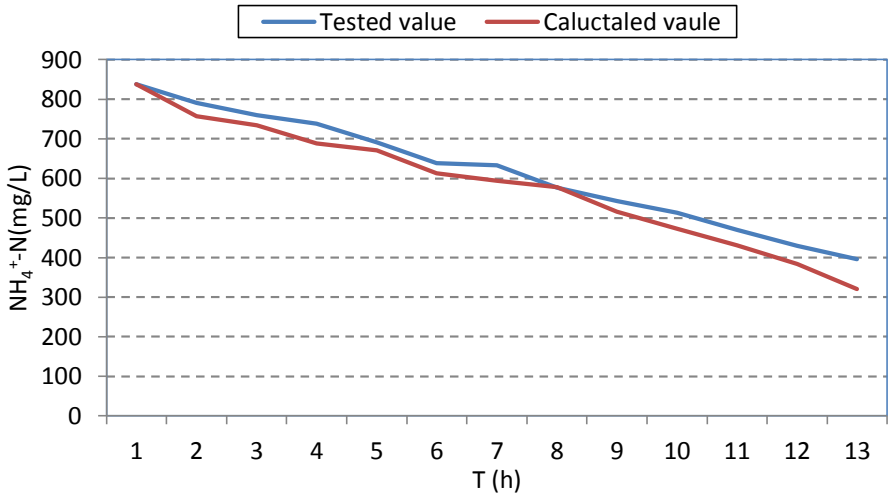


**Figure 7.3** The evolution of calculated $NH_4^+$-N concentration and tested $NH_4^+$-N concentration in one operational cycle

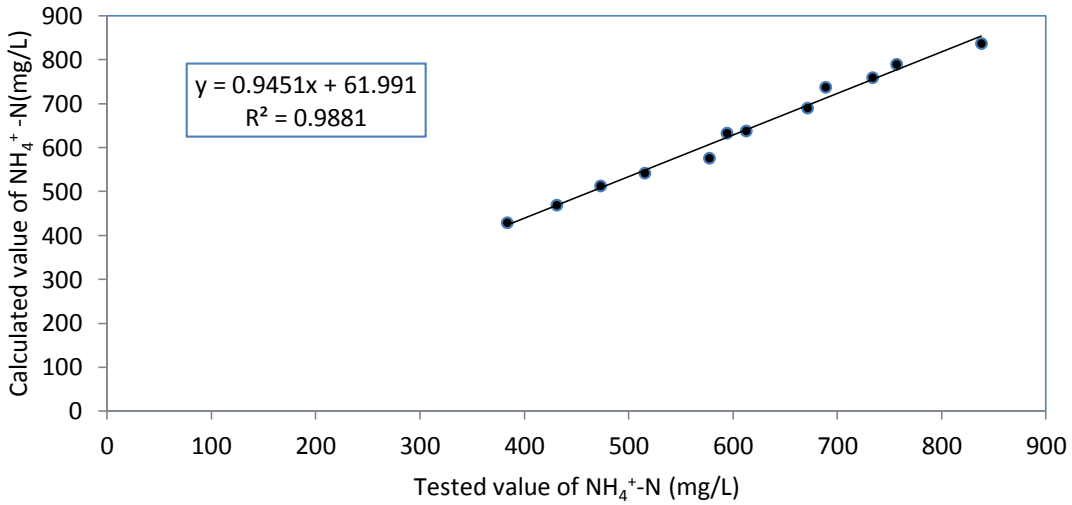


**Figure 7.4** Correlation between calculated values and test values of variation of $NH_4^+$-N concentration

Using Eq7-14, the correlation between the partial nitrification rate *vs.* $NH_4^+$-N concentration (Fig 7.5) and the change in $NH_4^+$-N concentration *vs.* reaction time (Fig 7.6) at DO concentrations of 0.1, 0.3, 0.5, 0.7and 0.9 mgDO$L^{-1}$ were simulated. Through this result of simulation, it is observed that higher conversion rate and better $NH_4^+$-N removal pattern were observed at relatively higher DO concentrations (Fig 7.6). However, the simulated data show that the $NH_4^+$-N removal extent was almost identical for DO of 0.5 ~0.9 mg $L^{-1}$ after reaction for 8h (Fig7.5). This suggests that relatively lower DO such as 0.5 ~0.9 mg $L^{-1}$ may be favourable for the operation to save aeration

energy. Operation at low DO also provides negative selection pressure for the growth of NOB in SBAB with FO.

The kinetic model for partial nitrification in SBGB with FO was not only used to predict the performance of the nitrogen removal but more important also offer the optimized operation parameter for the future work. Therefore the model construction has very important significance for the potential pilot or full scale application of this novel biological nitrogen removal technology, especially when the microbubble generation system was employed.

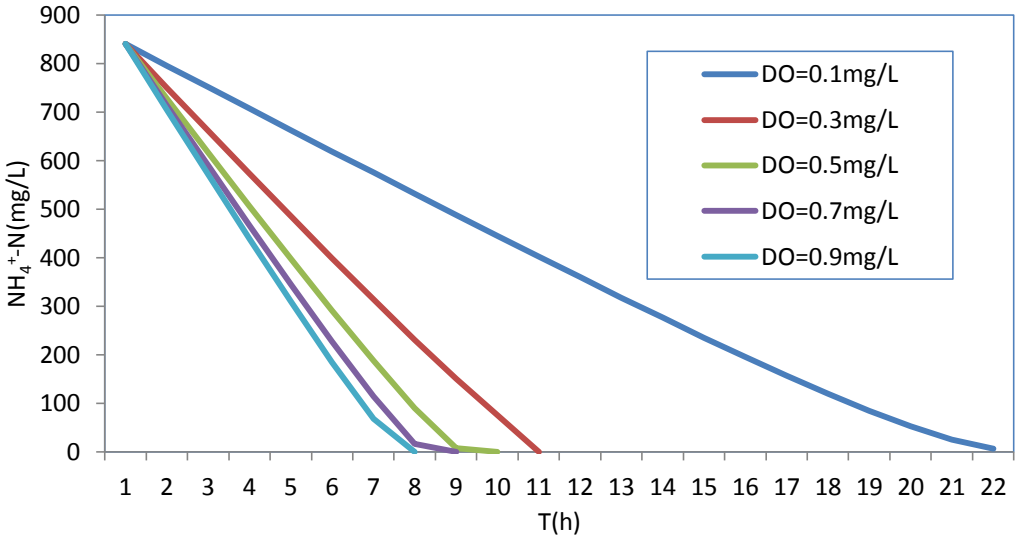


**Figure 7.5** Changes in ammonium concentration during nitrification process in a SBR at five different DO concentrations

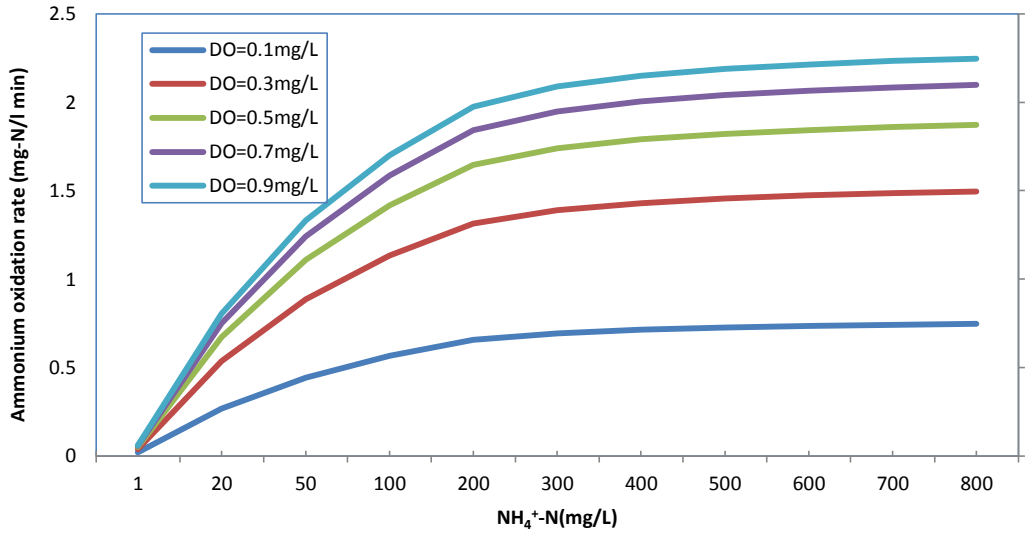


**Figure 7.6** Simulated shortcut nitrification rate vs. ammonium concentration

## 7.4 Model Development for Anammox Process

### 7.4.1 Kinetic Model for Anammox Process

Process kinetics can present necessary information for granular anammox process but little study was focused on the nitrogen removal kinetics of Anammox granular process in SBGB. In this study, the substrate removal kinetics in a lab-scale Amox-SBGB with fluidic oscillator were investigated, which was then operated at different hydraulic retention times and nitrogen loading rates. The bioreactor showed good tolerance to substrate concentration shock and hydraulic shock. Evaluation of the nitrogen removal kinetics indicated that the modified Stover–Kincannon model turned out to be appropriate to describe nitrogen removal of anammox granules, rather than the Monod substrate removal model. Model evaluation was then carried out via assessing the linearity between the experimental data and predicted values, which proved the applicability of modified Stover–Kincannon model. The information derived from the current study could guide and optimize the design of pilot-scale anammox SBGB with fluidic oscillator.

***Monod model**

Since Monod model is the most popular model to describe the kinetics of pollutant biodegradation, similarly to partial nitrification process, the maximal substrate conversion rate ($q_{max}$) and half saturation constant (Ks) for Anammox process can be obtained according to Monod model. The model is represented as follows:

$$\frac{dS/dt}{X} = v_{MAX}\frac{S}{K_S+S} \quad (7\text{-}15)$$

Where: $K_S$-half saturation constant ($mgL^{-1}$); and S-substrate concentration ($mgL^{-1}$).

The assumptions of kinetic model for partial nitrification are also foundation for Anammox model establishment. Base on those assumptions the concentration of granular anammox sludge could be characterized by mean value and the substrate concentrations inside the reactor were considered same as the substrate concentrations in the effluent.

Nitrogen balance in the steady-state operation of SBAB can be expressed as:

$$QS_0 - QS - V\left(\frac{dS}{dt}\right) = 0 \quad (7\text{-}16)$$

Eq7-16 is transformed to be

$$\frac{dS}{dt} = \frac{Q}{V}(S_0 - S) = \frac{(S_0 - S)}{HRT} \text{ (7-17)}$$

where: Q is influent and effluent volume (L); V is reactor working volume(L); $S_0$, S – substrate concentrations in influent and effluent ($mgL^{-1}$); (dS/dt) is substrate degraded rate [$mg(L\ h)^{-1}$].

The specific substrate degraded rate v is defined as

$$v = \frac{1}{X}\frac{dS}{dt} = \frac{d(S_0 - S)}{Xdt} \quad \text{(7-18)}$$

Emerge 7.16, 7.17 and 7.18

$$\frac{(S_0 - S)}{X \cdot HRT} = v_{MAX}\frac{S}{K_S + S} \quad \text{(7-19)}$$

$$\frac{HRT \cdot X}{(S_0 - S)} = \frac{K_S}{v_{MAX}} \cdot \frac{1}{S} + \frac{1}{v_{MAX}} \text{ (7-20)}$$

The term has the linear relationship with $\frac{1}{S}$. By plotting $\frac{HRT \cdot X}{(S_0 - S)}$ versus $\frac{1}{S}$. The vertical intercept is $\frac{1}{v_{MAX}}$. The $\frac{K_S}{v_{MAX}}$ could be determined from the slope of the line.

***Stover–Kincannon model**

Stover–Kincannon is also a widely used mathematical models for determining the kinetic constants in immobilized system as well as has been applied to continuously operated, for instance mesophilic and thermophilic upflow anaerobic filters for the treatment of paper-pulp liquors and simulated starch wastewater (Guo et al., 2002), anaerobic filter for soybean wastewater treatment (Yong and McCarty, 1998), anaerobic hybrid reactor , and anaerobic migrating blanket reactor (Kuşçu and Sponza , 2009), rotate biological contactor (Hosseiny,2002). However, this model has not been applied for the determination of nitrogen removal kinetic constants in SBGB with microbubble generation system for Anammox process. The Stover–Kincannon model considers the substrate removal rate as a function of substrate loading rate at steady state as in Equation (7-21)

$$\frac{dS}{dt} = \frac{Q}{V}(S_0 - S_e) \quad \text{(7-21)}$$

Where dS/dt is defined as

$$\frac{dS}{dt} = \frac{U_{MAX}(\frac{QS_0}{V})}{K_B + (\frac{QS_0}{V})} \quad \text{( 7-22)}$$

The modified Stover–Kincannon model for the SBGB for Anammox is (Hooshyari et al., 2009)

$$\frac{dS}{dt} = \frac{Q}{V}(S_0 - S_e) = \frac{U_{MAX}(\frac{QS_0}{V})}{K_B + (\frac{QS_0}{V})} \quad (7\text{-}23)$$

Linearization of Eq7-23 gives the following relationship

$$(\frac{\mathrm{dS}}{\mathrm{dt}})^{-1} = \frac{\mathrm{V}}{\mathrm{Q}(\mathrm{S_0} - \mathrm{S_e})} = \frac{\mathrm{K_B}}{\mathrm{U_{MAX}}} \cdot \frac{\mathrm{V}}{\mathrm{QS_0}} + \frac{1}{\mathrm{U_{MAX}}} \quad (7\text{-}24)$$

where d*S*/d*t*, substrate removal rate ($gL^{-1}$ day); $U_{max}$, the maximum utilization rate constant ($gL^{-1}$ $day^{-1}$) and $K_B$ is the saturation value constant ($gL^{-1}$ $day^{-1}$).

### 7.4.2 Determination of Anammox Kinetic Parameters

**Monod model**

Experimental data at steady states were used to get the kinetic parameters for the Monod type model. If $\frac{dS/dt}{X}$ is taken as $\frac{\mathrm{X \cdot HRT}}{(\mathrm{S_0 - S})}$, which is the inverse of the loading removal rate and this is plotted against the inverse of $\frac{1}{\mathrm{S}}$, a straight line portion of intercept $\frac{1}{\mathrm{v_{MAX}}}$ and a slope of $\frac{\mathrm{K_S}}{\mathrm{v_{MAX}}}$ result.

A plot of Eq. (7-20) gave the necessary information for the Monod kinetic coefficients. From Fig. 7.7, the values of the maximum rate of substrate conversion ($v_{MAX}$) and half saturation concentration (Ks) were calculated to be 0.331/d and 0.153g/L, respectively. The correlation coefficient 0.67, being much lower than correlation coefficient for Modified Stover-Kincannon model, confirmed its inapplicability for Amox-SBGB with FO.

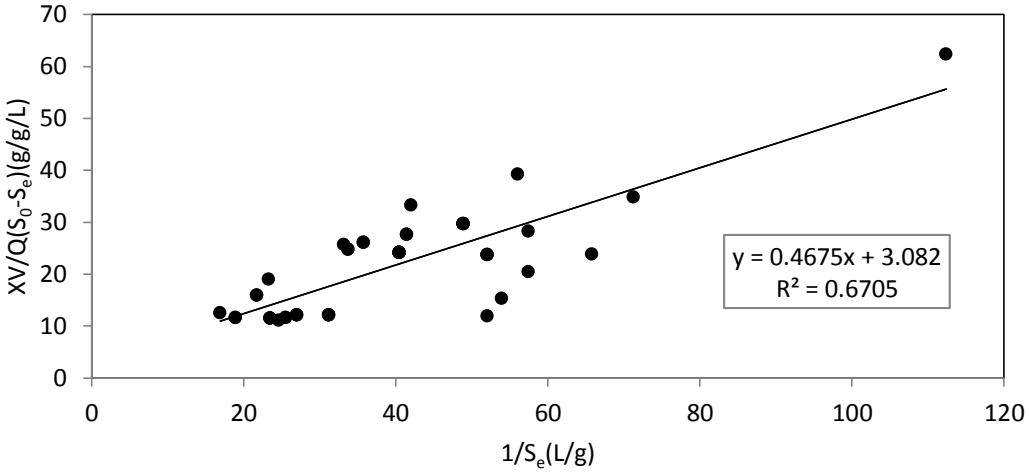


**Figure 7.7** Monod model plot

**Modified Stover–Kincannon model**

The major difference between the Stover-Kincannon model and the Monod model is the introduction of the concept of total substrate loading rate, $QS_e/V$, to the Stover-Kincannon model.

The modified Stover–Kincannon model was applied to experimental results of the Anammox process for nitrogen removal in Amox-SBGB with fluidic oscillator. The kinetic parameters of total nitrogen conversion rate were estimated.

Fig.7.8 shows the graph plotted between reciprocal of total substrate removal rate, $V/[Q(S_0 - S_e)]$, against the reciprocal of NLRs, $V/(QS_0)$. According to Eq.7-24, where $K_B/U_{max}$ is the slope and $1/U_{max}$ is the intercept point, saturation constant ($K_B$) value and maximum total substrate utilization rate ($U_{max}$) were calculated from the line plotted on graph in Fig.7.8 to be 58.17 and 57.8 g N/Lday. This indicated that the maximum total nitrogen removal rate was 73.75 g N/Lday in this Anammox reactor. The correlation coefficient is 0.997, confirming the applicability of the modified Stover – Kincannon model.

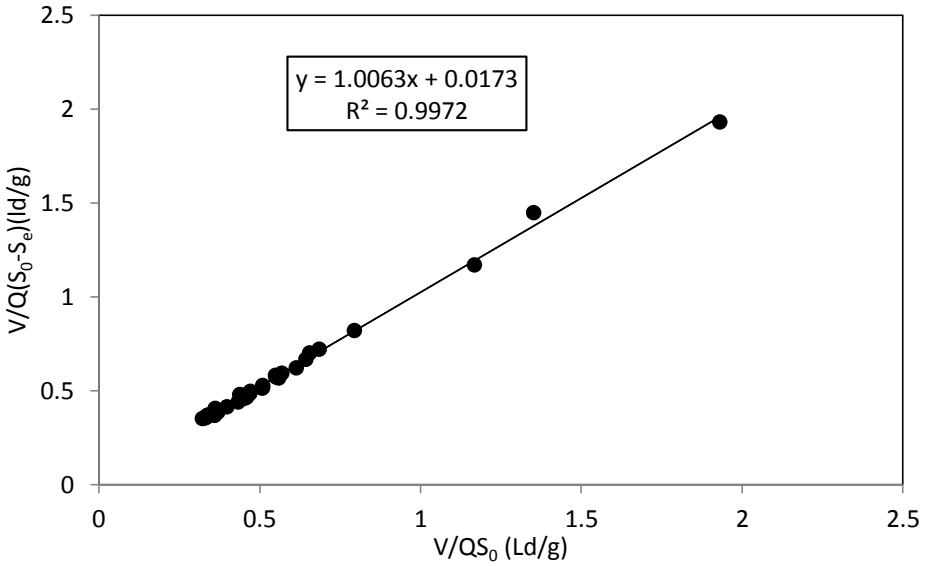


**Figure 7.8** Stover-Kincannon model plot

In the present study the two substrate removal models were applied to model the Amox-SBGB with FO. All kinetic coefficients obtained from these models are summarized in Table 7.1. The results showed that the modified Stover-Kincannon model were more reliable to predict the nitrogen removal performance of the Amox SBGB rather than the Monod model. The similar result was obtained by the other authors. (Jin, 2009; Hooshyari et al, 2009)

The low correlation coefficients of the Monod model indicated that this model was not suitable for the Amox-SBGB with FO with fair degree of precision (Table 7.1). The Monod model was proposed as an empirical model to describe microbial reactor (Monod, 1949), and it was the most widely used model for different reactors and wastewaters (Isik and Sponza, 2005; Yu et al., 1998). Although, in present study the Monod model was found not appropriate for describing the Anammox process kinetics in the Amox-SBGB, it was reliable enough to predict the parital nitrification process in SBAB with FO as discussed previously. Even the kinetics of the anaerobic process are more complicated than the aerobic process, the Stover-Kincannon model was applicable to the kinetic analysis of the Amox-SBGB. This model is capable of predicting substrate removal at any loading conditions, no matter which order kinetics. More important, this model did not model substrate diffusion, hydraulic dynamics and other parameters, which may be important to the reactor performance but were difficult to measure at the present study.

**Table 7.1** Summary of kinetic constants in Monod model and Modified Stover–Kincannon model

| Kinetic Models | Kinetic constants | Values | $R^2$ |
|---|---|---|---|
| Monod model | $K_B$ | 0.153 | 0.67 |
| | $v_{MAX}$ | 0.33 | 0.67 |
| Modified Stover-Kincannon model | $K_B$ | 58.17 | 0.9973 |
| | $U_{MAX}$ | 57.8 | 0.9973 |

The maximum total nitrogen removal rate ($U_{max}$) turned out to be 57.8g N/Lday in the Anammox reactor from the analysis of modified Stover-Kincannon model, while in this study, the actual maximum total nitrogen removal rate was 5 kg/$m^3$/d, only 8.8% of the calculated $U_{max}$ suggesting that the Amox-SBAB with FO in the present study might possess a good nitrogen removal potential. By introducing the values of $K_B$ and $U_{max}$ to Eq 7-24, the effluent nitrogen concentrations can be predicted by using Eq7-26.

$$S = S_0 - \frac{57.8S_0}{58.17+QS_0/V} \quad (7\text{-}26)$$

The model developed for prediction of total substrate removal efficiency in the present work is as follow

$$E = 1 - \frac{72.9957.8}{58.17+QS_0/V} \quad (7\text{-}27)$$

Although the Monod model was not appropriate to simulate the nitrogen removal kinetics in the granular Amox-SBGB, the $v_{max}$ value of 0.33 per day in this study was higher than that (0.1693 per day) found by Ni et al. (2010). The difference in $v_{max}$ values was probably due to the adoption of different reactor configurations, wastewater characteristics and microorganisms used in various studies. The Modified Stover-Kincannon model kinetic constants in this study are much higher than the values from other researches (Jin and Zheng, 2009; Ni et al., 2010c). The Modified Stover-Kincannon model constant depends on the influent substrate (Si) and bacteria concentration (X) in the reactor and increases with the increase of substrate removal efficiency (Isik and Sponza, 2005). Due to the different reactor configuration, working volume, inoculums and operational conditions, the maximum total nitrogen removal rate ($U_{max}$) turned out to be higher than the values. According to the Modified Stover-Kincannon model, low $U_{max}$ value results in a drop of substrate removal rate. Therefore,

the substrate removal rates calculated in this study were higher than values in the study mentioned above. This deduction was also proved by the experimental data.

The validation of the kinetic model for Amox-SBAB with FO was performed and shown in Fig 7.10. A series of new experiments were conducted for validation purpose. The simulated effluent nitrogen concentrations were compared with the new measured values. From 7.10 it is observed that the estimated values had correlation coefficient of 82% with experimental results indicating that the occurrence of denitrification interfere the accuracy of prediction by using modified Stover-Kincannon model. Therefore the more complicated biological nitrogen removal process in Amox-SBGB should be taken into account into the kinetic models. But in present study the correlation coefficient as high as 82% could be considered that the kinetic model Eq 7-27 can be used to simulate the Anammox process in PN-SBGB.

These models were developed based on the most common wastewaters containing limited or no organic nitrogen matter. For a wastewater containing high concentration of proteins and other organic nitrogen sources, ammonification reaction has to be included in the process and anaerobic or anoxic treatment is needed to degrade these compounds prior to nitrogen removal.

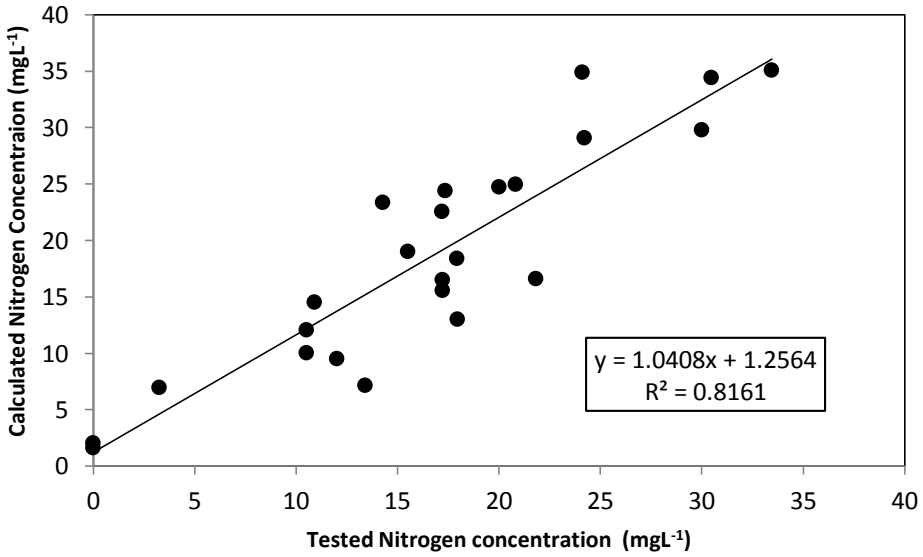


**Figure 7.10** Correlation between calculated values and test values of variation of nitrogen concentration

# Chapter. 8 Conclusions

These studies were mainly focused on the evaluation of influence of application of microbubble on the novel partial nitrification and Anammox processes. Literature review and experimental work carried out in this project confirmed the sustainability and the potential advantages of application of microbubble in the partial nitrification and Anammox process and also established theory and experiment foundation for its the industrial implementation. The major conclusions for this doctoral thesis was drawn as follows

## 8.1. Effect of Microbubble on Mass Transfer Efficiency for Airlift Loop Bioreactor

The higher mass transfer efficiency in the gas lift loop bioreactor with the microbubble generation system was experimentally demonstrated. In the oxygenating process the mass transfer coefficient $K_La$ were impressively elevated by 38.9% by using fluidic oscillator to produce microbubble. In the deoxygenating process the improvement for mass transfer of oxygen removal was surprisingly as high as 70%, meanwhile the enhancement was also found in mass transfer from $CO_2$ phase into liquid phase. The modeling for simulating the inner motion of the airlift loop bioreactor represented more convincing visual results which indicated the finer mixing and higher mass transfer inside bioreactor were obtained by introduction of fluidic oscillator. The alternation of low DO concentration in downcomer region and high DO concentration in rising region provided a favorable environment for the partial nitrification process. In addition, the deoxygenating study in a gas lift loop bioreactor with fluidic oscillator flushed with mixture of $10\%CO_2/N_2$ provided a novel concept for implementation of Anammox process. Better mixing effects, higher oxygen removal rates and pH adjustment with the aid of $H^+$ produced by dissolving $CO_2$ would not only ensure a potential better anaerobic conditions for the growth of Anammox bacteria but also save more energy and operating costs.

## 8.2. Effect of Application of Microbubble on Partial Nitrification Process in SBAB

The performances of partial nitrification processes carried out in two laboratory-scale sequencing batch airlift loop bioreactor equipped with different aeration systems were studied. The laboratory scale investigation allowed understanding the features of effluent and parameters involved in both PN reactors and directly examine the influence of microbubble on the behaviours of partial nitrification. The following conclusion can be stated.

1. The study proved the feasibility to achieve successful and long term stable partial nitrification in sequencing batch airlift loop bioreactor inoculated with return aerobic activated sludge. On the basis of the conditions of PN system and according to the previous literature it is reasonable concluded that this half nitrite build up was achieved by the out-competition of AOB over NOB, IC limitations and limited dissolved oxygen, however operational factors such as inhibition by FA or FNA, high temperature, short HRT contributed to the partial nitrification as well, but were not very essential.

2. Although both aeration systems allow partial nitrification to be successfully achieved, the microbubble aeration system yielded a more suitable treatment performance. Its overall performance was more efficient and more stable and was linked to the advantages of microbubble i.e. higher mass transfer efficiency, hydrodynamic shear force and better mixing. In addition, the shorter feedback loop in the fluidic oscillator related to the higher frequency of the impulse air flow slightly enhanced the improvement of treatment performance caused by smaller microbubble.

3. From the point view of treatment efficiency, the cycle profiles obtained in batch experiment illustrated that when microbubble aeration was applied, the duration time (9 hours) of the half ammonium oxidizing reaction was dramatically shortened compared to that of fine bubble aeration system (16 hours). The DO and ORP file values in PN-SBAB with FO were higher throughout the cycle operation under same airflow rate which indicated microbubble contributed to the higher AOB activity. The OUR file also demonstrated that higher ammonium oxidation occurred in the PN system with microbubble leading to faster reach its valley point. In contrast, 44% time saving implied that 44% energy savings.

4. In terms of the treatment capacity, the observed maximum NLR of 2.08kg-N $m^{-3}day^{-1}$ in PN-SBAB with FO was much higher than maximum NLR of 1.23 kg-N $m^{-3}day^{-1}$ in a PN system with the normal bubble aeration system. When NLR exceeded 1.23 kg-N $m^{-3}day^{-1}$, the inhibition by FA would cause the deterioration of the AOB activity. Whereas throughout the entire experimental period, there was no inhibition by the FA concentratin on partial nitrification behaviours was detected in SBAB with FO which suggested the real maximum NLR for this PN system should be higher than observed maximum NLR of 2.08kg-N $m^{-3}day^{-1}$. Therefore it is concluded that the treatment capacity was increased by 69% at least through using the microbubble aeration system.

5. This study allowed identifying bicarbonate as the key to control the half ammonium conversions. The assessment of effluent $NO_2^-$-N/$NH_4^+$-N ratio revealed that the more appropriate effluent composition was achieved in the PN-SBAB with FO. In this bioreactor the effluent $NO_2^-$-N/$NH_4^+$-N ratio stabilized at $1.3 \pm 0.2$ which satisfactorily met the requirement for the subsequent Anammox process. While in the other PN system the result showed a large fluctuation between 0.5 and 1.4 presenting on the profile of effluent $NO_2^-$-N/$NH_4^+$-N ratio, suggesting that the lower tolerance of AOB to the substrate concentration shock under condition of fine bubble was observed in the experiment.

6 The better performance of partial nitrification in the PN-SBAB with FO was closely linked to the biomass characteristics. The microbubble applied not only created a desirable hydraulic environment for the growth of AOB but also enhanced the settability of the biomass, therefore the higher biomass retention ability of the bioreactor guaranteed more effective bacteria involved in the ammonium oxidation.

7. Molecular techniques enabled the identification the AOB phylotype as the dominant species presenting in the bioreactors under different aeration systems. *Nitrobacter* was not detected in both PN systems, nevertheless the nitration function gene (*nxrA*) was observed around 1%. In addition, QPCR analyses allowed a relative higher quantification of AOB enrichment in PN-SBAB with the microbubble generation system, with a percentage of 22.4%. In contrast the percentage of AOB population in the sludge in PN-SBAB without microbubble was around 17%.

## 8.3. Effect of Application of Microbubble and $CO_2$-rich Mixed Gas on the Anammox Process in SBGB

1. The mixed gas of 10%CO2/N2 was first employed in the Anammox process as operational strategy to keep anaerobic condition. The satisfactory nitrogen removal performance obtained in this study proved that Anammox process was successfully carried out in the SBGB. Compared with the conventional inert gas used for oxygen exchange in Anammox process, the impressed benefits achieved by using the mixture of 10%$CO_2/N_2$ were summarized as follows: ① controlling the values of pH in proper range even in the absence of automatic pH regulator in the Anammox bioreactor followed by saving considerable operational cost; ② keeping desirable anaerobic condition for the growth of the Anammox bacteria; ③ Dissolved $CO_2$ reacting with $H_2O$ would produce $H^+$ and $HCO^-_3$ acting as reactant for Anammox (Eq 2-15). According to the reaction equilibrium theory, the additional reactant produced drove the Anammox reaction towards to the right hand side. ④Feeding the Anammox bacteria with extra $HCO^-_3$ enhanced cell synthesis as well as overcame the shortage of carbon source ; ⑤As promising environmental-friendly strategy, continuously flushing mixed gas of $CO_2/N_2$ into Anammox bioreactor means the massive demand of $CO_2$ which is feasible recycled from the industrial plant. As a result the emission of greenhouse gas was reduced; ⑥ By contrast it was very disappointing that in the pH adjusting devicedjusting device, the Amox-SBGB continuously flushed with argon lost over 90% Anammox activity, which denitrificationdenitrification process, not our target. In addition the high temperature stack gas from the power plant is potentially capable of providing the heat required by Anammox process so as to save operational cost.

2. The microbubble generation system was also first introduced into the Anammox process to flush the mixture of 10 $CO_2/O_2$ into SBGB in order to keep the desirable environment for the activity of Anammox bacteria and a positive influence of microbubble on the Anammox activity was observed in this study. Through comparing treatment performance of both Amox-SBGBs with different bubble generation systems during the operating period of 63days, it is evident that the Amox-SBGB with FO was carried out the Anammox process with higher nitrogen removal efficiency, more stable operation and more tolerance to substrate shock. The maximum NLR of 5 kg-$Nm^{-3}day^{-1}$ and maximum total nitrogen removal efficiency of 97.8% was achieved in Amox-SBGB

with FO, whereas the maximum NLR and maximum TN removal efficiency for the Amox-SBGB without FO was only 3.39 kg-$Nm^{-3}day^{-1}$ and 2.87% respectively under the same operational conditions. During the stable operational period, the nitrogen removal efficiency for the former was stabilized above 90% in comparison with 80% for the latter. From the point view of the stability of the treatment performance, the instability indices i.e. coefficient of variation ratio, coefficient of range ratio and coefficient of regression function derivative for the both bioreactors were studied and compared. The results showed us a more stable performance belonged to the bioreactor equipped with the microbubble generation system.

The operational strategy, based on the microbubble, increased the mass transfer efficiency between gas-liquid phases and strengthened the removal of oxygen and the production of $H^+$ and $HCO3^-$, therefore the inhibition of oxygen was diminished and the more IC can strengthen the tolerance of Anammox bacteria to the high FNA, which promoted the Anammox bacteria activity.

Anammox bacteria activity is very sensitive to the substrate especially nitrite thus inhomogeneous substrate tended to suppress the Anammox process fractionally. For this reason the obtaining good mixing conditions inside the bioreactor is required to avoid the presence of high concentrations of nitrite or ammonia in the medium. This better mixing can be achieved by means of high liquid velocity caused by the recirculation of the mixed gas microbubble.

The coexistence of the denitrification process in the Anammox bioreactor was considered as a favourable factor in respect of improving TN nitrogen removal efficiency. On the other hand, the presence of denitrifying bacteria caused the original stoichiometric relationship between $NO_2^-$-N and $NH_4^+$ -N in the influent increased from 1.32 to around 1.4 in order to maintain well-pleasing treatment performance.

4. The higher hydraulic shear force was regarded as a key factor to exert a positive effect on the formation, structure and stability of Anammox granular sludge in aerobic conditions. In the present study, due to the same operational condition applied, the microbubble was responsible for the higher shear stress. The higher shear force enhanced the formation of anaerobic granules and the granule compactness so that settling property of the sludge was improved during the operational period. The retention ability of the biomass could ensure abundant sludge volume in the reactor,

which is of primary importance to provide the foundation for high-rate nitrogen removal and stable performance. The smaller size of the biomass granules was visually observed in the Amox-SBGB with FO, which should benefit the substrate diffusion and improve the activity of the biomass placed in the inner cores of the granules.

5. Molecular techniques confirmed the coexistence of Anammox species and denitrifiers in both Amox-SBGBs. The analyse of QPRC revealed that at least two well-known anammox species (*Kuenenia stuttgartiensis and Candidatus Brocadia fulgida*) and anammox cells accounted for 71.9% of total cells in SBGB with the microbubble generation system compared to 61.9% in SBGB without a microbubble generation system.

## 8.4. Kinetic Modelling of Partial nitrification and Anammox Process in SBGB

Base on the Monod equation and the Stover–Kincannon model, the kinetic models were successfully developed to describe the partial nitrification process in SBAB with fluidic oscillator and Anammox process in SBGB with fluidic oscillator respectively. Through using the laboratory-scale SBGB treating synthetic wastewater the kinetic parameters were estimated as follows

The kinetic model for partial nitrification process in SBAB with FO

$$\frac{dS_{NH}}{dt} = -0.069 \cdot \frac{S_{NH}}{38.5 + S_{NH}} \cdot \frac{S_O}{0.302 + S_O} \cdot M \cdot X$$

The kinetic model for Anammox process in SBGB with FO

$$S = S_0 - \frac{57.8 S_0}{58.17 + Q S_0 / V}$$

The kinetic models were validated by comparison between calculated data and experimental data with the correlation coefficient as high as 98.8% and 81% respectively. As a result, these models were capable of accurately predicting the main outcomes of the systems; therefore the optimization of the operation of biological nitrogen removal process could be accomplished. In addition, this study also provided the basic kinetic parameters (i.e. $K_S$ and $\mu_{max}$) which are helpful for the establishment of further mathematical models.

Based on the simulation results with the model, relatively low DO (0.5~0.9mg $L^{-1}$) could be favourable for the partial nitrification process and the duration time of the aeration should be adjusted to prevent the over aeration for the sake of avoiding the nitrate production and saving energy in operation. Whereas the kinetic parameters of the substrate-removal model for Anammox process showed us the higher potential of the Amox-SBGB with FO. In this study, we tested the model at only one temperature condition (30 ℃). For application, the impact of temperature on the system performance for both partial nitrification and Anammox process must be evaluated. The influence of pH should also be addressed when designing a SBGB system for the nitrogen removal. More operational conditions including different temperature and pH should be tested prior to applying the model for full scale SBGB design.

# Future Work

Future research and studies are still needed to further understand and improve this novel technology. Increasing the scientific knowledge is essential for its future full-scale application. Some of directions for the future research have emerged from this study.

Firstly more research on the relationship between the length of feedback loop and microbubble size would help us achieve more satisfying designs for finer microbubble cloud generation. The modeling of mass transfer of the mixed gas in the gas lift loop bioreactor could be further investigated.

Secondly, in this study NLR for the PN-SBAB with fluidic oscillator reached up to 2.08kg-N $m^{-3}day^{-1}$ however there is no obvious inhibition was found in the bioreactor, which means the PN-SBAB with FO is potentially capable of treating the higher ammonia loading stream. Therefore the performance of PN-SBAB with higher substrate load under microbubble aeration system needs to be studied to detect the highest NLR. The real-time controlled system could be employed to improve the efficiency of the partial nitrification system. It is admitted that the low ammonium concentration presenting in the influent is easy to be converted to nitrate. The application of microbubble aeration system on the partial nitrification process with real-time control for the low nitrogen loading could be another significantly research direction. The kinetics of the partial nitrification study could be further investigated, especially with regard to NOB. The nitrate production was neglected due to the little yield in the present study. If the kinetic models for both AOB and NOB were built, the operation of the partial nitrification system would be optimized based on more accurate model. Studies about $N_2O$ emission from the treatment are important in order to reduce and minimize the impacts from the emission of this strong greenhouses gas.

Regarding the Anammox process, more study are needed to investigate feasibility of Anammox process with injecting authentic stack gas including $NO_x$, $SO_x$ by using microbubble generation system. Long term influence of microbubble on the Anammox sludge could be in-depth investigate. It is potential that the heat presenting in hyperthermal stack gas from the industrial plant could be used to maintain the high temperature required by Anammox process. The heat transfer from the stack gas into Anammox system is another important research direction.

More research on acclimation of bacteria population responsible for partial nitrification and Anammox process under different conditions using different molecular biology techniques for instance FISH or DNA sequencing could provide a thorough understanding of the perspectives to run this process.

Continued investigation of pilot scale of combined process of partial nitrification and Anammox is recommended. The effect of treating various wastewater streams with this novel technology could be investigated.

Taking account of various reactions presenting in the partial nitrification and Anammox system such as nitration and denitrification, it is very significant to establish the more comprehensive mathematical model of PN-SBAB with FO and Amox-SBGB with FO based on ASM1.2.3 in order to predicting the effluents in more details such as ammonium, nitrite, nitrate, inorganic carbon concentration and pH.

## References

A, B. H., Truper.M, Dworkin.W, Harder.K, KH,Schleifer (2001). An Evolving Electronic Database for the Microbiological Community. New York, Springer-Verlag

Abeling, U. and C. Seyfried (1992). "Anaerobic-aerobic treatment of high strength ammonium wastewater nitrogen removal using nitrite." Water Science Technology **26**: 1007-1015.

Ahn, J. H. and C. F. Forster (2000). "Kinetic analyses of the operation of mesophilic and thermophilic anaerobic filters treating a simulated starch wastewater." Process Biochemistry **36**(1–2): 19-23.

Ahn, J. H. and C. F. Forster (2002). "A comparison of mesophilic and thermophilic anaerobic upflow filters treating paper–pulp–liquors." Process Biochemistry **38**(2): 256-261.

Ahn, Y.-H. (2006). "Sustainable nitrogen elimination biotechnologies: A review." Process Biochemistry **41**(8): 1709-1721.

Aktan, C. K., K. Yapsakli and B. Mertoglu (2012). "Inhibitory effects of free ammonia on Anammox bacteria." Biodegradation **23**(5): 751-762.

Alphenaar, P. A., A. Visser and G. Lettinga (1993). "The effect of liquid upward velocity and hydraulic retention time on granulation in uasb reactors treating wastewater with a high sulfate content." Bioresource Technology **43**(3): 249-258.

Amann, R. I., L. Krumholz and D. A. Stahl (1990). "Fluorescent-oligonucleotide probing of whole cells for determinative, phylogenetic, and environmental-studies in microbiology." Journal of Bacteriology **172**(2): 762-770.

American Water Works Association, W. E. F. (1997). Standard Methods for the Examination of Water and Wastewater, American Public Health Association.

Anceno, A. J., P. Rouseau, F. Beline, O. V. Shipin and P. Dabert (2009). "Evolution of N-converting bacteria during the start-up of anaerobic digestion coupled biological nitrogen removal pilot-scale bioreactors treating high-strength animal waste slurry." Bioresource Technology **100**(14): 3678-3687.

Anthonisen, A. C., R. C. Loehr, T. B. Prakasam and E. G. Srinath (1976). "Inhibition of nitrification by ammonia and nitrous acid." J Water Pollut Control Fed **48**(5): 835-852.

Antoniou, P., J. Hamilton, B. Koopman, R. Jain, B. Holloway, G. Lyberatos and S. A. Svoronos (1990). "Effect of temperature and ph on the effective maximum specific growth rate of nitrifying bacteria." Water Research **24**(1): 97-101.

A.O. Smith Harvestore Products, (1993), Harvestore Products Today, Communications Group, Freeport, IL,. 32,(2).

Araujo, J. C., AC. Correa, MM. Silva, EC. Matté, MH. Matté, GR. Von Sperling, M. Chernicharo, CA. (2011). "Anammox bacteria enrichment and characterization from municipal activated sludge." Water Sci Technol **64**(7): 1428-1434.

Arcand, Y., S. R. Guiot, M. Desrochers and C. Chavarie (1994). "Impact of the reactor hydrodynamics and organic loading on the size and activity of anaerobic granules." Chemical Engineering Journal and the Biochemical Engineering Journal **56**(1): B23-B35.

Arrojo, B., A. Mosquera-Corral, J. L. Campos and R. Méndez (2006). "Effects of mechanical stress on Anammox granules in a sequencing batch reactor (SBR)." Journal of Biotechnology **123**(4): 453-463.

Aslan, S. and M. Dahab (2008). "Nitritation and denitritation of ammonium-rich wastewater using fluidized-bed biofilm reactors." Journal of Hazardous Materials **156**(1-3): 56-63.

Astrid, A. v. d. G. P. d. B. R., Lesley A . Jetten ,Mike M. Gijs Kuenen,J. (1997). "Metabolic pathway of anaerobic ammonium oxidation on the basis of I5N studies in a fluidized bed reactor." Microbiology **143**(24): 2415-2421.

Behm, Don,( 1989). “Ill Waters: The Fouling of Wisconsin's Lakes and Streams”

(Special Report), The Milwaukee Journal,

Berner, E., and Berner, R.,(1987). The Global Water Cycle, Prentice Hall, New Jersey, p. 102-119. Barron County Land Conservation Department (producer),( 1993), Lagoon

Reclamation

Bernhard, A. (2010). “The Nitrogen Cycle: Processes, Players, and Human Impact”. Nature Education Knowledge **2**(2):12

Bertino, A. (2010). Study on one-stage partial nitritation-anammox process in moving bed biofilm reactors: a sustainable nitrogen removal. Land and water Resources Engineering. Stokholm, Royal Instituite of Technology. **Master**.

Blum, D. J. W. and R. E. Speece (1991). "Quantitative structure-activity relationships for chemical toxicity to environmental bacteria." Ecotoxicology and Environmental Safety 22(2): 198-224

Bocher, Lori Ward,( 1995). “Tracing the Flow of Chemicals: How to Reduce Nitrate and Pesticide Leaching”, Turf Science,:64-67.

Bougard, D., N. Bernet, D. Cheneby and J. P. Delgenes (2006). "Nitrification of a high-strength wastewater in an inverse turbulent bed reactor: Effect of temperature on nitrite accumulation." Process Biochemistry **41**(1): 106-113.

Bredwell, M. D. and R. M. Worden (1998). "Mass-Transfer Properties of Microbubbles. 1. Experimental Studies." Biotechnology Progress **14**(1): 31-38.

Brochier, C. and H. Philippe (2002). "Phylogeny - A non-hyperthermophilic ancestor for bacteria." Nature **417**(6886): 244-244.

Broda, E. (1977). "2 kinds of lithotrophs missing in nature." Zeitschrift Fur Allgemeine Mikrobiologie **17**(6): 491-493.

Bruce E, R. P. L., McCarty (2001). Environmental Biotechnology: Principles and Applications, McGraw-Hill.

Buisine, A. and M. Paget (1953). "Cyanosis in infants caused by ingestion of well water." Annales de biologie clinique **11**(10-12): 625-627.

Burkart, M. R. and D. W. Kolpin (1993). "Hydrologic and land-use factors associated with herbicides and nitrate in near-surface aquifers." Journal of Environmental Quality **22**(4): 646-656.

Büyükkamaci, N. and A. Filibeli (2002). "Determination of kinetic constants of an anaerobic hybrid reactor." Process Biochemistry **38**(1): 73-79.

CEH (2011). "Excessive nitrogen harms the economy and environment ". from http://www.ceh.ac.uk/news/news_archive/EuropeanNitrogenAssessment.html.

Chamchoi, N. and S. Nitisoravut (2007). "Anammox enrichment from different conventional sludges." Chemosphere **66**(11): 2225-2232.

Chamchoi, N., S. Nitisoravut and J. E. Schmidt (2008). "Inactivation of ANAMMOX communities under concurrent operation of anaerobic ammonium oxidation (ANAMMOX) and denitrification." Bioresource Technology **99**(9): 3331-3336.

Chang, H. T., B. E. Rittmann, D. Amar, R. Heim, O. Ehlinger and Y. Lesty (1991). "Biofilm detachment mechanisms in a liquid-fluidized bed." Biotechnology and Bioengineering **38**(5): 499-506.

Chen, H. H., S. T. Liu, F. L. Yang, Y. Xue and T. Wang (2009). "The development of simultaneous partial nitrification, ANAMMOX and denitrification (SNAD) process in a single reactor for nitrogen removal." Bioresource Technology **100**(4): 1548-1554.

Chen, M. J., Z. Zhang and T. R. Bott (1998). "Direct measurement of the adhesive strength of biofilms in pipes by micromanipulation." Biotechnology Techniques **12**(12): 875-880.

Chen, T. T., P. Zheng, L. D. Shen, S. Ding and Q. Mahmood (2011). "Kinetic characteristics and microbial community of Anammox-EGSB reactor." Journal of Hazardous Materials **190**(1-3): 28-35.

Cheremisinoff, N. P. (2011). Handbook of Water and Wastewater Treatment Technologies, St. Louis: Butterworth-Heinemann.

Chisti, Y. (2000). "Animal-cell damage in sparged bioreactors." Trends in Biotechnology **18**(10): 420-432.

Cho, S., N. Fujii, T. Lee and S. Okabe (2011). "Development of a simultaneous partial nitrification and anaerobic ammonia oxidation process in a single reactor." Bioresource Technology **102**(2): 652-659.

Chuang, H. P., A. Ohashi, H. Imachi, M. Tandukar and H. Harada (2007). "Effective partial nitrification to nitrite by down-flow hanging sponge reactor under limited oxygen condition." Water Research **41**(2): 295-302.

Chung, J., H. Shim, Y. W. Lee and W. Bae (2005). "Comparison of Influence of Free Ammonia and Dissolved Oxygen on Nitrite Accumulation Between Suspended and Attached Cells." Environmental Technology **26**(1): 21-33.

Collins, M. J., D. M. Arciero and A. B. Hooper (1993). " Optical spectropotentiometric resolution of the hemes of hydroxylamine oxidoreductase. Heme quantitation and pH dependence of Em." Journal of Biological Chemistry **268**(20): 14655-14662

Dalsgaard, T. and B. Thamdrup (2002). "Factors Controlling Anaerobic Ammonium Oxidation with Nitrite in Marine Sediments." Applied Environmental Microbiology **68**(8): 3802–3808.

Dalsgaard, T., B. Thamdrup and D. E. Canfield (2005). "Anaerobic ammonium oxidation (anammox) in the marine environment." Research in Microbiology **156**(4): 457-464.

Dapena-Mora, A., J. L. Campos, A. Mosquera-Corral, M. S. M. Jetten and R. Méndez (2004). "Stability of the ANAMMOX process in a gas-lift reactor and a SBR." Journal of Biotechnology **110**(2): 159-170.

Dapena-Mora, A. C., JL. Mosquera-Corral, A. and R. Méndez (2006). "Anammox process for nitrogen removal from anaerobically digested fish canning effluents." Water Science Techology **53**(12): 265-274.

deGraaf, A. A. V., P. deBruijn, L. A. Robertson, M. S. M. Jetten and J. G. Kuenen (1996). "Autotrophic growth of anaerobic ammonium-oxidizing micro-organisms in a fluidized bed reactor." Microbiology-Uk **142**: 2187-2196.

Deshpande, K. B. and W. B. Zimmerman (2005). "Experimental study of mass transfer limited reaction—Part II: Existence of cross-over phenomenon." Chemical Engineering Science **60**(15): 4147-4156.

Deshpande, K. B. and W. B. Zimmerman (2005). "Experimental study of mass transfer limited reaction—Part I: Use of fibre optic spectrometry to infer asymmetric mass transfer coefficients." Chemical Engineering Science **60**(11): 2879-2893.

Dosta, J., I. Fernández, J. R. Vázquez-Padín, A. Mosquera-Corral, J. L. Campos, J. Mata-Álvarez and R. Méndez (2008). "Short- and long-term effects of temperature on the Anammox process." Journal of Hazardous Materials **154**(1–3): 688-693.

Driessen, W. and G. Reitsma (2011). "One-Step ANAMMOX Process a sustainable way to remove ammoniacal nitroge." Wastewater Treatment & Sewerage UK Water Projects 101-102.

Driscoll, C., Whitall, D, Aber, JD, Boyer, E, Castro, M, Cronan, C, Goodale, CL, Groffman, PM, Hopkinson, C, Lambert, K, Lawrence, G, Ollinger, S (2003). "Nitrogen pollution in the northeastern United States: Sources, effects and management options." BioScience **53**(4): 357-374.

Edwards, V. H. (1970). "The influence of high substrate concentrations on microbial kinetics." Biotechnology and Bioengineering **12**(5): 679-712.

Edzwald, J. (2010). "Dissolved air flotation and me." Water Research **44**(7): 2077-2106.

Egli, K., U. Fanger, P. J. J. Alvarez, H. Siegrist, J. R. van der Meer and A. J. B. Zehnder (2001). "Enrichment and characterization of an anammox bacterium from a rotating biological contactor treating ammonium-rich leachate." Archives of Microbiology **175**(3): 198-207.

Environment Directorate, (1974)," Waste Water Treatment Processes for Phosphorus and Nitrogen Removal", Organization for Economic Co-Operation and Development, Paris, :**109**.

Fang, F., B.-J. Ni, X.-Y. Li, G.-P. Sheng and H.-Q. Yu (2009). "Kinetic analysis on the two-step processes of AOB and NOB in aerobic nitrifying granules." Applied Microbiology and Biotechnology **83**(6): 1159-1169.

Feng, Y.-J., S.-K. Tseng, T.-H. Hsia, C.-M. Ho and W.-P. Chou (2007). "Partial nitrification of ammonium-rich wastewater as pretreatment for anaerobic ammonium oxidation (Anammox) using membrane aeration bioreactor." Journal of Bioscience and Bioengineering **104**(3): 182-187.

Fernández, I. (2010). Towards the improvement of start-up and operation of Anammox reactors. Santiago de Compostela, Universidad de Santiago de Compostela. **PhD**.

Ferris, M. J. M., G and W. DM (1996). "Denaturing gradient gel electrophoresis profiles of 16S rRNA-defined populations inhabiting a hot spring microbial mat community." Appl Environ Microbiol **62**(2): 340-346.

Finley, B., (1990), Well-water Nitrates Endanger N. Colorado, Denver (Colorado)

Post, 16 November.

Forman, D., S. Al-Dabbagh and R. Doll (1985). "Nitrates, nitrites and gastric cancer in Great Britain." Nature **313**(6004): 620-625.

Franco, A., E. Roca and J. M. Lema (2006). "Granulation in high-load denitrifying upflow sludge bed (USB) pulsed reactors." Water Research **40**(5): 871-880.

Frear, D. S. and R. C. Burrell (1955). "Spectrophotometric method for determining hydroxylamine reductase activity in higher plants." Analytical Chemistry **27**(10): 1664-1665.

Fujii, T., H. Sugino, J.D. Rouse, K.J. Furukawa, (2002), "Characterization of the microbial community in an anaerobic ammonium-oxidizing biofilm cultured on a nonwoven biomass carrier", Biosci. Bioeng. **94** 412–418.

Furukawa, K., Y. Inatomi, S. Qiao, L. Quan, T. Yamamoto, K. Isaka and T. Sumino (2009). "Innovative treatment system for digester liquor using anammox process." Bioresource Technology **100**(22): 5437-5443.

Fux, C., M. Boehler, P. Huber, I. Brunner and H. Siegrist (2002). "Biological treatment of ammonium-rich wastewater by partial nitritation and subsequent anaerobic ammonium oxidation (anammox) in a pilot plant." Journal of Biotechnology **99**(3): 295-306.

Gaillard, J.F., February,(1995), Lecture on Nitrogen Cycle.

Gali, A., J. Dosta, S. Mace and J. Mata-Alvarez (2007). "Comparison of reject water treatment with nitrification/denitrification via nitrite in SBR and SHARON chemostat process." Environmental Technology **28**(2): 173-176.

Gal í, A., J. Dosta, M. C. M. van Loosdrecht and J. Mata-Alvarez (2007). "Two ways to achieve an anammox influent from real reject water treatment at lab-scale: Partial SBR nitrification and SHARON process." Process Biochemistry **42**(4): 715-720.

Gali, A., J. Dosta, et al. (2007). "Comparison of reject water treatment with nitrification/denitrification via nitrite in SBR and SHARON chemostat process." Environmental Technology **28**(2): 173-176.

Gallert, C. and J. Winter (2005). Bacterial Metabolism in Wastewater Treatment Systems. Environmental Biotechnology, Wiley-VCH Verlag GmbH & Co. KGaA: 1-48.

Galloway J.N., J.D. Aber, J.W. Erisman, S.P. Seitzinger, R.H. Howarth, E.B. Cowling, B.J. Cosby (2003). "The nitrogen cascade". BioScience **53**: 341–356.

Ganigue, R., H. Lopez, M. D. Balaguer and J. Colprim (2007). "Partial ammonium oxidation to nitrite of high ammonium content urban land fill leachates." Water Research **41**(15): 3317-3326.

Ganigue, R., H. Lopez, M. Ruscalleda, M. D. Balaguer, J. Colprim (2008). Operational strategy for a partial nitritation-sequencing batch reactor treating urban landfill leachate to achieve a stable influent for an anammox reactor. J Chem Technol Biotecnol.**83**:365–71.

Ganigué, R. G., J. Sànchez-Melsió, A. Ruscalleda, M. López, H. Vila, X.Colprim, J. Balaguer, MD. (2009). "Long-term operation of a partial nitritation pilot plant treating

leachate with extremely high ammonium concentration prior to an anammox process." Bioresour Technology **100**(23): 5624-5632.

Gao, D. W., Y. Z. Peng and W. M. Wu (2010). "Kinetic Model for Biological Nitrogen Removal Using Shortcut Nitrification-Denitrification Process in Sequencing Batch Reactor." Environmental Science & Technology **44**(13): 5015-5021

Garrido, J. M., W. A. J. vanBenthum, M. C. M. vanLoosdrecht and J. J. Heijnen (1997). "Influence of dissolved oxygen concentration on nitrite accumulation in a biofilm airlift suspension reactor." Biotechnology and Bioengineering **53**(2): 168-178.

Gee, C. S., M. T. Suidan and J. T. Pfeffer (1990). "Modeling of nitrification under substrateinhibiting conditions." Journal of Environmental Engineering ASCE **116**: 18-31.

Gjaltema, A., M. C. M. van Loosdrecht and J. J. Heijnen (1997). "Abrasion of suspended biofilm pellets in airlift reactors: Effect of particle size." Biotechnology and Bioengineering **55**(1): 206-215.

Gonzalez-Domenech, C. M., F. Martinez-Checa, E. Quesada and V. Bejar (2009). "Halomonas fontilapidosi sp nov., a moderately halophilic, denitrifying bacterium." International Journal of Systematic and Evolutionary Microbiology **59**: 1290-1296.

Govoreanu, R., D. Seghers, I. Nopens, B. De Clercq, H. Saveyn, C. Capalozza, P. Van der Meeren, W. Verstraete, E. Top and P. A. Vanrolleghem (2003). "Linking floc structure and settling properties to activated sludge population dynamics in an SBR." Water Science and Technology **47**(12): 9-18.

Grau, P., M. Dohanyos and J. Chudoba (1975). "Kinetics of multicomponent substrate removal by activated-sludge." Water Research **9**(7): 637-642.

Gujer, W., M. H. Mino and M. v. Loosdrecht (1999). "Activated Sludge Model No. 3." Water Science and Technology **39**(1): 183–193.

Guo, J. H., Y. Z. Peng, H. J. Huang, S. Y. Wang, S. J. Ge, J. R. Zhang and Z. W. Wang (2010). "Short- and long-term effects of temperature on partial nitrification in a sequencing batch reactor treating domestic wastewater." Journal of Hazardous Materials **179**(1-3): 471-479.

Guo, J. H., Y. Z. Peng, S. Y. Wang, Y. N. Zheng, H. J. Huang and S. J. Ge (2009). "Effective and robust partial nitrification to nitrite by real-time aeration duration control in an SBR treating domestic wastewater." Process Biochemistry **44**(9): 979-985.

Gustafson, D. I., (1993), Pesticides in Drinking Water, Van Hostrand Reinhold, New York, : 241.

Gut, L., E. Plaza, M. Dlugolecka and B. Hultman (2005). "Partial nitritation process assessment." Vatten **61**: 175–182.

Gut, L., E. Plaza and B. Hultman (2007). "Assessment of a two-step partial nitritation/Anammox system with implementation of multivariate data analysis." Chemometrics and Intelligent Laboratory Systems **86**(1): 26-34.

Guter, Gerald A.,(1981), Removal of Nitrate from Contaminated Water Supplies for Public Use, Environmental Protection Agency, Cincinnati.

Guven, D., A. Dapena, B. Kartal, M. C. Schmid, B. Maas, K. van de Pas-Schoonen, S. Sozen, R. Mendez, H. J. M. Op den Camp, M. S. M. Jetten, M. Strous and I. Schmidt (2005). "Propionate oxidation by and methanol inhibition of anaerobic ammonium-oxidizing bacteria." Applied and Environmental Microbiology **71**(2): 1066-1071

Hallberg, G.R. and Keeney, D.R., (1993), Nitrate, Alley, William A., ed., Regional Ground-water Quality, Van Nostrand Reinhold, New York, p.297-322.

Haller, L., P. McCarthy, T. O'Brien, J. Riehle and T. Stuhldreher. "Nitrate pollution of groundwater." 2012, from http://www.reopure.com/nitratinfo.html.

Hanaki, K., C. Wantawin and S. Ohgaki (1990). "Nitrification at low-levels of dissolved-oxygen with and without organic loading in a suspended-growth reactor." Water Research **24**(3): 297-302.

Hanotu, J., H. C. H. Bandulasena and W. B. Zimmerman (2012). "Microflotation performance for algal separation." Biotechnology and Bioengineering **109**(7): 1663-1673.

Hellinga, C., A. A. J. C. Schellen, J. W. Mulder, M. C. M. van Loosdrecht and J. J. Heijnen (1998). "The sharon process: An innovative method for nitrogen removal from ammonium-rich waste water." Water Science and Technology **37**(9): 135-142.

Hellinga, C., M. C. M. Van Loosdrecht and J. J. Heijnen (1999). "Model based design of a novel process for nitrogen removal from concentrated flows." Mathematical and Computer Modelling of Dynamical Systems **5**(4): 351-371.

Henry, S., D. Bru, B. Stres, S. Hallet and L. Philippot (2006). "Quantitative detection of the nosZ gene, encoding nitrous oxide reductase, and comparison of the abundances of 16S rRNA, narG, nirK, and nosZ genes in soils." Applied and Environmental Microbiology **72**(8): 5181-5189.

Henze, M., W. Gujer, T. Mino and M. C. M. van Loosdrecht (2000). Activated Sludge Models ASM1, ASM2, ASM2d, and ASM3(Scientific & technical report). London,UK, IWA Publishing.

Henze, M., P. Harremoes, J. l. C. Jansen and E. Arvin (2001). Wastewater Treatment: Biological and Chemical Processes (Environmental Science and Engineering / Environmental Engineering), Springer.

Henze, M., M. C. M. V. Loosdrecht and G. A. Ekama (2008). Biological Wastewater Treatment: Principles, Modelling and Design, IWA Publishing.

Haycock, Nicholas, (1990). Handling Excess Nitrates, **Nature**, **348:** 291.

Hoage, J. B. M., L A. (2005). Apparatus for aeration without significant agitation to deplete and biodegrade sludge. U. S. Patent. United States. 6884353.

Hooshyari, B., A. Azimi and N. Mehrdadi (2009). "Kinetic analysis of enhanced biological phosphorus removal in a hybrid integrated fixed film activated sludge process." International Journal of Enviornmental Science and Technology **6**(1): 149-158.

Hu, B.-l., P. Zheng, C.-j. Tang, J.-w. Chen, E. van der Biezen, L. Zhang, B.-j. Ni, M. S. M. Jetten, J. Yan, H.-Q. Yu and B. Kartal (2010). "Identification and quantification of anammox bacteria in eight nitrogen removal reactors." Water Research **44**(17): 5014-50

Hu S, “Novel bubble aerator performance,” University of Sheffield, MSc in Environmental and Energy Engineering dissertation, 2006 20.

Hunik, J. H., H. V. M. Hamelers and I. W. Koster (1990). "Growth-rate inhibition of acetoclastic methanogens by ammonia and pH in poultry manure digestion." Biological Wastes **32**(4): 285-297.

Hwang, I. M., K S. Choi, E. and Z. Yun (2006). "Resource recovery and nitrogen removal from piggery waste using the combined anaerobic processes." Water Scienec Techology . **54**(8): 229-236.

Imajo, U., T. Tokutomi and K. Furukawa (2004). "Granulation of Anammox microorganisms in up-flow reactors." Water Science and Technology **49**(5-6): 155-163.

Institute, W. R. "Sources of Nutrient Pollution." 2012.

Isaka, K., T. Sumino and S. Tsuneda (2007). "High nitrogen removal performance at moderately low temperature utilizing anaerobic ammonium oxidation reactions." Journal of Bioscience and Bioengineering **103**(5): 486-490.

Işik, M. and D. T. Sponza (2005). "Substrate removal kinetics in an upflow anaerobic sludge blanket reactor decolorising simulated textile wastewater." Process Biochemistry **40**(3–4): 1189-1198.

Jauregi, P. V., J. (1999). "Colloidal gas aphrons: Potential applications in biotechnology." TrendsBiotechnology Advances **17**: 389–395.

Jetten, M. S. M., S. J. Horn and M. C. M. vanLoosdrecht (1997). "Towards a more sustainable municipal wastewater treatment system." Water Science and Technology **35**(9): 171-180.

Jetten, M. S. M., M. Wagner, J. Fuerst, M. van Loosdrecht, G. Kuenen and M. Strous (2001). "Microbiology and application of the anaerobic ammonium oxidation (‘anammox’) process." Current Opinion in Biotechnology **12**(3): 283-288.

Jetten, M. S. M. N., Laura van. Strous, Marc. Kartal, Boran. Keltjens, Jan T.Op den Camp, Huub J M. (2009). "Biochemistry and molecular biology of anammox Bacteria." Biochemistry and Molecular Biology **44**(2-3): 65–84.

Jin, R. C. and P. Zheng (2009). "Kinetics of nitrogen removal in high rate anammox upflow filter." Journal of Hazardous Materials **170**(2-3): 652-656.

Jin, R.-c., B.-l. Hu, P. Zheng, M. Qaisar, A.-h. Hu and E. Islam (2008). "Quantitative comparison of stability of ANAMMOX process in different reactor configurations." Bioresource Technology **99**(6): 1603-1609.

Jin, R.-C., P. Zheng, A.-H. Hu, Q. Mahmood, B.-L. Hu and G. Jilani (2008). "Performance comparison of two anammox reactors: SBR and UBF." Chemical Engineering Journal **138**(1–3): 224-230.

Johnson, C. J., P. A. Bonrud, T. L. Dosch, A. W. Kilness, K. A. Senger, D. C. Busch and M. R. Meyer (1987). "FATAL OUTCOME OF METHEMOGLOBINEMIA IN AN INFANT." Jama-Journal of the American Medical Association **257**(20): 2796-2797.

Junker, B., W. Maciejak, B. Darnell, M. Lester and M. Pollack (2007). "Feasibility of an in situ measurement device for bubble size and distribution." Bioprocess and biosystems engineering **30**(5): 313-326.

Kamrin, M. A., (1987), "Health Implications of Groundwater Contaminants"., Rural Groundwater Contamination, Lewis, Chelsea, MI :226 - 233.

Kapdan, I. K. (2005). "Kinetic analysis of dyestuff and COD removal from synthetic wastewater in an anaerobic packed column reactor." Process Biochemistry **40**(7): 2545-2550.

Kartal, B., J. Rattray, L. A. van Niftrik, J. van de Vossenberg, M. C. Schmid, R. I. Webb, S. Schouten, J. A. Fuerst, J. S. S. Damste, M. S. M. Jetten and M. Strous (2007). "Candidatus "Anammoxoglobus propionicus" a new propionate oxidizing species of anaerobic ammonium oxidizing bacteria." Systematic and Applied Microbiology **30**(1): 39-49.

Kartal, B., L. Van Niftrik, J. Rattray, J. L. C. M. Van De Vossenberg, M. C. Schmid, J. Sinninghe Damsté, M. S. M. Jetten and M. Strous (2008). "Candidatus 'Brocadia fulgida': an autofluorescent anaerobic ammonium oxidizing bacterium." FEMS Microbiology Ecology **63**(1): 46-55.

Khin, T. and A. P. Annachhatre (2004). "Novel microbial nitrogen removal processes." Biotechnology Advances **22**(7): 519-532.

Kilonzo, P. M., A. Margaritis, M. A. Bergougnou, J. Yu and Q. Ye (2007). "Effects of geometrical design on hydrodynamic and mass transfer characteristics of a rectangular-column airlift bioreactor." Biochemical Engineering Journal **34**(3): 279-288.

Kim, D. J., D. I. Lee and J. Keller (2006). "Effect of temperature and free ammonia on nitrification and nitrite accumulation in landfill leachate and analysis of its nitrifying bacterial community by FISH." Bioresource Technology **97**(3): 459-468.

Kim, D. J. and D. Seo (2006). "Selective enrichment and granulation of ammonia oxidizers in a sequencing batch airlift reactor." Process Biochemistry **41**(5): 1055-1062

Kim, J. H., X. J. Guo and H. S. Park (2008). "Comparison study of the effects of temperature and free ammonia concentration on nitrification and nitrite accumulation." Process Biochemistry **43**(2): 154-160.

Kimura, Y., K. Isaka, F. Kazama and T. Sumino (2010). "Effects of nitrite inhibition on anaerobic ammonium oxidation." Applied Microbiology and Biotechnology **86**(1): 359-365

Klotz, M. G., M. C. Schmid, M. Strous, H. J. M. Op Den Camp, M. S. M. Jetten and A. B. Hooper (2008). "Evolution of an octahaem cytochrome c protein family that is key to aerobic and anaerobic ammonia oxidation by bacteria." Environmental Microbiology **10**(11): 3150-3163.

Knowles, G., A. L. Downing and M. J. Barrett (1965). "Determination of kinetic constants for nitrifying bacteria in mixed culture with aid of an electronic computer." Journal of General Microbiology **38**(2): 263-278.

Kommareddy, A. and G.anderson (2004). "Analysis of Currents and Mixing in a modified Bubble Column Reactor." The American Society of Agricultural and Biological Engineers.

Koops, H.-P. and A. Pommerening-Röser (2005). The Lithoautotrophic Ammonia-Oxidizing Bacteria Bergey's Manual® of Systematic Bacteriology. D. J. Brenner, N. R. Krieg, J. T. Staley and G. M. Garrity, Springer US**:** 141-147.

Kross, B. C., Hallberg, G.R.,Bruner,R., Cherryholmes, K., and Johnson, K. J., (1993). "The Nitrate Contamination of Private Well Water in Iowa", American Journal of Public Health. **83**: 270-272.

Kuai, L. and W. Verstraete (1998). "Ammonium Removal by the Oxygen-Limited Autotrophic Nitrification-Denitrification System." Appl Environ Microbiol **64**(11): 4500–4506.

Kuenen, J. (2008). "Anammox bacteria: from discovery to application." Nat Rev Microbiol **6**(4): 320-326.

Kuenen, J. and M. Jetten (2001). "Extra ordinary anaerobic ammonium oxidizing bacteria." ASM News **67**: 456–463.

Kuşçu, Ö. S. and D. T. Sponza (2009). "Kinetics of para-nitrophenol and chemical oxygen demand removal from synthetic wastewater in an anaerobic migrating blanket reactor." Journal of Hazardous Materials **161**(2–3): 787-799.

Kuypers, M. S., AO. Lavik, G. Schmid, M.Jørgensen, BB. Kuenen, JG. Sinninghe, Damsté JS. Strous, M. Jetten, MSM. (2003). "Anaerobic ammonium oxidation by anammox bacteria in the Black Sea." Nature **422**: 608-611.

Kwok, W. K., C. Picioreanu, S. L. Ong, M. C. M. van Loosdrecht, W. J. Ng and J. J. Heijnen (1998). "Influence of biomass production and detachment forces on biofilm structures in a biofilm airlift suspension reactor." Biotechnology and Bioengineering **58**(4): 400-407.

Lai, Q. L. and Z. Z. Shao (2008). "Pseudomonas xiamenensis sp nov., a denitrifying bacterium isolated from activated sludge." International Journal of Systematic and Evolutionary Microbiology **58**: 1911-1915.

Lau, Y. L. and D. Liu (1993). "Effect of Flow Ratio Biofilm Accumulation in Open Channel." Water Research **27**: 355-360.

Legrys, G. A. (1978). "Power demand and mass transfer capability of mechanically agitated gas-liquid contactors and their relationship to air-lift fermenters." Chemical Engineering Science **33**(1): 83-86.

Lek Noophan, P., S. Sripiboon, M. Damrongsri and J. Munakata-Marr (2009). "Anaerobic ammonium oxidation by Nitrosomonas spp. and anammox bacteria in a sequencing batch reactor." Journal of environmental management **90**(2): 967-972.

Lewis, Chelsea, MI.,(1974), “Waste Water Treatment Processes for Phosphorus and Nitrogen Removal” Environment Directorate p. 213 - 223

Li, J. P., D. Elliott, M. Nielsen, M. G. Healy and X. M. Zhan (2011). "Long-term partial nitrification in an intermittently aerated sequencing batch reactor (SBR) treating ammonium-rich wastewater under controlled oxygen-limited conditions." Biochemical Engineering Journal **55**(3): 215-222.

Li, Z., Y. Ma, D. Hira, T. Fujii and K. Furukawa (2011). "Factors affecting the treatment of reject water by the anammox process." Bioresource Technology **102**(10): 5702-5708.

Lim, J., H. Do, S. G. Shin and S. Hwang (2008). "Primer and probe sets for group-specific quantification of the genera Nitrosomonas and Nitrosospira using real-time PCR." Biotechnology and Bioengineering **99**(6): 1374-1383.

Lin, Y. T. and W. Y. Shieh (2006). "Zobellella denitrificans gen. nov., sp nov and Zobellella taiwanensis sp nov., denitrifying bacteria capable of fermentative metabolism." International Journal of Systematic and Evolutionary Microbiology **56**: 1209-1215.

Lindner, J. R. (2004). "Microbubbles in medical imaging: current applications and future directions." Nat Rev Drug Discov **3**(6): 527-533.

Lindsay, M. R., R. I. Webb, M. Strous, M. S. Jetten, M. K. Butler, R. J. Forde and J. A. Fuerst (2001). "Cell compartmentalisation in planctomycetes: novel types of structural organisation for the bacterial cell." Archives of Microbiology **175**(6): 413-429.

Liu, S., F. Yang, Y. Xue, Z. Gong, H. Chen, T. Wang and Z. Su (2008). "Evaluation of oxygen adaptation and identification of functional bacteria composition for anammox consortium in non-woven biological rotating contactor." Bioresource Technology **99**(17): 8273-8279.

Liu, Y. and J.-H. Tay (2002). "The essential role of hydrodynamic shear force in the formation of biofilm and granular sludge." Water Research **36**(7): 1653-1665.

Livansky K. (1990). Losses of CO2 in outdoor mass algal cultures: Determination of the mass transfer coefficient KL by means of measured pH course in NaHCO3 solution. Algological Studies **58**: 87-97.

Looker, Dan, (1991), Nitrogen Use Still Too High, Experts Say, Des Moines (Iowa) Register.

Lopez, I., F. Ruiz-Larrea, L. Cocolin, E. Orr, T. Phister, M. Marshall, J. VanderGheynst and D. A. Mills (2003). "Design and evaluation of PCR primers for analysis of bacterial populations in wine by denaturing gradient gel electrophoresis." Applied and Environmental Microbiology **69**(11): 6801-6807.

Lukens, J. N. (1987). "THE LEGACY OF WELL-WATER METHEMOGLOBINEMIA." Jama-Journal of the American Medical Association **257**(20): 2793-2795.

Mahmood, k. H. AL-Mashhadani, S. J. W., William B. Zimmerman (2012). Removal of acid-gases from digested sludge using microbubble generated by fluidic oscillation. International Conference on Environmental Science and Technology 2012. USA.

Mahmood, K. H. A.-M. B., H C Hemaka. and W. B. Zimmerman (2012). "CO2 Mass Transfer Induced through an Airlift Loop by a Microbubble Cloud Generated by Fluidic Oscillation." Industrial & Engineering Chemistry Research **51**(4): 1864-1877.

Mahne, I. P., A. Megusar, F. (1996). "Nitrification/denitrification in nitrogen high-strength liquid wastes." Water Sci.Technol **30**(9): 2107-2111.

Malovanyy, A., E. Plaza and J. Trela (2009). Evaluation of factors influencing specific Anammox activity (SAA) using surface modelling. Polish-Swedish-Ukrainian seminar. Stockholm, Sweden**:** 35-45.

Malovanyy, A., E. Plaza and J. Trela (2010): Evaluation of factors influencing specific Anammox activity (SAA) using surface modelling In: and application of new technologies in wastewater treatment and municipal solid waste disposal in Ukraine, Sweden and Poland, E. Plaza, E. Levlin (Editors) Report 16, Proceedings of a Polish-Swedish-Ukrainian seminar, 23 – 25

Manipura, A., J. R. Duncan, H. J. Roman and J. E. Burgess (2005). "Potential biological processes available for removal of nitrogenous compounds from metal industry wastewater." Process Safety and Environmental Protection **83**(B5): 472-480.

Mart ń de la Vega, P. T., E. Mart ínez de Salazar, M. A. Jaramillo and J. Cros (2012). "New contributions to the ORP & DO time profile characterization to improve biological nutrient removal." Bioresource Technology **114**(0): 160-167.

Matsumoto, S., A. Terada and S. Tsuneda (2007). "Modeling of membrane-aerated biofilm: Effects of C/N ratio, biofilm thickness and surface loading of oxygen on feasibility of simultaneous nitrification and denitrification." Biochemical Engineering Journal **37**(1): 98-107.

Merchuk, J. C. and M. Gluz (2002). Bioreactors, Air-lift Reactors. Encyclopedia of Bioprocess Technology, John Wiley & Sons, Inc.

Merchuk, J. C. and M. H. Siegel (1988). "Air-lift reactors in chemical and biological technology." Journal of Chemical Technology & Biotechnology **41**(2): 105-120.

Molinuevo, B. G., M.C. Karakashev, D. Angelidaki, I. (2009). "Anammox for ammonia removal from pig manure effluents: effect of organic matter content on process performance." Bioresour Technol **100**: 2171–2175.

Monod, J., (1949). The growth of bacterial cultures. Ann. Rev. Microbiol. 3, 371–376

Moore, James W., 1991, Inorganic Contaminants of Surface Water: Research and Monitoring Priorities, Springer-Varlag, New York City, p. 333.

Moraveji, M. K. and R. Davarnejad (2011). "CFD Modeling of Geometrical Parameters Effects on the Hydrodynamics and Mass Transfer in an airlift Reactor." World Applied Sciences Journal **15**(6): 890-898.

Mosquera-Corral, A., F. Gonzalez, J. L. Campos and R. Mendez (2005). "Partial nitrification in a SHARON reactor in the presence of salts and organic carbon compounds." Process Biochemistry **40**(9): 3109-3118.

Mulder, A., A. A. van de Graaf, L. A. Robertson and J. G. Kuenen (1995). "Anaerobic ammonium oxidation discovered in a denitrifying fluidized bed reactor." FEMS Microbiology Ecology **16**(3): 177-184.

Neef, A. A., Rudolf. Schlesner, Heinz. Schleifer,Karl-Heinz. (1998). "Monitoring a widespread bacterial group: in situ detection of planctomycetes with 16S rRNA-targeted probes." Microbiology **144**(12): 3257-3266.

Neal, L.,1995, Turf grass Nitrogen Evaluated, Water Environment and Technology, : 57.

Ni, S. Q., S. W. Sung, Q. Y. Yue and B. Y. Gao (2012). "Substrate removal evaluation of granular anammox process in a pilot-scale upflow anaerobic sludge blanket reactor." Ecological Engineering **38**(1): 30-36.

Ni, S.-Q., P.-H. Lee and S. Sung (2010). "The kinetics of nitrogen removal and biogas production in an anammox non-woven membrane reactor." Bioresource Technology **101**(15): 5767-5773.

Ni, S.-Q., J.-Y. Ni, D.-L. Hu and S. Sung (2012). "Effect of organic matter on the performance of granular anammox process." Bioresource Technology **110**(0): 701-705.

Ni, S. Q., S. W. Sung, et al. (2012). "Substrate removal evaluation of granular anammox process in a pilot-scale upflow anaerobic sludge blanket reactor." Ecological Engineering **38**(1): 30-36.

Nitrification & Denitrification. New London, The water planet company.

Oflaherty, V., P. N. L. Lens, D. deBeer and E. Colleran (1997). "Effect of feed composition and upflow velocity on aggregate characteristics in anaerobic upflow reactors." Applied Microbiology and Biotechnology **47**(2): 102-107.

Okabe, S., M. Oshiki, Y. Takahashi and H. Satoh (2011). "Development of long-term stable partial nitrification and subsequent anammox process." Bioresource Technology **102**(13): 6801-6807.

Oviatt, C., P. Doering, B. Nowicki, L. Reed, J. Cole and J. Frithsen (1995). "An ecosystem-level experiment on nutrient limitation in temperate coastal marine environments." Marine Ecology-Progress Series **116**(1-3): 171-179.

Pages, R. G. (2009). partial nitrification of land leachate in a sbr prior to an Anammox reactor: operation and modelling, University de Girona. **PhD**.

Park, S. and W. Bae (2009). "Modeling kinetics of ammonium oxidation and nitrite oxidation under simultaneous inhibition by free ammonia and free nitrous acid." Process Biochemistry **44**(6): 631-640.

Pawlowska, M. and L. Pawlowski (2007). Management of Pollutant Emission from Landfills and Sludge, Taylor & Francis.

Paustian, Timothy (2000). "Lithotrophic Bacteria - Rock Eaters." 2012, from http://dwb4.unl.edu/Chem/CHEM869P/CHEM869PLinks/www.bact.wisc.edu/microtextbook/metabolism/lithotrophs.html.

Payne, M. R., (1993), Farm waste and nitrate pollution, in Jones, J. G., ed., Agriculture and the Environment, Ellis Horwood Limited, New York,63-73.

Peng, Y. and G. Zhu (2006). "Biological nitrogen removal with nitrification and denitrification via nitrite pathway." Applied Microbiology and Biotechnology **73**(1): 15-26.

Penton, C. D., AH. Tiedje, JM. (2006). "Molecular evidence for the broad distribution of anaerobic ammonium-oxidizing bacteria in freshwater and marine sediments." Appl Environ Microbiology **72**: 6829–6832.

Puig, S., L. Corominas , M. T. Vives , M. D. Balaguer and J. Colprim (2005). "Development and Implementation of a Real-Time Control System for Nitrogen Removal Using OUR and ORP as End Points." Ind. Eng. Chem. Res. **44**(9): 3367–3373.

Purkhold, U., A. Pommerening-Roser, S. Juretschko, M. C. Schmid, H. P. Koops and M. Wagner (2000). "Phylogeny of all recognized species of ammonia oxidizers based on comparative 16S rRNA and amoA sequence analysis: Implications for molecular diversity surveys." Applied and Environmental Microbiology **66**(12): 5368-5382.

Qiao, S., Y. Kawakubo, T. Koyama and K. Furukawa (2008). "Partial Nitritation of Raw Anaerobic Sludge Digester Liquor by Swim-Bed and Swim-Bed Activated Sludge Processes and Comparison of Their Sludge Characteristics." Journal of Bioscience and Bioengineering **106**(5): 433-441.

Qiao, S., N. Matsumoto, T. Shinohara, T. Nishiyama, T. Fujii, Z. Bhatti and K. Furukawa (2010). "High-rate partial nitrification performance of high ammonium containing wastewater under low temperatures." Bioresource Technology **101**(1): 111-117.

Quan, Z.-X., S.-K. Rhee, J.-E. Zuo, Y. Yang, J.-W. Bae, J. R. Park, S.-T. Lee and Y.-H. Park (2008). "Diversity of ammonium-oxidizing bacteria in a granular sludge anaerobic ammonium-oxidizing (anammox) reactor." Environmental Microbiology **10**(11): 3130-3139.

Ra, C. S., K. V. Lo and D. S. Mavinic (1998). "Real-Time Control of Two-Stage Sequencing Batch Reactor System for the Treatment of Animal Wastewater." Environmental Technology **19**(4): 343-356.

Rail, C. D., 1989, Groundwater Contamination: Sources, Control, and Preventive Measures, Technomic, Lancaster, PA, p. 139.

Raj, S. A. and D. V. S. Murthy (1999). "Comparison of the trickling filter models for the treatment of synthetic dairy wastewater." Bioprocess and Biosystems Engineering **21**(1): 51-55.

Richards, F. A. (1965). "Aoxic basins and Fjords " In Chemical Oceanography: 611-643

Rittmann, B. E. (2001). Environmental Biotechnology.

Rittmann, B. E. and P. L. Mccarty (2001). Environmental Biotechnology: Principles and Applications. London, McGraw-Hill Higher Education.

Rodr ǵuez, I. F. (2010). Towards the improvement of start-up and operation of Anammox reactors, University of Santiago de Compostela. **PhD**.

Rubio, F. C., F. G. A. Fernández, J. A. S. Pérez, F. G. Camacho and E. M. Grima (1999). "Prediction of dissolved oxygen and carbon dioxide concentration profiles in tubular photobioreactors for microalgal culture." Biotechnology and Bioengineering **62**(1): 71-86.

Ruscalleda, M., H. Lopez, R. Ganigue, S. Puig, M. D. Balaguer and J. Colprim (2008). "Heterotrophic denitrification on granular anammox SBR treating urban landfill leachate." Water Science and Technology **58**(9): 1749-1755.

Rysgaard, S., R. N. Glud, N. Risgaard-Petersen and T. Dalsgaard (2004). "Denitrification and Anammox activity in Arctic marine sediments." Limnology and Oceanografy **49**(5): 1493–1502.

Ryther JH, Dunstan W.(1971). "Nitrogen, phosphorus and eutrophication in the coastal marine environment". Science **171**: 1008–1012.

Sabumon, P. C. (2007). "Anaerobic ammonia removal in presence of organic matter: a novel route." J Hazard Mater. **149**(1): 49-59.

Schalk, J., H. Oustad, J. G. Kuenen and M. S. M. Jetten (1998). "The anaerobic oxidation of hydrazine: a novel reaction in microbial nitrogen metabolism." FEMS Microbiology Letters **158**(1): 61-67.

Schmid, M., U. Twachtmann, M. Klein, M. Strous, S. Juretschko, M. Jetten, J. W. Metzger, K.-H. Schleifer and M. Wagner (2000). "Molecular Evidence for Genus Level Diversity of Bacteria Capable of Catalyzing Anaerobic Ammonium Oxidation." Systematic and Applied Microbiology **23**(1): 93-106.

Schmid, M., K. Walsh, R. Webb, W. I. C. Rijpstra, K. van de Pas-Schoonen, M. J. Verbruggen, T. Hill, B. Moffett, J. Fuerst, S. Schouten, J. S. S. Damste, J. Harris, P. Shaw, M. Jetten and M. Strous (2003). "Candidatus "Scalindua brodae", sp nov., Candidatus "Scalindua wagneri", sp nov., two new species of anaerobic ammonium oxidizing bacteria." Systematic and Applied Microbiology **26**(4): 529-538.

Schmid, M. C., B. Maas, A. Dapena, K. V. de Pas-Schoonen, J. V. de Vossenberg, B. Kartal, L. van Niftrik, I. Schmidt, I. Cirpus, J. G. Kuenen, M. Wagner, J. S. S. Damste, M. Kuypers, N. P. Revsbech, R. Mendez, M. S. M. Jetten and M. Strous (2005). "Biomarkers for in situ detection of anaerobic ammonium-oxidizing (anammox) bacteria." Applied and Environmental Microbiology **71**(4): 1677-1684.

Schmid, M. C., A. B. Hooper, M. G. Klotz, D. Woebken, P. Lam, M. M. M. Kuypers, A. Pommerening-Roeser, H. J. M. Op Den Camp and M. S. M. Jetten (2008). "Environmental detection of octahaem cytochrome c hydroxylamine/hydrazine oxidoreductase genes of aerobic and anaerobic ammonium-oxidizing bacteria." Environmental Microbiology **10**(11): 3140-3149.

Schmid, M. C., N. Risgaard-Petersen, J. Van De Vossenberg, M. M. M. Kuypers, G. Lavik, J. Petersen, S. Hulth, B. Thamdrup, D. Canfield, T. Dalsgaard, S. Rysgaard, M. K. Sejr, M. Strous, H. J. M. Op den Camp and M. S. M. Jetten (2007). "Anaerobic ammonium-oxidizing bacteria in marine environments: widespread occurrence but low diversity." Environmental Microbiology **9**(6): 1476-1484.

Schmidt, I., O. Sliekers, M. Schmid, E. Bock, J. Fuerst, J. G. Kuenen, M. S. M. Jetten and M. Strous (2003). "New concepts of microbial treatment processes for the nitrogen removal in wastewater." FEMS Microbiology Reviews **27**(4): 481-492.

Schmidt, J. E. and B. K. Ahring (1996). "Granular sludge formation in upflow anaerobic sludge blanket (UASB) reactors." Biotechnology and Bioengineering **49**(3): 229-246.

Schmidt, J. E. E. and B. K. Ahring (1994). "Extracellular polymers in granular sludge from different upflow anaerobic sludge blanket (UASB) reactors." Applied Microbiology and Biotechnology **42**(2): 457-462.

Selman, M., S. Greenhalgh, E. Branosky, C. Jones, and J. Guiling. 2009. “Water Quality Trading: An International Overview.” Washington, DC: World Resources

Shorrock, C., Driessen, W., Snelson, P and Chadha, M. (2012). "Minworth STW the first UK Anammox® plant to yield an environmentally friendly and budget beating biological phosphorous solution." From http://www.waterprojectsonline.com/case_studies/2012/Severn_Trent_Minworth_2012.pdf.Institute

Shi, H., 2006, Novel Bubble Aerator Performance, University of Sheffield, MSc in Environmental and Energy Engineering dissertation.

Shivaraman, N. (2003). "Anammox - A novel microbial process for ammonium removal." Current Science **84**(12): 1507-1508.

Shuval, Hillel I., 1977, Water Renovation and Reuse, Academic Press, New York City, p. 463.

Shuler, Michael L. and Fikret Karqi (2003). Bioprocess Engineering: Basic Concepts, Pearson

Siegrist, H. H., W. and H. H. (2006). "Anaerobic digestion of slaughterhouse waste with UF-membrane separation and recycling of permeate after free ammonia stripping." Water Science Technology **52**: 531-536.

Sinninghe Damste, J. S., M. Strous, W. I. Rijpstra, E. C. Hopmans, J. A. Geenevasen, A. C. van Duin, L. A. van Niftrik and M. S. Jetten (2002). "Linearly concatenated cyclobutane lipids form a dense bacterial membrane." Nature **419**(6908): 708-712.

Sliekers, A. O., N. Derwort, J. L. C. Gomez, M. Strous, J. G. Kuenen and M. S. M. Jetten (2002). "Completely autotrophic nitrogen removal over nitrite in one single reactor." Water Research **36**(10): 2475-2482.

Sliekers, A. O., K. A. Third, W. Abma, J. G. Kuenen and M. S. M. Jetten (2003). "CANON and Anammox in a gas-lift reactor." FEMS Microbiology Letters **218**(2): 339-344.

Smith, C. J. and A. M. Osborn (2009). "Advantages and limitations of quantitative PCR (Q-PCR)-based approaches in microbial ecology." FEMS Microbiology Ecology **67**(1): 6-20.

Soto, M. M., R. Lema, J.M (1991). "Biodegradability and toxicity in the anerobic treatment of fish canning wastewaters." Environ. Technol **12**: 669-677.

Sozen, M. S., M. D. Orhon and H. A. San (1996). "A new approach for the evaluation of the maximum specific growth rate in nitrification." Water Research **30**(7): 1661-1669.

Stara, W. R. L. v. d., W. R. Abmab, D. Blommersc, J.-W. Mulderc, T. Tokutomid, M. Strouse, C. Picioreanua and M. C. M. v. Loosdrechta (2007). "Startup of reactors for anoxic ammonium oxidation:Experiences from the first full-scale anammox reactor in Rotterdam." Water Research **41**: 4149-4163

Strous, M. (2000). Microbiology of anaerobic ammonium oxidation. Delft, Technical University of Delft. **PhD**.

Strous, M., J. A. Fuerst, E. H. M. Kramer, S. Logemann, G. Muyzer, K. T. van de Pas-Schoonen, R. Webb, J. G. Kuenen and M. S. M. Jetten (1999). "Missing lithotroph identified as new planctomycete." Nature **400**(6743): 446-449.

Strous, M. G. K., J.Jetten, Mike S M. (1999). "Key Physiology of Anaerobic Ammonium Oxidation." Appl Environ Microbiol **65**(7): 3248–3250.

Strous, M., J. J. Heijnen, J. G. Kuenen and M. S. M. Jetten (1998). "The sequencing batch reactor as a powerful tool for the study of slowly growing anaerobic ammonium-oxidizing microorganisms." Applied Microbiology and Biotechnology **50**(5): 589-596.

Strous, M., E. Pelletier, S. Mangenot, T. Rattei, A. Lehner, M. W. Taylor, M. Horn, H. Daims, D. Bartol-Mavel, P. Wincker, V. Barbe, N. Fonknechten, D. Vallenet, B. Segurens, C. Schenowitz-Truong, C. Médigue, A. Collingro, B. Snel, B. E. Dutilh, H. J. M. Op den Camp, C. van der Drift, I. Cirpus, K. T. van de Pas-Schoonen, H. R. Harhangi, L. van Niftrik, M. Schmid, J. Keltjens, J. van de Vossenberg, B. Kartal, H. Meier, D. Frishman, M. A. Huynen, H.-W. Mewes, J. Weissenbach, M. S. M. Jetten, M. Wagner and D. Le Paslier (2006). "Deciphering the evolution and metabolism of an anammox bacterium from a community genome." Nature **440**(7085): 790-794.

Strous, M., E. VanGerven, P. Zheng, J. G. Kuenen and M. S. M. Jetten (1997). "Ammonium removal from concentrated waste streams with the anaerobic ammonium oxidation (anammox) process in different reactor configurations." Water Research **31**(8): 1955-1962.

Strous, M. G., E Van .Kuenen,J G. Jetten,M (1997). "Effects of Aerobic and Microaerobic Conditions on Anaerobic Ammonium-Oxidizing (Anammox) Sludge." Applied and Environmental Microbiology **63**(6): 2446–2448.

Strous, M. G. K., J.Jetten, Mike S M. (1999). "Key Physiology of Anaerobic Ammonium Oxidation." Appl Environ Microbiol **65**(7): 3248–3250.

Sustainable-Website, T. "Water Pollution." Retrieved 1 June, 2012, from http://www.sustainabletable.org/issues/waterpollution/.

Tang, C. J., P. Zheng and Q. Mahmood (2009). "The shear force amendments on the slugging behavior of upflow Anammox granular sludge bed reactor." Separation and Purification Technology **69**(3): 262-268.

Tang, C.-j., P. Zheng, C.-h. Wang and Q. Mahmood (2010). "Suppression of anaerobic ammonium oxidizers under high organic content in high-rate Anammox UASB reactor." Bioresource Technology **101**(6): 1762-1768.

Tang, C.-J., P. Zheng, C.-H. Wang, Q. Mahmood, J.-Q. Zhang, X.-G. Chen, L. Zhang and J.-W. Chen (2011). "Performance of high-loaded ANAMMOX UASB reactors containing granular sludge." Water Research **45**(1): 135-144.

Tang, C.-J., P. Zheng, et al. (2011). "Performance of high-loaded ANAMMOX UASB reactors containing granular sludge." Water Research 45(1): 135-144.

Tesař, V. H., C-H. and W. Zimmerman (2006). "No moving part hybrid synthetic jet mixer." Sensors and Actuators A **125**(2): 159–169.

Tesar, V. c. (2007). Pressure driven microfluidics. Integrated microsystems series. Boston,USA, Artech house.

Thiele, J. H., W.-M. Wu, M. K. Jain and J. G. Zeikus (1990). "Ecoengineering high rate anaerobic digestion systems: Analysis of improved syntrophic biomethanation catalysts." Biotechnology and Bioengineering **35**(10): 990-999.

Third, K. A., J. Paxman, M. Schmid, M. Strous, M. S. M. Jetten and R. Cord-Ruwisch (2005). "Enrichment of Anammox from Activated Sludge and Its Application in the CANON Process." Microbial Ecology **49**(2): 236-244.

Throbäck, I. N., K. Enwall, Å. Jarvis and S. Hallin (2004). "Reassessing PCR primers targeting nirS, nirK and nosZ genes for community surveys of denitrifying bacteria with DGGE." FEMS Microbiology Ecology **49**(3): 401-417.

Toh, S. K., R. I. Webb and N. J. Ashbolt (2002). "Enrichment of Autotrophic Anaerobic Ammonium-Oxidizing Consortia from Various Wastewaters." Microbial Ecology **43**(1): 154-167.

Toh, S. T. and N. A. Ashbolt (2002). "Adaptation of anaerobic ammonium-oxidising consortium to synthetic coke-ovens wastewater." Applied Microbiology and Biotechnology **59**(2): 344-352.

Trigo, C., J. L. Campos, J. M. Garrido and R. Méndez (2006). "Start-up of the Anammox process in a membrane bioreactor." Journal of Biotechnology **126**(4): 475-487.

Tsushima, I., Y. Ogasawara, T. Kindaichi, H. Satoh and S. Okabe (2007). "Development of high-rate anaerobic ammonium-oxidizing (anammox) biofilm reactors." Water Research **41**(8): 1623-1634.

Turk, O. and D. S. Mavinic (1989). "Stability of nitrite buildup in an activated-sludge system." Journal Water Pollution Control Federation **61**(8): 1440-1448.

Turk, O. and D. S. Mavinic (1989). "Maintaining nitrite buildup in a system acclimated to free ammonia." Water Research **23**(11): 1383-1388.

Uyanik, S., O. K. Bekmezci and A. Yurtsever (2011). "Strategies for Successful ANAMMOX Enrichment at Laboratory Scale." CLEAN – Soil, Air, Water **39**(7): 653-657.

Vadivelu, V. M., J. Keller and Z. Yuan (2007). "Free ammonia and free nitrous acid inhibition on the anabolic and catabolic processes of Nitrosomonas and Nitrobacter." Water Science and Technology **56**(7): 89-97

van Benthum, W. A. J., M. C. M. van Loosdrecht and J. J. Heijnen (1997). "Process design for nitrogen removal using nitrifying biofilm and denitrifying suspended growth in a biofilm airlift suspension reactor." Water Science and Technology **36**(1): 119-128.

Van de Graaf, A. A. d. B., P Robertson, L A. Jetten, M S M.Kuenen, J.G. (1996). "Autotrophic growth of anaerobic ammonium-oxidizing micro-organisms in a fluidized bed reactor." Microbiology **142**(8): 2187–2196.

Van de Graaf, A. A. M., A. de Bruijn, P. Jetten, M S M. Robertson, L A. Kuenen,J G. (1995). "Anaerobic oxidation of ammonium is a biologically mediated process." Appl Environ Microbiol **61**: 1246–1251.

Van De Vossenberg, J., J. E. Rattray, W. Geerts, B. Kartal, L. Van Niftrik, E. G. Van Donselaar, J. S. Sinninghe Damsté, M. Strous and M. S. M. Jetten (2008). "Enrichment and characterization of marine anammox bacteria associated with global nitrogen gas production." Environmental Microbiology **10**(11): 3120-3129.

van der Star, W. R. L., A. I. Miclea, U. van Dongen, G. Muyzer, C. Picioreanu and M. C. M. van Loosdrecht (2008). "The membrane bioreactor: A novel tool to grow anammox bacteria as free cells." Biotechnology and Bioengineering **101**(2): 286-294.

van Dongen, U., M. S. Jetten and M. C. van Loosdrecht (2001). "The SHARON-Anammox process for treatment of ammonium rich wastewater." Water science and technology : a journal of the International Association on Water Pollution Research **44**(1): 153-160.

Van Hulle, S. W. H., E. I. P. Volcke, J. L. Teruel, B. Donckels, M. C. M. van Loosdrecht and P. A. Vanrolleghem (2007). "Influence of temperature and pH on the kinetics of the Sharon nitritation process." Journal of Chemical Technology and Biotechnology **82**(5): 471-480.

van Niftrik, L. A., J. A. Fuerst, J. S. S. Damsté, J. G. Kuenen, M. S. M. Jetten and M. Strous (2004). "The anammoxosome: an intracytoplasmic compartment in anammox bacteria." FEMS Microbiology Letters **233**(1): 7-13.

Vanotti, M., J. Martinez, A. Magrí, A. Szögi and T. Fujii (2011). Streamlined Ammonia Removal from Wastewater Using Biological Deammonification Process. The CIGR-Ageng Conference.

Vazquez-Padin, J., I. Fernadez, M. Figueroa, A. Mosquera-Corral, J. L. Campos and R. Mendez (2009). "Applications of Anammox based processes to treat anaerobic digester supernatant at room temperature." Bioresource Technology **100**(12): 2988-2994.

Vazquez-Padin, J. R. (2009). Autotrophic nitrogen removal in granular sequencing batch reactors. Spain, University of Santiago de Compostela. **PhD**.

Vazquez-Padin, J. R., M. J. Pozo, M. Jarpa, M. Figueroa, A. Franco, A. Mosquera-Corral, J. L. Campos and R. Mendez (2009). "Treatment of anaerobic sludge digester effluents by the CANON process in an air pulsing SBR." Journal of Hazardous Materials **166**(1): 336-341.

Villaverde, S., F. Fdz-Polanco and P. A. Garcia (2000). "Nitrifying biofilm acclimation to free ammonia in submerged biofilters. Start-up influence." Water Research **34**(2): 602-610.

Vitousek, P. M., J. D. Aber, R. W. Howarth, G. E. Likens, P. A. Matson, D. W. Schindler, W. H. Schlesinger and D. Tilman (1997). "Human alteration of the global nitrogen cycle: Sources and consequences." Ecological Applications **7**(3): 737-750.

Vogt, C., and Cotruvo, J., 1987, Drinking Water Standards: Their Derivation and Meaning, in D'Itri, F.M., Wolfson, L. G., eds., Rural Groundwater Contamination.

Wang, C.-C., P.-H. Lee, M. Kumar, Y.-T. Huang, S. Sung and J.-G. Lin (2010). "Simultaneous partial nitrification, anaerobic ammonium oxidation and denitrification (SNAD) in a full-scale landfill-leachate treatment plant." Journal of Hazardous Materials **175**(1–3): 622-628.

Wang, T., H. Zhang, F. Yang, S. Liu, Z. Fu and H. Chen (2009). "Start-up of the Anammox process from the conventional activated sludge in a membrane bioreactor." Bioresource Technology **100**(9): 2501-2506.

Watt, G. W. and J. D. Chrisp (1952). "Spectrophotometric Method for Determination of Hydrazine." Anal. Chem. **24**(12): 2006–2008.

Wertz, S., F. Poly, X. Le Roux and V. Degrange (2008). "Development and application of a PCR-denaturing gradient gel electrophoresis tool to study the diversity of Nitrobacter-like nxrA sequences in soil." FEMS Microbiology Ecology **63**(2): 261-271.

Wett, B., S. Murthy, Tak, I. cs, M. Hell, G. Bowden, A. Deur and M. O'Shaughnessy (2007). "Key Parameters for Control of DEMON Deammonification Process." Water Practice **1**(5): 1-11.

Wiesmann, U. (1994). Biological nitrogen removal from wastewater Biotechnics/Wastewater, Springer Berlin / Heidelberg. **51:** 113-154.

Wilén, B.M. and Balmer, P. (1999). The effect of dissolved oxygen concentration on the structure, size and size distribution of activated sludge flocs. Wat. Res., **33**(2), 391–400.

William, B. Z., Z. Mohammad, H. C. H. Bandulasena, T. Václav, D. J. Gilmour and Y. Kezhen (2011). "Design of an airlift loop bioreactor and pilot scales studies with fluidic oscillator induced microbubbles for growth of a microalgae Dunaliella salina." Appl Energy **88**(10): 3357-3369

Woebken, D., P. Lam, M. M. M. Kuypers, S. W. A. Naqvi, B. Kartal, M. Strous, M. S. M. Jetten, B. M. Fuchs and R. Amann (2008). "A microdiversity study of anammox bacteria reveals a novel Candidatus Scalindua phylotype in marine oxygen minimum zones." Environmental Microbiology **10**(11): 3106-3119.

Worden, R. M. and M. D. Bredwell (1998). "Mass-Transfer Properties of Microbubbles. 2. Analysis Using a Dynamic Model." Biotechnology Progress **14**(1): 39-46.

World Resources Institute (2002) "Sources of Nutrient Pollution." 2012, from http://www.wri.org/project/eutrophication/about/sources.

Xu, Q., M. Nakajima, Z. Liu and T. Shiina (2011). "Biosurfactants for Microbubble Preparation and Application." International Journal of Molecular Sciences **12**(1): 462-475.

Xue, Y., F. L. Yang, S. T. Liu and Z. M. Fu (2009). "The influence of controlling factors on the start-up and operation for partial nitrification in membrane bioreactor." Bioresource Technology **100**(3): 1055-1060.

Yamamoto, T., K. Takaki, T. Koyama and K. Furukawa (2008). "Long-term stability of partial nitritation of swine wastewater digester liquor and its subsequent treatment by Anammox." Bioresource Technology **99**(14): 6419-6425.

Yang, Q., Y. Z. Peng, X. H. Liu, W. Zeng, T. Mino and H. Satoh (2007). "Nitrogen removal via nitrite from municipal wastewater at low temperatures using real-time control to optimize nitrifying communities." Environmental Science & Technology **41**(23): 8159-8164.

Yang, Y., J.-e. Zuo, P. Shen and X.-s. Gu (2006). "Influence of temperature, pH value and organic substance on activity of ANAMMOX sludge." Huanjing Kexue **27**(4): 691-695.

Yap, K. "Micro Bubbles and Its Applications." 2012, from http://www.suwaprecision.com/SIV/micro_bubbles_applications.html.

Yu, H., F. Wilson and J.-H. Tay (1998). "Kinetic analysis of an anaerobic filter treating soybean wastewater." Water Research **32**(11): 3341-3352.

Yu, J., X. Wang and P. L. Yue (2001). "Optimal Decolorization and Kinetic Modeling of Synthetic Dyes by Pseudomonas Strains." Water Research **35**(15): 3579-3586.

Yuan, L.-M., C.-Y. Zhang, Y.-Q. Zhang, Y. Ding and D.-L. Xi (2008). "Biological nutrient removal using an alternating of anoxic and anaerobic membrane bioreactor (AAAM) process." Desalination **221**(1–3): 566-575.

Yuan, Z., A. Oehmen, Y. Peng, Y. Ma and J. Keller (2008). "Sludge population optimisation in biological nutrient removal wastewater treatment systems through on-line process control: a re/view." Reviews in Environmental Science and Bio/Technology **7**(3): 243-254.

Zajic, J. E., (1971), Water Pollution Disposal and Reuse, Marcel Dekker, New York City, Volume 1p. 389.

Zeng, W., Y. Zhang, L. Li, Y. Z. Peng and S. Y. Wang (2009). "Control and optimization of nitrifying communities for nitritation from domestic wastewater at room temperatures." Enzyme and Microbial Technology **45**(3): 226-232.

Zhang, D., N. G. Deen and J. A. M. Kuipers (2006). "Numerical simulation of the dynamic flow behavior in a bubble column: A study of closures for turbulence and interface forces." Chemical Engineering Science **61**(23): 7593-7608.

Zhang, L. (2009). The study of performance of anaerobic ammonium oxidation. Hangzhou, University of Zhejiang. **PhD**.

Zhang, L., J. Yang, D. Hira, T. Fujii, W. Zhang and K. Furukawa (2011). "High-rate nitrogen removal from anaerobic digester liquor using an up-flow anammox reactor with polyethylene sponge as a biomass carrier." Journal of Bioscience and Bioengineering **111**(3): 306-311.

Zhang, L., J. Yang, Y. Ma, Z. Li, T. Fujii, W. Zhang, N. Takashi and K. Furukawa (2010). "Treatment capability of an up-flow anammox column reactor using polyethylene sponge strips as biomass carrier." Journal of Bioscience and Bioengineering **110**(1): 72-78.

Zhang, Z.-P., S. S. Adav, K.-Y. Show, J.-H. Tay, D. T. Liang, D.-J. Lee and A. Su (2008). "Characteristics of rapidly formed hydrogen-producing granules and biofilms." Biotechnology and Bioengineering **101**(5): 926-936.

Zheng, P. H., Baolan. (2001). "Kinetics of Anaerobic Ammonia Oxidation." Chinese Journal of Biotechnology, **17**(2): 193-198.

Zheng, P. W., M S.Jin, R C. (2006). "Effect of organic matter on performance of anammox reactor." Acta Scientiae Circumstantiae 26: 1087–1092.

Zhou, Y., A. Oehmen, M. Lim, V. Vadivelu and W. J. Ng (2011). "The role of nitrite and free nitrous acid (FNA) in wastewater treatment plants." Water Research **45**(15): 4672-4682.

Zimmerman, William B., Buddhika N. Hewakandamby, Václav Tesař, H. C. Hemaka Bandulasena and Olumuyiwa A. Omotowa (2009). "On the design and simulation of an airlift loop bioreactor with microbubble generation by fluidic oscillation." Food and Bioproducts Processing 87(3): 215-227.

Zimmerman, William B., Václav Tesař and H. C. Hemaka Bandulasena (2011). "Towards energy efficient nanobubble generation with fluidic oscillation." Current Opinion in Colloid & Interface Science 16(4): 350-356.

Zimmerman. William B., Lozano-Parada, Jaime H., Bandulasena, H.C. Hemaka., (2010). "Ozone regenerated: low power consumption and high dispersal rates with microbubbles." J. Sewerage & Water.

Zimmerman, William B., Tesar, Vaclav, Butler, Simon, Bandulasena, Himiyage C.H, (2008). "Microbubble Generation." Recent Patents on Engineering **2**: 1-8.